

IAEA-TECDOC-1361

***Assessment and management of
ageing of major nuclear
power plant components
important to safety***

Primary piping in PWRs



INTERNATIONAL ATOMIC ENERGY AGENCY

IAEA

July 2003

The originating Section of this publication in the IAEA was:

Engineering Safety Section
International Atomic Energy Agency
Wagramer Strasse 5
P.O. Box 100
A-1400 Vienna, Austria

ASSESSMENT AND MANAGEMENT OF AGEING OF
MAJOR NUCLEAR POWER PLANT COMPONENTS IMPORTANT TO SAFETY
IAEA, VIENNA, 2003
IAEA-TECDOC-1361
ISBN 92-0-108003-4
ISSN 1011-4289

© IAEA, 2003

Printed by the IAEA in Austria
July 2003

FOREWORD

At present, there are over four hundred operational nuclear power plants (NPPs) in IAEA Member States. Operating experience has shown that ineffective control of the ageing degradation of the major NPP components (caused for instance by unanticipated phenomena and by operating, maintenance or manufacturing errors) can jeopardize plant safety and also plant life. Ageing in these NPPs must therefore be effectively managed to ensure the availability of design functions throughout the plant service life. From the safety perspective, this means controlling, within acceptable limits, the ageing degradation and wearout of plant components important to safety so that adequate safety margins remain, i.e. integrity and functional capability in excess of normal operating requirements.

This TECDOC is one in a series of reports on the assessment and management of ageing of the major NPP components important to safety. The reports are based on experience and practices of NPP operators, regulators, designers, manufacturers, technical support organizations and a widely accepted Methodology for the Management of Ageing of NPP Components Important to Safety, which was issued by the IAEA in 1992. Since the reports are written from a safety perspective, they do not address life or life cycle management of plant components, which involves economic considerations.

The current practices for the assessment of safety margins (fitness-for-service) and the inspection, monitoring and mitigation of ageing degradation of selected components of Canada deuterium–uranium (CANDU) reactors, boiling water reactors (BWRs), pressurized water reactors (PWRs), and water moderated, water cooled energy reactors (WWERs) are documented in the reports. These practices are intended to help all involved directly and indirectly in ensuring the safe operation of NPPs, and to provide a common technical basis for dialogue between plant operators and regulators when dealing with age-related licensing issues. The guidance reports are directed at technical experts from NPPs and from regulatory, plant design, manufacturing and technical support organizations dealing with specific plant components addressed in the reports.

This report addresses the primary piping in PWRs including main coolant piping, surge and spray lines, Class 1 piping in attached systems, and small diameter piping that cannot be isolated from the primary coolant system. Maintaining the structural integrity of this piping throughout NPP service life in spite of several ageing mechanisms is essential for plant safety.

The work of all contributors to the drafting and review of this publication, identified at the end, is greatly appreciated. In particular, the IAEA would like to acknowledge the contributions of C. Faidy (EdF, France), J. Schmidt (Siemens, Germany), and V. Shah (ANL, USA). The IAEA officer responsible for the preparation of the report was J. Pachner of the Division of Nuclear Installation Safety.

EDITORIAL NOTE

The use of particular designations of countries or territories does not imply any judgement by the publisher, the IAEA, as to the legal status of such countries or territories, of their authorities and institutions or of the delimitation of their boundaries.

The mention of names of specific companies or products (whether or not indicated as registered) does not imply any intention to infringe proprietary rights, nor should it be construed as an endorsement or recommendation on the part of the IAEA.

CONTENTS

1. INTRODUCTION.....	1
1.1. Background.....	1
1.2. Objective.....	3
1.3. Scope.....	3
1.4. Structure.....	4
References to Section 1	4
2. DESCRIPTION: DESIGN, MATERIALS, FABRICATION, AND WATER CHEMISTRY	6
2.1. US design and materials	6
2.1.1. Main coolant loop piping design.....	6
2.1.2. Surge and spray line design and materials	9
2.1.3. Charging system design and materials	16
2.1.4. Safety injection system design and materials.....	17
2.1.5. Design and materials of residual heat removal system	20
2.2. French design.....	24
2.3. Japanese design.....	25
2.4. German design	26
2.5. Russian design	30
2.5.1. WWER 440	30
2.5.2. WWER 1000	37
2.6. Main coolant loop piping materials and fabrication	39
2.6.1. Clad carbon steel main coolant loop piping	40
2.6.2. Stainless steel main coolant loop piping	51
2.6.3. Dissimilar metal welds	53
2.7. Pre-service inspections	54
2.8. Pre-service testing.....	60
2.9. Reactor coolant system water chemistry	60
References to Section 2	61
3. DESIGN BASIS: REGULATIONS, CODES AND GUIDES	62
3.1. US Regulations, codes and standards	62
3.1.1. US regulations	62
3.1.2. US referenced codes and standards.....	63
3.1.3. Other US codes and standards.....	63
3.2. Regulations, codes and standards in other countries	63
3.3. Design basis (expected) transients.....	64
3.4. Design fatigue analysis of piping.....	69
3.4.1. Present ASME Code Design Requirements	69
3.4.2. Fatigue analysis practice in Germany	70
3.4.3. Fatigue analysis practice in France	70
3.5. Assessment of fracture toughness.....	70
References to Section 3	72
4. AGEING MECHANISMS AND OPERATING EXPERIENCE	73
4.1. Thermal fatigue of pipes and nozzles	74

4.1.1. Thermal fatigue of surge line	74
4.1.2. Thermal fatigue of spray line and nozzles.....	82
4.1.3. Thermal fatigue of other connected lines	84
4.1.4. Thermal fatigue of dissimilar metal welds	102
4.2. Vibratory fatigue of small lines	104
4.2.1. Excitation mechanisms.....	106
4.2.2. Characteristics of socket welds	106
4.2.3. Experience in the USA	108
4.2.4. French experience.....	111
4.3. Thermal ageing of cast stainless steel piping and welds	111
4.3.1. Thermal ageing of cast stainless steel piping	112
4.3.2. Thermal ageing of austenitic stainless steel welds	117
4.4. Primary water stress corrosion cracking of alloy 600.....	118
4.4.1. Initiation key parameters	118
4.4.2. Crack growth rate key parameters.....	120
4.4.3. Primary water stress corrosion cracking — operating experience	122
4.5. Boric acid corrosion.....	125
4.6. Atmospheric corrosion.....	126
References to Section 4	127
5. ASSESSMENT METHODS	133
5.1. Assessment of thermal fatigue.....	133
5.1.1. Fatigue analysis of piping by ASME code method.....	133
5.1.2. Thermal fatigue assessment of surge line.....	148
5.1.3. Thermal fatigue assessment of branch lines and connections.....	152
5.1.4. Consequences of fatigue damage on dynamic load carrying capacity of pipings	154
5.2. Assessment of vibratory fatigue of piping connections.....	154
5.3. Assessment of thermal ageing	156
5.3.1. Cast stainless	156
5.3.2. Stainless steel welds	162
5.4. Primary water stress corrosion cracking of alloy 600.....	162
5.4.1. Crack initiation	162
5.4.2. Crack growth	163
5.5. Assessment of boric acid corrosion	166
5.6. Assessment of atmospheric corrosion of dissimilar metal welds	166
5.7. Leak-before-break analysis.....	167
5.7.1. The approach in the USA	167
5.7.2. The approach in Germany	169
5.7.3. The approach in France	174
5.7.4. The approach in Japan	177
5.7.5. Russian approach.....	178
5.7.6. Calibration of leak detection system (LDS).....	178
5.7.7. Check of leak/break reaction forces	179
5.7.8. LBB safety margins.....	179
5.7.9. Toughness assessment.....	179
References to Section 5	183
6. INSPECTION, MONITORING AND LEAK DETECTION	187

6.1. Inspections of PWR primary piping	187
6.1.1. Inspection requirements	187
6.1.2. Material considerations	190
6.1.3. Past experience/augmented examinations	193
6.1.4. In-service inspection methods/reliability	197
6.1.5. Emerging in-service inspection techniques	200
6.2. Monitoring of low-cycle fatigue	206
6.2.1. Design basis approach	208
6.2.2. On-line fatigue monitoring	208
6.3. Leak detection	211
6.3.1. USNRC Regulatory Guide 1.45 Recommendations	211
6.3.2. Effectiveness of current leakage detection systems	212
6.3.3. Capabilities of advanced leakage detection systems	215
6.4. Loose parts monitoring	216
6.5. Water chemistry monitoring	216
References to Section 6	216
7. AGEING MITIGATION METHODS	220
7.1. Mitigation of thermal fatigue	220
7.1.1. Operational changes	220
7.1.2. Maintenance to reduce valve leakage	221
7.1.3. Design changes	221
7.1.4. Examples of ageing mitigation actions for thermal fatigue	222
7.2. Mitigation of vibration fatigue	222
7.3. Mitigation of PWSCC of Alloy 600	223
7.4. Piping repair and replacement	223
References to Section 7	224
8. PWR PRIMARY PIPING AGEING MANAGEMENT PROGRAMME	225
8.1. Key elements of pwr primary piping ageing management programme	226
8.1.1. Understanding PWR primary piping ageing	226
8.1.2. Co-ordination of PWR primary piping ageing managemeprogramme	228
8.1.3. Operation of PWR primary piping	228
8.1.4. PWR primary piping inspection, monitoring and assessment	229
8.1.5. Maintenance of PWR primary piping	229
8.2. Application guidance	230
8.2.1. Fatigue	230
8.2.2. Thermal ageing	232
8.2.3. Corrosion	232
References to Section 8	234
CONTRIBUTORS TO DRAFTING AND REVIEW	235

1. INTRODUCTION

1.1. Background

Managing the safety aspects of nuclear power plant (NPP) ageing requires implementation of effective programmes for the timely detection and mitigation of ageing degradation of plant systems, structures and components (SSCs) important to safety, so as to ensure their integrity and functional capability throughout plant service life. General guidance on NPP activities relevant to the management of ageing (operation maintenance, surveillance, and inspection of SSCs) is given in the following IAEA Safety Standards on the Safety of NPPs: Operation Requirements [1.1] and associated Safety Guides on in-service inspection [1.2], maintenance [1.3], and surveillance [1.4].

The operation requirements require that an NPP operating organization prepares and carries out a programme of maintenance, testing, surveillance and inspection of plant systems, structures and components important to safety to ensure that their level of reliability and effectiveness remains in accordance with the design assumptions and intent throughout the service life of the plant. This programme is to take into account the operational limits and conditions, any other applicable regulatory requirements, ageing characteristics of SSCs and be re-evaluated in the light of operating experience. The associated Safety Guides provide further guidance on NPP programmes and activities that contribute to timely detection and mitigation of ageing degradation of SSCs important to safety.

The Safety Guide on In-Service Inspection provides recommendations on methods, frequency and administrative measures for the in-service inspection programme for critical systems and components of the primary reactor coolant system aimed at detecting possible deterioration caused by stressors such as stress, temperature, radiation, vibration and water chemistry and at determining whether they are acceptable for continued safe operation of the plant or whether remedial measures are needed. Organizational and procedural aspects of establishing and implementing an NPP programme of preventive and remedial maintenance to achieve design performance throughout the operational life of the plant are covered in the Maintenance Safety Guide. Guidance and recommendations on surveillance activities, for SSCs important to safety (i.e. monitoring plant parameters and systems status, checking and calibrating instrumentation, testing and inspecting SSCs, and evaluating results of these activities) are provided in the Surveillance Safety Guide. The aim of the surveillance activities is to verify that the plant is operated within the prescribed operational limits and conditions, to detect in time any deterioration of SSCs as well as any adverse trend that could lead to an unsafe condition, and to supply data to be used for assessing the residual life of SSCs. The above Safety Guides provide general guidance, but do not give detailed technical advice for particular SSCs.

Programmatic guidance on ageing management is given in Technical Reports Series No. 338 “Methodology for the Management of Ageing of NPP Components Important to Safety” [1.5] and in a Safety Practices Publication “Data Collection and Record Keeping for the Management of NPP Ageing” [1.6]. Guidance provided in these reports served as a basis for the development of component specific technical publications (TECDOCs) on the Assessment and Management of Ageing of Major NPP Components Important to Safety. This publication on PWR primary piping is one such TECDOC. TECDOCs already issued address: steam generators [1.7], concrete containment buildings [1.8], CANDU pressure tubes [1.9],

PWR reactor pressure vessels [1.10], PWR reactor vessel internals [1.11], metal components of BWR containment systems [1.12], in-containment I&C cables [1.13] and CANDU reactor assemblies [1.14].

The PWR primary system piping constitutes a barrier to the release of fission products and activated species to the containment during normal, off-normal, accident and test conditions. The large diameter primary system piping (main coolant piping) carries the hot coolant from the reactor pressure vessel to the steam generators and then provides cold coolant back to the vessel. The other piping facilitates plant operation and plays a role in mitigating any off-normal or accident conditions. Therefore, maintaining the structural integrity of this piping is essential to the safe operation of a PWR plant.

The reactor coolant components are subjected to several different ageing mechanisms:

- the surge and spray lines and several branch lines and nozzles (charging line, safety injection lines ...) experience significant low cycle thermal fatigue caused by thermal stratification and cycling, and high cycle fatigue caused by striping
- the bimetallic welds made with stainless steel filler metal experience low cycle fatigue damage caused by heat-up and cooldown transients and some corrosion sensitivity
- the cast stainless steel piping experiences a loss of fracture toughness caused by thermal ageing and low cycle fatigue in the inclined nozzle of the safety injection line
- the ferritic steel base metal may experience boric acid corrosion if exposed to the primary coolant
- the socket welds between instrument penetration lines and piping experience cracking caused by vibration fatigue
- thermal sleeves experience cracking caused by vibration and thermal fatigue
- Alloy 600 penetrations experience cracking caused by primary water stress corrosion cracking.

The most likely mode of failure is a through-wall crack and leakage; some piping components have experienced such cracking. In the presence of these mechanisms, it is possible but unlikely, depending on crack morphology and growth rate, that a pipe may rupture without giving an adequate warning by leakage. Primary system piping has not experienced such ruptures in the field, except some small diameter piping that failed by vibration fatigue. The potential failure modes are small, intermediate or large break loss of coolant accidents, which can lead to severe accidents.

Effective ageing management of reactor coolant piping requires in depth understanding of interactions between component design, materials, fabrication, operating environment and operational transients. Effective ageing management of the piping mainly includes reliable and accurate in-service inspection at susceptible locations including welds and base metal, monitoring of thermal transients causing fatigue damage, reliable and accurate leak detection, accurate assessment of flaws by fracture mechanics and changes in operating procedures.

1.2. Objective

The objective of this report is to identify significant ageing mechanisms and degradation locations, and to document the current practices for the assessment and management of the ageing of PWR primary system piping. The report emphasizes safety aspects and also provides information on current inspection, monitoring and mitigation practices for managing ageing of PWR primary system piping.

The underlying objective of this report series is to ensure that the information on the current assessment methods and ageing management techniques is available to all involved, directly and indirectly, in the operation of NPPs in IAEA Member States. The target audience includes NPP operators, regulators, technical support organizations, designers and manufacturers.

The readers who are not interested in technical details related to ageing degradation of PWR primary system piping but are interested in ageing management strategy for PWR piping utilizing a systematic ageing management approach should go directly to Section 8. This section presents a strategy for managing each of the five significant ageing mechanisms: thermal fatigue, vibratory fatigue, thermal ageing, stress corrosion cracking and boric acid corrosion.

1.3. Scope

This report provides the technical basis for understanding and managing the ageing of PWR (including WWER) reactor coolant system piping to ensure that acceptable safety and operational margins are maintained throughout the plant service life. The reactor coolant system piping is a part of the reactor coolant pressure boundary and includes main coolant piping, surge and spray lines, Class 1 piping in attached systems, and small diameter piping (diameter ≤ 25.4 mm) that cannot be isolated from the primary coolant system. The attached systems in US PWRs include safety injection system, charging and purification system, residual heat removal system, auxiliary spray system, and core flood and incore monitoring systems. In addition, vents, drains and instrumentation lines up to and including isolation valves or flow restricting orifices contain Class 1 piping. The Class 1 piping in the attached systems penetrates the reactor coolant pressure boundary and extends up to and including any and all of the following as defined by Definitions 10 CFR 50.2. [1.15]:

- the outermost containment isolation valve in system piping which penetrates the primary reactor containment,
- the second of two valves normally closed during normal reactor operation in system piping which does not penetrate primary reactor containment,
- the RCS safety and relief valves.

The scope of the report includes passive components in the primary system piping (straight pipes, fittings, safe ends, nozzles and thermal sleeves, but no active components such as valves and pumps).

1.4. Structure

The designs, materials of construction, physical features and water chemistry of the various PWR reactor coolant system piping are described in Section 2. The codes, regulations and guides used in a number of countries to design reactor coolant system piping are summarized in Section 3. The ageing mechanisms, susceptible degradation sites, and operating experience are presented in Section 4. Methods for assessing ageing degradation caused by significant ageing mechanisms and leak-before-break (LBB) analysis are discussed in Section 5. The in-service inspection techniques and procedures and monitoring methods to assess ageing degradation of reactor coolant system piping are described in Section 6. Mitigation of age-related degradation is discussed in Section 7. The report concludes, in Section 8, with a description of a systematic ageing management programme for PWR primary piping.

REFERENCES TO SECTION 1

- [1.1] INTERNATIONAL ATOMIC ENERGY AGENCY, Safety of Nuclear Power Plants: Operation Requirements, Safety Standards Series No. NS-R-2, IAEA, Vienna (2000).
- [1.2] INTERNATIONAL ATOMIC ENERGY AGENCY, In-Service Inspection for Nuclear Power Plants, Safety Series No. 50-SG-O2, IAEA, Vienna (1980).
- [1.3] INTERNATIONAL ATOMIC ENERGY AGENCY, Maintenance of Nuclear Power Plants, Safety Series No. 50-SG-O7 (Rev. 1), IAEA, Vienna (1990).
- [1.4] INTERNATIONAL ATOMIC ENERGY AGENCY, Surveillance of Items Important to Safety in Nuclear Power Plants, Safety Series No. 50-SG-O8 (Rev. 1), IAEA, Vienna (1990).
- [1.5] INTERNATIONAL ATOMIC ENERGY AGENCY, Methodology for the Management of Ageing of Nuclear Power Plant Components Important to Safety, Technical Reports Series No. 338, IAEA, Vienna (1992).
- [1.6] INTERNATIONAL ATOMIC ENERGY AGENCY, Data Collection and Record Keeping for the Management of Nuclear Power Plant Ageing, Safety Series No. 50-P-3, IAEA, Vienna (1991).
- [1.7] INTERNATIONAL ATOMIC ENERGY AGENCY, Assessment and Management of Ageing of Major Nuclear Power Plant Components Important to Safety: Steam Generators, IAEA-TECDOC-981, Vienna (1997).
- [1.8] INTERNATIONAL ATOMIC ENERGY AGENCY, Assessment and Management of Ageing of Major Nuclear Power Plant Components Important to Safety: Concrete Containment Buildings, IAEA-TECDOC-1025, Vienna (1998).
- [1.9] INTERNATIONAL ATOMIC ENERGY AGENCY, Assessment and Management of Ageing of Major Nuclear Power Plant Components Important to Safety: CANDU Pressure Tubes, IAEA-TECDOC-1037, Vienna (1998).
- [1.10] INTERNATIONAL ATOMIC ENERGY AGENCY, Assessment and Management of Ageing of Major Nuclear Power Plant Components Important to Safety: PWR Pressure Vessels, IAEA-TECDOC-1120, Vienna (1999).
- [1.11] INTERNATIONAL ATOMIC ENERGY AGENCY, Assessment and Management of Ageing of Major Nuclear Power Plant Components Important to Safety: PWR Vessel Internals, IAEA-TECDOC-1119, Vienna (1999).
- [1.12] INTERNATIONAL ATOMIC ENERGY AGENCY, Assessment and Management of Ageing of Major Nuclear Power Plant Components Important to Safety: Metal Components of BWR Containment Systems, IAEA-TECDOC-1181, Vienna (2000).

- [1.13] INTERNATIONAL ATOMIC ENERGY AGENCY, Assessment and Management of Ageing of Major Nuclear Power Plant Components Important to Safety: In-containment Instrumentation and Control Cables, Vols I and II, IAEA-TECDOC-1188, Vienna (2000).
- [1.14] INTERNATIONAL ATOMIC ENERGY AGENCY, Assessment and Management of Ageing of Major Nuclear Power Plant Components Important to Safety: CANDU Reactor Assemblies, IAEA-TECDOC-1197, Vienna (2001).
- [1.15] USNRC, 10 CFR 50.2, "Definitions," *Code of Federal Regulations*, US Office of the Federal Register (1993).

2. DESCRIPTION: DESIGN, MATERIALS, FABRICATION, AND WATER CHEMISTRY

This section is organized according to the configuration of the main coolant piping employed in the reactor coolant system design. There are of three different types of main coolant piping configuration, which are employed in (1) Babcock & Wilcox-designed and Combustion Engineering-designed PWRs, (2) Westinghouse-type PWRs, and (3) WWER plants designed in the former Soviet Union. The Babcock & Wilcox- and Combustion Engineering-designed PWRs are operating mainly in the USA. The Westinghouse-type PWRs are the most typical PWRs and include those designed by Westinghouse, Framatome, Siemens and Mitsubishi Heavy Industries (MHI). The WWER plants are designed by the Russian Federation and are operating mainly in eastern European countries.

Detailed design descriptions of the reactor coolant system piping for Babcock & Wilcox-, Combustion Engineering-, and Westinghouse-designed PWRs in the USA are presented in Section 2.1. The designs for French, Japanese, and German PWRs are similar to that in Westinghouse-designed PWRs in the USA, except that the materials of German PWRs are different. Therefore, Sections 2.2, 2.3, and 2.4 on French, Japanese, and German PWR designs, respectively, are brief and identify any differences from the Westinghouse-designed PWRs. Detailed design description of the reactor coolant system piping for WWER plants is presented in Section 2.5. The related materials and fabrication are described in Section 2.6. The preservice inspections and testing are summarized in Sections 2.7 and 2.8, respectively. Primary water chemistry specifications are summarized in Section 2.9.

2.1. US design and materials

There are 71 operating PWRs in the USA: 7 Babcock & Wilcox plants, 14 Combustion Engineering plants, and 50 Westinghouse plants.¹ The main difference in the piping configuration of these plants is that the Babcock & Wilcox and all but one Combustion Engineering plant have two RCS loops with two reactor coolant pumps (RCP) in each loop, whereas the Westinghouse plants have 2, 3, or 4 loops with one RCP in each loop. The remainder of the primary system piping in all the design consists of a surge line, main and auxiliary spray lines, safety injection lines, charging lines, and residual heat removal lines.

2.1.1. Main coolant loop piping design

The Babcock & Wilcox and Combustion Engineering main coolant loop designs are shown in Figures 2-1 and 2-2, respectively. Each loop has a hot leg that takes coolant from the reactor to the steam generator, and two cold legs that return the coolant from the steam generator to the reactor pressure vessel via an RCP. An exception is the three-loop Combustion Engineering plant shown in Figure 2-3, which has a steam generator, a pump, and two isolation valves on each loop (one each on a hot leg and a cold leg).

A major difference between the B&W and CE main coolant loop designs is that the B&W steam generators are once-through, straight-tube steam generators, whereas the CE steam generators are recirculating, U-tube steam generators. The primary coolant in the once-

¹ PWRs in commercial operation as of June 1999.

through steam generators flows from the upper head (hot-leg side) vertically down to the lower head (cold-leg side), whereas in recirculating steam generators, it flows from the bottom of the hot-leg side up to the top of the tube bundle, then down to the bottom of the cold-leg side.

Consistent with the steam generator designs, the primary system hot-leg piping in the Babcock & Wilcox design runs vertically up from the reactor vessel outlet nozzles to the top of the steam generators. The hot leg piping in the Combustion Engineering design runs directly from the reactor vessel outlet nozzles to the bottom head of the steam generators. The overall arrangement of the cold-leg piping for these two designs is quite similar.

The main coolant loop piping in a Westinghouse plant consists of two, three or four loops as shown in Figure 2-4. The number of loops in any given plant depends on a number of factors, but the most important is the capacity of the plant. Each loop increases the amount of power that may be extracted from the reactor.

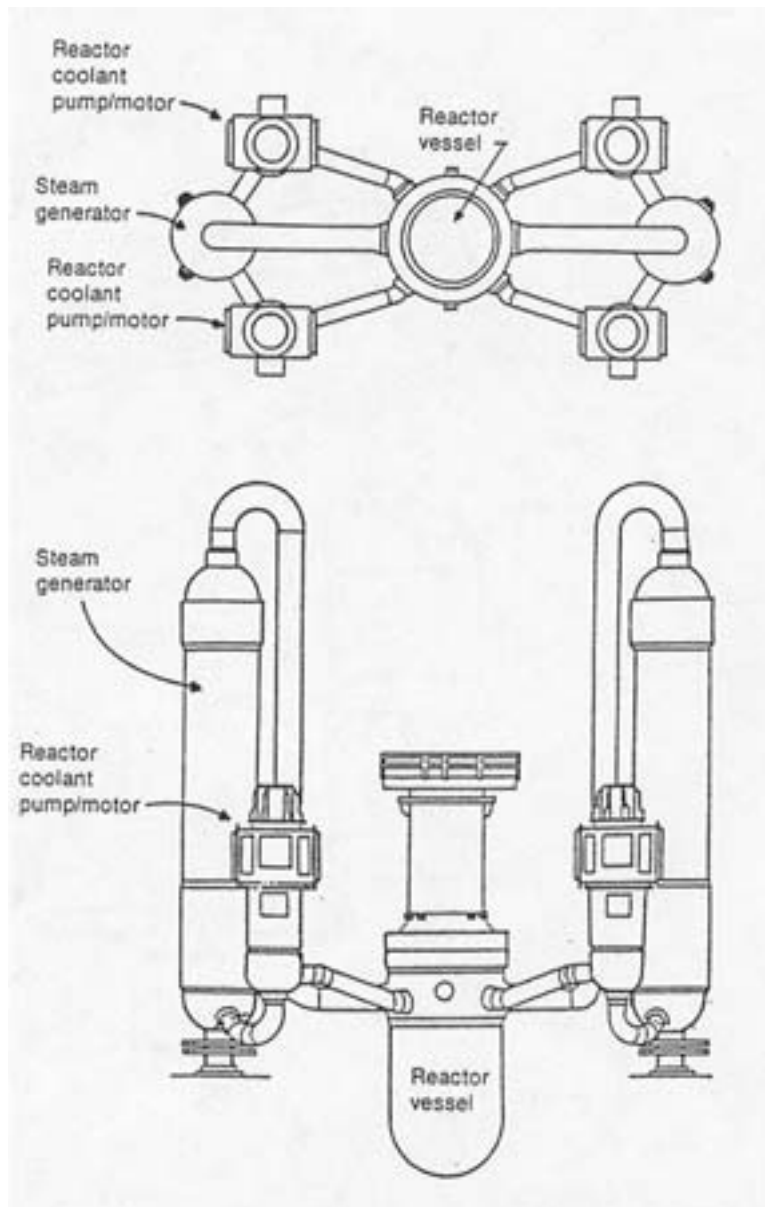


FIG. 2-1. Schematic of a Babcock and Wilcox PWR reactor coolant system.

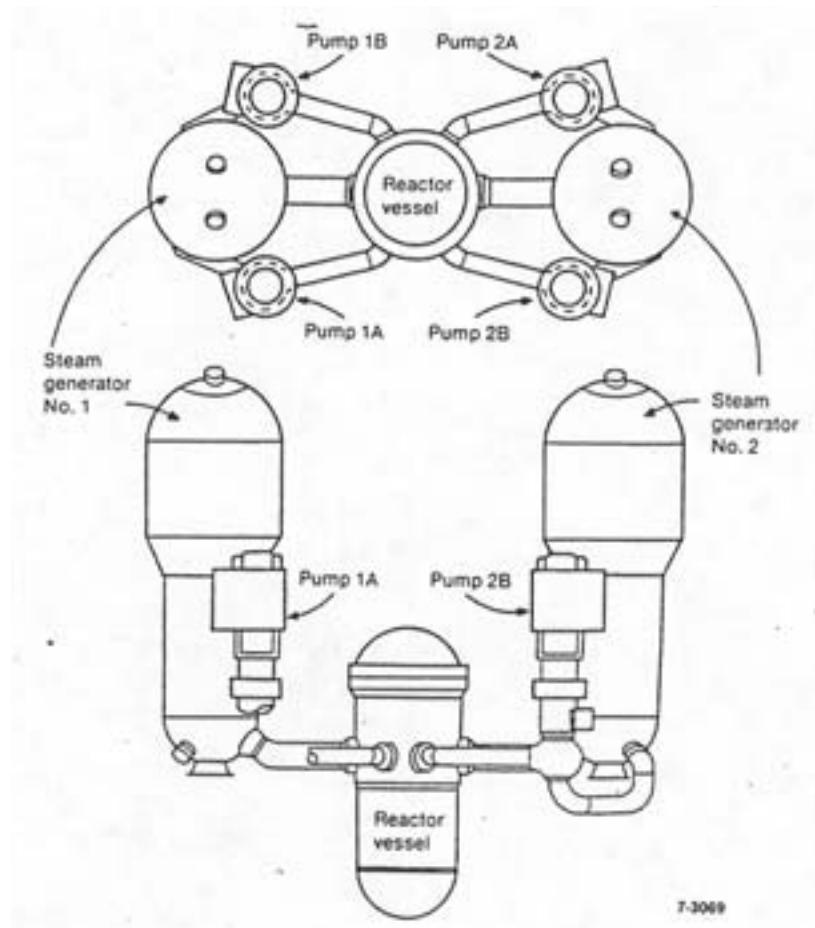


FIG. 2-2. Schematic of a combustion engineering PWR reactor coolant system.

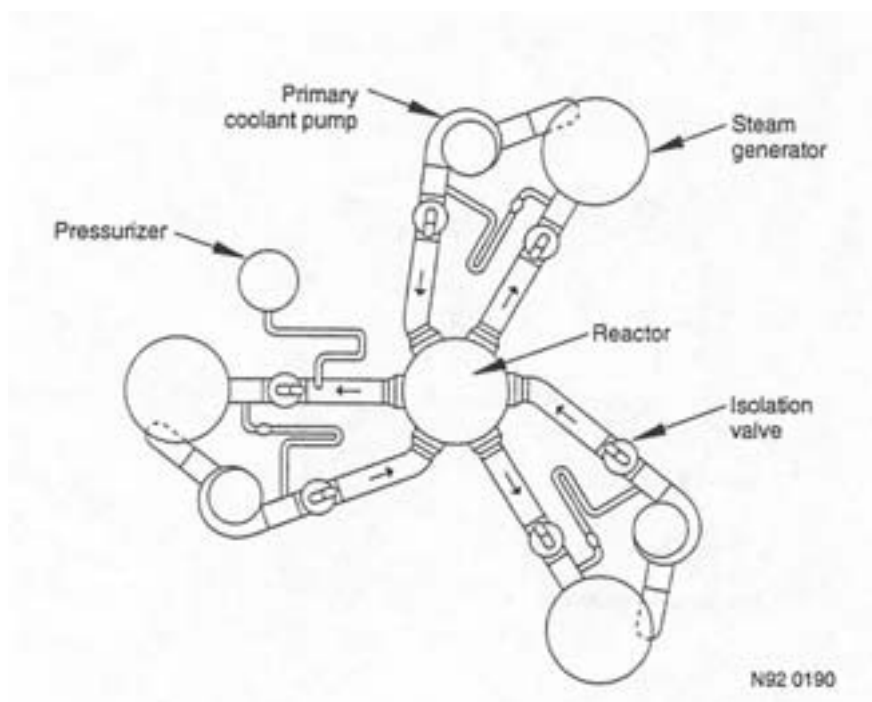


FIG. 2-3. Plan view of a combustion engineering three-loop reactor coolant system with an isolation valve.

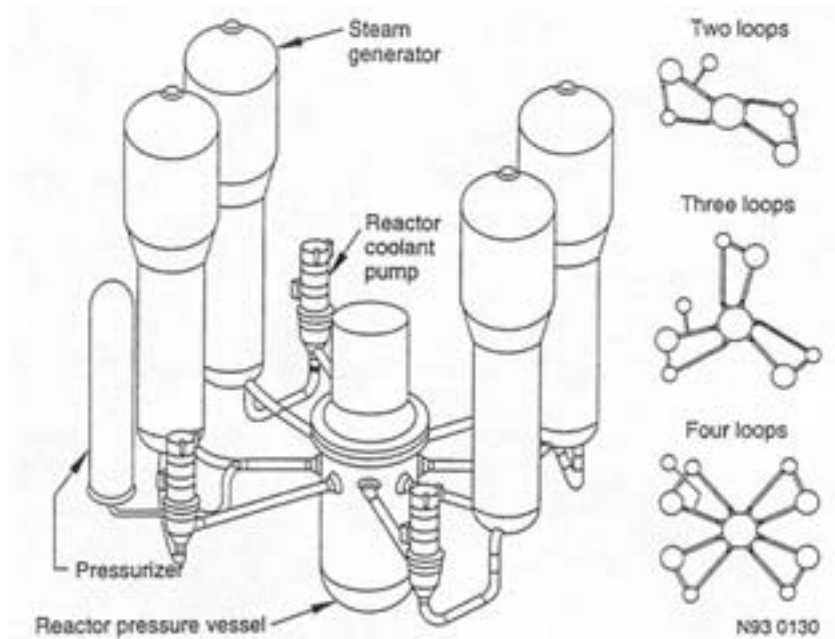


FIG. 2-4. Schematic of a Westinghouse PWR reactor coolant system.

The design of the Westinghouse main coolant loop is conceptually different from the Babcock & Wilcox and most Combustion Engineering designs in that each exchange loop has only one reactor coolant pump. Each loop has a hot leg from the reactor to the recirculating steam generator, a crossover leg from the steam generator to the pump, and a cold leg from the pump to the reactor. Some plants of the Westinghouse design also have two isolation valves on each loop, one on hot leg and one on cold leg.

Typical pipe inside diameters and thicknesses for a Babcock & Wilcox, Combustion Engineering, and a four-loop Westinghouse plant are given in Table I. The materials for main coolant piping are discussed in Section 2.6.

2.1.2. Surge and spray line design and materials

Figure 2-5 is a schematic of a portion of a typical Combustion Engineering reactor coolant system, which includes the pressurizer, surge line, main and auxiliary spray lines, and charging lines. Pressure, temperature, and level sensing locations; valves; and bypass lines are also shown in this figure. The surge line connects the bottom, liquid-filled region of the pressurizer to one of the hot legs. The spray line connects the upper, steam-filled region of the pressurizer to the main and auxiliary spray valves, which in turn are connected to various cold legs. The auxiliary spray valve is connected to the charging pumps via the charging line, which permits pressurizer spray during such plant conditions as heat-up and cooldown when one or more reactor coolant pumps are not operating and main spray is, therefore, not available.

TABLE I. TYPICAL DIMENSIONS OF PWR PRIMARY COOLANT PIPING. ALL DIMENSIONS ARE IN INCHES (1 IN. = 25.4 MM)

Piping	Babcock & Wilcox		Combustion Engineering		Westinghouse (four-loop plant)	
	Inside diameter	Thickness	Inside diameter	Thickness	Inside diameter	Thickness
Hot leg	36	3.75	42	3.74 to 4.125	29	2.33 to 2.5
Cold leg	28	2.50	30	2.50 to 3.156	27.5	2.21 to 2.56
Crossover leg					31	2.48 to 2.88

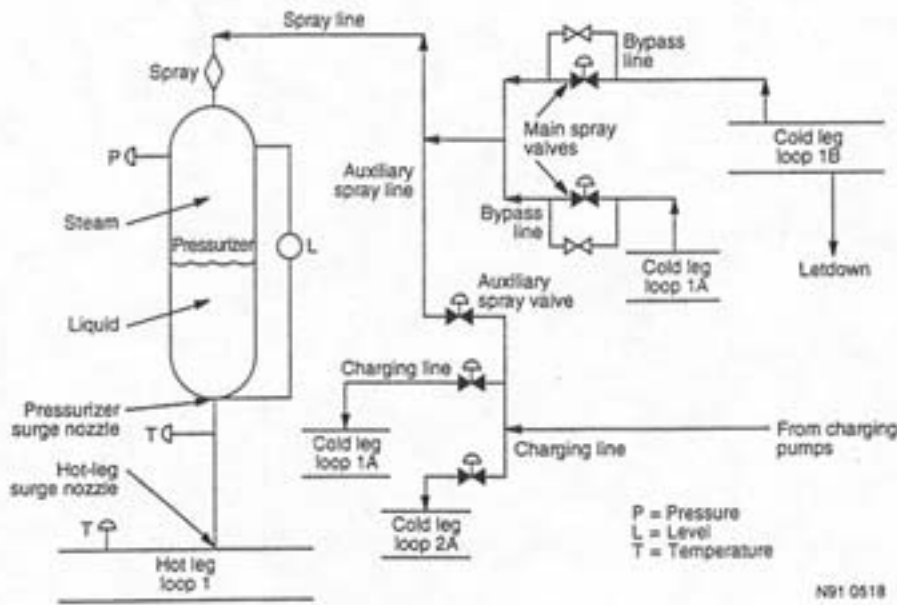


FIG. 2-5. Typical combustion engineering pressurizer spray and surge line systems.

The pressurizer controls the reactor coolant system pressure by maintaining the temperature of the pressurizer liquid at the saturation temperature corresponding to the desired system pressure. Pressurizer temperature is controlled and maintained by internal heaters and the spray systems. The heaters supply energy to heat the pressurizer liquid to the required temperature and to offset heat losses to the containment atmosphere. The spray system acts to reduce pressurizer pressure, should it increase during a transient, by injecting cold leg water into the steam space.

When the demand for steam from a NPP is increased, the average reactor coolant temperature is raised in accordance with a coolant temperature programme. Figure 2-6 illustrates a typical temperature control programme for Combustion Engineering plants with recirculating steam generators. The normal operating pressurizer temperature at full power, for example, is 343°C (650°F), with the cold and hot leg temperatures being about 285°C (545°F) and 316°C (600°F), respectively. Westinghouse plants have a similar temperature control programme. At any given steam generator power output, T_{cold} is the primary fluid inlet temperature into the reactor vessel, which is kept constant as the power level changes, T_{hot} is the outlet temperature, and T_{avg} is the average temperature in the reactor core. In contrast, the

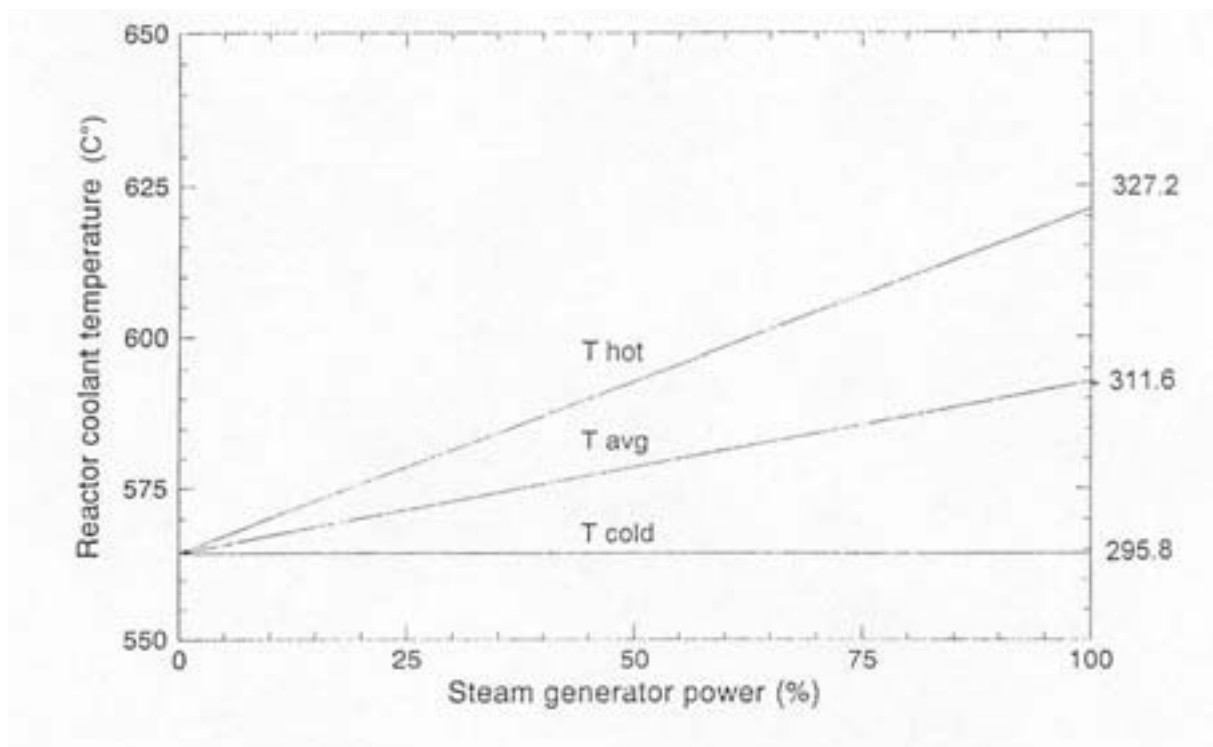


FIG. 2-6. Typical combustion engineering temperature control program.

average temperature in the reactor core, rather than the cold leg temperature, is kept constant at all power levels in the Babcock & Wilcox plants, except at less than 20% power. When core power is increased, the expanding coolant from the hot leg enters the bottom of the pressurizer through the surge line, compressing the steam and raising the system pressure. This increase in pressure is moderated by the condensation of the steam in the pressurizer during compression and by the decrease in average liquid temperature in the pressurizer resulting from the insurge of cooler surge line water. The water temperature in the surge line may be slightly lower than the hot leg temperature during some flow conditions because of the heat loss to the containment building. When the transient pressure reaches an upper limit, the pressurizer spray valves open, spraying coolant from the reactor coolant pump discharge (cold leg) into the pressurizer steam space. The relatively cold spray water condenses more of the steam and, therefore, limits the system pressure increase. When the core power and steam demand is decreased, the pressurizer heaters are used to keep the primary coolant system pressure constant.

Surge Lines. Figures 2-7, 2-8, and 2-9 show the layout of a typical pressurizer surge line in a Combustion Engineering, Babcock & Wilcox, and Westinghouse plant, respectively. The surge lines in US PWRs range in diameter from about 250 to 400 mm (10 to 16 in.) and are generally made of Schedule 140 or 160 pipe. The surge lines generally begin in a short vertical run out of the pressurizer, then travel in a horizontal or near horizontal plane for most of their length, and finally terminate in a surge nozzle, which is located on one of the hot legs. For example, in one plant the horizontal portion is about 91% of the 21m (70 ft) long surge line. The surge lines were designed with the assumption that coolant surges would sweep the full cross section of the piping.

The surge lines are generally fabricated from Type 316 stainless steel except in some Combustion Engineering plants where they are fabricated from Grade CF-8M cast stainless steel. In Combustion Engineering and Babcock & Wilcox plants, the weld between the surge line and the hot-leg surge nozzle is a dissimilar metal weld because the hot-leg is made of

carbon steel; a stainless-steel safe end is used between the hot-leg surge nozzle and surge line. A dissimilar metal weld is not needed in a Westinghouse plant because the hot leg is made of stainless steel. A sketch of a Combustion Engineering hot-leg surge nozzle is shown in Figure 2-10. Thermal sleeves are installed inside both pressurizer and hot-leg surge nozzles to protect the nozzle wall from thermal transients, which could develop high thermal stresses. However, thermal sleeves have failed in some plants, and these plants have been allowed to operate without sleeves. The thermal sleeves are typically made of Alloy 600 or Type 304 stainless steel. A typical sleeve is fitted in the nozzle with an interference fit.

Spray Lines. As mentioned, the cold legs supply the coolant to the pressurizer spray nozzle via main spray piping. Automatic main and auxiliary spray valves control the amount of spray as a function of pressurizer pressure. Components of the pressurizer main spray system are sized to use the differential pressure between the reactor coolant pump discharge and the pressurizer to pass the amount of spray required to maintain the pressurizer steam pressure during normal operational transients. Since the main spray valves are generally closed, a small, continuous flow, referred to as the bypass flow, is also maintained through the spray line when all reactor coolant pumps are running. The flow bypasses the main spray valves as indicated in Figure 2-5, and serves to keep the spray piping and nozzle at a constant temperature in order to reduce the severity of thermal transients during main spray usage. The bypass flow also serves to keep the chemistry and boric acid concentration of the pressurizer water the same as that of the reactor coolant loops. The auxiliary spray line is connected to the charging line.

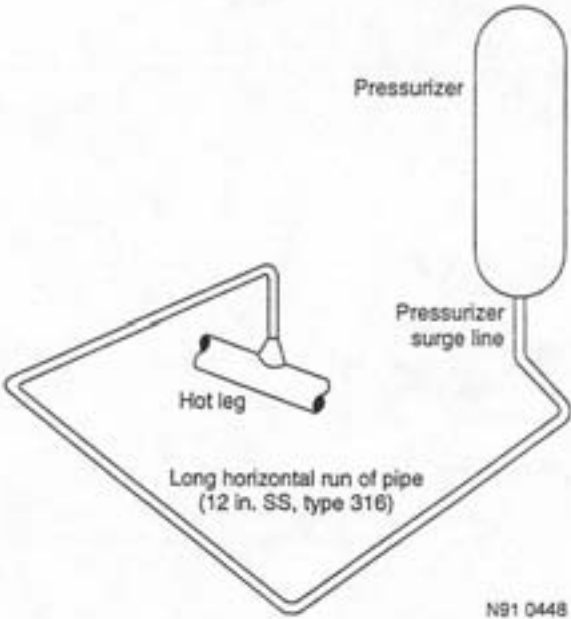


FIG. 2-7. Typical combustion engineering pressurizer surge line layout.

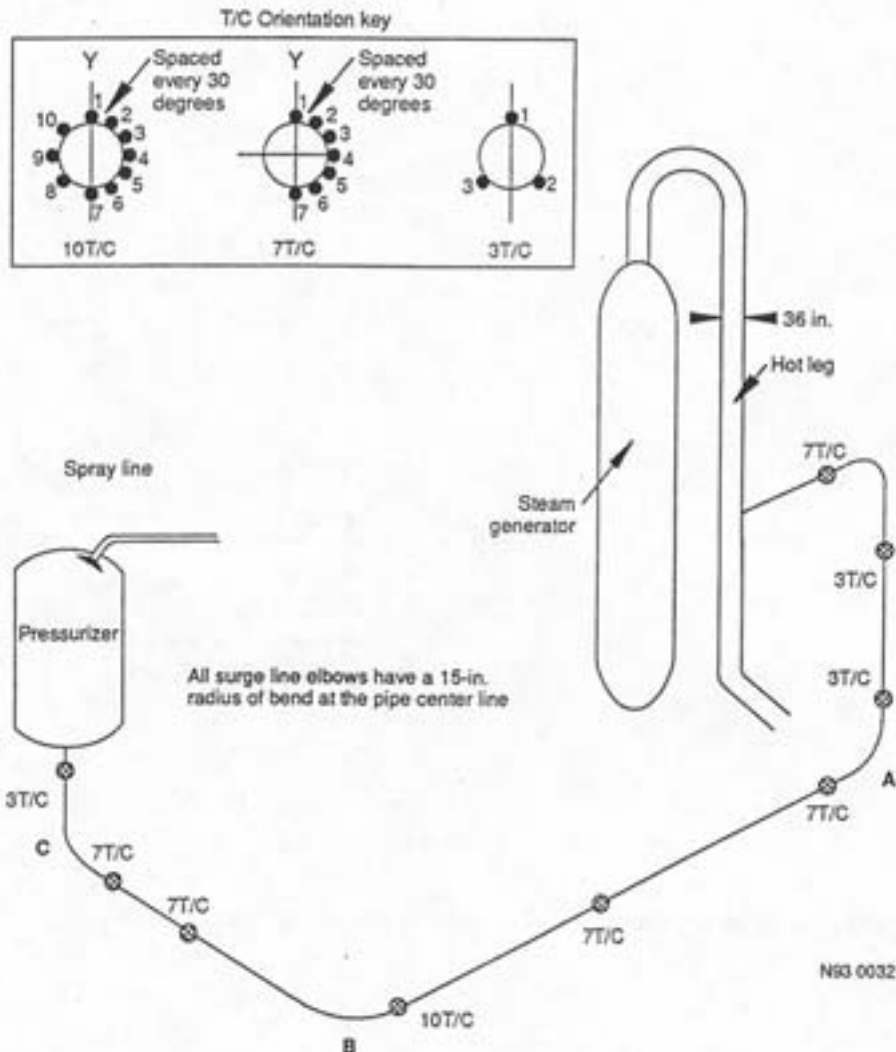


FIG. 2-8. Typical Babcock & Wilcox pressurizer surge line layout. Locations of thermocouples for monitoring outside-surface temperatures are shown.

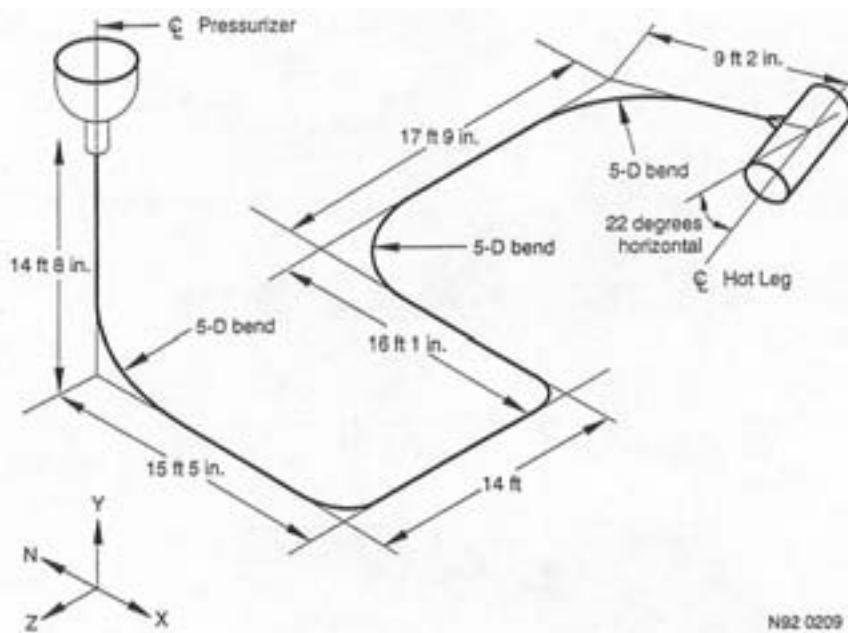


FIG. 2-9. Examples of a Westinghouse pressurizer surge line layout.

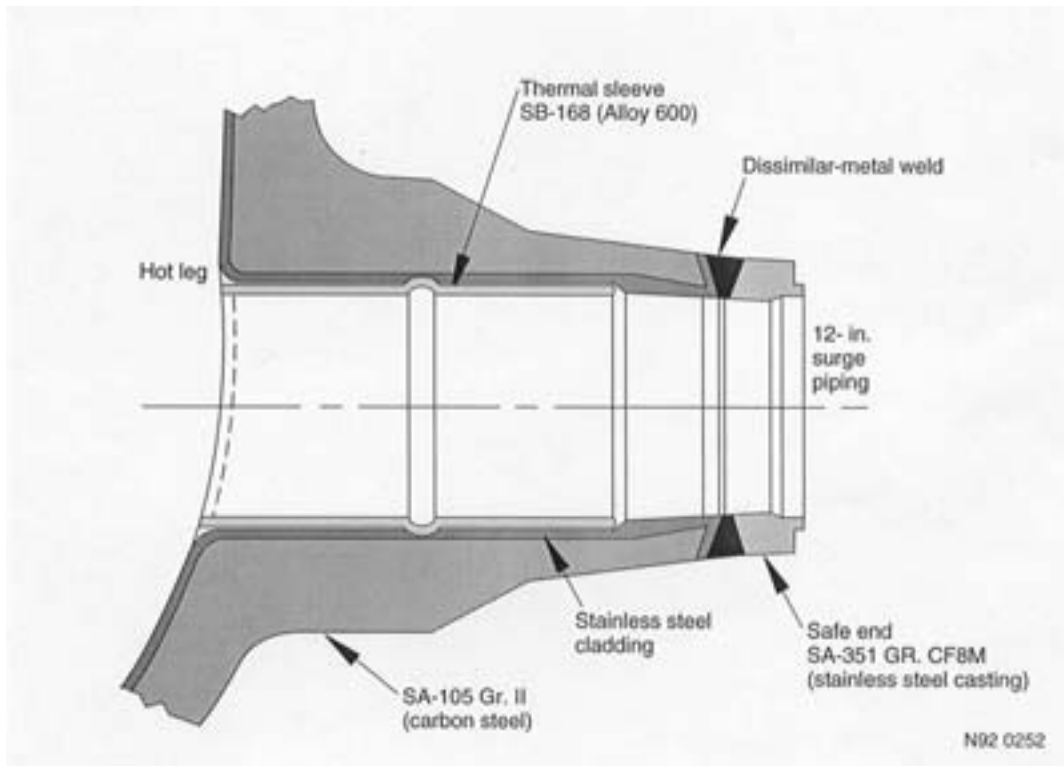


FIG. 2-10. Typical combustion engineering surge nozzle at the hot leg (12 in. schedule 160).

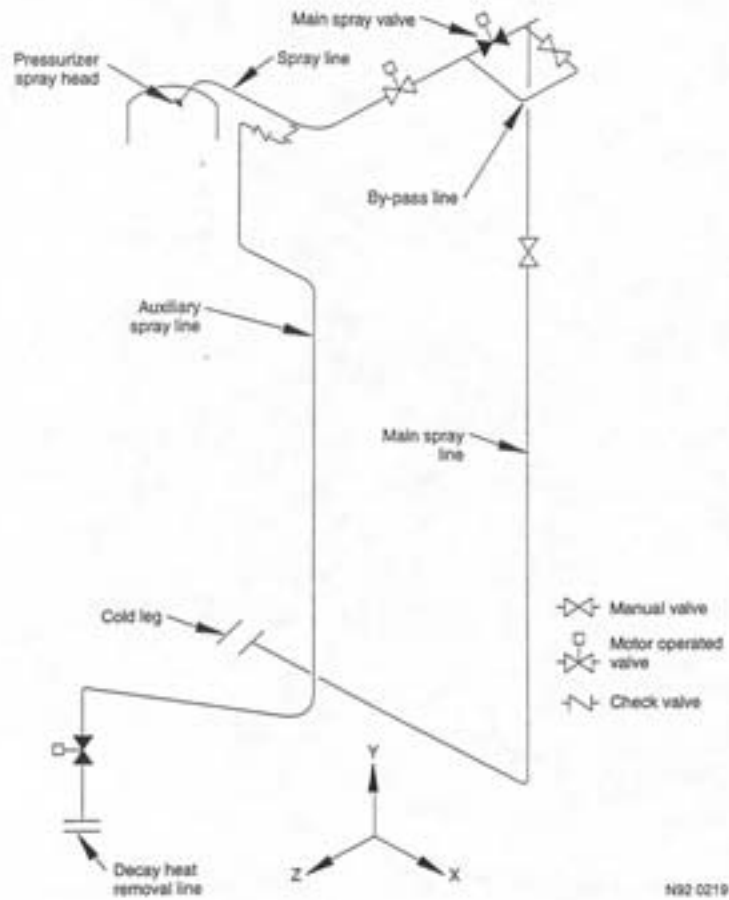


FIG. 2-11. Typical Babcock & Wilcox pressurizer spray line layout.

The typical Babcock & Wilcox spray line layout is shown in Figure 2-11. The main spray line connects to one of the cold legs (near the bottom of Figure 2-11). From there the main spray line travels a certain distance horizontally (back left to front right in the figure), runs vertically up to the pressurizer spray nozzle elevation, and then runs horizontally to the pressurizer. The coolant enters the pressurizer through a spray nozzle on the top head, which connects to a spray head. A short portion of the spray line inside the top head of the pressurizer is bent in a V-shape (not shown), which, being filled with liquid coolant, prevents steam entering the spray line and thus aids in mitigating thermal stratification loads on the spray line. One end of the auxiliary spray line is connected to the auxiliary spray nozzle on the main spray line, the other end is connected either to the decay heat removal system, which is a low-pressure system, or to the charging line, which is a high-pressure system. The main and auxiliary spray lines are, respectively, either 63-mm and 28-mm (2.5 and 1.125 in.) diameter or 100-mm and 50-mm (4 and 2 in.) in diameter, Schedule 160, stainless steel pipes (wall thickness equal to 0.531 and 0.344 in., respectively, for 4- and 2-in. diameter pipe). The length of the horizontal portion of the main spray line near the spray nozzle is about 5 m (16 ft).

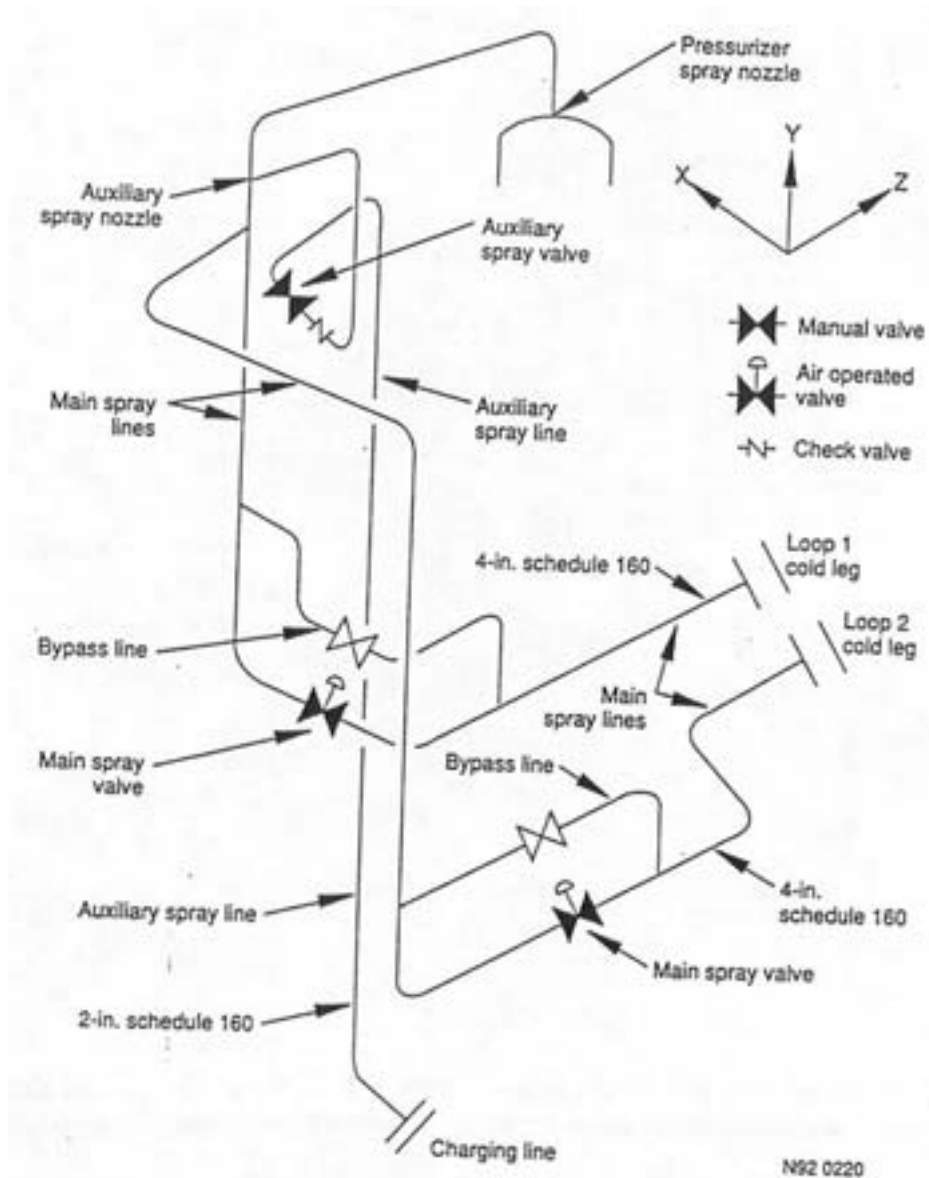


FIG. 2-12. Typical Westinghouse pressurizer spray line layout.

The layout of a typical Westinghouse spray line is shown in Figure 2-12. One end of the main spray line connects to two cold legs, and the other end connects to the pressurizer spray nozzle. One end of the auxiliary spray line connects to the auxiliary spray nozzle on the main spray line, the other end connects to the charging line. The overall layout of the Combustion Engineering spray line is similar to that of the Westinghouse spray line except that there is a T-connection between the auxiliary and main spray lines. In some Combustion Engineering plants, the horizontal portion of the spray line outside the pressurizer and adjacent to the spray nozzle has been modified by incorporating a *goose neck*, also called loop seal, to mitigate thermal stratification loads on the spray line [2.1]. The main and auxiliary spray lines in Westinghouse plants are, respectively, with a diameter of 100 mm and 50 mm (4 and 2 in.), Schedule 160, stainless steel pipes. The length of the horizontal portion near the spray nozzle elevation is generally about 3.1 to 4.6 m (10 to 15 ft) long.

The weld between the carbon steel (or low-alloy pressure vessel steel) spray nozzle and the austenitic stainless steel safe end is a dissimilar metal weld in all three USA reactor vendor designs. A typical Combustion Engineering spray nozzle is shown in Figure 2-13. A thermal sleeve is installed inside the pressurizer spray nozzle.

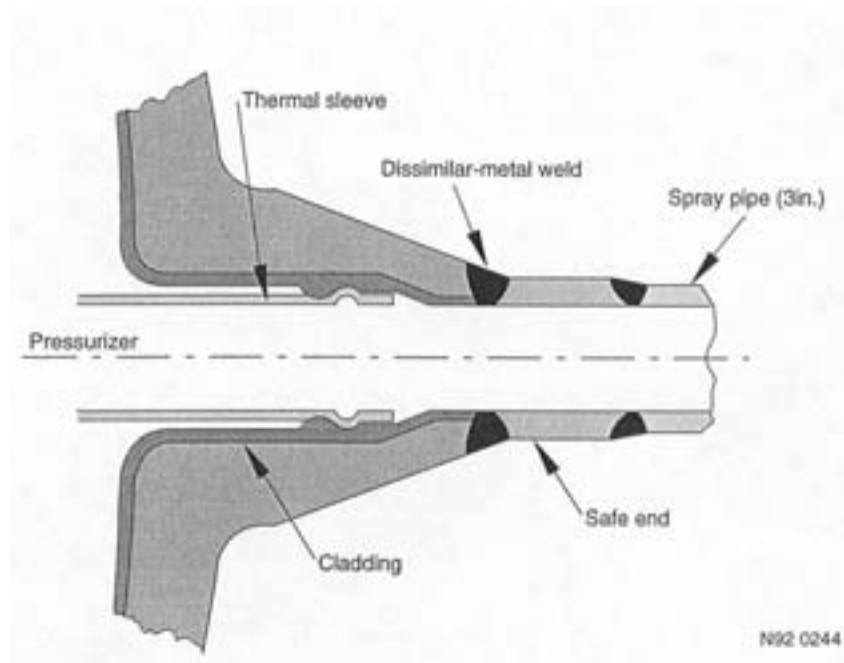


FIG. 2-13. Typical combustion engineering spray nozzle (3 in. Schedule 160).

2.1.3. Charging system design and materials

The charging and letdown functions of the chemical and volume control system maintain a programmed water level in the pressurizer, maintain a proper concentration of boric acid and corrosion inhibiting chemicals in the reactor coolant, and provide the required flow to the reactor coolant pump shaft seals. A proper inventory of the reactor coolant is maintained during all different modes of plant operation by a continuous make-up and letdown process wherein the pressurizer water level automatically controls the feed rate.

A typical Combustion Engineering letdown and charging system is shown in Figure 2-14. Coolant from the cold leg of the reactor coolant system passes through the tube

side of a regenerative heat exchanger for an initial temperature reduction. The cooled fluid is then reduced to the operating pressure of the letdown heat exchanger by the letdown control valves. The flow is then reduced to the operating temperature and pressure of the purification system by the letdown heat exchanger and letdown backpressure valve. Finally, the flow passes through a purification filter, one of the three ion exchangers, and a strainer (not shown in Figure 2-14) and is then sprayed into the volume control tank.

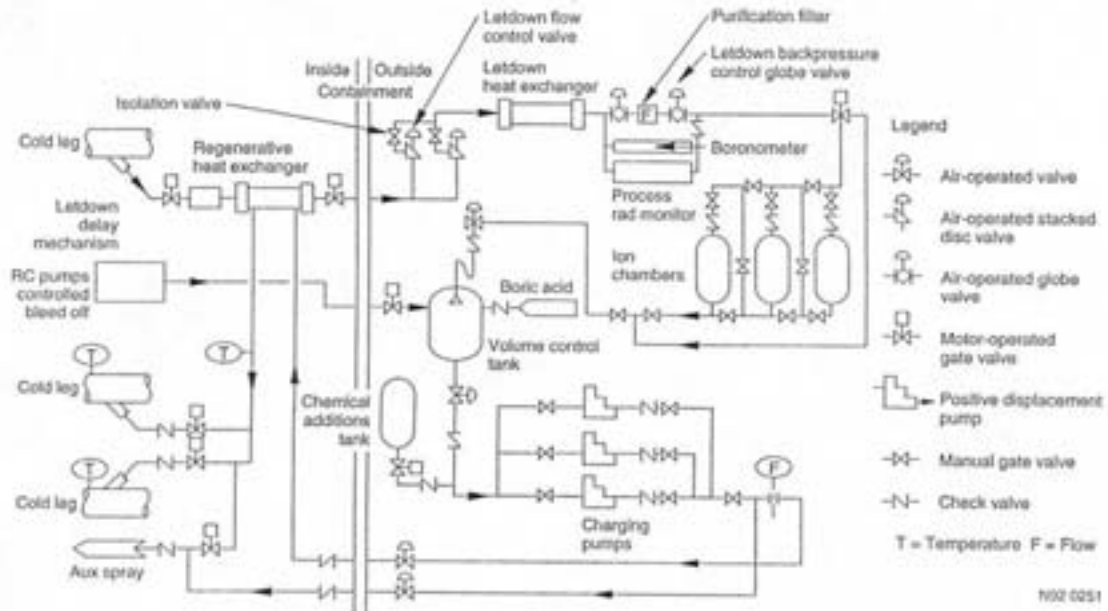


FIG. 2-14. Schematic diagram of a typical combustion engineering letdown and charging system.

The charging pumps draw from the volume control tank and pump the coolant (sometimes called makeup water) to the reactor coolant system. During normal operation, charging flow is equal to letdown flow plus reactor coolant pump bleedoff flow and other system leakage. The charging flow passes through the shell side of the regenerative heat exchanger for recovery of heat from the letdown flow before returning to the reactor coolant system cold leg via the charging nozzles. The charging fluid is always cooler than the reactor coolant in the cold leg. The Babcock & Wilcox design does not use a regenerative heat exchanger in the make-up coolant circuit [2.2], and uses one nozzle per cold leg for both charging and safety injection. The Westinghouse design uses a regenerative heat exchanger in the make-up coolant circuit, and uses one or two nozzles per cold leg for charging and safety injection.

The charging inlet nozzles are generally 50-mm (2-in.) nozzles with thin, Type 304 stainless steel or Alloy 600 thermal sleeves that protect the nozzles from thermal shocks. Combustion Engineering and Babcock & Wilcox plants in the United States use low-alloy steel nozzles with a dissimilar metal weld to the stainless steel charging line. Westinghouse plants use stainless steel nozzles and stainless steel connecting piping. A typical Combustion Engineering charging nozzle is shown in Figure 2-15. The charging nozzles are part of the reactor coolant pressure boundary and their structural integrity is therefore required for continued plant operation.

2.1.4. Safety injection system design and materials

The safety injection system is designed to provide core cooling in the unlikely event of a loss of coolant accident (LOCA). The cooling is intended to prevent excessive core heat-

up, significant cladding-water reactions, fuel melting, or significant alteration of the core geometry. The safety injection system is also designed to remove the core fission product decay heat for an extended period of time following a LOCA. The safety injection system fluid contains sufficient neutron absorber (borated water) to maintain the core subcritical following a LOCA. In addition, the safety injection system can be used to inject borated water into the reactor coolant system to prevent fuel damage and to increase the shutdown margin of the core in the unlikely event of a steam line rupture. The system is actuated automatically upon a low-pressure signal. Typical Combustion Engineering high pressure safety injection systems operate at about 12.5 MPa (1800 psig) and 50°C (120°F).

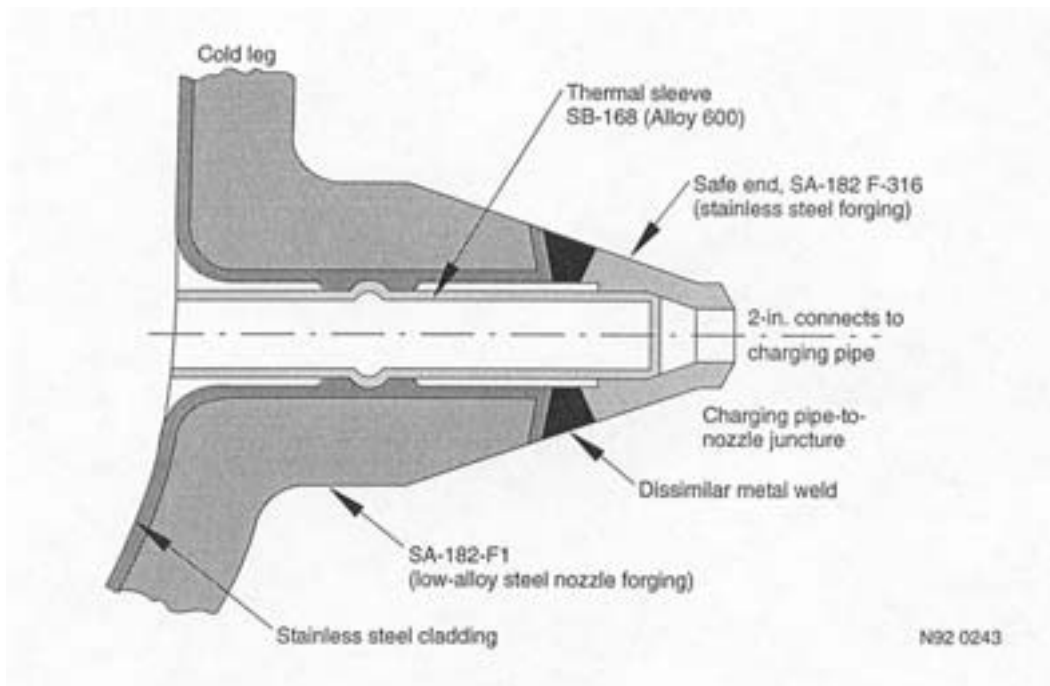


FIG. 2-15. Typical combustion engineering charging nozzle (2-in. Schedule 160).

A typical Combustion Engineering safety injection system is shown in Figure 2-16. It consists of two high-pressure and two low-pressure safety injection pumps and four safety injection tanks (only one of each is shown). Automatic operation of the pumps is actuated by either a low pressurizer pressure signal or a high containment pressure signal. If the leak in the reactor coolant system is small enough so that one charging pump can maintain the reactor coolant pressure, the safety injection flow is not initiated. However, the safety injection flow is initiated when the cold-leg pressure drops below the pump shut-off heads or the safety injection tank pressure.

The high-pressure safety injection system is designed to supply water for reactor core cooling for breaks of all sizes, including a double-ended break of the largest size piping in the reactor coolant system. The Combustion Engineering high-pressure safety injection pumps are actuated when the reactor coolant pressure drops below about 12.5 MPa (1800 psig). The pumps draw from the refueling water tank or from the containment sump when the water level in the refueling water tank is low, and discharge into the reactor coolant system through the nozzles located in the cold legs. (Some PWR plants have additional safety injection nozzles in the hot legs.) The minimum temperature specification for the refueling water tank water, which is borated, is 5°C (40°F) to prevent boron precipitation.

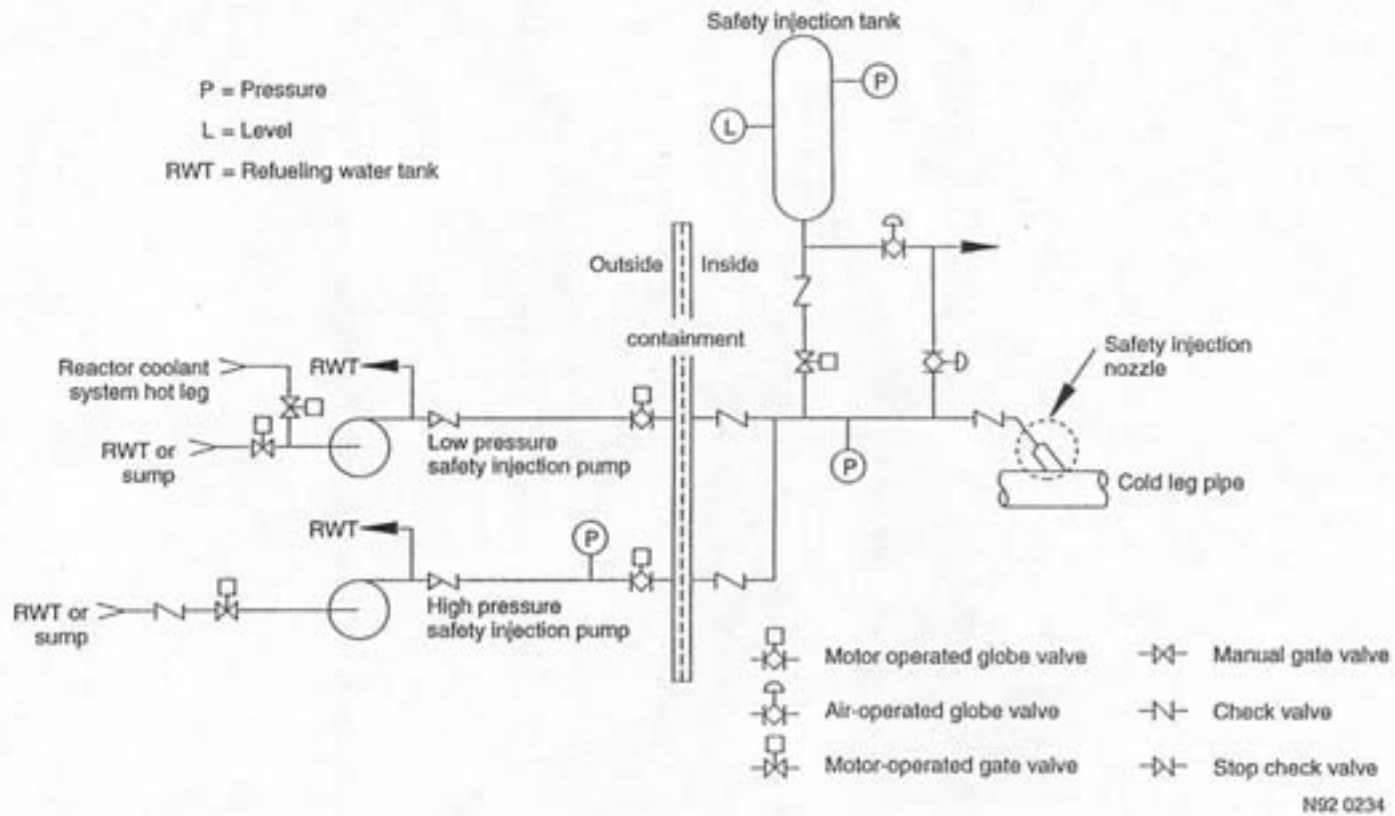


FIG. 2-16. Typical combustion engineering safety injection system (simplified).

The low-pressure safety injection system is designed to supply a high volume of low-pressure water to complete the reflooding of the core following a large LOCA. The Combustion Engineering low-pressure safety injection pumps are actuated when the reactor coolant pressure drops below about 1.4 MPa (200 psig). These pumps also draw from the refueling water tank or the containment sump and discharge into the reactor coolant system. In addition to the safety functions, this system is designed to provide a second phase of cooldown, called shutdown cooling. During the shutdown cooling mode, the low-pressure safety injection pumps take water from the reactor coolant system, pass it through the shutdown cooling heat exchangers, and return it to the reactor coolant system through the safety injection nozzles.

The function of the safety injection tanks is to supply sufficient coolant to completely cover the core following a large break LOCA. The tanks are passive components that do not require any actuation signal. They contain borated water (³2000 ppm boron) pressurized to about 4.2 MPa (600 psig). This water is discharged into the cold legs through the safety injection nozzles when the reactor coolant pressure drops below about 4.2 MPa (600 psig) during the accident. The discharge lines from the safety injection tanks are equipped with valves to isolate the tanks when the reactor coolant system is depressurized.

Some PWR plants have dual-purpose pumps used for both adding coolant during normal reactor operation and injecting emergency core coolant at high pressure following an accident. A schematic diagram of the high-pressure safety injection and residual heat removal systems in a three-loop Westinghouse plant with dual-purpose pumps is shown in Figure 2-17 [2.3]. The charging pumps supply the coolant to the safety injection system. All valves in the safety injection system are closed during normal operation. The globe valve A, which has leaked in one US and one non-US plant, is in a bypass line around the boron injection tank. The safety injection and residual heat removal systems are connected to the reactor coolant system through the same nozzles, located one on each of the three cold legs. The charging system (not shown in Figure 2-17) is connected to the cold leg through a different nozzle. Accumulator tanks, also not shown in Figure 2-17, serve a function similar to that of the safety injection tanks but are connected to the primary system cold legs through separate nozzles.

The safety injection nozzles are generally 150 to 300 mm (6 to 12 in.) nozzles with thin, Type 304 stainless steel or Alloy 600 thermal sleeves that protect the nozzles from thermal shock. Each sleeve is held in place with an interference fit or attachment welds. The safety injection nozzles in Combustion Engineering and Babcock & Wilcox plants are low-alloy steel nozzles clad with stainless steel, similar, except in size, to the charging nozzles. The welds between the nozzles and the stainless steel safety injection lines are dissimilar metal welds. Westinghouse plants have stainless steel nozzles welded to stainless steel safety injection lines. A typical Combustion Engineering safety injection nozzle is shown in Figure 2-18. The safety injection nozzles are also part of the reactor coolant pressure boundary and their structural integrity is required for continued plant operation.

2.1.5. Design and materials of residual heat removal system

The residual heat removal system is designed to remove the decay heat from the core and reduce the temperature of the reactor coolant system during the second phase of cooldown. (The first phase of cooldown is accomplished by the auxiliary feedwater system and the steam generators.) In addition, the residual heat removal system is designed to transfer

refueling water between the refueling water storage tank and the refueling cavity before and after refueling. The residual heat removal system is also designed to provide low pressure injection for core cooling following a LOCA.

A typical residual heat removal system for a four-loop Westinghouse plant is shown in Figure 2-19. The system consists of two heat exchangers, two residual heat removal pumps, and the associated piping, valves, and instrumentation necessary for operational control. The inlet lines to the residual heat removal system for the second phase of cooldown are connected to the hot legs of reactor coolant Loos 1 and 4, whereas the return lines are connected to each cold leg of the reactor coolant system. These return lines also provide low pressure injection for core cooling during LOCA.

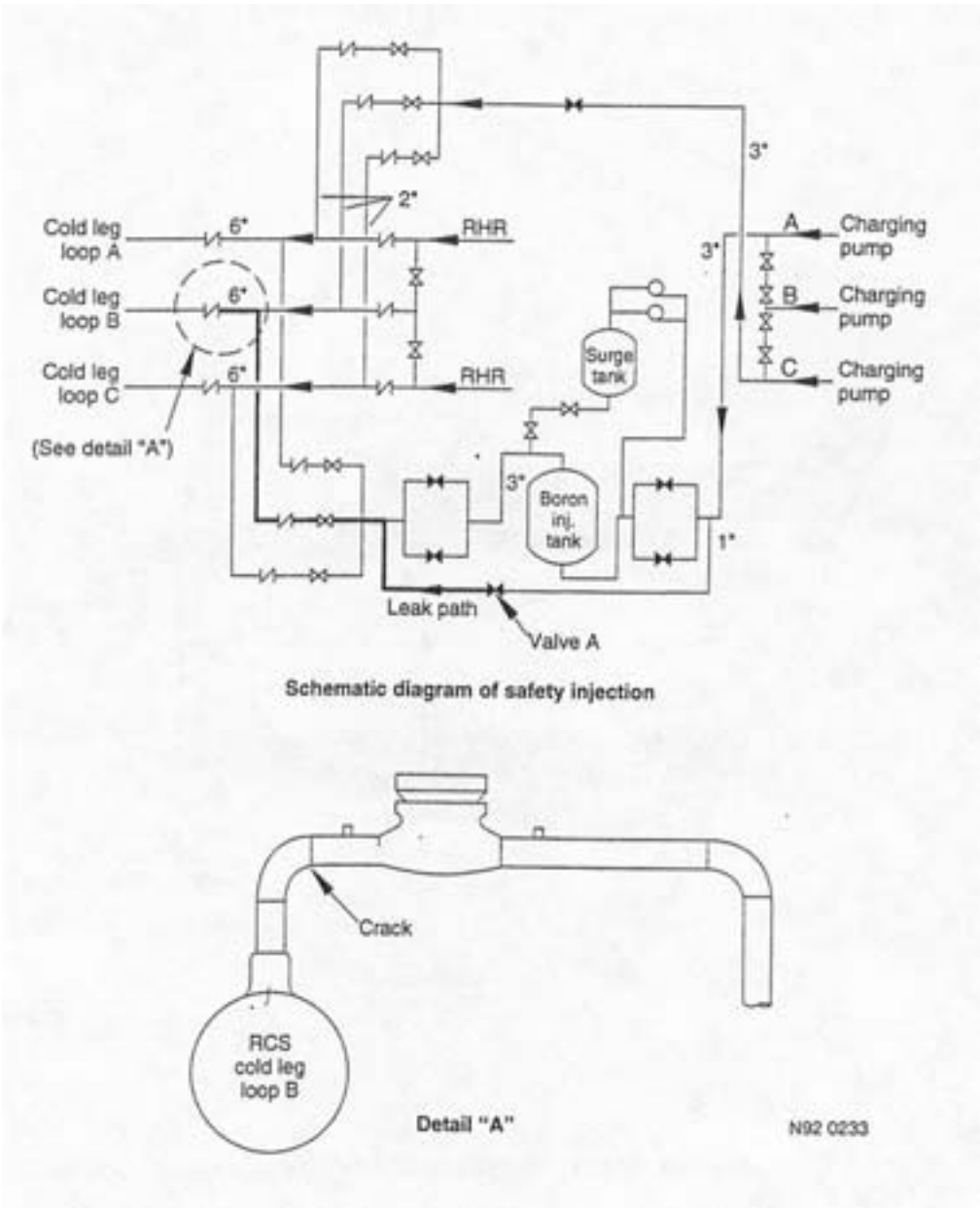


FIG. 2-17. Schematic diagram of a safety injection and residual heat removal system in a three-loop Westinghouse plant.

Each residual heat removal pump suction line from the reactor coolant system is normally isolated by two motor-operated valves (8701 A,B and 8702 A,B) located inside the containment. Each residual heat removal pump discharge line is isolated from the reactor coolant system by two check valves located inside the containment and by two normally open motor-operated valves (8809 A&B) located outside the containment. During the second phase cooldown, reactor coolant flows from the reactor coolant system to the residual heat removal pumps, through the tube side of the residual heat removal heat exchangers, and back to the reactor coolant system. The heat from the reactor coolant is transferred to the component cooling water which is circulating through the shell side of the heat exchangers.

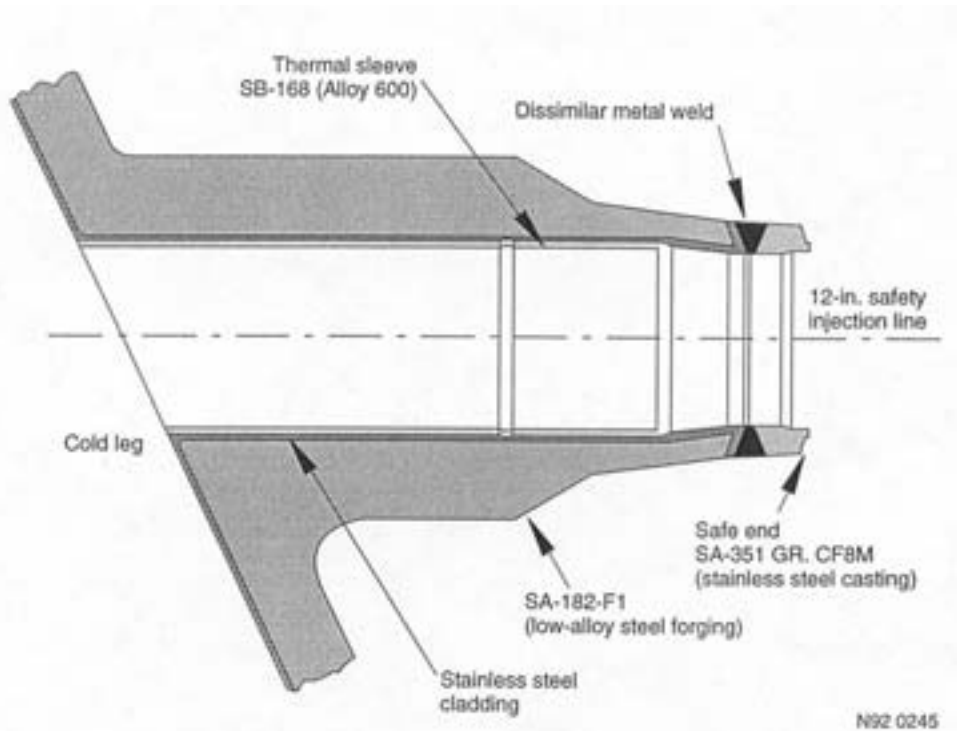


FIG. 2-18. Typical combustion engineering safety injection nozzle (12-in. Schedule 160).

The residual heat removal system is designed to reduce the temperature of the reactor coolant from 177°C to 60°C (350°F to 140°F) in 16 hours during the second phase cooldown. The heat load handled by the residual heat removal system during the cooldown includes residual and decay heat from the core, and reactor coolant pump heat. The reactor coolant system cooldown rate is limited by component cooldown rates based on allowable stress limits.

The residual heat removal system is designed to transfer the heat associated with the shutdown plant until the plant is restarted. During the shutdown, if solid plant operations are desired, the residual heat removal system is used in conjunction with the chemical and volume control system (see Section 2.1.4) for solid plant pressure control; this function is not presented in Figure 2-19.

The materials used to fabricate the residual heat removal system components are in accordance with the applicable ASME code requirements. All components in contact with boric acid coolant are fabricated of, or clad with austenitic stainless steel or an equivalent corrosion resistant material. Typical material for the residual heat removal system piping is Type 304 stainless steel.

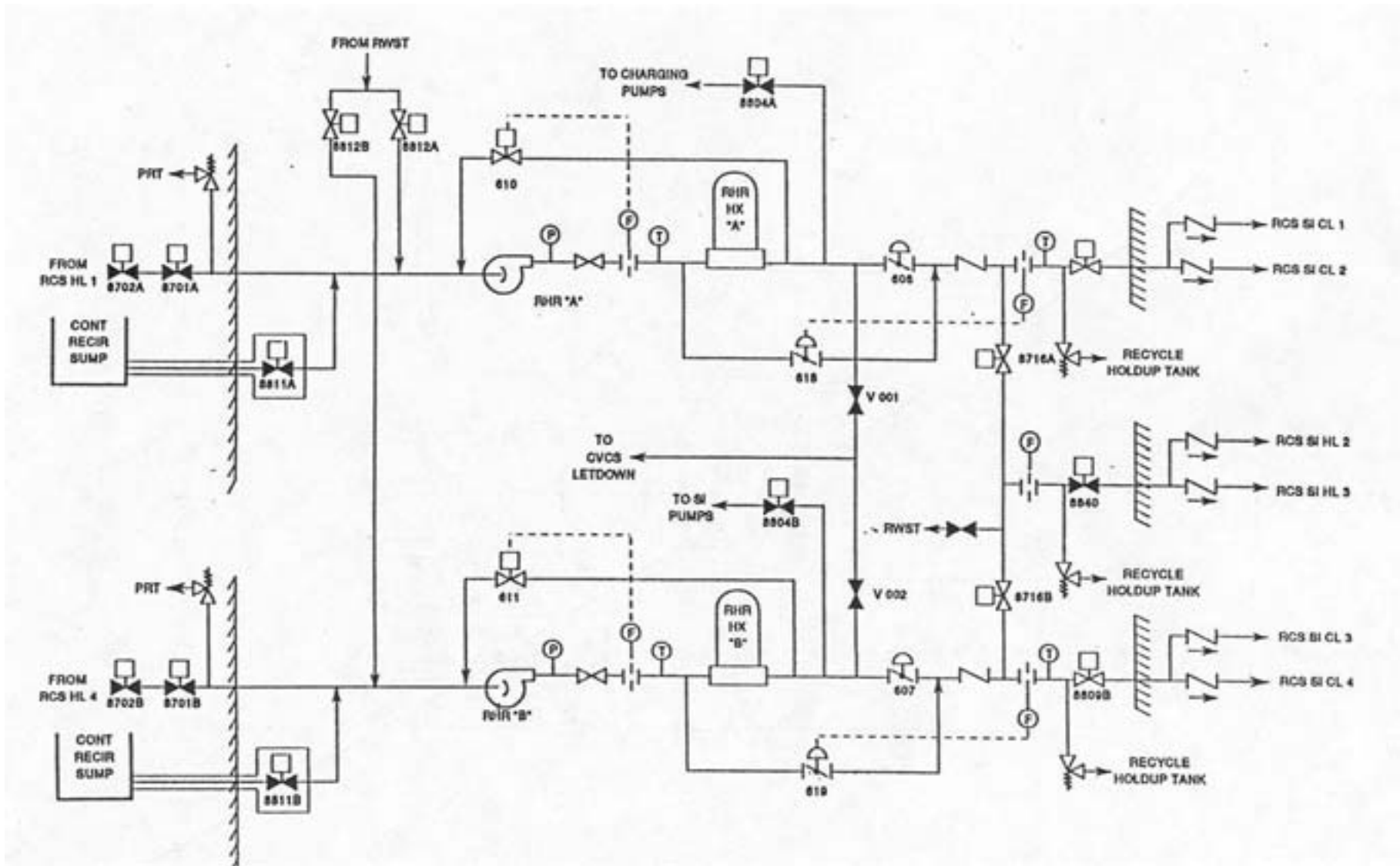


FIG. 2-19. Schematic diagram of a residual heat removal system in a Westinghouse-type PWR.

2.2. French design

The designer of French PWRs is Framatome. These plants are similar as those designed by Westinghouse in all essential respects except for the following major design changes:

- cast elbows instead of two shell elbows
- use of centrifugated and forged stainless steel piping for main coolant lines
- design modifications of connected line nozzles and thermal sleeve attachments (replacement of crack like defect at the attachment weld level by an integrated thermal sleeve)
- one piece cold leg (without any weld and integration of nozzle) for the last 4-loop plants

A typical French PWR reactor coolant loop is shown in Figure 2-20. Typical main coolant pipe inside diameters and thickness for a French plant are given in Table II.

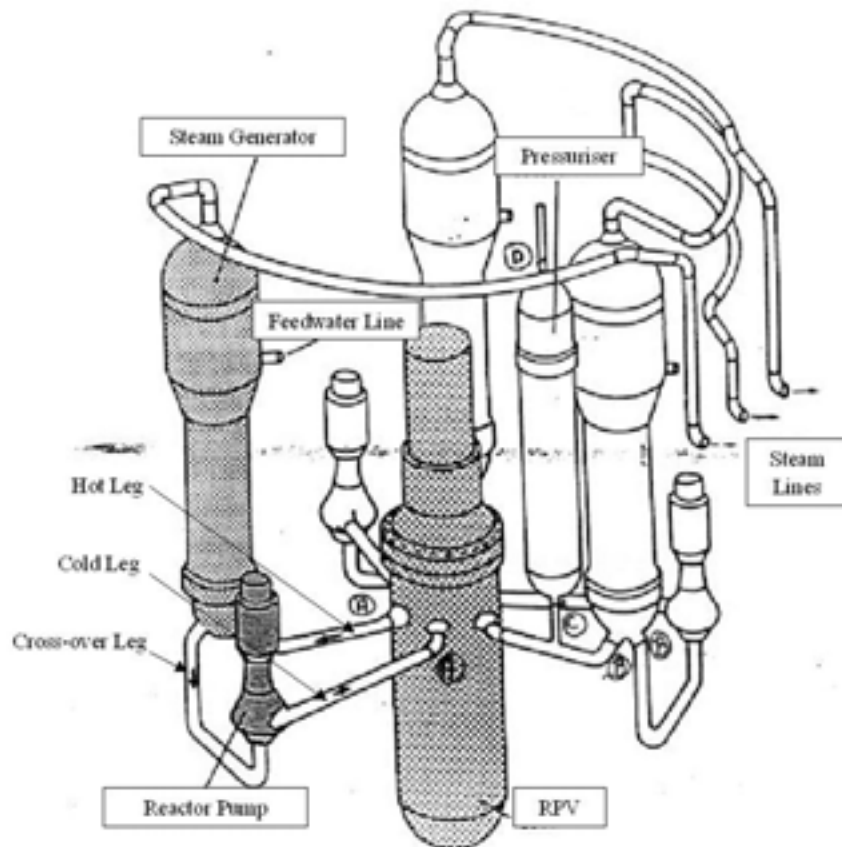


FIG. 2-20. Sketch of a typical French PWR reactor coolant loop.

TABLE II. TYPICAL DIMENSIONS OF PWR PRIMARY COLLANT PIPING. ALL (NOMINAL) DIMENSIONS ARE IN MM

Piping	Framatome		Siemens		VVER 440/V-230	
	Inside diameter	Thickness	Inside diameter	Thickness	Inside diameter	Thickness
Hot leg	740	72 to 78	780	40 to 57*	500	32
Cold leg	700	68	780	40 to 57	500	32
Crossover leg	780	78	780	40 to 57	500	32

* in earlier plants (built prior to the mid-1970s): pipes/elbows = 40/50 mm
in later plants: pipes/elbows/pipes with integrated nozzles = 52/57/70 mm

2.3. Japanese design

The designer of Japanese PWRs is Mitsubishi Heavy Industries (MHI). These plants are the same as those designed by Westinghouse in all essential respects. Typical branch connections for these plants are shown in Figures 2-21 to 2-25. The surge and spray line nozzles at the pressurizer are shown in Figures 2-21 and 2-22, respectively. The welds between the nozzles and piping are dissimilar metal welds made with Alloy 600 buttering and filler material. The charging line, accumulator injection, and residual heat removal nozzles are shown in Figures 2-23 to 2-25, respectively.

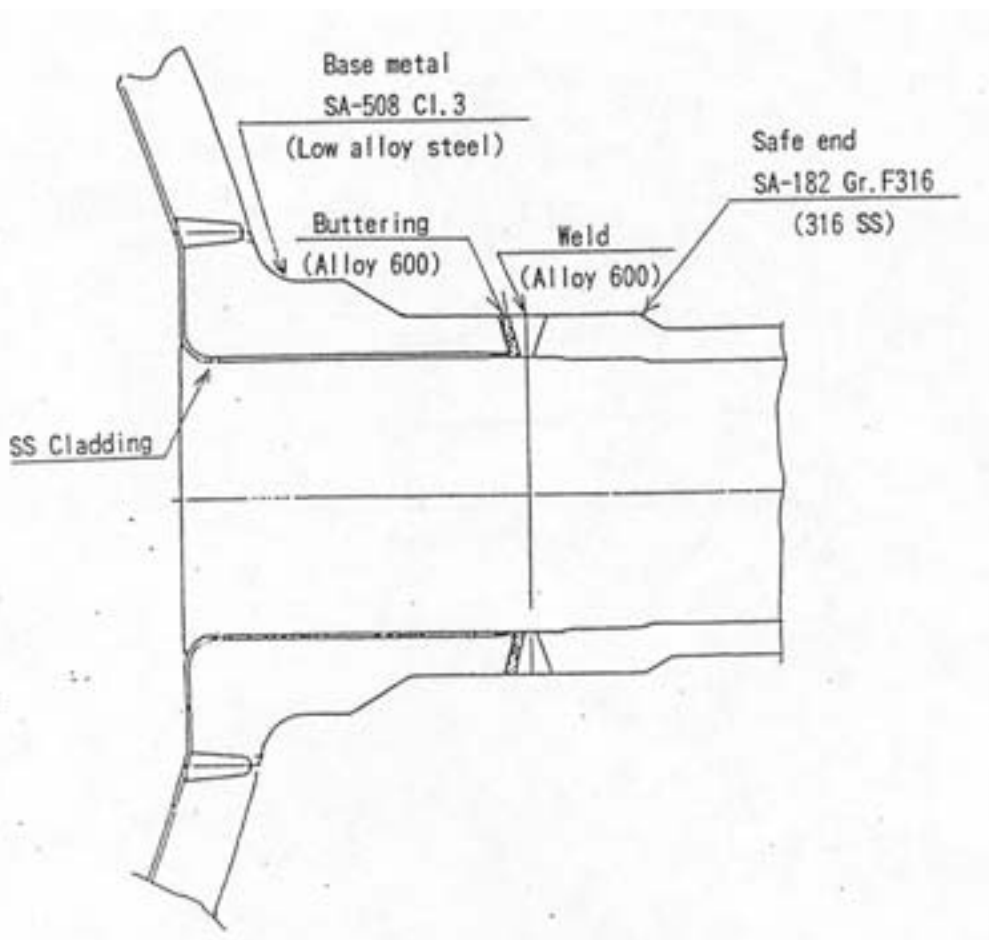


FIG. 2-21. Sketch of a Japanese surge line nozzle.

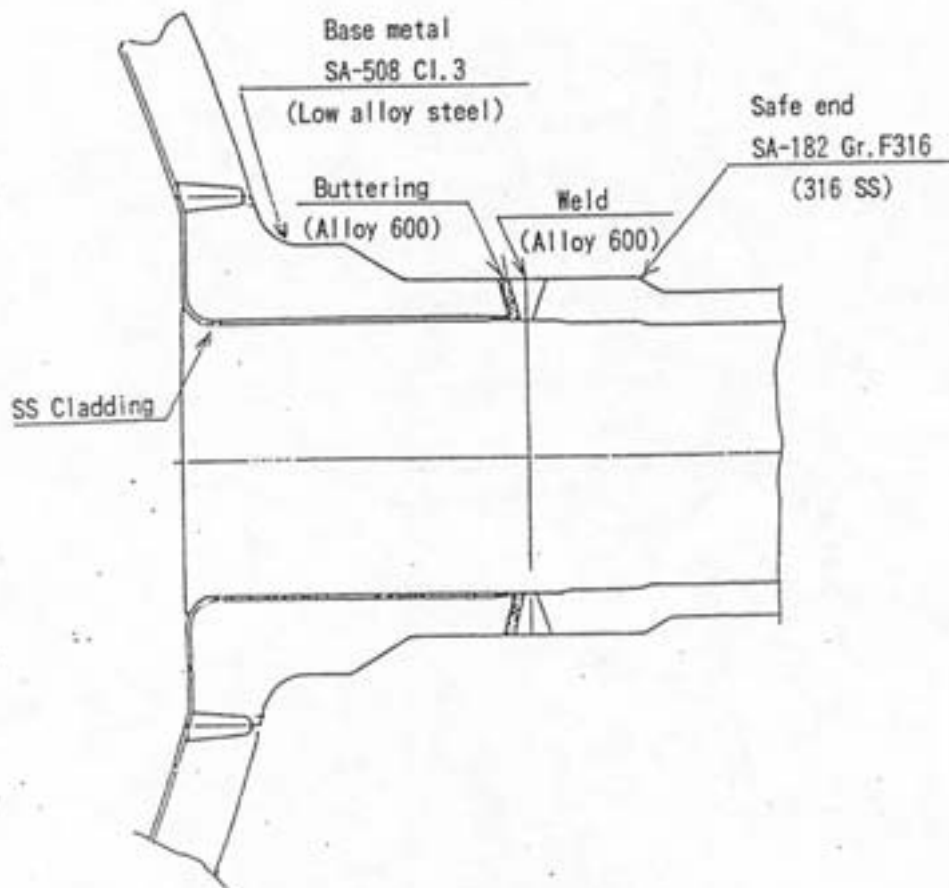


FIG. 2-22. Sketch of a Japanese spray line nozzle.

2.4. German design

The German design (see Figure 2.26) is similar to the Westinghouse/French design only with respect to the rough layout of the primary loop. The main difference is a uniform material concept related to all primary loop components (reactor pressure vessel, steam generator, main coolant pump, and main coolant line) allowing to avoid material changes throughout the loop and consequently large diameter dissimilar welds in the connections of the main coolant piping (except surge line) to these components. Straight pipes and elbows of the main coolant piping are seamless since the late seventies (in former time elbows were made of two pressed halves with longitudinal welds at the extrados and the intrados).

The layout of the surge line in their joints to the main coolant line and the pressurizer is also different and there are two DN 100 (nominal diameter 100 mm) spray lines connected to two cold legs of the reactor coolant piping; each line branches into two DN 80 lines and connects to two spray nozzles at the top of the pressurizer as shown in Figure 2-26. Typical main coolant pipe inside diameters and thicknesses for a German plant are given in Table II.

The branch line nozzles in earlier plants (prior to about 1978) designed as “set on” or “set through” nozzles, whereas those in later plants are integrally forged with the straight pipe as listed in Table III, except the cold leg injection nozzle, which is inclined as shown in Figure 2-27. Nozzles with a higher calculated cumulative fatigue usage factor are designed with a thermal sleeve made of niobium-stabilized stainless steel (similar to Type 347 stainless steel).

All nozzles have a shop welded safe end as shown in Figure 2-27 in order to realize homogeneous welding (similar metal weld) in the field. Nozzles with nominal diameter smaller than DN 100 are made of stabilized stainless steel and designed as “set through” nozzles; they are attached to main coolant piping by a dissimilar metal weld as shown in Figure 2-28. A stainless steel or Inconel buttering is applied to the pipe, which is stress relieved prior to welding to the branch nozzle.

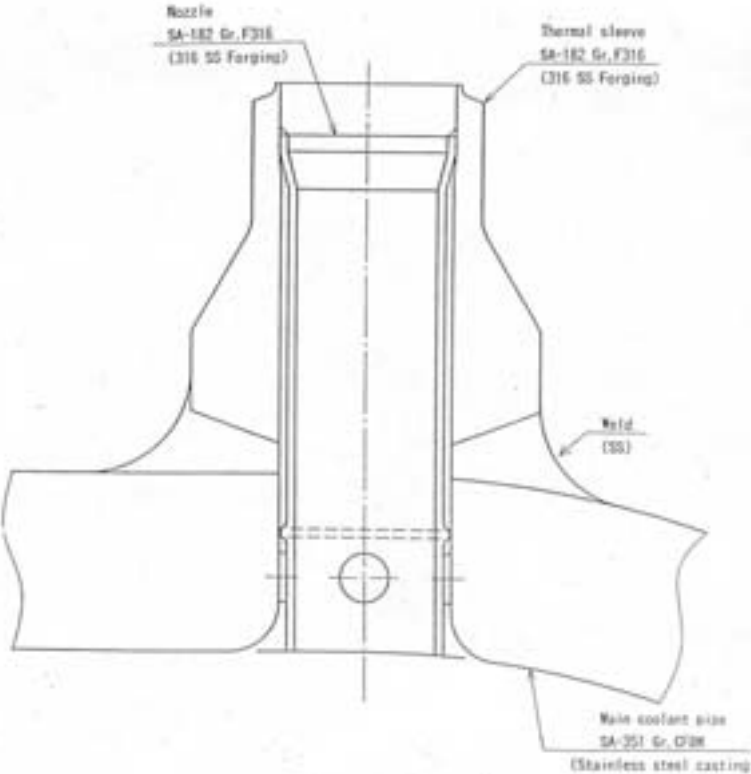


FIG. 2-23. Sketch of a Japanese charging line nozzle.

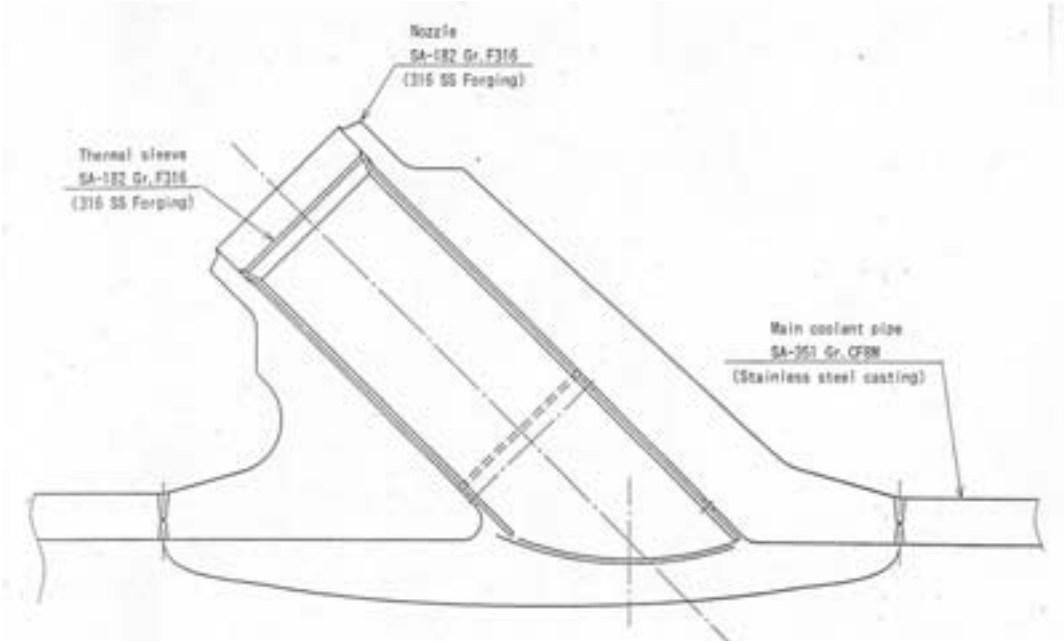


FIG. 2-24. Sketch of a Japanese accumulator injection nozzle.

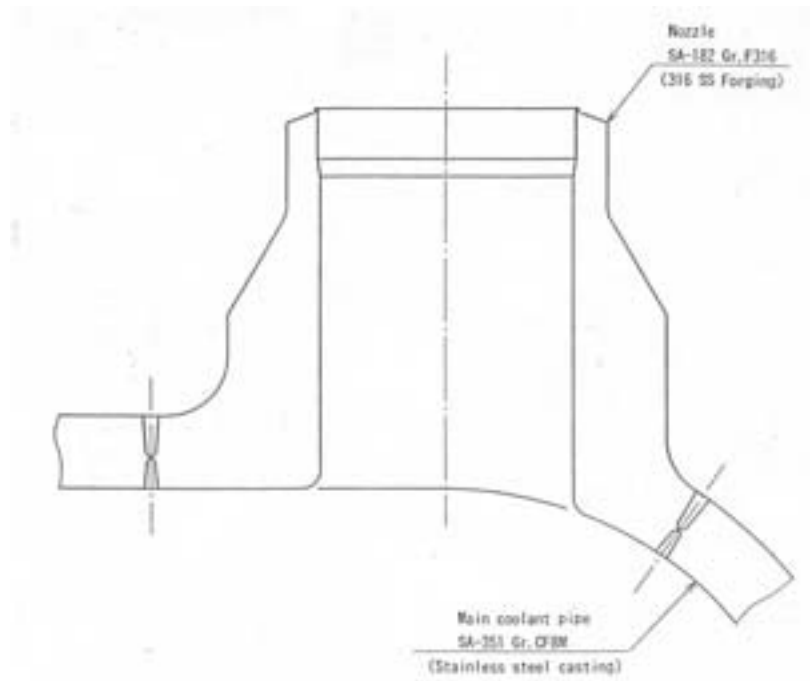


FIG. 2-25. Sketch of a Japanese residual heat removal line nozzle.

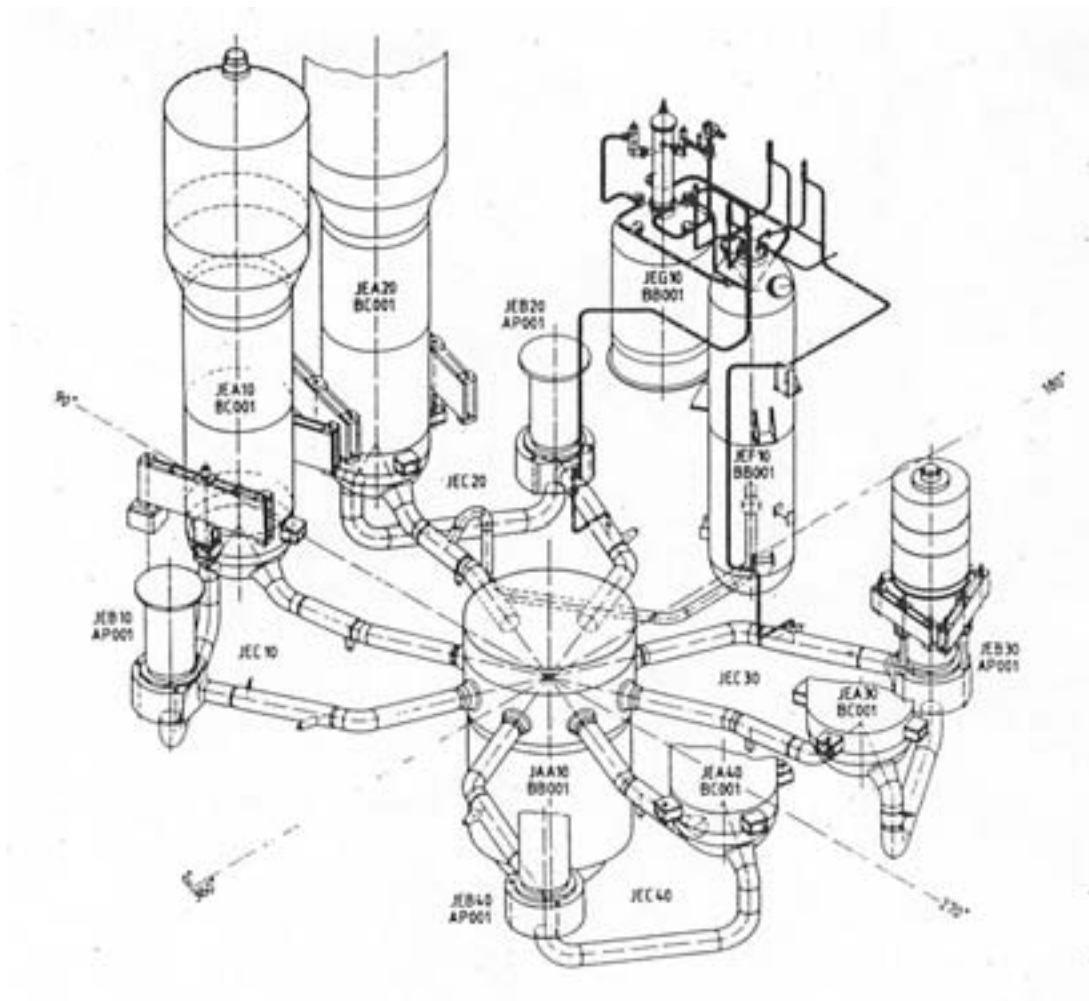


FIG. 2-26. Schematic of a typical German PWR primary coolant system.

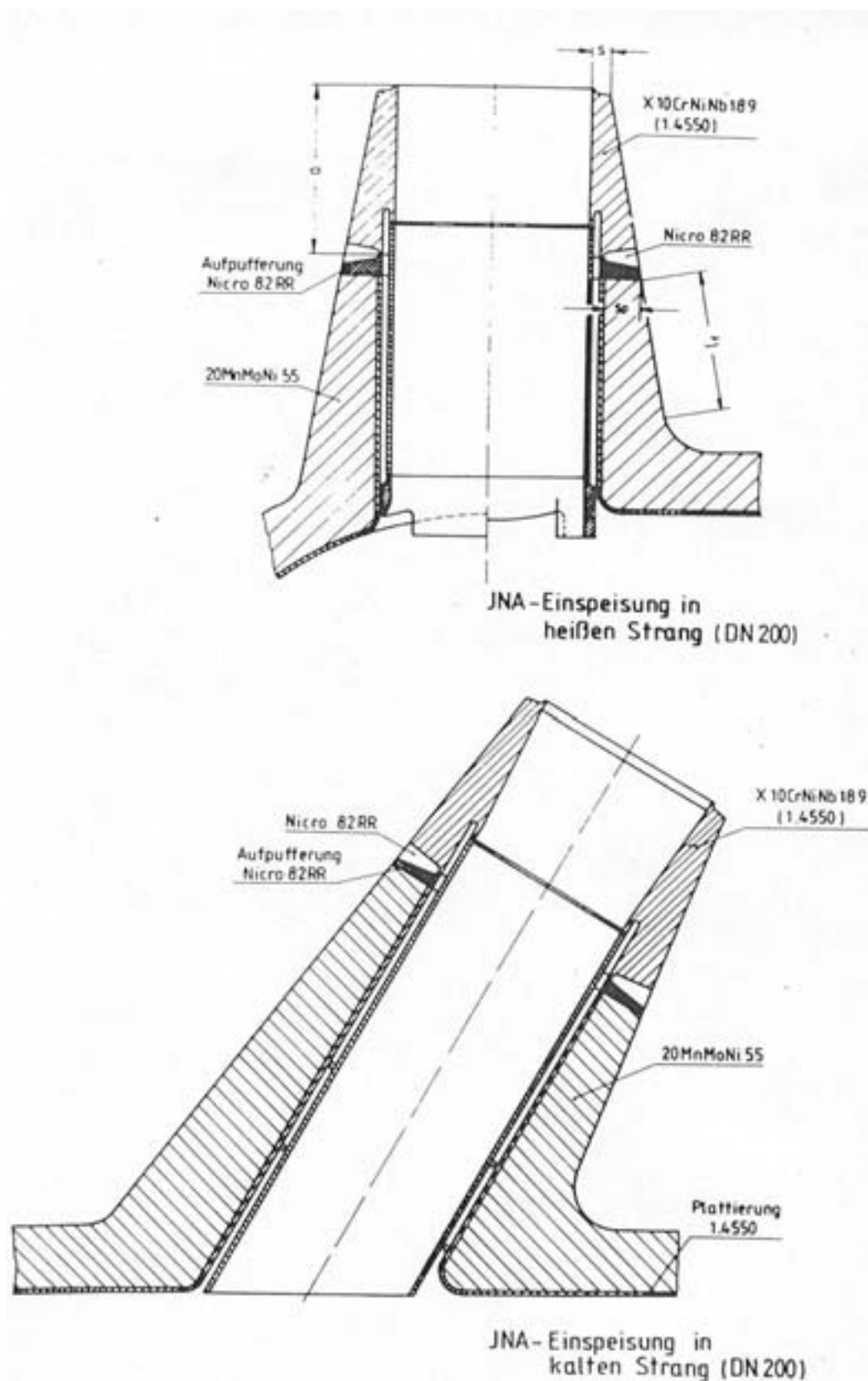


FIG. 2-27. Integrally forged auxiliary line nozzles in the German PWR primary coolant system.

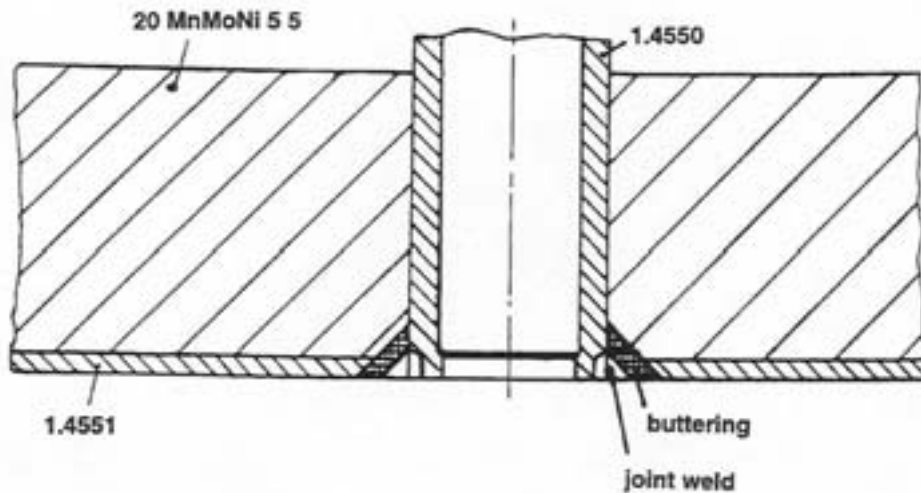


FIG. 2-28. Small diameter nozzles in the German PWR primary coolant system.

TABLE III. BRANCH LINE NOZZLE DESIGNS IN GERMAN PWRs

PIPING SYSTEM	DN	NUMBER OF NOZZLES	COMPONENT CONNECTION	DESIGN
JEF	350	1/1	MCL	Straight nozzle, thermal sleeve
	350	1/1	PRESSURIZER	Straight nozzle, thermal sleeve
JNA	200	4/3	MCL	Straight nozzle, thermal sleeve
	200	4/3	MCL	Inclined nozzle, thermal sleeve
KBA	50	4/3	MCL	Straight nozzle, thermal sleeve
	100	1/1	MCL	Straight nozzle, no sleeve
JEF	100	2/2	MCL	Straight nozzle, no sleeve

2.5. Russian design

Although it shares a basic engineering concept with its counterparts in the United States, France, Germany and Japan, the Russian pressurized water WWER design is very different. Two major differences are (1) horizontal steam generators, and (2) two motor operated isolation valves located on hot and cold legs of each of the six loops in the WWER 440 design. The WWER 1000 design has four loops and does not have isolation valves.

2.5.1. WWER 440

The WWER 440, Model 230 plant is one of the earlier designs employed between 1956 and 1970. Twelve units of this model are presently in operation in Bulgaria, the Russian Federation and the Slovak Republic. It has six primary coolant loops shown in Figure 2-29, one of which is shown in Figure 2-30. Typical main coolant pipe inside diameters and thicknesses for a WWER 440, Model 230 plant are given in Table II. Each loop has a horizontal steam generator which provides better heat transfer; together, the six steam generators provide a large volume of coolant.

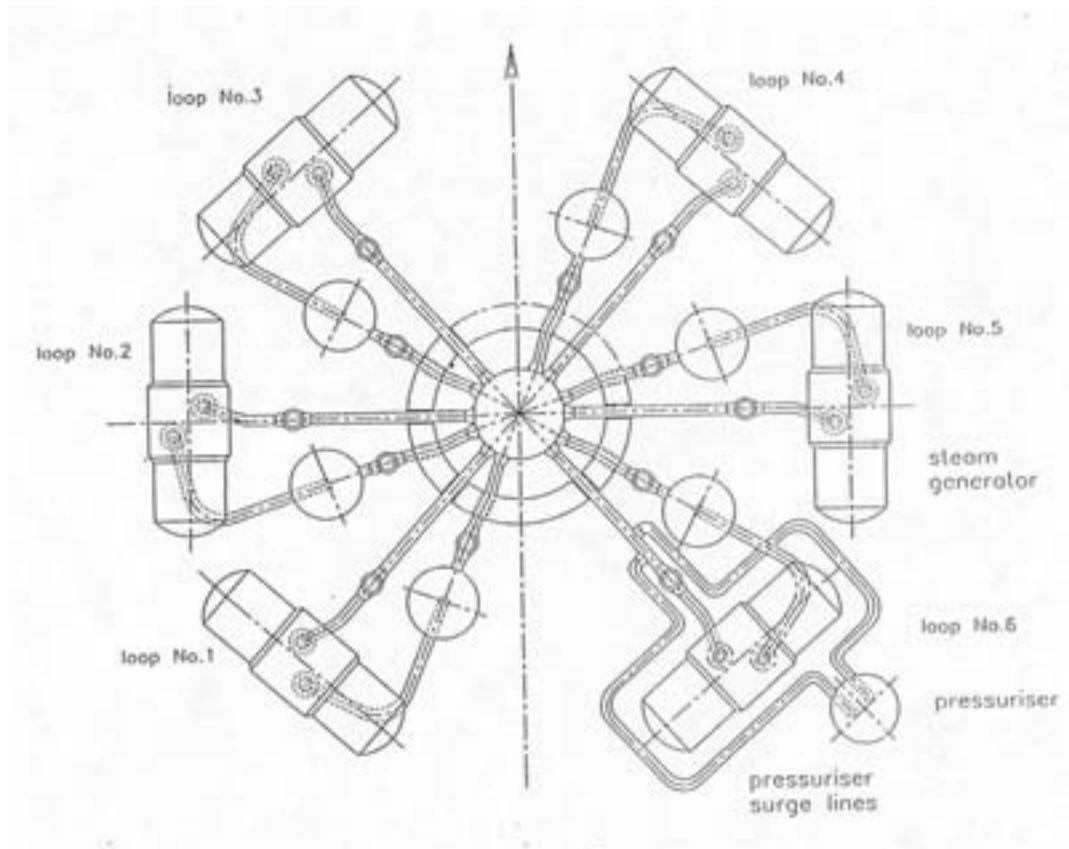


FIG. 2-29. Schematic view on the primary system layout of a WWER 440, Model 230 reactor.

In some respects this design is more forgiving than Western plant designs with 2, 3, or 4 large vertical steam generators. Each loop in a WWER 440 plant also has two main isolation valves. The hot leg includes an U-shaped section near the steam generator inlet in order to reduce primary coolant elevations. This feature provides loop seal effects during a LOCA accident. As a result, the main coolant piping layout incorporates several bends and elbows and the hot and cold legs are much longer than those in the standard western PWRs. Isolation valves allow plant operators to take one or more of the six coolant loops out of service for repair while continuing to operate the plant. But this mode of operation is not recommended because of asymmetrical distribution of flow in individual loops. This mode of operation is administratively excluded in some plants, for example in Paks plants. The 230 plant does not have an accumulator and, therefore, has a limited capability for emergency core cooling. The emergency core cooling system designs differ considerably among various 230 plants. These plants are not designed with an appropriate confinement system to cope with a large failure of the primary loop piping. The WWER 440, Model 230, was designed with two pressurizer surge lines connecting a hot leg to the bottom side of the pressurizer, and a third line, the pressurizer relief pipe, connecting the same hot leg to the top of the pressurizer as shown in Figure 2-30(a). The top and side views of the 230 plant reactor coolant loop with pressurizer surge lines are shown, respectively, in Figures 2-30(b) and 2-30(c). The 230 plant surge line nozzles on the pressurizer and the hot leg are shown, respectively, in Figures 2-31(a) and 2-31(b). The 230 plant spray line nozzle on the cold leg is shown in Figure 2-32. The WWER 440, model 213 plants were designed between 1970 and 1980. Over 20 units of this model are in operation or in the final stage of construction in the Russian Federation, Ukraine, Finland, Hungary, and the Czech and Slovak Republics.

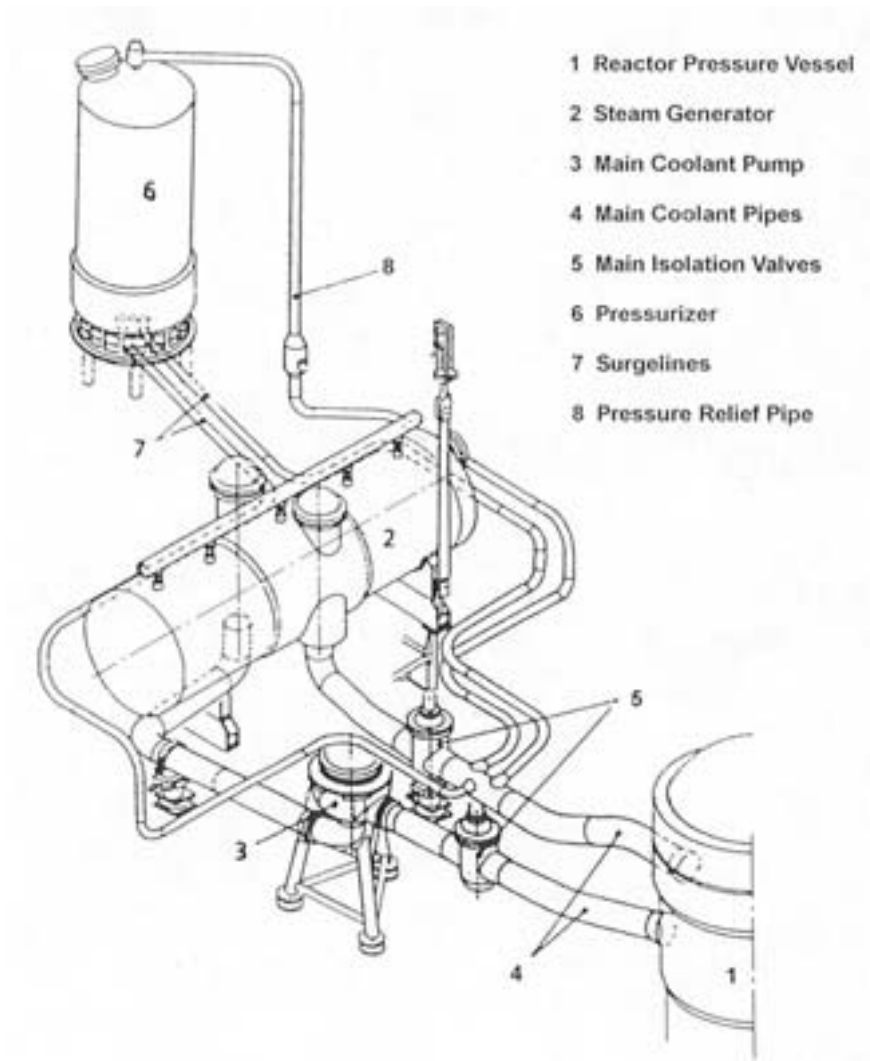


FIG. 2-30(a). Typical reactor coolant loop for a WWER 440, Model 230 plant.

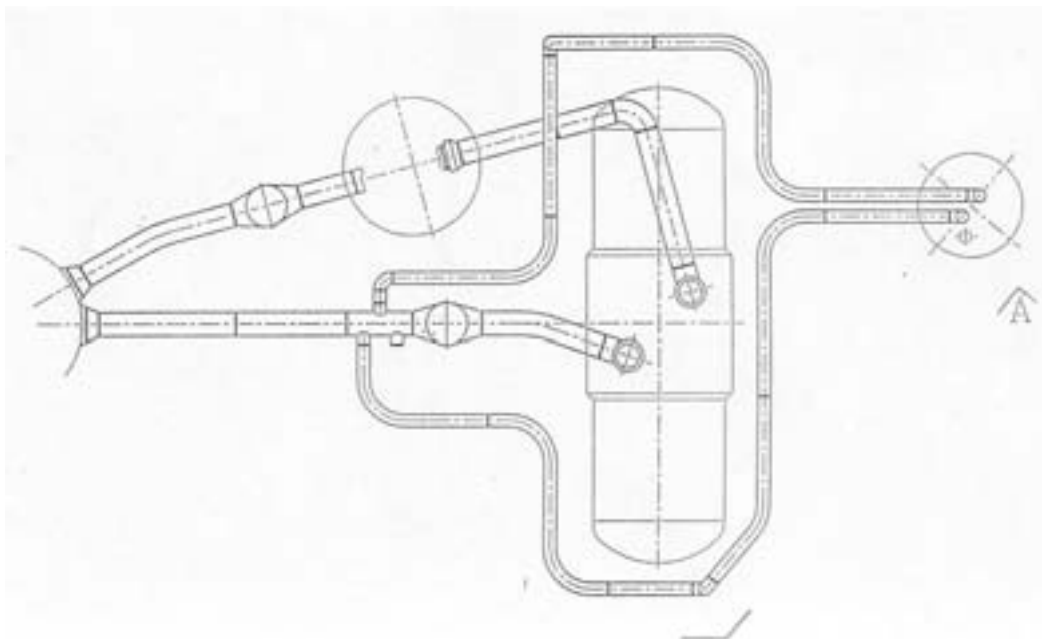


FIG. 2-30(b). Top view of a WWER 440, Model 230, reactor coolant loop with pressurizer surge lines.

The Model 213 continues the use of 6 coolant loops and horizontal steam generators. Other features of the Model 213 differ substantially from the older Model 230. The Model 213 has incorporated standard emergency core cooling system and accident localization features, which include a pressure suppression system. However, these plants are not equipped with pipe whip restraints to absorb the dynamic effects of breaks in the primary loop piping. Each reactor coolant pump is equipped with a high inertia flywheel to increase the pump coast down. Three different views of the WWER 440, Model 213, reactor coolant loops with pressurizer surge lines are shown in Figure 2-33. The 213 plant surge and spray line nozzles on the pressurizer are shown in Figures 2-34(a) and 2-34(b), respectively.

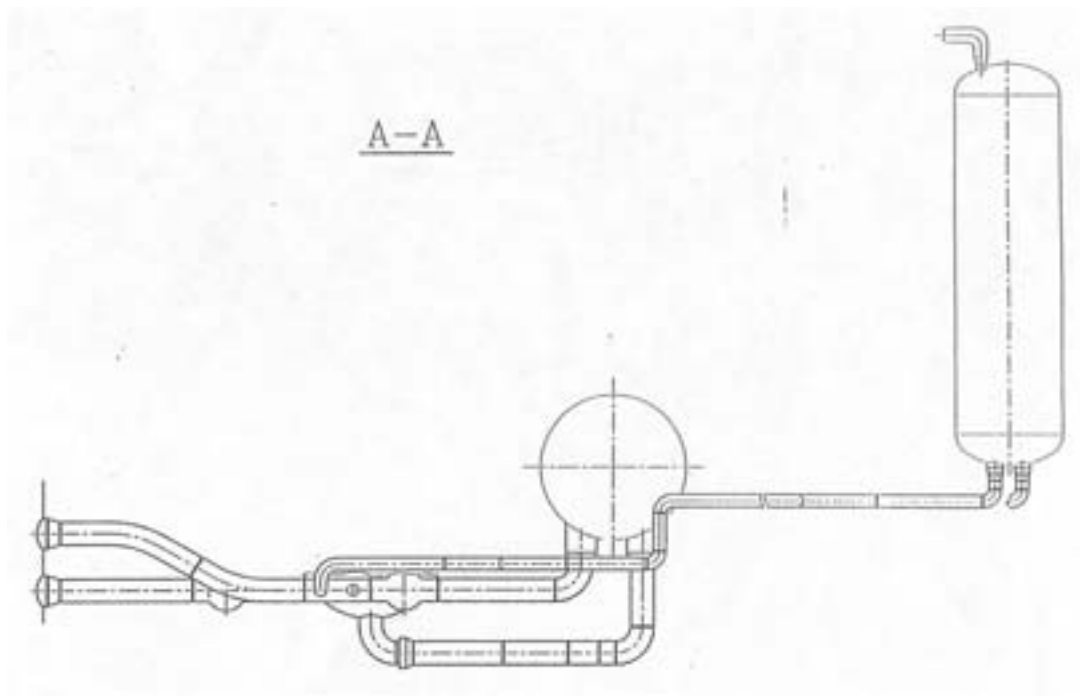


FIG. 2-30(c). Side view of a WWER 440, Model 230, pressurizer surge lines.

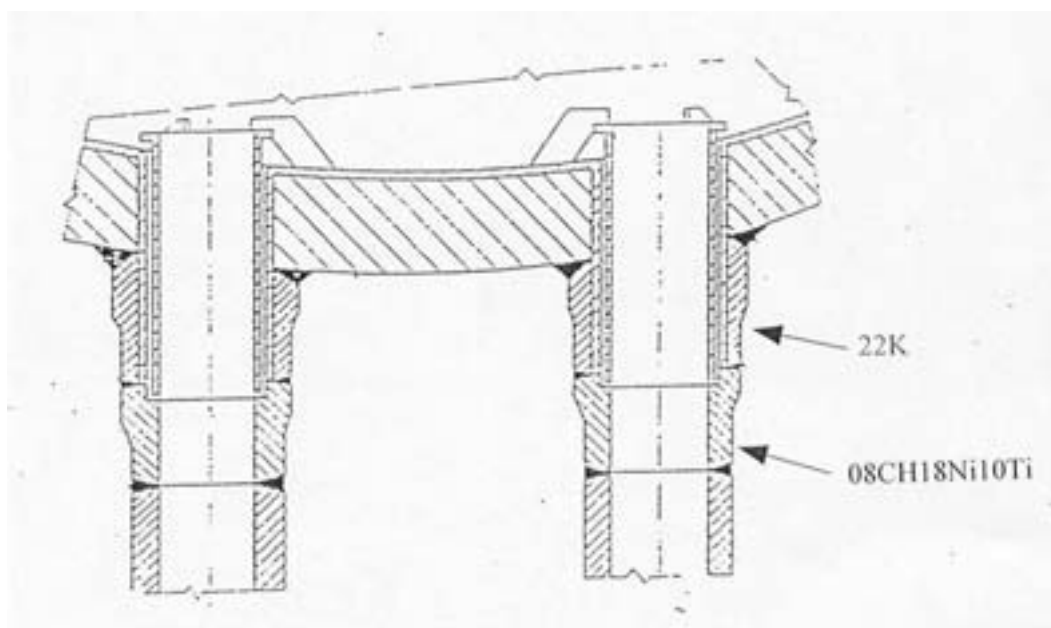


FIG. 2-31(a). WWER 440, Model 230, surge line nozzles on the pressurizer.

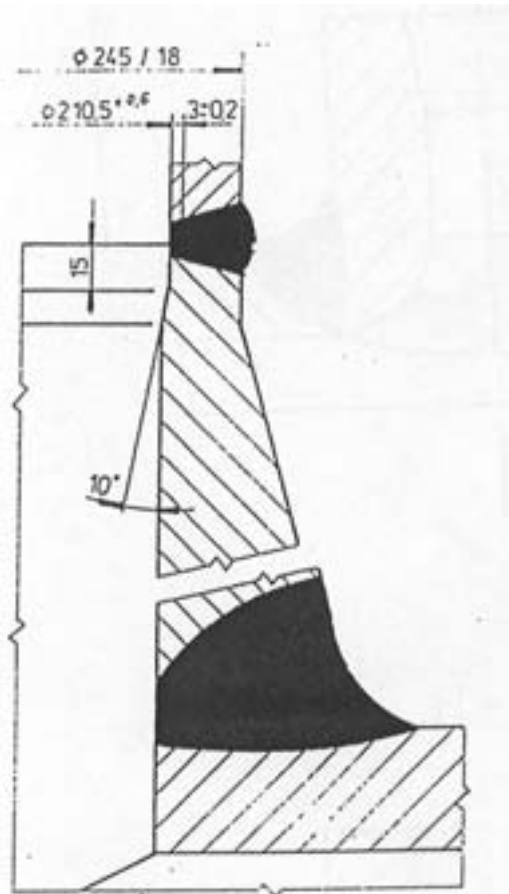


FIG. 2-31(b). WWER 440, Model 230, surge line nozzle on the hot leg.

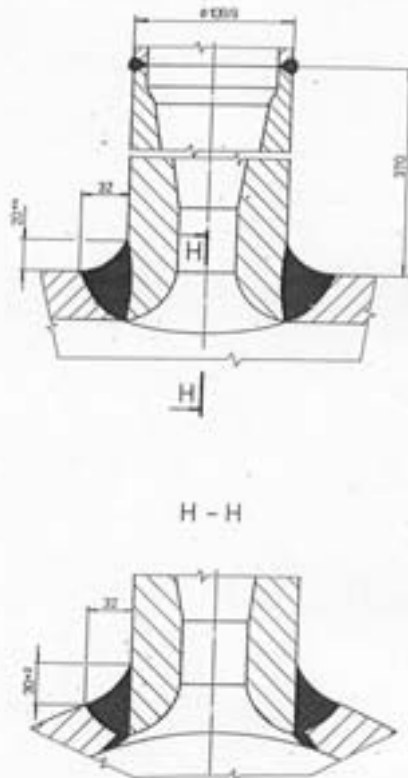


FIG. 2-32. WWER 440, Model 230, spray line nozzle on the primary piping.

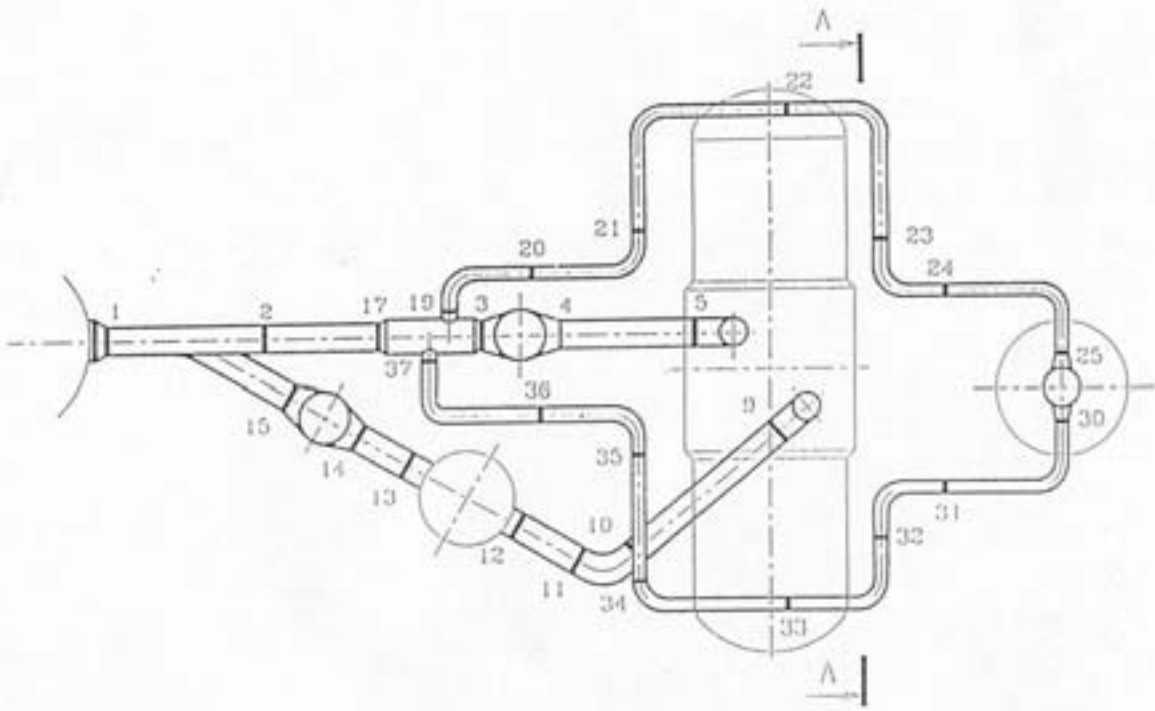


FIG. 2-33(a). Top view of a WWER 440, Model 213, reactor coolant loop with pressurizer surge lines.

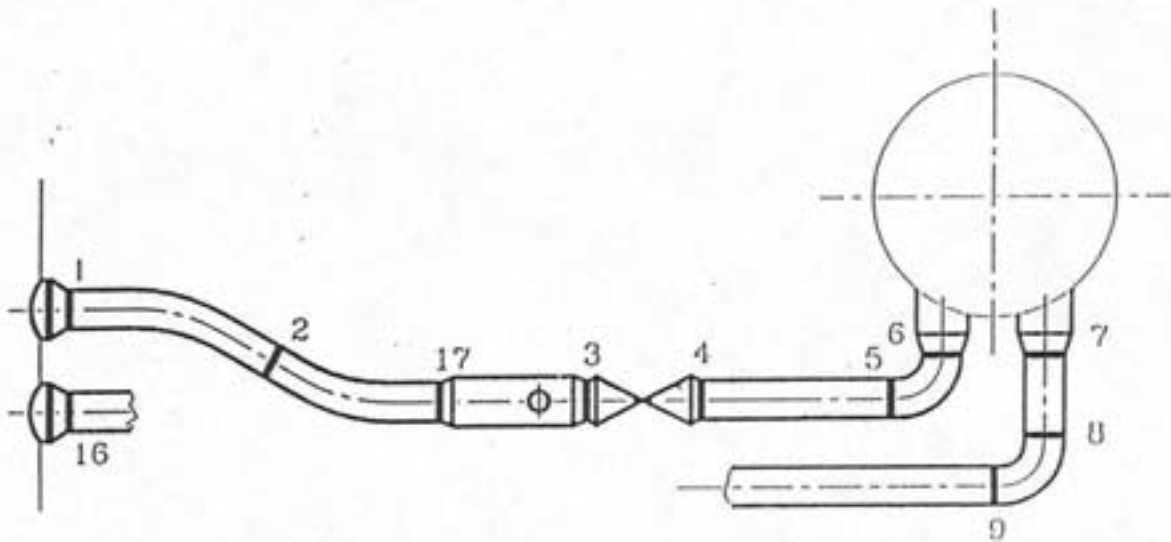


FIG. 2-33(b). Side view of a WWER 440, Model 213, reactor coolant loop with pressurizer surge lines.

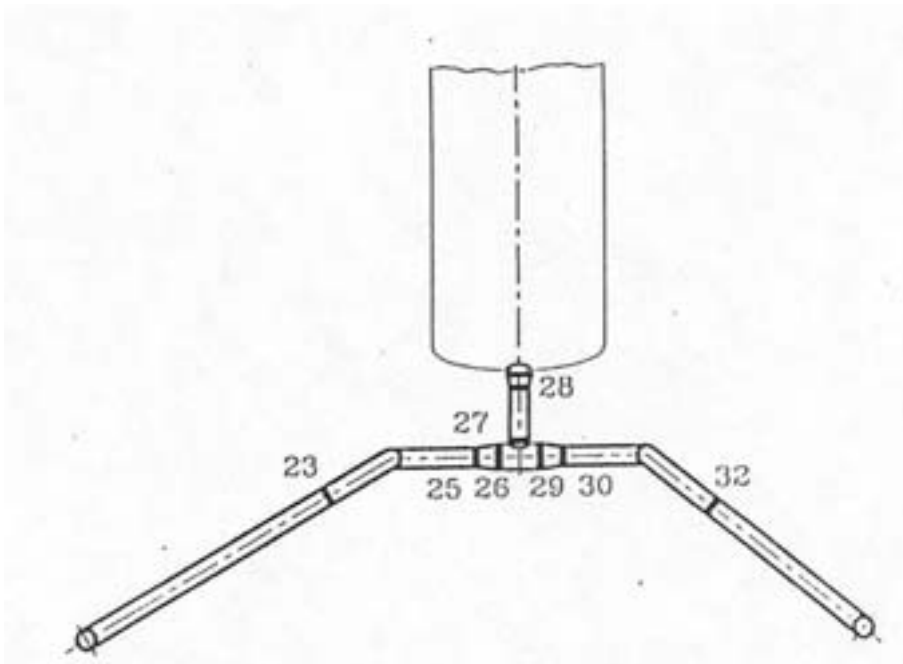


FIG. 2-33(c). Front view of a WWER 440, Model 213, reactor coolant loop with pressurizer surge lines.

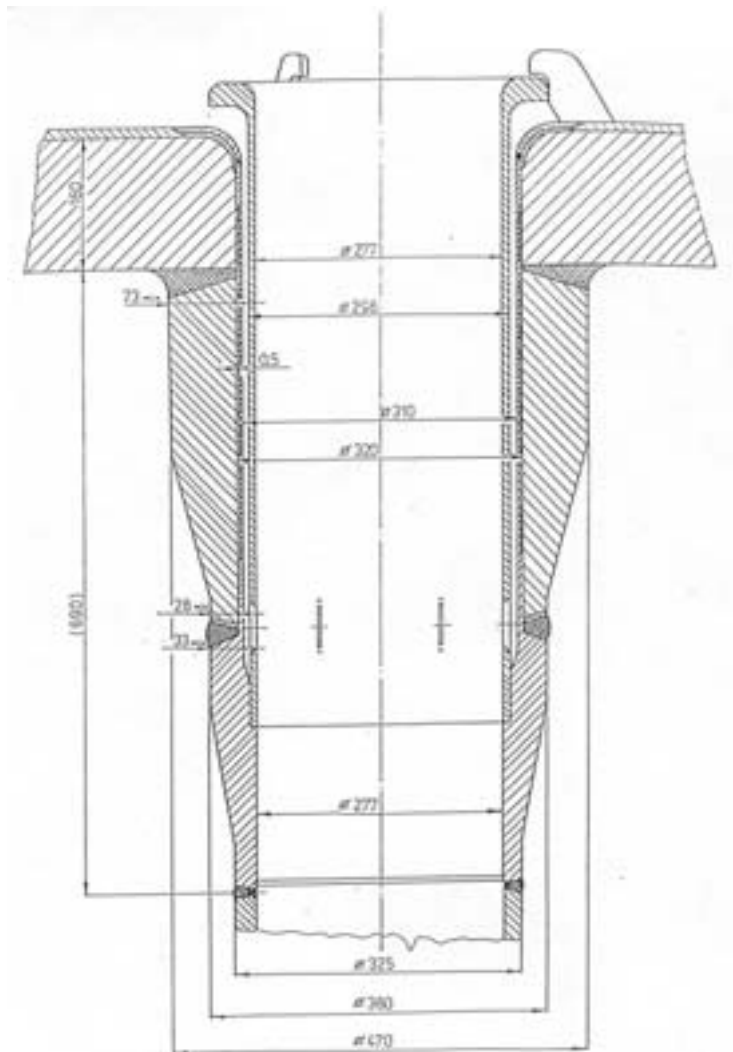


FIG. 2-34(a). WWER 440, Model 213, surge line nozzle on the pressurizer.

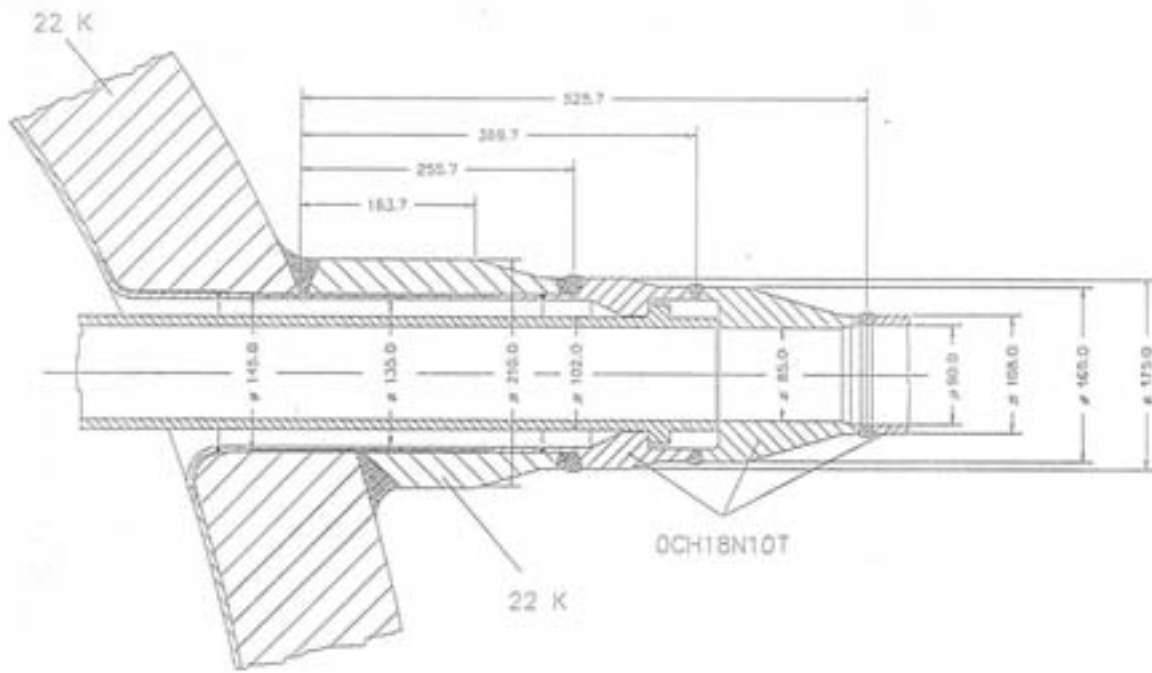


FIG. 2-34(b). WWER 440, Model 213, spray line nozzle on the pressurizer.

2.5.2. WWER 1000

The WWER 1000 design was developed between 1975 and 1985 and was based on the requirements of a new Soviet nuclear standard that incorporated some international practices. The basic design parameters for WWER 1000 main coolant piping are given in Table IV. The model has four coolant loops and horizontal steam generators, as shown in Figure 2-35. The hot leg of loop No.4 is connected to the pressurizer by a surge line and the cold leg of loop No. 1 is connected to the pressurizer steam space by a spray line. There are several nozzles connecting the residual heat removal, coolant purification, make-up, boron injection, drainage and process parameters measuring systems. Each loop of primary piping of WWER-1000 type 302 plants (South Ukraine NPP Units 1 and 2, Kalinin NPP Units 1 and 2, and Novovoronezh Unit 5) has two motor operated valves, one on the hot leg and one on the cold leg. The WWER-1000 Type 320 design has four loops and does not have isolation valves. The layout of pressurizer surge line is shown in Figure 2-36.

TABLE IV. MCL BASIC DESIGN PARAMETERS FOR WWER 1000

Design pressure	17,6 MPa
Design temperature	350° C
Design lifetime	30 years
Design length	148 m
Design heat-up rate	Less or equal to 20° C/h
Design cooldowns, rate normal	70 cycles 30° C/h
Design cooldowns, rate accelerated	30 cycles 60° C/h
Design coolant flow	21000 m ³ /h

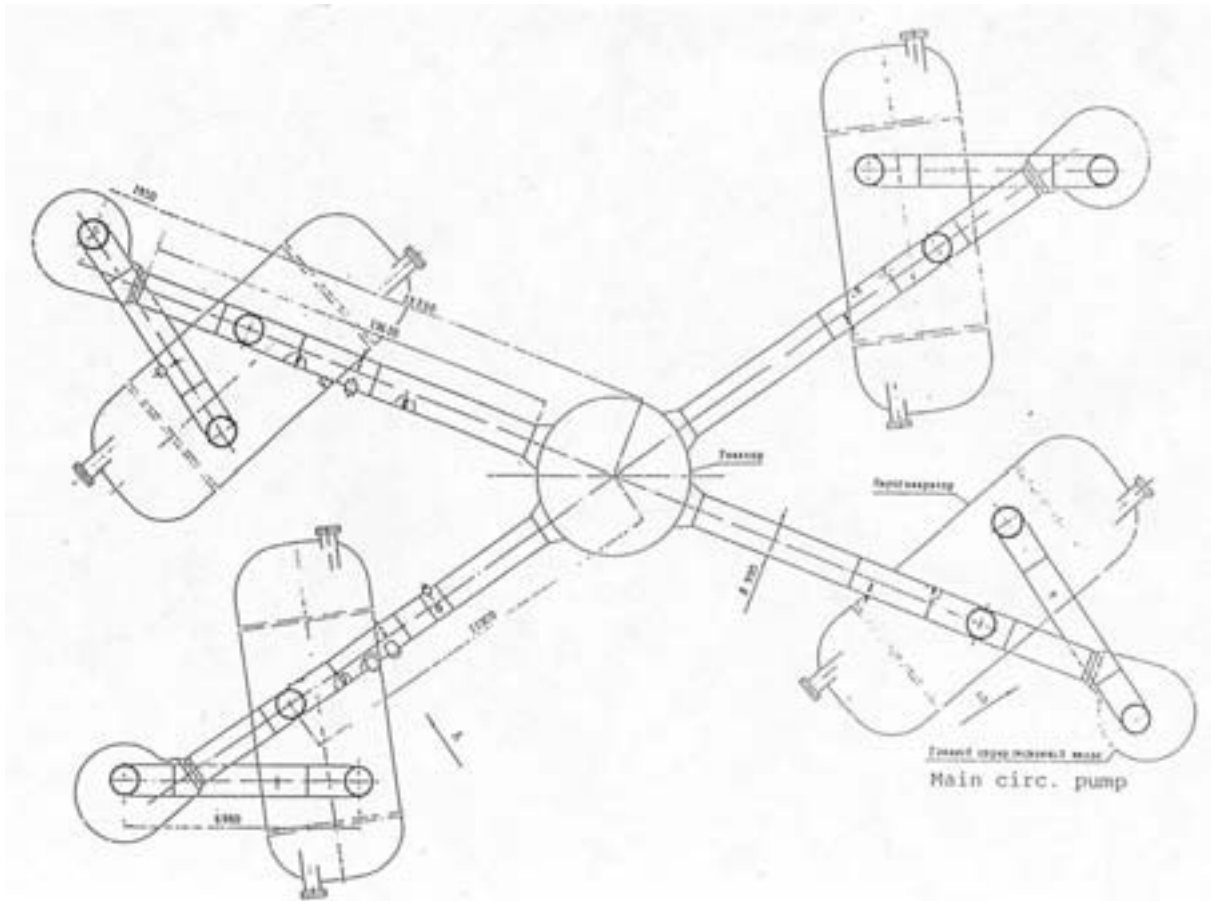


FIG. 2-35. Schematic of a typical primary coolant loop for WWER 1000, Model 320 reactor.

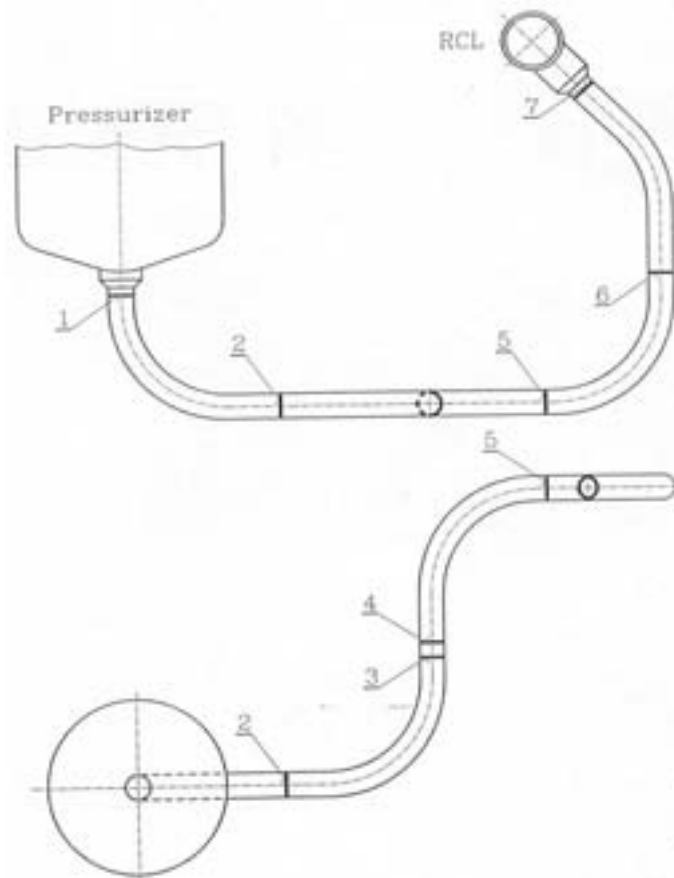


FIG. 2-36. Position of weldments on WWER 1000, Model 320, pressurizer surge line.

2.6. Main coolant loop piping materials and fabrication

The materials used for the PWR main coolant loop piping include carbon steel piping clad with austenitic stainless steel, austenitic stainless steel piping, both cast and wrought form, Alloy 600, and weld filler and buttering materials. The austenitic stainless steel used for cladding and piping is either stabilized or non-stabilized. The materials for main coolant piping and branch lines are listed in Tables V and VI, respectively. The fabrication methods used by various vendors for main coolant piping are summarized in Table VII.

TABLE V. MCL PIPING MATERIALS

MCL Material		Materials	Weld	Remarks Experience
Westinghouse	Pipe/Elbow	CF8M, CF8A 316 316L & 304N	308, 309, A182 A82, 308, 308L A152/52 for replacement	Experience on safe end replacement BWR, no cladding, requirement on temper bead welding see ASME grinding of BMW external surface
<i>VOGTLE</i>	<i>Pipe</i>	<i>S4-351, GR CF8A Cent cast seamless</i>		
<i>BRAIDWD BYRON</i>	<i>Pipe</i>	<i>S4-376, GR 304N Forged seamless</i>		
Framatome	Pipe/Elbow	See Westinghouse		
Siemens	Pipe/Elbow	508 cl 2, cl3 Cladding: stabil. SS, Welded, (>4 mm thick)	adj. To 508 cl 2, cl 3	Experience on long term behaviour (Obrigh.: 508 cl 2). PWHT after cladding/welding typically 580°C/2h
B&W	Pipe Elbow Cladding	106 or 516 GR C 516 GR 70 18/8-type, welded (pipe) and explosive bonding (elbows)		
<i>OCONEE, CRYS: RWR3</i>	<i>Pipe Elbow</i>	<i>A-106 GR C 516 GR 70</i>		
WWER 440 1000	Cladding	08Cr18Ni10T or Ni 12 10Gni2MFA (Russian): stabil,	04Cr19Ni11Mo3 10Gni1MA SS, welded	Elbows made of clad straight pipes
CE	Pipe Elbow Nozzle Cladding:	SA-516 GR 70 SA-516 GR 70 SA-182 F SA-109 GR 11 Roll bonded		
<i>CALV CL., MILL.STO.3</i>	<i>Pipe Cladding</i>	<i>S4-516 GR 70 304L (>1/8" thick)</i>		

General remarks:

1. By the "Bend Pipes" watch the heat treatment very carefully!!!!
2. Heat treatment-ASME code requirements are being evaluated!!!!!!

TABLE VI. MCL BRANCH LINE MATERIALS

MCL Branch Line Material	Piping	Elbows	Nozzles
Westinghouse	316/304, cast SS	Cast SS, bent pipe	Forged SS
Framatome	See Westinghouse		
Siemens	347 mod.	347 mod. Bent Pipe	Forged 347 mod.
B&W	316 S/304	Cast SS, bent pipe	Forged SS
WWER (440) (1000)	08Cr18Ni10T 10GN2MFA	08Cr18Ni10T 10GN1MA	Forged SS Forged CS
Combustion*	316S, CF8M	CF8M	Forged SS

* ABB-CE (USA) and KAERI (Korea) changed surge line piping material from CF8M to 347 SS in order to increase strength (to meet ASME stress limit because severe loading condition due to flow stratification) and toughness (application of LBB concept and ageing concern in cast SS) of the piping material

TABLE VII. FABRICATION METHODS FOR MCL PIPING COMPONENTS

	Pipes	Elbows	Nozzles, Tees
Westinghouse, Framatome	Centrif. Cast, forged (SS)	Cast SS long welds (some) forged	Forged SS cast SS
Westinghouse future plans: Avoid cast material. French: Tendency to forge the hot leg. Other elbows with cylindrical ends (bendings) generally.			
Siemens	Extruded CS forging	Plates with long welds forged (since about 1978)	Forget CS integral
Siemens: no change envisaged			
WWER (440) (1000)	Extruded SS Extruded (CS)	Forged (SS) long welds (some) bent CS	Forged SS Same CS
Russia: No change envisaged			
B&W/Combustion	Plates CS long welds	Plates CS long welds	Forged CS SA-182-F1 SA-105-GR.4
Mitsubishi	Cast SS	Cast SS	Forged SS

General remark: elbows with cylindrical endings have a tendency to bend.

2.6.1. Clad carbon steel main coolant loop piping

US Plants. The main coolant piping, fitting, and nozzle material for the Babcock & Wilcox and Combustion Engineering plants is wrought ferritic steel clad with austenitic stainless steel, as presented in Table V. The inside surface of the piping adjacent to penetrations, however, is clad with Alloy 182. Cladding provides corrosion resistance to carbon steel piping. The cladding is normally deposited by welding or installed by roll

bonding. Some nuclear steam supply system manufacturers (NSSS) have applied it to elbows by an explosive process and, therefore, its thickness varies with the location in the piping system. Babcock & Wilcox employed weld-deposited cladding on the piping inside surfaces and explosively bonded cladding in the piping elbows, which were fabricated with two half elbows (clam shells), the clad applied before the halves are welded together. The Combustion Engineering piping was constructed of roll-bonded cladded plates. The plates, cladded during the rolling process, were formed into rounds and seam welded. The ferrite content of the stainless steel weld overlay was controlled to preclude microfissuring during the cooling process. Non-destructive examinations were performed following the post weld heat treatment (PWHT) to ensure the integrity of the bond between the cladding and carbon steel. Careful weld preparation permitted use of austenitic weld material on the cladding and ferritic weld material on the ferritic material forming the main pipe wall.

German plants. The main coolant piping, fitting, and nozzle material and in one case also the material of the surge line for the German PWR plants is fine-grained, low-alloy steel clad with stabilized austenitic stainless steel. The types of low-alloy steels commonly used are SA-508 Class 2 (German Type 22NiMoCr3 7), and SA-508 Class 3 (German Type 20MnMoNi5 5).

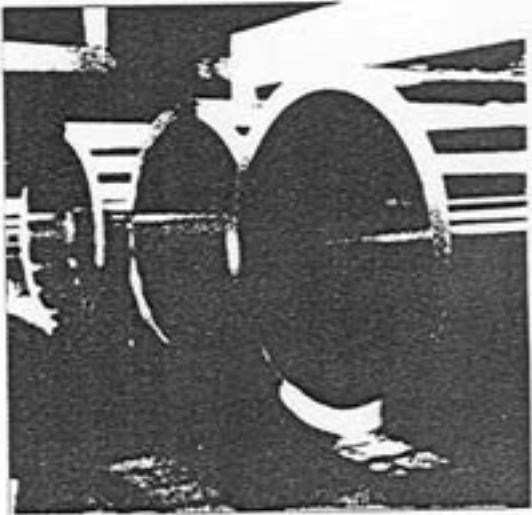
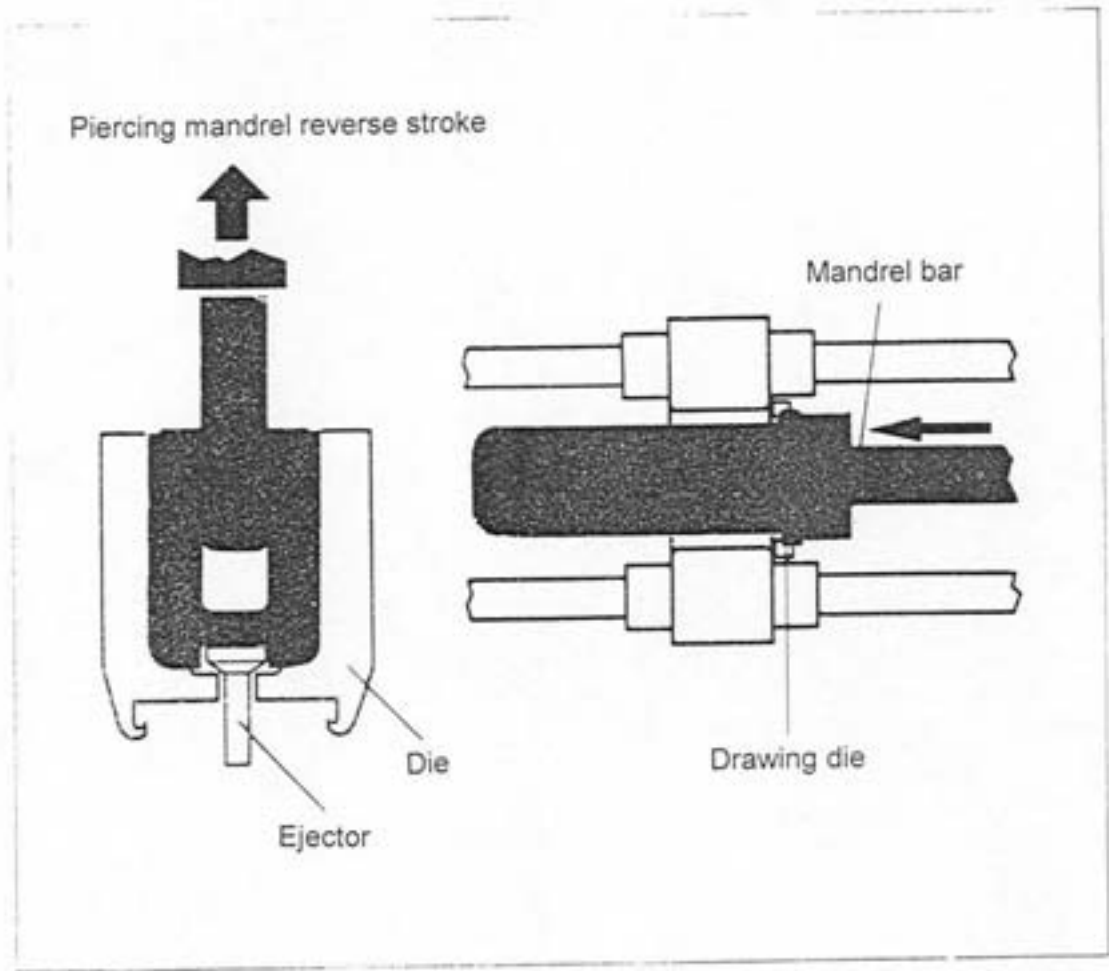
Straight pipes are normally produced by the Erhardt-process shown in Figure 2-37, by the Pilger-rolling process shown in Figure 2-38, or forged with integral nozzles as shown in Figure 2-39. Elbows are made from 2 halves (pressed plates) with longitudinal welds on extrados and intrados; seamless elbows are produced by inductive bending of straight pipes as shown in Figures 2-40 and 2-41, or by cold bending in a die as shown in the lower part of Figure 2-42 and in Figure 2-43 and quenched and tempered. Hamburger bends made by pressing and simultaneously expanding pipe over a conical bent mandrel. The result is a product with a small bending radius and only small changes in wall thickness in the intrados and extrados as shown in the upper part of Figure 2-42.

All pipes, forgings, and elbows of the main coolant piping in the German plants have been seamless since the late 1970s. Earlier, elbows were made of two pressed halves with longitudinal welds at the extrados and the intrados. The piping material is 20 MnMoNi5 5, whose chemical composition is similar to SA 508 cl 3 as shown in Table VIII. The cladding material is niobium-stabilized austenitic stainless steel. To guarantee corrosion resistance, the composition of the upper 2 mm of the cladding weld deposit is specified as follows:

$$C \leq 0.045, Nb \leq 0.9 \text{ (aimed } \leq 0.65), Nb/C \geq 12.0.$$

This specification is similar to US Type 347 stainless steel. The clad piping components in German plants are fabricated as follows. Straight pipes and elbows are clad individually and then butt welded together. The cladding is deposited by welding at least one-layer on each component. Typical cladding operations are:

- elbows are cladded automatically by longitudinal strip submerged arc weld (SAW) with subsequent PWHT (1 layer)
- straight pipes are cladded by automatic helicoidal strip SAW (1 layer)
- nozzles are cladded by manual or automatic tungsten inert gas (TIG) process with subsequent PWHT (2 or 3 layers)
- manual (2 or 3 layers) or automatic (1 to 2 layers strip SAW) cladding recompletion of butt weld areas with subsequent PWHT.



Class 1 Primary Piping
Class 2 Main Steam Piping
Class 2 Header Pipes

FIG. 2-37. Tube manufacture: hot pierce and draw process.

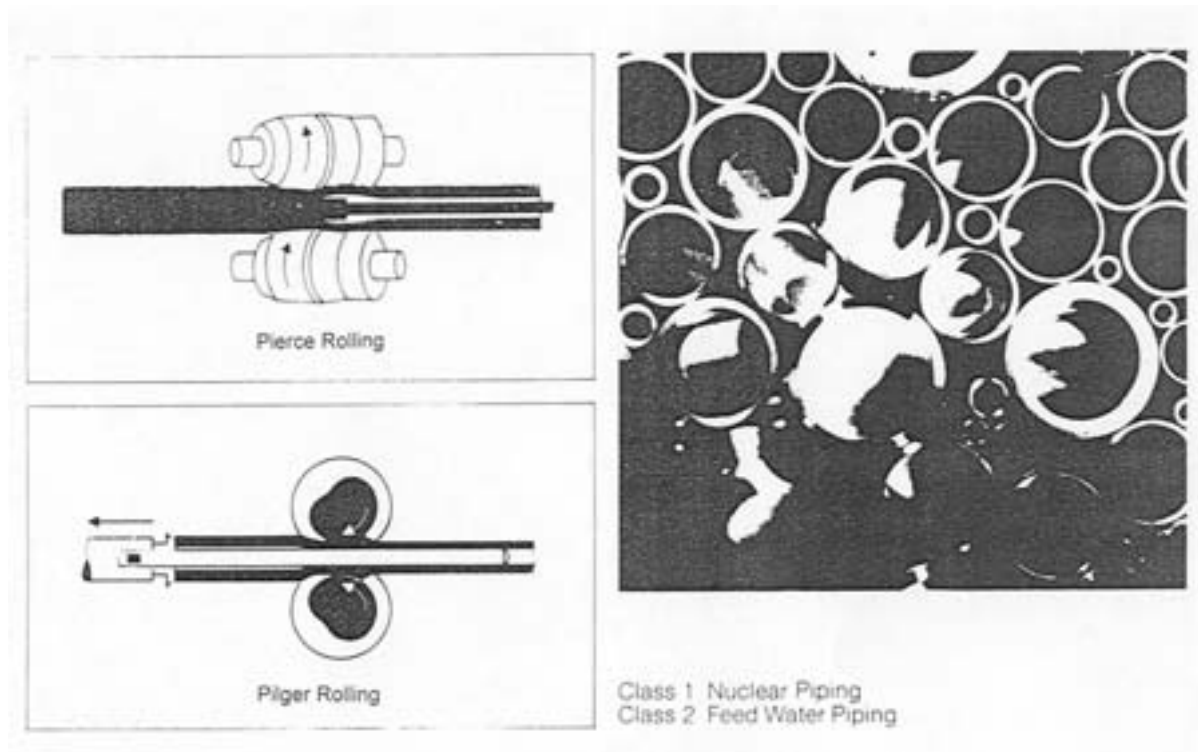


FIG. 2.38. Tube manufacture: pierce and pilger rolling process.

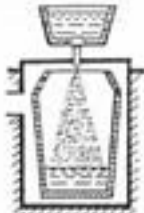
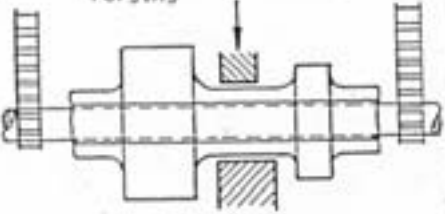
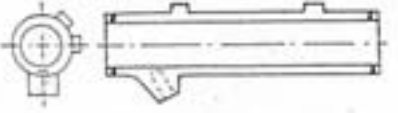
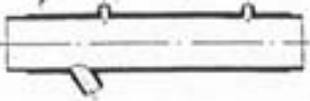
<p>Melting and Pouring</p> 	<p>Melting in electric furnace Degassing and desulphurization Pouring of ingot with stream degassing or VCD</p>
<p>Forging</p> 	<p>Upsetting and punching Straightening over mandrel Contour-forging of nozzle collars Preliminary heat treatment</p>
<p>Heat Treatment</p> 	<p>Flame cutting to nozzle contours Machining of straight pipe Water quenching and tempering Hardness test Mechanical tests</p>
<p>Finished Pipe</p> 	<p>NC-Machining Manual surface conditioning in nozzle areas Nondestructive examination Dimensional control</p>

FIG. 2-39. Manufacture of forged ferritic pipes with integral nozzles.

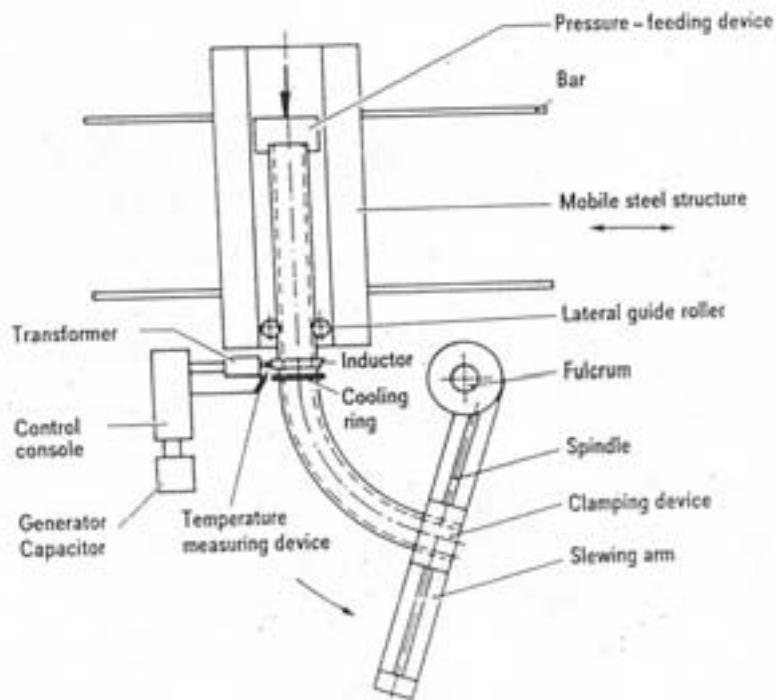


FIG. 2-40. Schematic diagram of an inductive bending appliance.

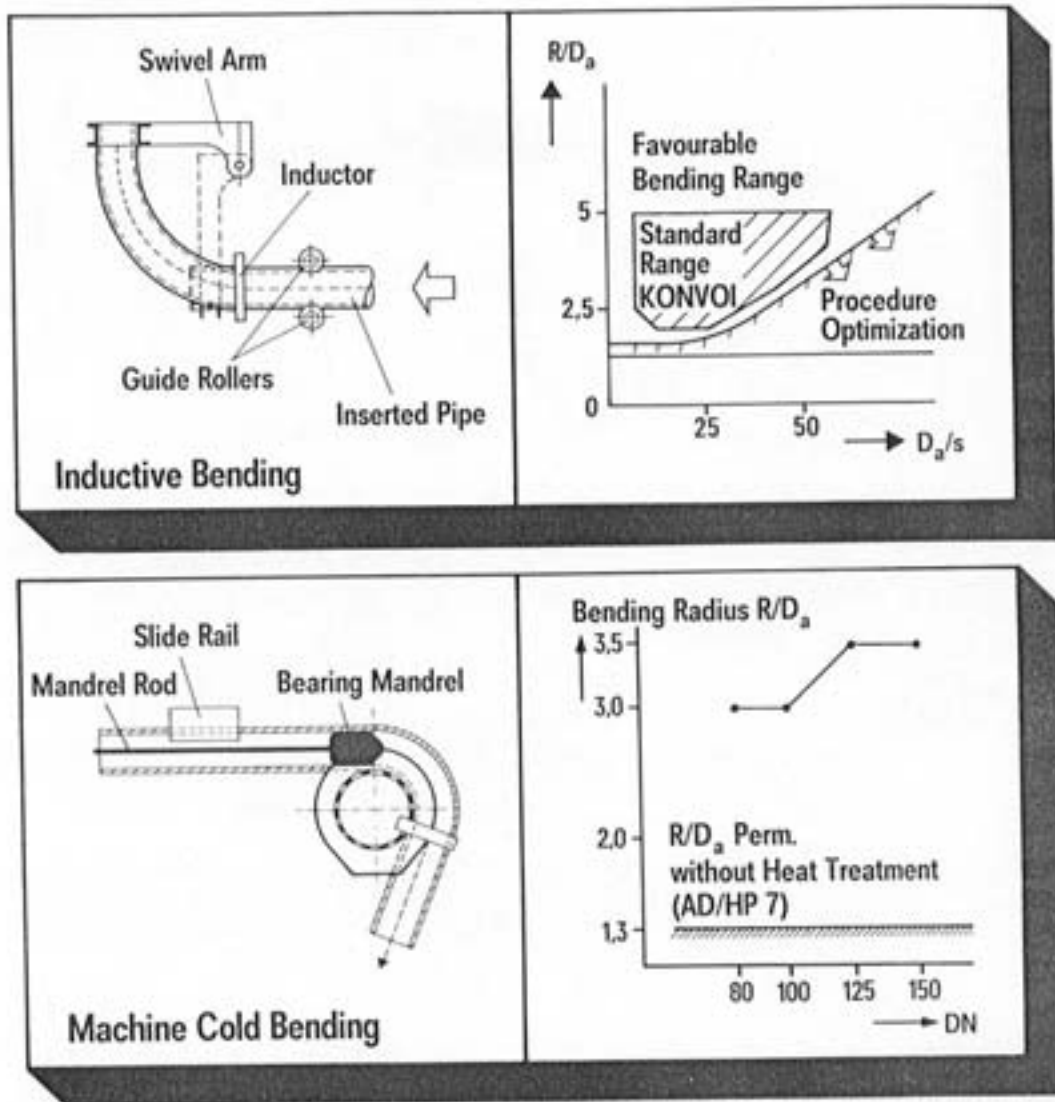


FIG. 2-41. Use of inductive bends and machine cold bends.

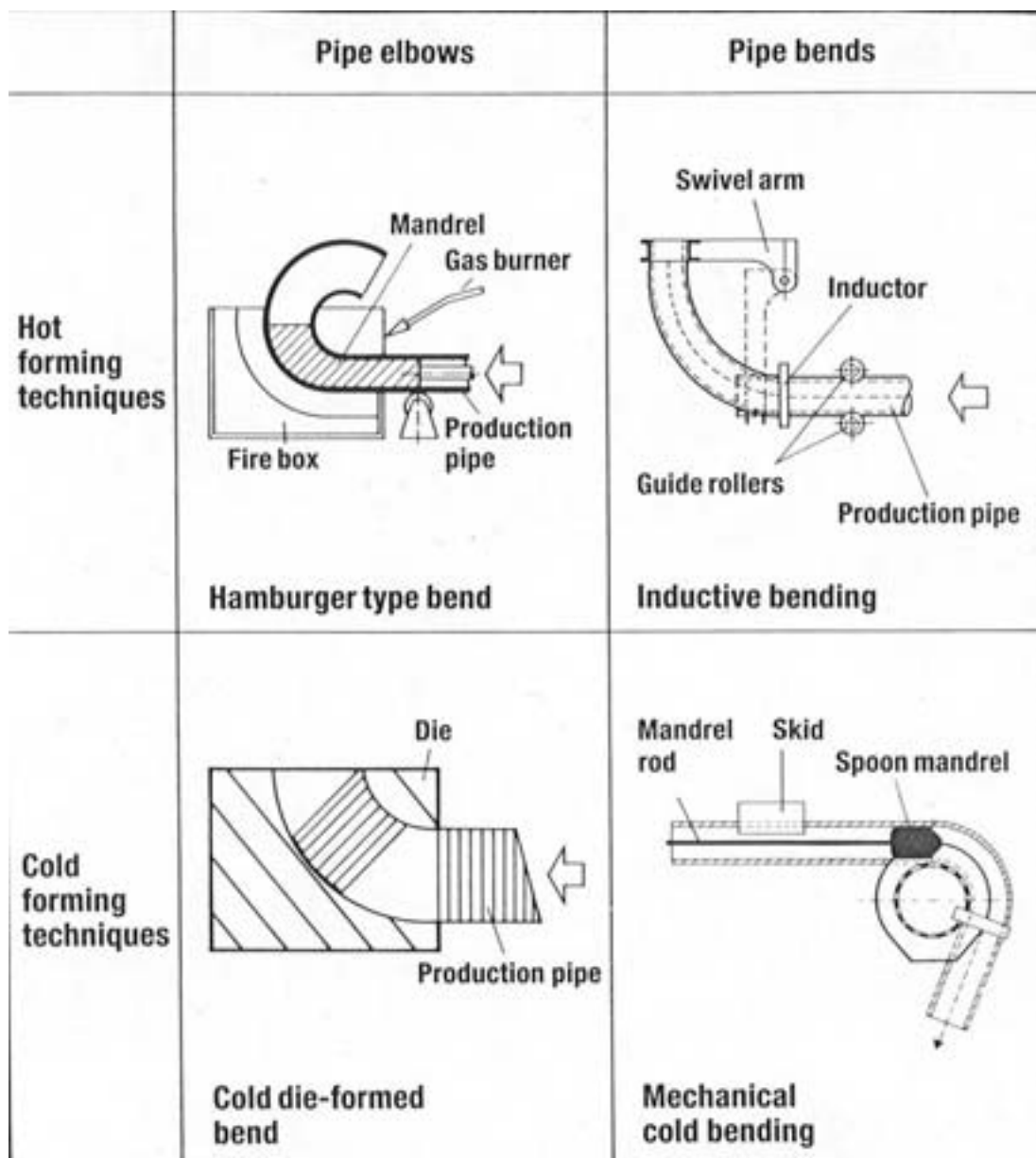


FIG. 2-42. Hot and cold forming techniques used to fabricate seamless pipe bends and elbows.

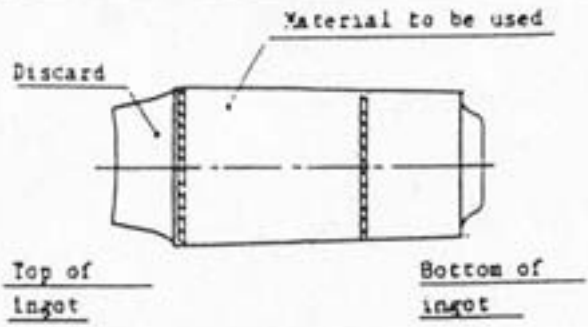
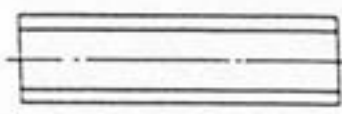
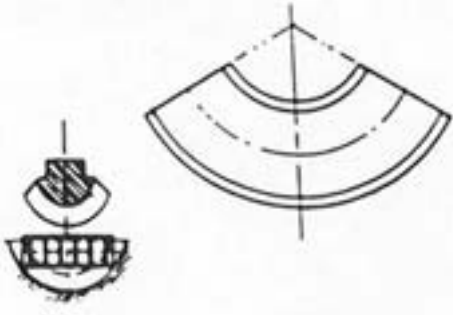
	Process	Sketch
1	Flame cutting	 <p>The sketch shows a cylindrical ingot with a horizontal centerline. The top end is labeled 'Top of ingot' and the bottom end is labeled 'Bottom of ingot'. A vertical dashed line indicates the cutting plane. The material to be discarded is labeled 'Discard' and the material to be used is labeled 'Material to be used'.</p>
2	Piercing	 <p>The sketch shows a rectangular cross-section of a metal piece with a vertical centerline and two vertical lines representing the piercing process.</p>
3	Enlarging	 <p>The sketch shows a rectangular cross-section of a metal piece with a horizontal centerline and two horizontal lines representing the enlarging process.</p>
4	Finish forging	 <p>The sketch shows a rectangular cross-section of a metal piece with a horizontal centerline and two horizontal lines representing the finish forging process.</p>
5	Hot forming	 <p>The sketch shows two views of a hot forming process. On the left is a cross-sectional view of a metal piece being formed into a curved shape. On the right is a plan view of the same metal piece, showing the curved shape and the hot forming process.</p>

FIG. 2-43. Manufacture of ferritic elbows.

TABLE VIII. COMPARISON BETWEEN 20MnMoNi 55 and SA 508 cl 3

Chemical Composition

20 MnMoNi 55		SA 508 cl 3		
Acc. To VdTÜV Material specification 401/3 7/83		Acc. To Material specification SA 508		
C	0.17–0.23	≤ 0.25		
Si	0.15–0.30	0.15–0.40 ²⁾		
Mn	1.20–1.50	1.20–1.50		
P	≤ 0.012	≤ 0.025	≤ 0.012 ³⁾	≤ 0.015 ⁴⁾
S	≤ 0.008	≤ 0.025		≤ 0.015 ⁵⁾
Cr	≤ 0.20	≤ 0.20		
Mo	0.40–0.55	0.45–0.60		
Ni	0.50–0.80	0.40–1.00		
Al	0.010–0.040	-		
Cu	≤ 0.12 ¹⁾	-	≤ 0.10 ³⁾	≤ 0.15 ⁴⁾
V	≤ 0.020	≤ 0.05		
Sn	≤ 0.011	-		
N	≤ 0.013	-		
As	≤ 0.025	-		
1) ≤ 0.10 Core of RPV		2) Si ≤ 0.12 (VCD) 3) S 9.1 (1) 4) S 9.1 (2) 5) S 9.2		

The material is preheated for all cladding operations whether automatic or manual welding is performed. No machining of the cladding is necessary for ultrasonic examination. The as-welded surface roughness of the cladding is smooth enough for ultrasonic examination from the outside. The clad components are post-weld heat treated in the temperature range of 580–600°C. With the exception of one case all surgelines are made of the stabilized stainless steel of German type 1.4550 (US-type 347). The auxiliary lines in German plants are made of the Nb- or Ti-stabilized SS materials (German type 1.4550, 1.4541, 1.4571).

Russian WWER 1000 plants. An example of the Russian design and fabrication practice is those used for the WWER 1000. The material used for piping is 10GNi2MFA with the following typical chemical composition: 0.08–0.12%C, 0.07–0.9%Mn, 1.7–2.0%Ni, 0.4–0.6%Mo, <0.30%Cr, <0.04%V, <0.02%S, and <0.02%P. The room temperature yield and ultimate strengths are in the range of 343–490 and 539–673 N/mm², respectively. Specifications for mechanical properties of base metal, weld materials, and cladding for main coolant piping are presented in Table IX. The main coolant loop elbows for WWER 1000 are made of weld clad Erhardt pipes. These pipes are pressed and simultaneously expanded over a conical bent mandrel. The elbow is quenched and tempered after the bending process.

TABLE IX. SPECIFICATION REQUIREMENTS OF MECHANICAL PROPERTIES OF BASE MATERIALS, METAL OF WELDMENTS AND CLADDINGS OF MAIN CIRCULATION LINES WWER-1000 (MCL)

Material	Temperature of tests 20°C				Temperature of tests 350°C				Critical temperature of brittleness
	Ultimate Strength R _m , MPa	Yield Strength R _{p0,2} , MPa	Elongation A ₅ , %	Reduction of area Z, %	Ultimate Strength R _m , MPa	Yield Strength R _{p0,2} , MPa	Elongation A ₅ , %	Reduction of area Z, %	
1	2	3	4	5	6	7	8	9	10
	not less				not less				not higher
10GN2MFA (pipes and elbows dia 850 mm)	539–637	343–490	16	55	490	249	14	50	–10
Sv-04Ch20N10G2B (cladding on internal surface of pipes and elbows dia 850 mm)	490	265	16	30	353	176	10	30	—
10GN2MFA (nozzles dia 350, 300, 180, 130, 126, 105, 50 mm)	540	345	16	55	490	295	14	50	+15
22K (nozzle 30 mm)	355	195	18	45	355	185	18	45	+40
08Ch18N10T (sleeving of all nozzles, except 50mm and 30mm)	490	195	38	40	355	165	25	40	—
Welding wire Sz-08A, Sv-08AA under flux, welding of root weldment of MCL, automatic welding	353	196	20	55	314	176	13	50	—

TABLE IX. SPECIFICATION REQUIREMENTS OF MECHANICAL PROPERTIES OF BASE MATERIALS, METAL OF WELDMENTS AND CLADDINGS OF MAIN CIRCULATION LINES WWER-1000 (MCL) (CONT'D)

1	2	3	4	5	6	7	8	9	10
	not less				not less				not higher
Electrode UONII-13/45A, welding of root weldment of circumferential welds of MCL (manual welding)	353	216	22	60	314	176	22	55	-10
Electrode UONII-13/55, welding of root weldment of circumferential welds of MCL (manual welding)	431	255	20	50	372	216	18	50	0
Welding wire Sv-10GN1MA (under flux), welding of circumferential welds of MCL (automatic welding)	539	343	16	55	490	294	14	50	+15
Electrode PT-30, welding of circumferential welds of MCL (manual welding)	539	343	16	55	490	294	14	50	+15

2.6.2. Stainless steel main coolant loop piping

US plants. The main coolant piping, fitting, and nozzle materials for Westinghouse plants include both wrought and cast stainless steels [2.4]. The cast stainless steel components include statically cast fittings, present in all the Westinghouse plants, and centrifugally cast straight piping, present in some plants, as listed in Table V. The 90-degree elbows in the earlier plants were cast in two half-sections and joined by longitudinal electroslag welds, whereas the elbows in the later plants were cast in one piece without any longitudinal welds. The cast stainless steel materials include Grades CF-8, CF-8A, and CF-8M. The compositions of Grades CF-8 and CF-8M are similar to those of wrought grades Type 304 and Type 316 stainless steel, respectively. Grade CF-8A is similar to Grade CF-8 in chemical composition but has different tensile properties. The physical metallurgy of the different grades of cast stainless steel is discussed in Section 4.5.1. The straight pipe used in Westinghouse plants is seamless, and because it is fabricated from stainless steel, needs no cladding.

The stainless steel welds such as those in the Westinghouse main coolant piping are fabricated using either a shielded metal-arc or gas-tungsten-arc welding process. Type 308 stainless steel is generally used as the weld filler material. The ferrite content in the welds varies over a wide range: a measurement of the delta ferrite in about 1450 production stainless steel pipe welds showed that the ferrite content ranged from about 3.0 to 17.5 FN (ferrite number) [2.5]. A typical value for the delta ferrite in a piping weld is about 10FN. (The ferrite number defines the ferrite content in austenitic stainless steel weld metal as measured by a magnetic method. For an FN less than 10, the ferrite content is equivalent to the volume percent ferrite. However, an exact one-to-one relationship between the FN and the percent of ferrite is not maintained as the ferrite number increases.)

French plants. Main coolant lines are made of 316L stainless steel and centrifugated cast stainless steel; the elbows are made of cast duplex stainless steel (CF8 or CF8M), except for three old plants where the elbows are made in two stainless steel shells with longitudinal welds. The connections with the major large components is done through safe end and stainless steel dissimilar metal welds [2.6]. For some younger plants the cold leg is done in one piece without any welds and with included forged nozzles.

Typical chemical composition and mechanical properties of materials used in French main coolant lines are presented Tables X, XI and XII.

TABLE X. STRAIGHT PIPE – MINIMUM SPECIFIED MATERIAL PROPERTIES

Material	Z3 CND 17.12	Z2 CN 19.10	Z3 CN 20.09
0.2% yield strength at 20°C, in MPa	206	206	206
Ultimate strength at 20°C, in MPa	520	510	480
Max elongation	36	36	36
0.2% yield strength at 20°C, in MPa	130	130	126
KCV value at 20°C, in daJ/cm ²	12	12	10

TABLE XI. ELBOW AND CONE – MINIMUM SPECIFIED MATERIAL PROPERTIES

Material	Z4 CN 20.09	Z3 CN 20.09	Z3 CND 17.12	Z5 CND 19.10	Z3 CND 19.10	Z2 CN 19.10
0.2% yield strength at 20°C, in MPa	206	206	206	206	206	210
Ultimate strength at 20°C, in MPa	480	480	520	483	483	510
Max elongation	36	36	36	36	36	36
0.2% yield strength at 20°C, in MPa	120	120	100	146	128	126
KCV value at 20°C, in daJ/cm ²	10.0	10.0	12.0	8.0	12.0	12.0

TABLE XII. ELBOW AND CONE – SPECIFIED MATERIAL CHEMICAL COMPOSITION

In %	Z4 CN 20.09	Z3 CN 20.09	Z3 CND 17.12	Z5 CND 19.10	Z3 CND 19.10	Z2 CN 19.10
Carbon	0.060	0.040	0.046	0.060	0.040	0.036
Silicon	1.60	1.60	1.00	1.60	1.60	1.00
Manganese	1.60	1.60	2.00	1.60	1.60	2.00
Phosphorus	0.036	0.036	0.040	0.040	0.030	0.040
Sulfure	0.026	0.026	0.030	0.030	0.020	0.030
Chromium	19.00–21.00	19.00–21.00	17.00–18.20	18.00	18.00–21.00	18.50–20.00
Nickel	8.00–11.00	8.00–11.00	11.60–12.60	9.00–12.00	9.00–12.00	9.00–10.00
Molybdenum	—	—	2.30–2.80	2.30–2.80	2.30–2.80	—
Copper	1.00	1.00	1.00	1.00	1.00	1.00
Cobalt	0.20	0.20	0.20	0.20	0.20	0.20
Nitrogen	—	—	0.080	—	—	0.080

Russian WWER 440 plants. All piping of primary circuit of the Russian design with reactors WWER 440 is made of titanium-stabilized stainless austenitic steels. In particular, the main coolant piping is made of seamless rolling pipes (diameter 560 × 34 mm) of the grade 08Ch18N12T steel. Chemical composition of these pipes is presented in Table XIII. The mechanical properties specification requirements of the pipe steel should correspond to the requirements (control on tangent specimens along circumferential direction (weak direction) of a middle pipe wall) given in Table XIV.

TABLE XIII. CHEMICAL COMPOSITION OF MATERIALS USED IN MAIN COOLANT PIPING IN WWER 440 PLANTS

Grade steel	Chemical elements content in percentage of weight							
	C	Si	Mn	Cr	Ni	Ti	S	P
08Ch1 8N12T	Not more 0,08	Not more 0,08	Not more 2,0	17,0– 19,0	11,0– 13,0	0,5–0,6	Not more 0,020	Not more 0,035

TABLE XIV. MECHANICAL PROPERTIES OF MATERIALS USED IN MAIN COOLANT PIPING AND BRANCH LINES IN WWER 440 PLANTS

Test temperature = 20°C				Test temperature +350°C		
Rm, MPa	Rp _{0,2} , MPa	A ₅ , %	Z, %	Rm, MPa	Rp _{0,2} , MPa	Z, %
Not more				Not more		
491	196	40	55	353	177	50

2.6.3. Dissimilar metal welds

A thick layer of weld material, also called *buttering*, or a *safe end*, also called *transition piece*, have been used in the design of PWR reactor coolant piping to facilitate field welding between the stainless steel and ferritic steel components. The welds between the two metals are called *dissimilar* or *bimetallic welds*. In the Westinghouse plants, the stainless steel main coolant piping is attached to the ferritic steel reactor pressure vessel and steam generator nozzles with the dissimilar welds. In addition, the surge and spray lines are attached to the ferritic steel pressurizer nozzles with the dissimilar welds. The *buttering* at the nozzle ends avoids any postweld heat treatment of the ferritic steel nozzles after field welding to the stainless steel piping. The Westinghouse plants use the various *safe end* or *buttering* designs shown in Figure 2-44 [2.7]. The most common design includes a forged Type 316 stainless steel *safe end* welded to the nozzle with a NiCrFe alloy (Alloy 82/182) *buttering* material and a full-penetration weld of the same material. In another design, austenitic stainless steel *buttering* is weld-deposited on the nozzle end but no *safe end* is used. The least common design includes a NiCrFe alloy *buttering* on the nozzle end welded to a forged stainless steel *safe end* with a stainless steel full-penetration weld. In the French design, the dissimilar metal welds are done between forged 316 stainless steel *safe end* and 308/309 stainless steel 2-layer *buttering* of ferritic nozzle; the weld is a 308 stainless steel weld. Alloy 82/182 is also used both as a *buttering* and filler materials for dissimilar metal welds at the reactor coolant pump nozzles and at the branch connections in Combustion Engineering plants and at the branch connections of auxiliary lines to the main coolant line and the butt weld of the *surgeline* to the pressurizer in German plants (designed by Siemens). Stainless steel *safe ends* are also employed between the main coolant piping branch nozzles and stainless steel branch lines. In one Combustion Engineering plant with isolation valves on the main coolant loop, *safe ends* are used between the valve and the piping (Combustion Engineering 1987).

Stainless steel safe ends were also used between the cast stainless steel primary coolant pump nozzles and the carbon steel cold leg piping in the Babcock & Wilcox and Combustion Engineering plants. The safe ends were welded in the shop to the stainless steel pump casing, and an Alloy 600 layer (buttering) was applied to the ends of the cold leg piping; then, an Alloy 600 field weld was made between each safe end and the buttered end of each ferritic steel pipe. All field welds were postweld heat treated.

The *dissimilar welds* are made in two steps. First, at least two (in some cases three) thin layers of buttering material are applied to the end of the ferritic steel vessel nozzles. The typical thickness of the buttering is 5 to 8 mm. In French plants, Type 308/309 stainless steel is used for buttering. The material for the first layer of buttering is overalloyed with respect to Cr- and Ni-content in order to compensate the dilution resulting from the diffusion to the base metal. These materials are also used in some Westinghouse plants as shown in Figure 2-44. In Combustion Engineering-designed plants, German plants, and majority of the Westinghouse plants, Alloy 182/82 are used for all buttering layers. In WWER plants, type 25Ni/16Cr material is used for the first layer and type 19Cr/11Ni/3Mo is used for the subsequent layers as shown in Figure 2-45 to 2-48.

The buttering is postweld heat treated at a temperature related to the needs of the ferritic base material and duration determined by the thickness of the ferritic steel components. For example, the postweld heat treatment temperature for A508, cl 3 nozzle is about 580°C. The stainless steel safe ends, if used, are welded to the nozzles after the vessel postweld heat treatment to avoid sensitization of the safe end. The joint to the stainless steel safe end is performed using the same filler material as taken for the second buttering layer; it gets no further heat treatment. The materials for the main coolant piping, including safe ends, are identified in Table V.

Germany. A typical dissimilar weld fabrication employed in a later German NPP is shown in Figure 2-49. It has to be pointed out, that the buttering at the inside surface and the root pass of the weld joint (including at least one cover layer) are made with stainless steel filler material. This design realizes an inside diameter (ID) surface totally free from Ni-base alloy, which facilitates inspection of weld root during an in-service ultrasonic examination as shown in Figure 2-50.

France. In French plants, the connections with the major large components is done through safe end and dissimilar metal welds. The safe ends are always welded in shop. The buttering, the weld and the cladding use 308, 309 type stainless steels, except for 3 last plants where the reactor pressure vessel dissimilar welds use Alloy 82.

2.7. Pre-service testing inspections

Non-destructive examinations ensure that there are no flaws in a component that exceed the acceptance standards. These examinations are performed during fabrication of the component and to a certain extent after the hydrostatic pressure test. Non-destructive volumetric examination is performed normally throughout 100% of the volume of each pipe, fitting, and forging. In the USA the volumetric NDE used during fabrication is generally radiography, whereas ultrasonic examination is generally used in other countries. However, preservice volumetric examination is universally performed with ultrasonic testing. Surface examination is performed on the entire outer and inner surface of piping. Austenitic surfaces are examined by liquid penetrant method; ferritic surfaces by the magnetic particle method.

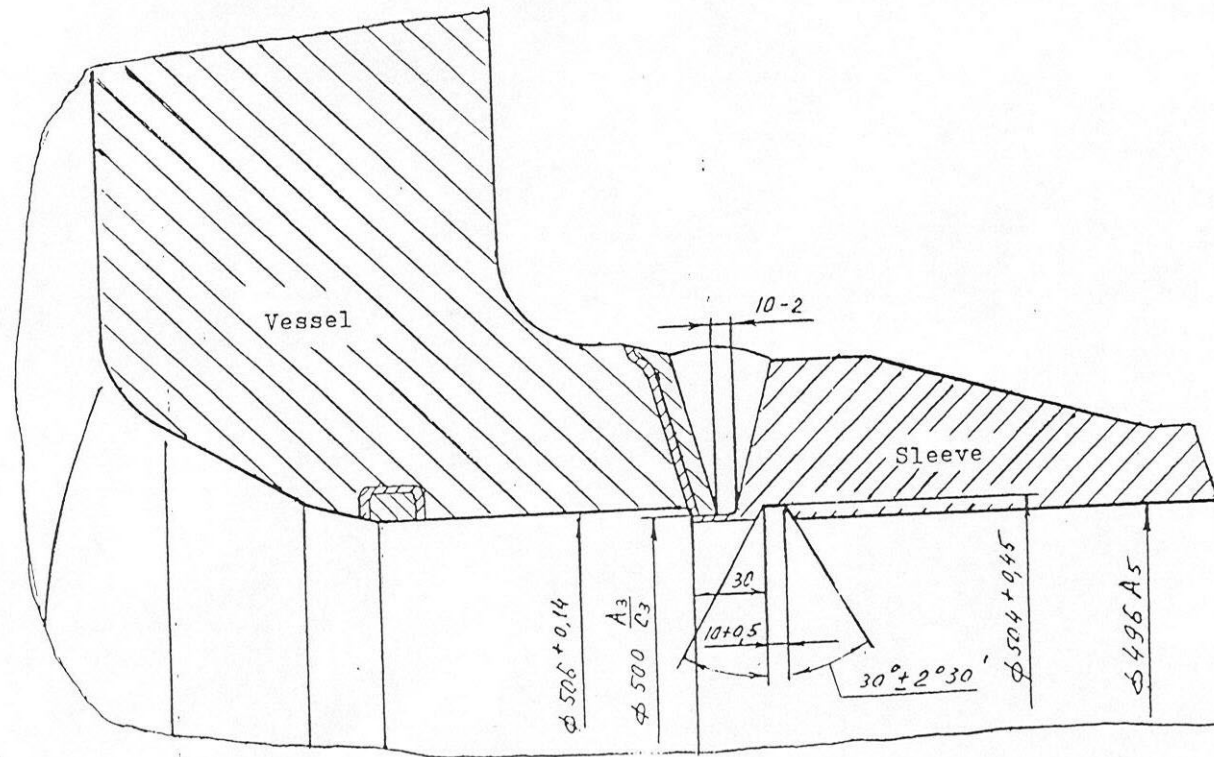
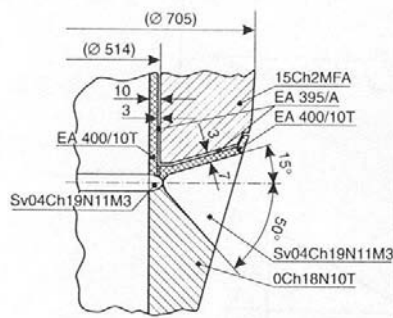
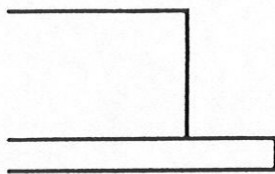


FIG. 2-47. Design of nozzle Dnom 500 of reactor vessels, NV NPP – Units 3, 4, and Kola NPP – Unit 1, showing completed weld between reactor nozzle and sleeve.

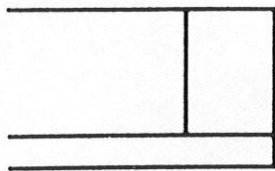


Type of Welding Material	Welding and Surfacing Materials	Chemical Composition in Weight Percent										%	
		C	Si	Mn	P	S	Cr	Ni	Mo	Co	Other	N	δ -Fe
CrNiMo 16/25/6	Electrode EA 395/A	max. 0.12	0.35 0.70	1.20 2.80	max. 0.030	max. 0.018	13.50 17.50	22.0 27.0	4.50 7.0	max. 0.05	0.10 0.15	-	
CrNiMo 19/11/3	Electrode EA 400/10T	max. 0.10	max. 0.60	1.15 3.10	max. 0.030	max. 0.025	16.80 19.0	9.0 12.0	2.0 3.50	max. 0.05	V 0.30 0.75	2 8	
	Welding Wire Sv 04Ch19N11M3	max. 0.08	0.30 1.20	0.80 2.0	max. 0.030	max. 0.020	16.0 20.0	9.0 12.0	1.5 3.0	max. 0.05	-	2 8	

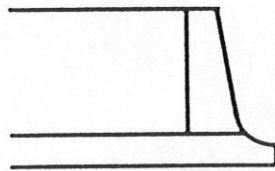
FIG. 2-48. Detail of dissimilar metal weld between reactor pressure vessel and reactor coolant line in a WWER 440 plant.



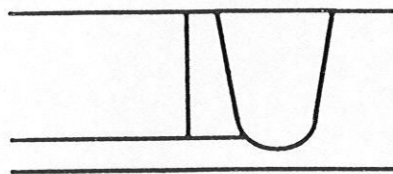
penetration testing of weld edges



after stress relieving (PWHT):
penetration testing of buttering,
ultrasonic testing for bonding



after machining:
penetration testing of weld edges



after OD -/ ID - machining/grinding:
penetration testing of OD -/ ID - surface,
radiographic testing,
ultrasonic testing of ID - surface in root
area

FIG. 2-49. Fabrication and testing sequence for bimetallic (dissimilar metal) welds.

A typical inspection programme for stainless steel piping welds includes radiographic/ultrasonic inspection of all welds including dissimilar welds as shown in Figure 2-51, and ultrasonic inspection of buttered surfaces prepared for dissimilar welds. Liquid penetrant testing is used for all weld surfaces and for all internal and external surfaces of cast components.

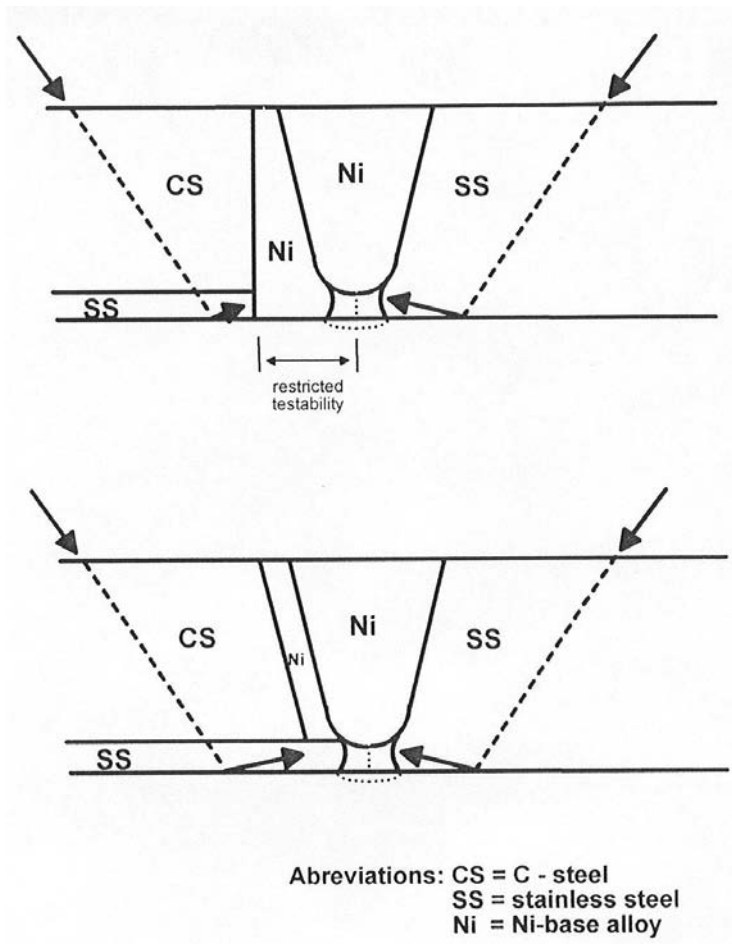


FIG. 2-50. In-service inspectability of inside diameter surface of a bimetallic weld.

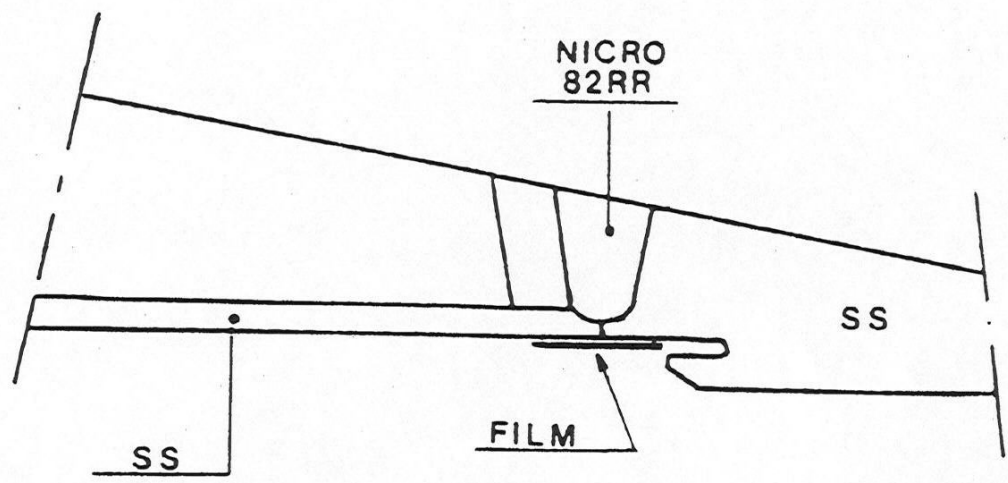


FIG. 2-51. Radiographic preservice inspections of a bimetallic weld on a large nozzle.

An example of typical inspection programme used for carbon steel piping is that performed in Germany. Siemens performed ultrasonic inspection of the cladding from the outside surface on the total component surface to inspect for disbonding of the cladding and to detect postulated underclad cracks on production test coupons, which are taken directly from the straight clad pipe or clad elbow. It performs the following:

- a chemical analysis on chips taken from the skin of the cladding on production test coupons for dilution control of the welding process
- radiographic and ultrasonic testing of the butt welds
- liquid penetrant testing of the cladding
- magnetic particle testing of the ferritic weld surface.

2.8. Pre-service testing

The preservice pressure tests in German PWRs are performed according to the Standard KTA 3201.4. The specified test pressure is 1.3 times the design pressure. The specified test temperature should be at least 33°C, but not more than 55°C, above the actual (calculated) nil-ductility transition temperature. The test procedure also specifies the gradient of pressure and temperature across the pipe wall thickness. The preservice pressure test in French PWR's is performed according to French regulation and the RCC-M Code [2.7]. The specified test pressure is 1.3 time the design pressure for wrought material and 1.5 time the design pressure for cast material.

Code OM-3 [2.8] states the requirements for preoperational and initial startup vibration tests of piping systems, which is intended to identify and correct problems in piping vibrations before the plant begins commercial operation. There are requirements for both steady-state and transient vibration monitoring. Some systems are accessible for visual inspection, while local monitoring systems that transmit data to remote collecting and analyzing stations must be used for inaccessible (for example, because of radiation or temperature) locations. Acceptance criteria are ASME Code stress limits or limiting deflections. Further, piping systems are subject to preoperational testing following system turnover. These procedures are also used in France.

2.9. Reactor coolant system water chemistry

The requirements on the primary circuit with respect to the water chemistry can be summarized as follows:

- the metal release rate of structural materials has to be minimized
- selective corrosion has to be avoided
- deposits on heat transfer surfaces has to be minimized
- the dose rate buildup has to be reduced
- radiological oxygen formation has to be suppressed as far as possible.

The important parameters of the primary reactor coolant chemistry are the boric acid, lithium hydroxide, and hydrogen concentrations, and the resulting pH level. For current PWR operation, the typical range of $\text{pH}_{300^\circ\text{C}}$ (pH measured at 300°C) is 6.9 to 7.4. A minimum value of 6.9 is required to avoid heavy crud deposits on fuel rods, which can cause accelerated corrosion of fuel rod cladding and increased radiation fields [2.9]. Some test results show that operation at $\text{pH}_{300^\circ\text{C}}$ of 7.4 results in less crud deposits than that at 6.9. The $\text{pH}_{300^\circ\text{C}}$ for most of the EDF plants is 6.9, whereas six plants are experimenting with a value of 7.1 [2.10].

Boron is added in the form of boric acid (H_3BO_3) as a neutron absorber for reactivity control. The boric acid concentration is changed throughout a reactor cycle to compensate for other changes in reactivity and is not varied independently. The boron levels are relatively high (1000–2500 ppm) at the beginning of the fuel cycle, depending on the length of the cycle. Then, they are gradually reduced by 100 ppm/month. The concentration of lithium hydroxide (LiOH) is coordinated with the boric acid concentration to achieve the desired $pH_{300^\circ C}$ of approximately 6.9 or higher at operating temperature. At the beginning of the fuel cycle, for $pH_{300^\circ C} = 6.9$, the typical lithium concentration is in the range of 1.8 to 4 ppm for a corresponding boron level in the range of 1000 to 2000 ppm, and then it is reduced as the boron concentration reduces [2.9]. One exception is the B&W plants, where the lithium concentration is limited to 2.2 ppm maximum, independent of the boron level. So, in some B&W plants, depending on the initial boron level, initial $pH_{300^\circ C}$ can be less than 6.9.²

Hydrogen is added to the primary coolant to suppress the buildup of oxygen from radiolysis. A hydrogen concentration of 25 to 50 cm^3/kg has typically been used.

REFERENCES TO SECTION 2

- [2.1] EDMUNDSON, J., (ABB Combustion Engineering), Private communication with V.N. Shah (1992).
- [2.2] USNRC, “Cracking in Piping of Makeup Coolant Lines at B&W Plants,” USNRC Information Notice 82-09 (1982).
- [2.3] SU, N.T., Special Study Report — Review of Thermal Stratification Operating Experience, AEOD/S902, U.S. Nuclear Regulatory Commission Office of Analysis and Evaluation of Operating Data (1990).
- [2.4] EGAN, G.R., et al., Inspection of Centrifugally Cast Stainless Steel Components in PWRs, EPRI NP-5131, Electric Power Research Institute, Palo Alto, CA (1987).
- [2.5] HEBBLE, T.L., et al., Analysis of Delta-ferrite Data from Production Stainless Steel Pipe Welds, NUREG-CR-3482, ORNL-6024, Oak Ridge National Lab. TN (1984).
- [2.6] RCC-M Code, “Design and Construction Rules for Mechanical Components of PWR Nuclear Islands”, Paris, AFCEN, 2000 edition.
- [2.7] ABBOTT, S.L., et al., The Westinghouse Reactor Vessel Life Extension Variance Study, Proc. Topical Meeting on Nuclear Power Plant Life Extension, snowbird, UT, Volume 2, American Nuclear Society, LaGrange Park, IL, 210–224.
- [2.8] ASME 1994, Requirements for preoperational and initial start-up vibration testing of nuclear power plant piping systems, ASME OM-3, American Society of Mechanical Engineers, 1994.
- [2.9] LOTT, R.G., et al., “Primary water stress corrosion crack growth rates in alloy 600 steam generator tubing”, Proceedings of the Fifth International Symposium on Environmental Degradation of Materials in Nuclear Power Systems — Water Reactors, Monterey, CA, 25–29 August 1991, American Nuclear Society, La Grange Park, IL (1992).
- [2.10] BERGE, P., et al., “The effects of chemical factors on stress corrosion of alloy 600 exposed to the cooling medium in pressurized water reactors”, Proceedings of the Fifth International Symposium on Environmental Degradation of Materials in Nuclear Power Systems — Water Reactors, Monterey, CA, 25–29 August 1991, American Nuclear Society, La Grange Park, IL (1992), 533–538.

² Shah, V.N. 1994. Private communication with S. Fyfitch, B&W Nuclear Technologies, August 26.

3. DESIGN BASIS: REGULATIONS, CODES AND GUIDES

The design, manufacture, processing and testing of materials and product forms for the reactor coolant system piping are generally subject to regulations, codes, and standards of the countries where the respective plants were designed and built. Further, the condition of the reactor coolant system piping is inspected and evaluated for operating NPPs. There are several levels of governing documents for nuclear plants. On the top level are federal (or national) regulations, on the next level, codes and standards referenced by the federal (or national) regulations, and on the next level, codes and guidance (such as regulatory guides) intended to ensure quality in fabrication.

3.1. US regulations, codes and standards

3.1.1. US regulations

The Code of Federal Regulations, Title 10, Part 50 (10 CFR Part 50), “Domestic Licensing of Production and Utilization Facilities,” contains rules for the design, construction, operation, and inspection of NPPs. 10 CFR 50.2, “Definitions”, defines the reactor coolant pressure boundary (RCPB). 10 CFR 50.55a, “Codes and Standards,” establishes a set of acceptable standards, the Boiler and Pressure Vessel Code of the American Society of Mechanical Engineers (ASME Code), for design, fabrication and inspection. Only ASME Code Section III, “Rules for Construction of Nuclear Plant Components”, and Section XI, “Rules for In-service Inspection of Nuclear Power Plant Components,” are endorsed by the regulations. The three appendices of 10 CFR 50 relevant to the reactor coolant system piping are Appendices A, B, and G. Appendix A, “General Design Criteria for Nuclear Plants”, lists the criteria that plant design must meet. The relevant general design criteria (GDC) are as follows:

- GDC 1 and 30 relate to quality standards for design, fabrication, erection and testing.
- GDC 4 relates to compatibility of components with environmental conditions.
- GDC 14 and 31 relate to the extremely low probability of rapidly propagating fracture and gross rupture of the reactor coolant pressure boundary (RCPB).

Appendix B, “Quality Assurance Criteria for NPPs and Fuel Reprocessing Plants”, requires a description of the quality assurance programme to be applied to the design, fabrication, construction, and testing of the NPP structures, systems, and components that prevent or mitigate the consequences of postulated accident that could cause undue risk to the health and safety of the public.

Appendix G, “Fracture Toughness Requirements”, relates to materials testing and acceptance criteria for the fracture toughness of the reactor coolant pressure boundary components. It requires that the pressure retaining components made of ferritic materials meet the requirements for fracture toughness during system hydrostatic tests and any condition of normal operation, including anticipated operational occurrences.

The Code of Federal Regulations, Title 10 Part 54 (10 CFR 54), “Requirements for Renewal of Operating Licenses for Nuclear Power Plants”, contains the rules for license renewal. Continuation of the Current Licensing Basis into the period of extended operation is addressed in 10 CFR 54.33.

3.1.2. US referenced codes and standards

On the next level are the codes referenced in the federal regulations, which require that the reactor coolant pressure boundary design conform to the ASME Code. The part of the ASME Code applicable to fabrication is Section III, “Rules for Construction of NPP Components.” Before 1963 and the issuance of the ASME Code, Section III, piping and components were designed to ANSI/ASME B31.1, “Power Piping” or B31.7 “Nuclear Piping”. The ASME Code identifies specifications for permitted materials in Section III, Appendix I, “Design Stress Intensity Values, Allowable Stresses, Material Properties, and Design Fatigue Curves” [3.1].

The part of the ASME Code applicable to in-service inspection of operating power plants is Section XI, “Rules for In-service Inspection.” Section XI states the minimum in-service inspection requirements for those components. PWR in-service inspection requirements are typically written around four 10-year inspection intervals (Inspection Programme B of Section XI) to cover the 40-year operating life as well as the rules for evaluations of discontinuities, and the rules for repair [3.2]. License Renewal in the US is allowing some plants to extend the operating life to 60-years.

3.1.3. Other US codes and standards

On the third level are the other sections of the ASME Codes and other documents such as regulatory guides used for fabrication. These include Section II, “Materials”, Part A, “Ferrous Materials Specifications”, Part B, “Nonferrous Materials Specifications”, and Part C, “Specifications for Welding Rods, Electrodes, and Filler Metals”, Section V, “Nondestructive Examination”, and Section IX, “Welding and Brazing Qualifications.” There are numerous regulatory Guides that give guidance, not requirements, to control weld quality, prevent sensitization of stainless steels, and other such matters. For a list of relevant regulatory guides see the US NRC Standard Review Plan, NUREG 0800, Section 5.2.3, “Reactor coolant pressure boundary materials.”

3.2. Regulations, codes and standards in other countries

As a general rule, the design, the manufacture, processing and testing of materials and product forms for the pressure-retaining piping (as other components) in the reactor coolant systems of NPPs are subject to codes, standards and regulations of the countries where they are built at the time the respective plants were planned and constructed.

For instance, the “Regulation on the construction and safe operation of equipment in NPP, experimental and research reactors and facilities” in the former Soviet Union are the generic regulations on construction.

Regulations and specification determine the approved base materials on the product forms used; also welding materials are specified; welded connections are examined in accordance with regulations as well. Higher-level, more detailed requirements for base metals and welding materials are specified in related higher-level codes, standards, and guidelines, e.g. ASME in USA, RCC-M and government decree in France, KTA and RSK/GRS guidelines in Germany and PNAE in the Russian Federation. Usually component and part-specific requirements as well as manufacturing, materials and examination requirements are laid down in technical specifications as well as in planning and design documents.

The “1974 French Decree” for Class 1 components of NPPs is the generic regulation for design, fabrication, overpressure protection and in-service surveillance of these components. A new set of regulation will be issued in 1999 and 2000: one for surveillance during operation and one for design and fabrication of new NPP components and spare parts.

3.3. Design basis (expected) transients

Design of the reactor coolant system piping components is based on the expected number of transients during the plant operation. These expected transients are called design basis transients and include between 200 and 500 plant heat-up and cooldown cycles and several other cycles as listed in Tables XV through XVII. These transients are based on maximum anticipated events and in most cases consist of conservative assumptions both in terms of anticipated number of cycles and in the severity of the transients. These transients are originally estimated in plant design specifications and are included in the plant Final Safety Analysis Reports (FSARs). The fatigue analyses of the components subjected to these design transients are performed before the plant is actually built and operated. These fatigue analyses serve as a basis for verification of adequate margin of safety against the initiation of a fatigue crack.

Typical design basis transients and the associated numbers are shown in Tables 3.1 through 3.3 for the three US NSSS PWR vendors. However, different plants supplied by the same vendor may have a different set of design basis transients. For example, the number of earthquake cycles (not shown in Tables 3.1 through 3.3) vary depending on plant location. The NRC Standard Review Plan (NUREG-0800) mentions 5 OBE events with 10 cycles each for a total of 50 cycles. However, many plants predated the Standard Review Plan and the number of OBE cycles assumed ranged from 10 to 650 [3.3]. As another example, a large number of plant loading and unloading cycles were assumed in all designs to account for load following; however, the plants have typically been operated as base-loaded plants and the number of loading and unloading cycles has been relatively small.

In addition to the conservative numbers of cycles, thermal, stress, and fatigue analyses often include conservative assumptions related to the transients. As long as the cumulative usage factor can be demonstrated to be less than the ASME Code allowable limit of 1.0, analyses can be simplified to reduce computational effort. If the cumulative usage factor is greater than 1.0 in the initial calculations, then refinements reducing some of the conservatism in the assumptions may be applied so that the calculated cumulative usage factor becomes less than 1.0. This cumulative usage factor is reported in the Final Safety Analysis Report, but still is greater than would be calculated if all conservative assumptions were eliminated. As an example of a conservative assumptions in the thermal analysis, the actual heatup or cooldown rates may be considerably less than the corresponding design basis transient as shown in Figure 3-1. Therefore, the temperature gradients used in the thermal analyses are more severe than actually occur. Deardorff and Smith [3.4] identify several other conservatisms present in the initial thermal, stress, and fatigue analyses.

Tables XV through XVII are not a comprehensive list of all transients, but only provide an overview of different transients and the number of transients considered in the fatigue evaluations performed using the ASME Section III procedures. Several other Westinghouse plant transients, which are normally considered in addition to the transients listed within the table, are listed at the end of Table XVIII.

In calculating the cumulative fatigue usage factor for a particular component, the contributions from all applicable transients should be considered. However, in actual practice some transients are important, whereas other transients may be relatively unimportant for the same component.

Experience has shown that the exact loadings (and their frequency) cannot be anticipated entirely accurately during the design stage. For example, thermal stratification (not considered in the design) has occurred in the fluids flowing in lengths of horizontal piping and this has caused bowing of the pipe which may damage the pipe and the supports.

Testing of systems and equipment can be a major stressor for some components. Some of the testing conditions were anticipated in the design phase, whereas others, for example testing of safety injection and charging system valves, were added after the plant started operating.

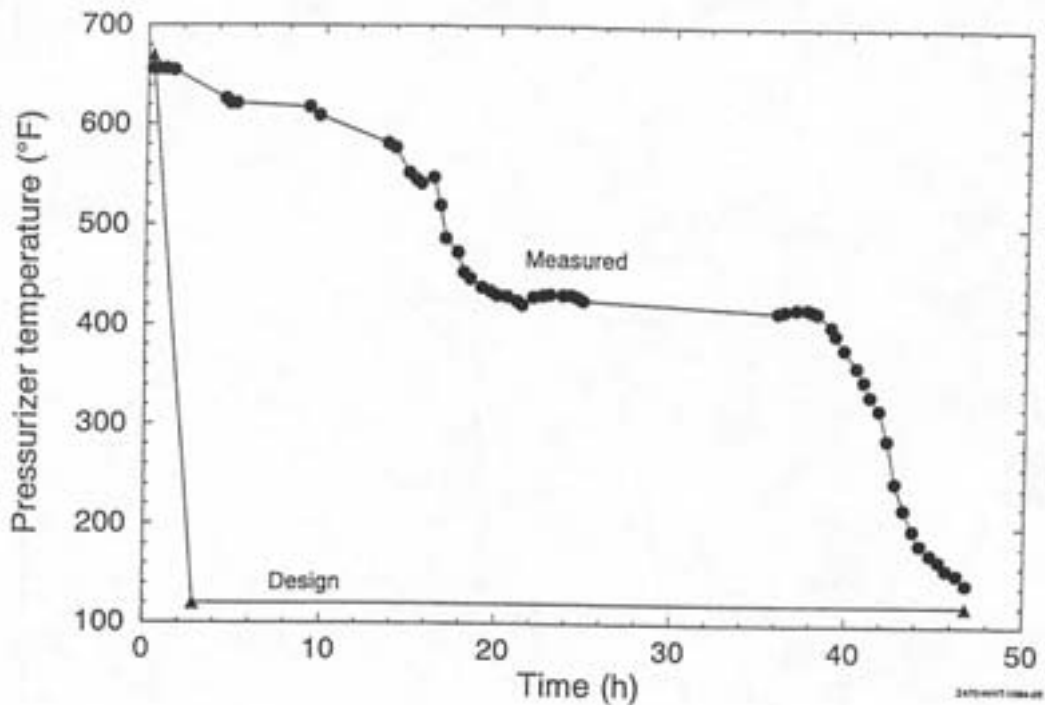


FIG. 3-1. Design basis and typical cooldown transients.

TABLE XV. DESIGN TRANSIENTS AND CYCLES FOR BABCOCK AND WILCOX REACTOR COOLANT SYSTEMS

Transient	Number	Description
More significant contributor to CUF		
Plant heat-up	240	21°C (70°F) to 292°C (557°F) at < 55°C/h (100°F/h)
Plant cooldown	240	292°C (557°F) to 21°C (70°F) at < 55°C/h (100°F/h)
Rapid depressurization	80	2200 to 300 psig in one hour; accompanying significant temperature drop
Reactor trip	400	Reactor trip from full power
Hydrotest	35	Test at 3125 psig
Less significant contributor to CUF		
Power change	1,440	277°C (532°F) to 304°C (579°F), 0% to 15% of full power at 5%/min and 306°C (582°F) to 277°C (532°F), 15% to 0% full power at 5%/min
Plant loading and unloading	48,000	8% to 100% of full power at 10% of full power/min, or 100% to 8% of full power at 10% full power/min
Step load change	8,000	Increase or decrease of 10% of full power
Turbine trip	310	Step load reduction from full power to auxiliary power
Rod withdrawal accidents	40	
Control rod drop	40	

(°F = 9/5° + 32; psi = 6895 Pa)

TABLE XVI. DESIGN TRANSIENTS AND CYCLES FOR THE COMBUSTION ENGINEERING REACTOR COOLANT SYSTEM

Transient	Number	Description
More significant contributor to CUF		
Heat-up	500	From <93°C/200°F (<21°C/70°F) to >285°C/545°F at <55°C/h (100°F/h)
Cooldown	500	From >285°C/545°F to <93°C/200°F (<21°C/70°F) at <55°C/h (100°F/h)
Pressurizer heat-up	500	Pressurizer temperature from <93°C/200°F (<21°C/70°F) to >345°C/653°F at <110°C/h (200°F/h)
Pressurizer cooldown	500	Pressurizer temperature from >345°C/653°F to <93°C/200°F (<21°C/70°F) at <110°C/h (200°F/h)
Hydrostatic test cycle	10	0 to 3110 psig (3125 psig to 0 psig)
Reactor trip	400	Trip from 100% rated thermal power
Less significant contributor to CUF		
Turbine trip	40	Total load rejection from 100% rated thermal power followed by resulting reactor trip
Leak test cycle	200	0 to 2250 psig to 0 psig with RCS temperature less than minimum for criticality (<350°C/400°F)
Loss of reactor coolant flow	40	Simultaneous loss of all reactor coolant pumps at 100% rated thermal power
Seismic load	200	1/2 design basis earthquake (full Operating Basis Earthquake)
Loss of secondary pressure	5	Loss of secondary pressure while in modes 1, 2 or 3
Pressurizer spray	—	Spray operation consisting of opening and closing either the main spray valves with spray water to pressurizer water temperature difference >93°C/200°F (>54°C/130°F), or auxiliary spray valves with spray water to pressurizer water temperature difference >93°C/200°F (>60°C/140°F)
Plant unloading at 5%/minute	15,000	
Plant loading at 5%/minute	15,000	

(°F = 9/5° + 32; psi = 6895 Pa)

TABLE XVII. DESIGN TRANSIENTS AND CYCLES FOR THE WESTINGHOUSE REACTOR COOLANT SYSTEM

Transient	Number	Description
More significant contributor to CUF		
Heat-up	250	T _{ave} from <93°C/200°F to >287°C/550°F at <55°C/h (100°F/h)
Cooldown	250	T _{ave} from >287°C/550°F to <93°C/200°F at <55°C/h (100°F/h)
Pressurizer cooldown	250	From T _{pressurizer} >343°C/650°F to <93°C/200°F at <110°C/h (200°F/h)
Loss of load, without reactor trip	100	>15 to 0% of rated thermal power
Loss of off-site ac	50	Loss of ac off-site electrical
Reactor trip	500	100 to 0% of rated thermal power
Reactor trip from full power	400	
Primary Hydrotest at 3125 psi, 204°C (400°F)	10	
Less significant contributor to CUF		
Large step load decrease	200	100 to 0% of rated thermal power
Inadvertent auxiliary spray actuation	10	Spray water temperature differential >160°C/320°F
Loss of flow in one loop	100	Loss of only one reactor coolant pump
Pipe break	1	Break in Reactor Coolant System pipe >152 mm (6 in.) equivalent diameter
Operating basis earthquake	400	20 earthquakes with 20 cycles/earthquake
Unloading between 0 and 15% power	500	
Loading between 0 and 15% power	500	
Plant unloading 5% full power/minute	13,200	
Plant loading at 5% full power/minute	13,200	
Reduced temperature return to power	2000	
Step load increase at 10% full power	2000	
Step load decrease at 10% full power	2000	
Feedwater cycling	2000	
Primary side leak test	200	

(°F = 9/5° + 32; psi = 6895 Pa)

TABLE XVIII. TRANSIENTS AFFECTING AUXILIARY LINES IN ADDITION TO OVERALL PLANT TRANSIENTS

Normal RHR operation
Inadvertent blowdown
Refueling
Post LOCA
Safety injection system actuation
Loss of charging and recovery
Loss of letdown
High head safety injection (HHSI)
Long term re-circulation with low head safety injection (LHSI) and HHSI

In France the transient list has to be review periodically by comparison with plant transient databank; if necessary (more severe transient or more numerous transient) the initial transient list will be revised and corresponding part of the stress report will be revised to assure a cumulative usage factor less than 1.

The plants are also designed to accept unusual conditions such as severe earthquakes and dynamic loadings resulting from other design basis events.

3.4. Design fatigue analysis of piping

This section outlines the fatigue analysis methods in the B31.1, B31.7, and ASME Codes that have been used for nuclear piping and branch nozzles. The present ASME Code analysis techniques are summarized in Section 3.4.1 and fatigue analysis practice in Germany is summarized in Section 3.4.2. Past and present ASME fatigue analysis practices are described in more details in Section 5.1.1 and 5.1.2, respectively.

3.4.1. Present ASME code design requirements

The basic stress (S) versus cycles (N) design fatigue curves (sometimes referred to as S-N curves) follow the relation proposed by Langer:

$$S = B N^{\frac{1}{2}} + S_e$$

where B and S_e are constants determined using linear, least-squares regression analyses to the data [3.5].

The ASME design curves were developed by applying a factor of 2 on stress or 20 on cycles, whichever is lower at a given point, to the mean best-fit curve for small, polished specimens. For less than 10 000 cycles, the factor 20 on the cycles gives the lower curve. These factors are intended to account for size effects, surface finish, statistical scatter of the data, and differences between laboratory and industry environments, but not the effects of a

specific coolant. The factor 20 on cycles is a product of three subfactors: a subfactor of 2.5 for size, 2.0 for data scatter, and 4.0 for surface finish and atmosphere [3.6]. Large scale carbon steel vessel fatigue tests have been performed in air at room temperature for the specific purpose of checking the ASME fatigue design curve [3.7]. It was shown by these tests that cracks may initiate below the ASME fatigue design curves, but that wall penetration is not expected until the fatigue cycles exceed the ASME design curves by about a factor of 3 [3.8]. Recent fatigue tests on ferritic and stainless steel elbows, subject to inplane bending moments in air at room temperature, have also shown that cracks initiate when the fatigue design curve is reached, and that full-wall penetration occurs when the fatigue cycles exceed the design curve by a factor between 2 and 3 [3.9]. Manjoine and Tome [3.10] assign equal weighing (about 20% each) to account for surface finish, size effects, material variability, environment, and residual stresses.

3.4.2. Fatigue analysis practice in Germany

The German practice is described in the KTA Standard (KTA 3201.2). The procedure is principally equivalent to the ASME Code. The fatigue design curves in this standard are identical to those in the ASME Code up to 10^6 cycles. The newer extension of the ASME design curve for austenitic material (up to 10^{11} cycles) was not adopted in the KTA Standard for piping because such extension was not considered to be necessary. But such extension has been adopted for reactor internals.

3.4.3. Fatigue analysis practice in France

The French design rules presented in the RCC-M [3.11] are derived from ASME fatigue analysis methods, but a lot of improvements are proposed on different aspects, some directly concern fatigue analysis of piping systems [3.12]:

- crack like defect fatigue analysis method (RCC-M appendix ZD)
- Ke optimisation for stainless steel piping (RCC-M B3650)
- combination of finite element approaches and piping rules (RCC-M appendix ZE).

Figure 3-2 presents a comparison between ASME and RCC-M Ke; in French practices the linear temperature gradient ΔT_1 has to be considered in the plastic shakedown rules. RCC-M fatigue curves are currently limited to 10^6 cycles.

3.5. Assessment of fracture toughness

Determination of the critical transition temperature for piping materials is performed in Western countries on the basis of Charpy impact testing as defined in the ASME Code, Section III/NB 2300, KTA 3201.1 and 3201.3, or RCCM; V-notches for ferritic material (preferably in USA and Germany also for austenitic material) or U-notches are used. A test shall consist of a set of three full-size 10 mm \times 10 mm specimens oriented in defined direction; according to ASME specimens from material for pipe shall be oriented in the axial direction, whereas according to KTA in the transverse direction. Normally absorbed energy (the requirement for the transition temperature is at least 68 J), lateral expansion (the requirement for the transition temperature is at least 1.0 mm (0.040 in.) for axial direction and 0.9 mm in transverse direction) and sometimes a percentage of the brittle/ductile fracture (in Germany) is measured.

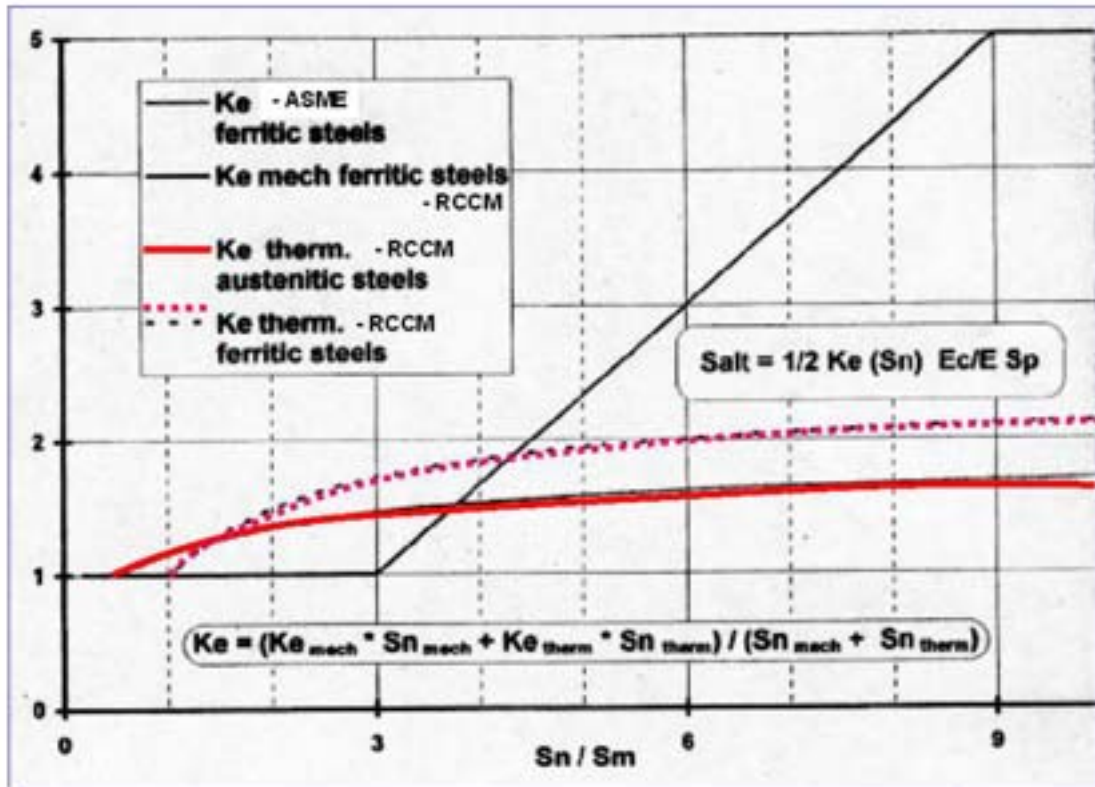


FIG. 3-2. Comparison of ASME and RCCM K_e formula.

Additional NDT drop weight tests are required in Germany for class 1 piping made of ferritic steel in order to fulfil the RT_{NDT} concept; this shall be done as follows:

- Determine a temperature T_{NDT} that is at or above the nil-ductility transition temperature by drop weight tests
- At a temperature not greater than $T_{NDT} + 33$ K, each specimen shall exhibit at least 0.9 mm lateral expansion and not less than 68 J absorbed energy. When these requirements are met, T_{NDT} is the reference temperature RT_{NDT} .
- In the event that the requirements above are not met, additional Charpy-tests have to be conducted to determine the temperature T_{CV} at which they are met. In this case the reference temperature $RT_{NDT} = T_{CV} - 33$ K. Thus, the reference temperature is the higher of T_{NDT} and $(T_{CV} - 33K)$.

The critical transition temperature according to Russian concept is that temperature, which meets the following requirements:

- the mean notch toughness determined in transverse specimens at a temperature T_k or greater shall not be below 32 J (for yield strength 300 to 400 MPa)
- the single value of notch toughness at a temperature T_k shall not be below 70% of the mean value
- the mean notch toughness determined at a temperature $T_k + 30$ K and higher shall be at least 1.5 times the mean value at T_k
- the percent ductile fracture of each specimen shall not be less than 50% at $T_k + 30$ K.

Conclusions, especially with respect to LBB behavior, are based on the precondition that toughness properties of the regarded system, including base metal and welds (also bimetallic welds as far as involved) are good enough to assure ductile failure mode; that means according to common practice Charpy-V 68 J at lowest service temperature (German investigations on specimens and components) with different toughness properties confirmed that Charpy-V 45 J are sufficient to guarantee ductile failure, see Section 5.12). Consideration of environmental conditions during the service life of the component need to be done as a part of any assessment of toughness.

In France, the fracture analysis of all Class 1 components is formally required at the design stage for last 4-loop plants and for spare parts [3.13]. The end of life toughness of each material (base metal and welds) has to be sufficiently high for the design life of the component to accept a deep crack on the inner or outer surface in all conditions (normal, upset, emergency and faulted) with specific safety factors. A particular attention is done on component that can have an operating temperature less than the brittle-ductile transition temperature.

REFERENCES TO SECTION 3

- [3.1] ASME, ASME Boiler and Pressure Vessel Code, Section III Components — Rules for Construction of Nuclear Power Plant, American Society of Mechanical Engineers, New York (1995a).
- [3.2] ASME, ASME Boiler and Pressure Vessel Code, Section XI — Rules for Inservice Inspection, American Society of Mechanical Engineers, New York (1995b).
- [3.3] WARE, A.G., Fatigue Monitoring for Ageing Assessment of Major LWR Components, NUREG/CT-5824, EGG-2668, Draft (1994).
- [3.4] DEARDORFF, A.F., SMITH, J.K., Evaluations of Conservatisms and Environmental Effects in ASME Code Section III, Class 1 Fatigue Analysis, SAND-94-0187, UC-523, Sandia National Laboratories, (1994).
- [3.5] JASKE, C.E., O'DONNELL, W.J., Fatigue Design Criteria for Pressure Vessel Alloys, Journal of Pressure Vessel Technology, November 1977, 584–592.
- [3.6] HARVEY, J.E., Pressure Component Construction, Van Nostrand Reinhold Company, New York, NY (1980)
- [3.7] KOOISTRA, L.F., LANGE, E.A., and PICKETT, A.C., “Full size pressure vessel testing and its approach to fatigue”, Journal of Engineering for Power, Transactions of the American Society of Mechanical Engineers, 86, 4, (1961) 419–28.
- [3.8] COOPER, W.E., “The initial scope and intent of the Section III fatigue design procedures”, paper presented at the Pressure Vessel Research Council Workshop on Environmental Effects on Fatigue Performance, Clearwater Beach, Florida, 20 January 1992 (1992).
- [3.9] KUSSMAUL, K., et al., Deformation and Failure Behaviour of Elbows: Experimental Results and Analytical Predictions, University of Stuttgart (1988).
- [3.10] Manjoine and Tome 1983.
- [3.11] RCC-M Code, “Design and Construction Rules for Mechanical Components of PWR Nuclear Islands”, Paris, AFCEN, 2000 edition.
- [3.12] FAIDY, C., “Fatigue analysis in French Nuclear Codes”, ASME Pressure Vessel and Piping Conference, San Diego, USA, July 1998.
- [3.13] FAIDY, C., “Recent Changes in French Regulation and Codes for Nuclear and Non-Nuclear Pressure Equipments”, ICONE8, International Conference on Nuclear Engineering, paper 8636, Baltimore, USA, April 2000.

4. AGEING MECHANISMS AND OPERATING EXPERIENCE

Six ageing mechanisms are discussed in this section that tend to reduce the life of the reactor coolant system piping components: thermal fatigue, vibrational fatigue, thermal ageing, primary water stress corrosion cracking, boric acid corrosion and atmospheric corrosion.

Thermal fatigue is the major ageing mechanism for surge, spray and branch lines and their nozzles that are subject to thermal transients during plant startup/shutdown, thermal stratification, thermal shock, turbulent penetration, and thermal cycling. Fatigue design analyses of these piping components included the design basis transients. However, these initial analyses did not include thermal stratification phenomena present in the surge and spray lines, and thermal cycling phenomena present in the branch lines; these phenomena were discovered after the plants were placed in operation. These loads are only considered in the design for the latest French 4-loop plants in the stress report and must be considered for any type of piping replacement in French reactors.

Today, thermal fatigue is not a major ageing mechanism for the main coolant piping. This piping was designed for thermal transients during plant startup and shutdown. This piping has not experienced any unanticipated thermal fatigue loads during operation. No thermal fatigue cracking of this piping has been reported. Therefore, thermal fatigue of main coolant piping is not discussed in this section, the only location that must be considered are the nozzle weld areas in the loop side for connected lines experiencing high fatigue, such as the charging line.

The surge and spray lines, and branch lines are made of austenitic stainless steel in all PWRs, whereas the main coolant lines are made of either austenitic stainless steel (and cast stainless steel) or ferritic steel. The welds joining the austenitic stainless steel piping and ferritic piping are called dissimilar metal welds. These welds experience thermal fatigue damage because the ferritic materials have higher thermal expansion coefficient than that for the austenitic stainless steel materials. The dissimilar metal welds are also present between the stainless steel main coolant piping and ferritic pressure vessels, and are also susceptible to thermal fatigue.

Main coolant loop pipe and fittings made from cast stainless steel are susceptible to thermal ageing. The socket welds between the instrument penetration lines and the reactor coolant loop piping are susceptible to vibration fatigue (high-cycle mechanical fatigue). The Alloy 600 instrument penetrations in the reactor coolant piping are susceptible to primary water stress corrosion cracking.

Boric acid corrosion of carbon steel and low-alloy steel base metal may take place, if the base metal is exposed to the borated reactor coolant; for example, the outside surface of piping exposed to leaking coolant. The PWR licensees, for example, Babcock and Wilcox Owners Group, have identified this mechanism as an applicable ageing effect for reactor coolant system piping [4.1].

In many countries some degradations have been noticed in dissimilar metal welds [4.2]. In France some atmospheric corrosion has been attributed to outer surface degradation of some dissimilar metal welds.

For each ageing mechanism, the related transients and operating environmental factors are discussed, the most susceptible sites are identified, the field experience is summarized, and related activities of regulators and the industry are summarized. The in-service inspection of ageing degradation, particularly thermal fatigue damage, and monitoring of transients causing the damage are discussed in Section 6. The mitigation of ageing degradation is discussed in Section 7.

4.1. Thermal fatigue of pipes and nozzles

4.1.1. Thermal fatigue of surge line

A principal source of fatigue damage in the pressurizer surge line and nozzles is the thermal stresses associated with design-basis thermal transients and the thermal stratification and striping associated with plant heat-up and cooldown, which were not included in the original fatigue design analyses. Typical design-basis thermal transients for Combustion Engineering plants (such as plant heat-up and cooldown, plant leak testing, plant trips, and other plant operational functions) are listed in Table XVI with their specified cycles. Figures 4-1 and 4-2 provide typical temperature and pressure versus time curves, illustrating some of the major transients. Figure 4-1 illustrates a conservative envelope of the reactor coolant temperature and pressure profiles during a plant leak test. Figure 4-2 illustrates the surge nozzle temperature and pressure transients encountered during typical plant heatup and cooldown events. Note that the transient descriptions are for fatigue evaluations only and may not represent actual plant operations. Design calculations performed in accordance with the American Society of Mechanical Engineers Boiler and Pressure Vessel Code [4.3] have demonstrated that those design-basis transients result in acceptable fatigue usage during a 40-year operating life, i.e. the calculated fatigue usage factor is less than the allowable ASME Code value of 1.0. A typical maximum design-basis cumulative fatigue factor for the surge line and nozzle for Combustion Engineering plants is 0.2. The design-basis fatigue usage factors differ for the Westinghouse and Babcock & Wilcox plants but are also below 1.0. For example, one design-basis usage factor calculated for a Westinghouse surge line and nozzle was approximately 0.7 [4.4]. Actual fatigue usage is, of course, a function of plant operation rather than the design assumptions. The French design transients are slightly limiting this phenomenon by a limitation in maximum temperature during heatup and cooldown to 110°C. Some specific designs have an inclined surge line in in this case the more sensitive location for thermal fatigue is the nozzle on the main coolant line area.

Three phenomena responsible for thermal fatigue in surge line and nozzles are thermal stratification, thermal striping, and thermal shock. These phenomena are described next. Then the field observations of surge line thermal stratification are summarized. Finally, the USNRC Bulletin 88-11 and the utilities responses to the bulletin are discussed.

Thermal stratification. The most important loading on the surge line (straight pipe, nozzle ends and elbows) and nozzle is imposed by thermal stratification. Thermal stratification can occur in the horizontal sections of the surge line when, during insurge, cooler, heavier water from the hot leg flows under the warmer, lighter coolant from the pressurizer, and when, during outsurge, warmer, lighter water from the pressurizer flows over the cooler, heavier water, that resides in the surge line. The propensity for stratification of a fluid in a horizontal pipe can be correlated to its Froude number, which is the ratio of the inertial force (velocity head) to the force of gravity (buoyancy head) acting on the fluid. The buoyancy head is caused by the density difference between the hot and cold regions of the

fluid in the pipe, and the magnitude of the buoyancy head is, of course, related to the difference in temperature between the two regions. Therefore, thermal stratification of the fluid in the surge line is likely to occur when the flow velocity during an insurge or outsurge is low and the temperature difference between the pressurizer and the hot leg is large (small Froude number). Conversely, surge line thermal stratification is less likely to occur at high flow velocities and low temperature differences (large Froude numbers). Therefore, the potential for thermal stratification is greatest during heat-up and cooldown because the difference between the pressurizer and hot leg temperatures is then largest.

Prior to start of the reactor coolant pumps, the temperature of the coolant in the hot legs is typically about 55°C (130°F), and the temperature of the coolant in a pressurizer with a steam bubble can be as high as the saturation temperature that corresponds to the pressure at which the reactor coolant pumps can be started, typically 2.24 MPa (325 psi). Therefore, the difference between the coolant temperature in the pressurizer and in the hot leg during heatup may be as high as 180°C (325°F) in some plants. Such a temperature swing in a surge line was measured in a Babcock & Wilcox-designed PWR in Germany (INPO 1987). The maximum temperature difference during cooldown is about 75% of the maximum difference during heat-up. The maximum temperature difference during normal operation is about 28°C (50°F).

The magnitude of the top-to-bottom temperature differences also depends on the piping layout and is different at different cross-sections along the surge line. The temperature distributions are also different for pressurizer insurges and outsurges, several of which take place during reactor heat-ups, cooldowns, and scrams. Monitoring of the San Onofre Units 2 and 3 surge lines (which are identical) indicates that significant thermal stratification develops in the horizontal portion of a surge line near the hot leg only during outsurges, whereas significant stratification develops in the horizontal portion of the surge line near the pressurizer during both outsurges and insurges [4.5].

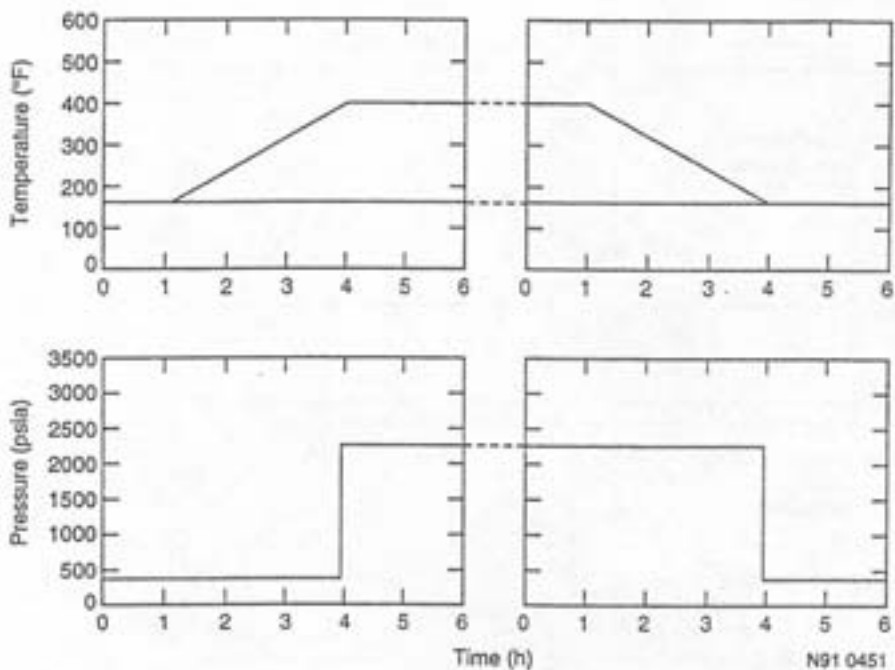


FIG. 4-1. Plant leak test, simulated for fatigue evaluations only.

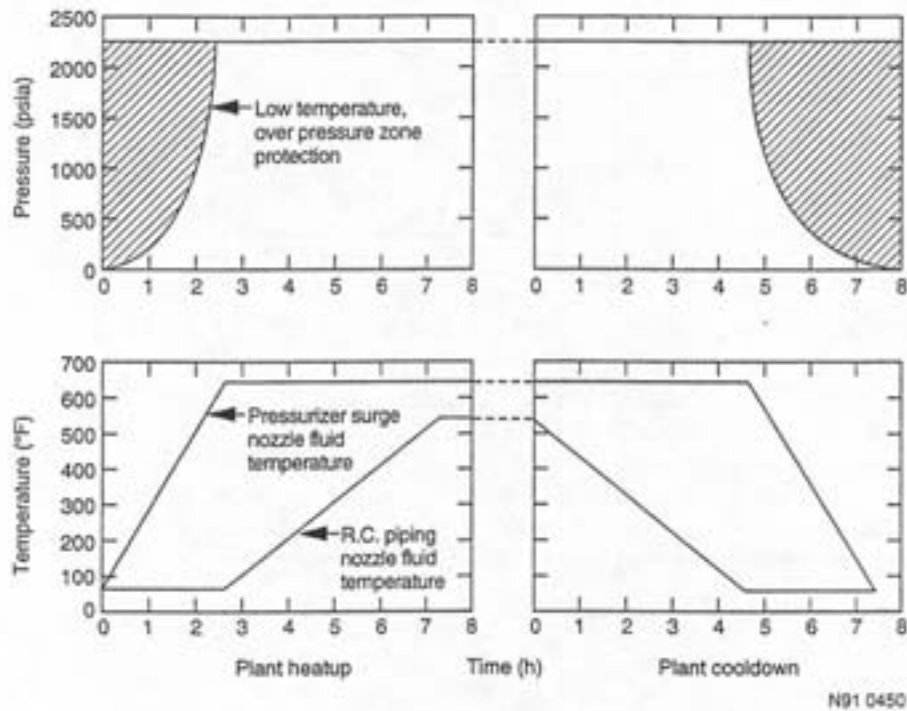


FIG. 4-2. Simulated surge nozzle transient heatup and cooldown for fatigue evaluation only.

The top-to-bottom temperature differences on the outside-surfaces of the surge line near the hot leg were as high as 60°C (110°F) during outsurges and only about 10°C (20°F) during insurges, whereas the differences near the pressurizers were 155°C (280°F) during outsurges and about 100°C (180°F) during insurges. The San Onofre surge lines extend vertically upward from the top of the hot legs, and then horizontally to under the pressurizers, and turn vertically up and connect to the pressurizer surge nozzles.

Stratified flows generate a non-linear temperature gradient across the pipe cross-section with, in some cases, an almost step change in temperature at the interface of the cold and hot coolant. This produces through-wall axial bending stresses and local hoop stresses caused by bending of the pipe cross-section. The magnitudes of the stresses are determined by the top-to-bottom temperature difference and temperature distribution in pipe sections. Axial compressive stresses develop in the hot upper region of the pipe, whereas axial tensile stresses develop in the cold lower region of the pipe. The maximum axial stresses are at the interface between the hot and cold coolants. The distribution of the through-wall bending stresses changes as the flow rate fluctuates and causes the interface between the hot and cold fluids to rise and fall. Thus, fluctuations in the flow rate cause fatigue damage.

When flow stratification persists over a long horizontal section of a line, the amplitude of the resulting cyclic stresses can be large because the flow condition changes from stratification to no stratification and back to stratification. This type of stratification causes significant low-cycle fatigue damage and is termed *global thermal stratification* [4.6]. The large stresses will cause the surge line to bow (macroscopic displacement). For example, thermal stratification caused a 76-mm (3-in.) deflection of the surge line at one plant in the United States [4.7]. Such large displacements result in high loads on the surge line supports along the horizontal run, on the elbows and on the nozzles at its ends. At another plant, thermal stratification caused the horizontal portion of the surge line to deflect downward and

against the pipe whip restraints, resulting in permanent deformation of the pipe [4.8]. The magnitudes of the loads and the bending stresses introduced by such large displacements depend on the surge line layout, end constraints, and the support system. For example, global thermal stratification in the horizontal portion of the surge line between elbows A and B in Figure 2-8 will produce inplane bending, out-of-plane bending, and torsion in elbows A, B, and C, respectively. The highest tensile stresses on a 90-degree elbow subject to in-plane bending are in the elbow mid-section ($\alpha=45$ degrees in Figure 4-3) at the inside-surface of the flank and at the outside-surface of the intrados; calculated fatigue usage factors at some of these sites on the surge line elbows are as high as 0.59.

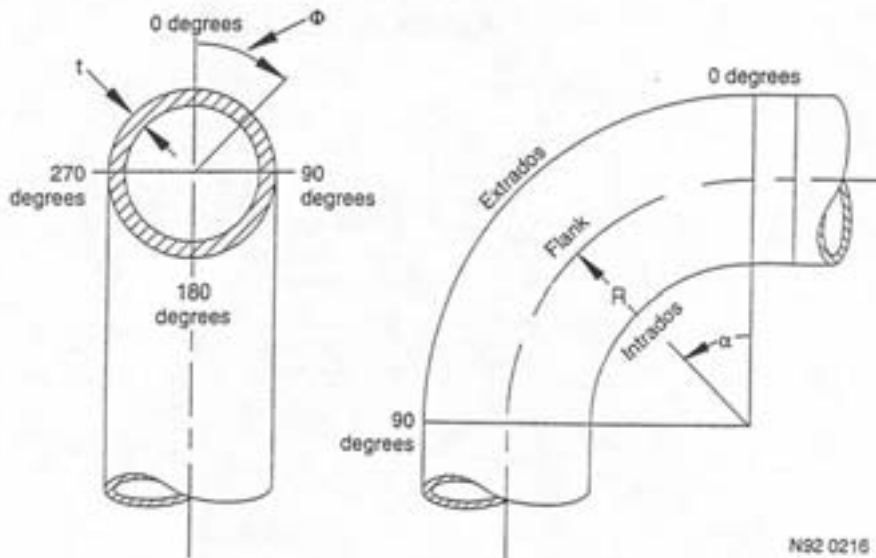


FIG. 4.3. High stress sites are on the midplane ($\alpha = 45$ degrees) at the inside-surface of the flank ($\Phi = 90$ and 270 degrees) and at the outside-surface of the intrados ($\Phi = 180$ degrees).

If thermal stratification is present in a short horizontal section of a pipe, changes in the elevation of the interface between the hot and cold coolants would impose cyclic through-wall bending stresses that cause fatigue damage without any macroscopic displacement of the pipe. To differentiate this type of stratification from global thermal stratification, it is termed *cyclic thermal stratification*.

The pressurizer temperature is about 343°C (650°F) during full-power operation, and the difference in temperatures between the pressurizer and the hot leg is about 28°C (50°F). The flow in the surge line is small and equal to the bypass flow in the spray line (typically 6 l/min) and, therefore, the flow during normal full power operation is also generally stratified. However, the corresponding thermal stresses will be much lower than those during heat-up and cooldown because the difference in temperature between the stratified flow layers is smaller.

Thermal striping. Thermal stratification can induce local cyclic stresses in the portion of the pipe near the inside-surface and adjacent to the interface between the hot and cold coolant layers, if the flow rates are sufficiently high. These stresses are caused by oscillations of the fluid temperature at the interface resulting from interfacial mixing of the hot and cold fluid layers. Such interfacial mixing results in a process called *thermal striping*. The onset of interfacial mixing that leads to thermal striping can approximately be correlated with the

initiation of a Kelvin-Helmholtz instability, which occurs when inertial forces overcome stratifying density differences between the fluid layers [4.9].

Wolf et al. [4.10] have conducted thermal stratification experiments in horizontal feedwater lines at the HDR (Heissdampfreaktor) test facility in Germany. The experiments were performed at several different flow rates with thermocouples mounted on the pipe inside-surface to measure the metal temperatures. Thermal striping was observed only at relatively high flow rates [4.11]. The test results and theory indicate that thermal striping is present when the gradient Richardson number through the interface is less than 0.25 [4.9, 4.12]. The gradient Richardson number is the ratio of the density gradient and horizontal velocity gradient. The typical frequency content of the metal temperature oscillations caused by thermal striping was between about 0.01 and 2 Hz, and the amplitude of the metal temperatures oscillations was less than 50% of the difference in the hot and cold coolant layer temperatures. The amplitude of the metal temperature oscillations was smaller because of the finite heat transfer coefficient and thermal inertia of the pipe wall. The magnitude of the thermal striping stresses is highest on the inside-surface and reduces rapidly through the thickness. Therefore, the high-cycle fatigue damage caused by these stresses is limited to the pipe inside surface adjacent to the interface.

Similarly, the French EDF-R&D programme COUFAST [4.13] performed tests on stratified pipes to confirm some tendency, like:

- the stress amplitude are high only for condition that leads to deep gradient in the piping section, and mainly for low cold flow;
- with constant boundary condition the stratified interface remains more or less stable (no striping).

Thermal shock. A slug of relatively cool fluid could pass through the hot leg surge line nozzle during pressurizer outsurges and impose thermal shock stress cycles on the nozzle and on the nearby surge line piping. Also, cooler water from the surge line piping could pass through the pressurizer surge line nozzle during a pressurizer insurge and impose thermal shock stress cycles on that nozzle. The severity of these stressors depends on the degree of local cooling and the frequency of the insurges and outsurges. There are more outsurges than insurges because of the main spray. Whenever the main spray is used while the pressurizer level remains constant, or decreases, there is an outsurge. During changes in power level, there is an equal number of outsurges and insurges as the power level is reduced and then increased. The occurrence of relatively cold slugs of water is based on evaluation but has not been measured [4.14].

Flow-induced vibration is another common stressor that affects components such as thermal sleeves, installed to protect the nozzles from thermal shock. That stressor could lead to fatigue failure of the thermal sleeve, with the possibility of the thermal sleeve breaking loose and moving through the piping. Some plants have analyzed the thermal shock loadings on the pressurizer surge nozzle and determined that the thermal sleeves are not needed; these plants are allowed to operate without them.

Operating experience on surge line thermal stratification. Unexplained movement of the surge line at a Westinghouse four-loop plant was first observed in 1982. At first the movement was believed to be associated with the removal of the thermal sleeve from the surge line hot leg nozzle. Although thermal stratification was postulated in 1985,

measurements during hot stand-by and power operation produced top-to-bottom temperature differences in the piping that were too low to explain the magnitude of the movement. Subsequently, in 1988 the surge line was found to be in contact with two shims and there was evidence of plastic deformation [4.15]. At this time it was discovered that high top-to-bottom temperature differences were occurring at the time of pressurizer bubble formation, and the subsequent heatup.

A summary of the plant surge line history is as follows:

- 1982 Surge line hot leg nozzle thermal sleeve removed because of failure.
- 1983 Contact observed at two whip restraints. Restraints reshimmed to adjust gap.
- 1984 Contact observed at whip restraint. Restraint reshimmed to adjust gap.
- 1985 Surge line movement noted again. Instrumentation installed. Stratification postulated at hot stand-by, but top-to-bottom temperature differences of only 56°C (100°F) at hot stand-by and 28°C (50°F) at power operations were measured. Two steam generator degraded snubbers were postulated to have restricted RCS thermal growth causing erratic surge line movement.
- 1986 Steam generator snubber lockup and inadequate restraint gaps identified during outage were evaluated. Whip restraint clamp found rotated.
- 1987 Whip restraint modified to change restraint design.
- 1988 Surge line found in contact with whip restraint during whip restraint gap measurement programme. Monitoring programme begun. Evaluation concluded that a potential temperature difference of 170°C (300°F) could occur during drawing pressurizer bubble and heatup. This would be sufficient to explain observed surge line movement.

The 1988 monitoring programme used resistance temperature detectors (RTDs) and linear potentiometers (LPs) [4.16]. General systems data (flow, temperature, and pressure) were also monitored and the following observations were noted. On three occasions stratification developed to the point that the nominal 1.5-in. gap at one pipe whip restraint was closed and contact was developed. The longest period of contact was approximately 45 min. The maximum top-to-bottom temperature difference was just over 140°C (250°F). No contact was observed at other whip restraint.

As a result of these observations, corrective actions were pursued by the licensee. These corrective actions included:

- Performing inspections and non-destructive examinations
- Conducting a piping integrity evaluation
- Establishing a monitoring programme to measure actual temperature distributions and line movements.

Stratification was also measured on other Westinghouse plants [4.17]. On one unit, data were obtained from continuous monitoring of the surge line piping outside surface, pipe displacements, and plant parameters. The data were sufficient to correlate measured temperature fluctuations to changes in plant operation, and confirmed the presence of thermal stratification. Thermal stratification has also been observed in France, with lower temperature

difference (less than 110°C) since the time that surge line temperature monitoring was initiated in 1981 [4.18]. The phenomenon was first observed at Dampierre 4. In 1984, a temperature monitoring programme at Cruas (a three-loop, 900 MW PWR) confirmed that steady state stratification exists on the horizontal portions of the piping and at a horizontal nozzle. The phenomenon is generic to all 900 MW surge lines and was not considered in original design stress reports. A temperature monitoring programme at Cattenom 1 (four-loop, 1300 MW PWR) found reduced thermal stratification, since the surge line joins the hot leg at a 45-degree angle. For the French four-loop plants stratification does not occur, but the interface between cold and hot water is, in this case, close to the primary nozzle, specific developments have been done to develop a complete databank of mixing ratio and heat transfer coefficient in all the nozzle area.

USNRC Information Notice 88-08 and Bulletin 88-11. Licensees were informed of the unexpected surge line movements in the plant in an NRC Information Notice 88-80, issued in October 1988. It reminded the licensees that they were required by the ASME Code to reconcile the pipe stresses between the measured data and analytical results for the thermal stratification condition. Two months later, the Information Notice was followed by Bulletin 88-11.

Bulletin 88-11 requested four actions from PWR licensees. These actions are summarized as follows:

- (1) Conduct a visual inspection (ASME Section XI, VT-3) of the pressurizer surge line. Search for any gross discernable distress or structural damage in the entire surge line, including piping, pipe supports, pipe whip restraints, and anchor bolts.
- (2) Demonstrate that the surge line meets the applicable design codes and other regulatory commitments, considering the effects of thermal stratification and thermal striping in the stress and fatigue evaluation. The fatigue analysis was to be performed in accordance with the latest ASME Code, including high-cycle fatigue.
- (3) If the analysis showed that the surge line did not meet the licensing requirements, submit justification for continued operation, or bring the plant to cold shutdown and develop a detailed analysis of the surge line.
- (4) Update the stress and fatigue analyses, based on the plant-specific or reference data and the observations in 1 above, to ensure compliance with the applicable codes. If the licensee was unable to demonstrate compliance, it was to submit a justification for continued operation and a description of the proposed corrective actions for effecting long term resolution.

Responses to USNRC Bulletin 88-11. Many of the licensee responses to Bulletin 88-11 were based on Owners Groups' submittals. Each Owners Group submitted a generic document (generally using the 1986 edition of the Code for the fatigue analysis) for review by the NRC and provided supporting information in response to NRC questions. In addition, each licensee submitted a plant-specific justification for continued operation, in general referencing the appropriate generic document. The following paragraphs summarize the Owners' Groups responses.

The B&W programme began with extensive local fatigue monitoring and analyses of a 177 fuel assembly plant surge line. For this programme 54 surface-mounted thermocouples

and 23 linear variable differential transformers (LVDTs) and string potentiometers were installed to monitor temperatures and displacements. The results of these programmes were applied to all six operational lowered-loop plants with similar designs [4.19–4.20]. A separate plant-specific evaluation was conducted for the single B&W raised-loop plant. Since the surge line layout was significantly different for this plant, an instrumentation package was installed which included 46 thermocouples mounted on the outside-surface of the surge line and 14 displacement instruments. Each plant conducted a plant-specific visual inspection in accordance with Bulletin 88-11. Both monitoring and a review of the past operational information was used to develop a set of revised design basis transients that included thermal stratification. The thermal stratification transients developed from the instrumentation monitoring were used as thermal input for stress models, and the models were verified by comparing the predicted displacements with the measured ones. Results of HDR tests were used to estimate the fatigue caused by thermal striping. Fatigue analyses were conducted for the both the surge line nozzle and piping. An elastic-plastic model of a surge line elbow was used to verify shakedown and to generate appropriate stress indices for use in an ASME Code NB-3600 fatigue analysis. (In a separate programme, elastic shakedown was computed after two cycles for a German PWR surge line subjected to insurge and outsurge sequences. A cumulative usage factor less than 1.0 was calculated for all locations (a maximum of 0.50 for lowered-loop plants and 0.59 for the raised-loop plant elbows, and 0.62 for the hot leg surge line nozzle).

Licenseses of 15 Combustion Engineering plants in the USA also worked together in an Owners Group (CEOG). A bounding analysis covering all plants was prepared in 1989, however, in addition each licensee had the responsibility for performing the visual inspections required by Bulletin 88-11, and ensuring that the analysis was applicable to its particular plant or plants. Combustion Engineering performed local monitoring of surge lines in three plants. Two plants were instrumented with thermocouples, and the third with RTDs and linear potentiometers (to measure deflections). The measured results were compared to plant operations to identify those evolutions that affected thermal loading significantly. A general similarity among the data indicated that the thermal loading characteristics were generic for all CEOG participants. Based on the instrumentation results, thermal hydraulic models were used to estimate the fluid and pipe wall temperature distributions for stress and fatigue analyses. Each of the plant-specific surge lines was modeled and a bounding, generic stratified flow loading was applied to each model. The $3S_m$ ASME Code limit for primary plus secondary stress range was exceeded. The most highly stressed line was chosen to be evaluated by inelastic analysis with a detailed finite element model. The analyses results indicated that the most highly stressed location was the elbow directly under the pressurizer. The elbows are the most critical component because of the stress and strain intensification that occurs in the crotch region. The model was verified by comparing predicted displacements with those measured by the plant instrumentation. A literature search on thermal striping was used to develop a thermal loading model (that included the test data), to demonstrate that striping does not significantly affect the integrity of the surge lines. The model was successfully able to establish that shakedown to elastic action would occur. The equivalent plastic-elastic strain after shakedown was used in the fatigue analysis rather than using the K_e factor. The fatigue analysis demonstrated that the cumulative usage factor was less than the ASME Code allowable value of 1.0 for the bounding case of assumptions.

There was also a Westinghouse Owners Group action to evaluate thermal stratification, similar to the descriptions given of the B&W and CEOG programmes. A bounding analysis covering all plants was prepared; again however, each licensee had the

responsibility for performing the visual inspections required by Bulletin 88-11, and ensuring the analysis was applicable to its particular plant or plants. Surge line data were obtained from several Westinghouse plants by continuous monitoring of the piping outside-surface temperature, displacements, and plant parameters. The data were used to verify that pipe movements were consistent with the analytical model predictions. Based on monitoring results, procedures, operators' experience, and plant operational data, a set of thermal stratification transients was developed. The design transients were updated to include the effects of stratification. The stress analysis showed that the worst case location was at the hot leg surge line nozzle. The $3S_m$ limit was exceeded, so the elastic-plastic analysis method of ASME Code NB-3600 was used. All stress limits were met and the cumulative usage factors were shown to be less than 1.0. Bhowmick, Bhavdani, and Swamy (1992) point out the important role that plant historical data plays in the qualification of the surge line. Obadiah et al. (1990) discuss the programme developed and implemented at the Surry and North Anna plants, which included field inspections, temperature and displacement measurements related to various operating transients, and analytical evaluations. Only minor hardware modifications to the pipe supports and pipe whip restraints were needed.

4.1.2. Thermal fatigue of spray line and nozzles

Typical design-basis thermal transients for the PWR spray lines and nozzles include the same plant heat-up and cooldown, power changes, and other operational evolutions as discussed in the previous section. Design analyses performed in accordance with the ASME Code have demonstrated that consideration of design-basis transients result in acceptable fatigue usage during a 40-year plant life. For example, a typical design-basis cumulative fatigue usage factor for the pressurizer spray piping and nozzle for a Combustion Engineering plant is 0.9. The design-basis fatigue usage factors will be different for the Westinghouse and Babcock & Wilcox plants, but also below 1.0. However, in addition to those typical design-basis transients, certain other thermal transients have a potential to cause fatigue damage in the PWR spray lines and nozzles. One such transient condition is the intermittent use of the pressurizer spray system during shutdown, an evolution contrary to the design-basis assumption of continuous spray usage during shutdown; an other one is the use of auxiliary spray system connected to charging line that leads to a high double thermal shock.

Reactor coolant system flow and reactor vessel pressure drop decrease when the first reactor coolant pump is tripped during cooldowns. Since the pressure drop across the reactor vessel provides the driving head for both the main and bypass sprays, bypass flow decreases as the driving head is reduced. The bypass flow can decrease as the pressure differential decreases to the point that it is no longer sufficient to maintain the uppermost horizontal section of the spray line full of water. Pressurizer steam will then partially fill the horizontal section of the spray piping while relatively cool water flows under the steam, thereby creating a stratified steam/water flow condition. Further reduction of the number of operating reactor coolant pumps causes the bypass flow to terminate and creates a no-flow condition in the spray piping. At this point, steam fills the spray nozzle and piping, moving to an elevation equivalent to the pressurizer level. Although when no bypass flow is present, auxiliary spray is available through the charging system. Main spray may also be available if the main spray valves are opened. The on-off use of main or auxiliary spray flows during periods when no bypass flow is available causes intermittent no-flow, stratified flow, or full-flow conditions. This results in cyclic thermal stresses and causes fatigue of the piping. The various stages of spray piping flow that may occur during a plant cooldown are depicted in Figure 4-4.

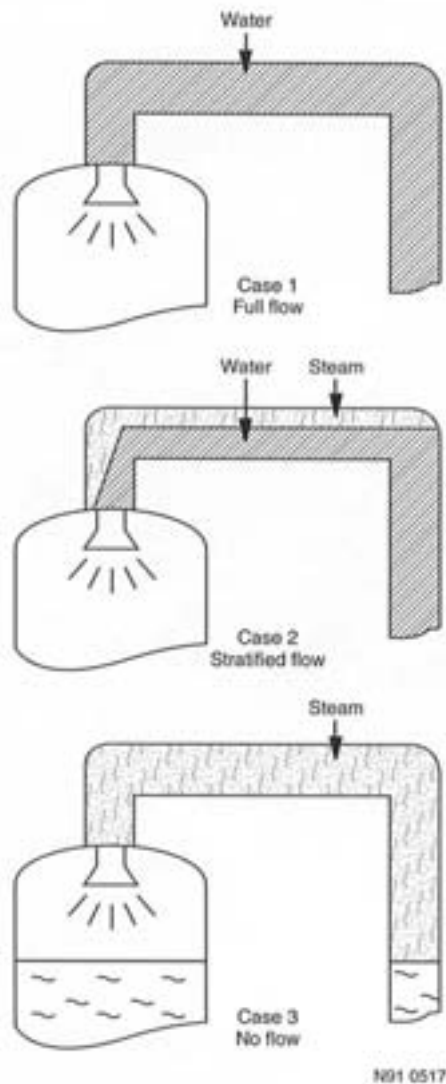


FIG.4-4. Various pressurizer spray system flow conditions.

Thermal transient may also occur without spray operation when a steam bubble is formed in the pressurizer and steam enters the spray piping during the plant heat-up. A thermal transient then occurs when a sufficient number of reactor coolant pumps are started to provide the driving head for a marginal amount of bypass flow, which causes flow stratification in the spray line. Another thermal cycle occurs when additional reactor coolant pumps are started and provide enough driving head for the bypass flow to fill the horizontal pipe and eliminate the stratified flow. In summary, spray system thermal transients can result from cyclic or throttling use of the main or auxiliary spray, or from altering the number of operating reactor coolant pumps without maintaining full-pipe flow conditions. The phenomenon of flow stratification in the piping of the pressurizer spray system was identified during startup testing at some Combustion Engineering PWR plants in 1984.

The alternating presence of steam and water may subject the upper portion of the spray piping and the spray nozzle to cyclic temperature differentials in the range of about 40 to 300°C (100–540°F) resulting in thermal shock loadings. These same temperature differences can exist in a top-to-bottom stratified flow condition under certain low spray line flow operations. However, the pressurizer spray nozzle cannot be subjected to stratified flow

loadings and is, therefore, not as limiting as the upper horizontal portion of the spray piping. Additional thermal shock loads occur when the auxiliary spray system (being much colder than the pressurizer steam) is initiated. The thermal shock loadings can be evaluated using the classical ASME Code Section III methods [4.21], whereas stratified flow loadings produce beam-bending behavior and can be evaluated using finite element methods. The shape of a typical spray line subjected to stratified flow is shown in Figure 4-5. The distribution of bending stress in the pipe for this loading can be calculated by finite element analysis, an example result of which is shown in Figure 4-6. One major difference between a thermal shock loading and a stratified flow loading is the duration of the stressed conditions. Thermal shock loadings happen quickly, whereas stratified flows tend to build up more gradually and last as long as the loading condition is applied. Figure 4-7 shows stress-versus-time plots for hypothetical thermal shock and stratified flow loadings. A thermal shock load can be a crack initiator, but it affects only a small portion of the wall thickness and, therefore, does not tend to extend an existing crack. However, a stratified flow load affects the entire wall thickness and, therefore, can drive or propagate existing cracks. In addition, stratified flows produce bending moments in the pipe elbows. Through-wall bending stresses have a more severe impact on fatigue usage than thermal shock-type skin stresses. A spray line fatigue analysis has been performed for both types of loadings. The allowable number of loading cycles required to reach a fatigue usage factor of 1.0 has been determined at the four locations in a horizontal run of spray piping, shown in Figure 4-8. The results are presented in Table XIX and demonstrate the more severe effects of stratified-flow loadings with high fluid temperature differences.

In France a specific analysis has been done on this spray line through different plant measurements to confirm the possibility to have steam in the upper part of the elbow, and consequences on fatigue behavior of that area (top of pressurizer). Finally, the cumulative usage factor is around 1, including all loads, the auxiliary spray line use has been limited to few cycle, the pressurizer spray nozzle thermal sleeve cannot be released.

Flow-induced vibration is another common stressor that affects components such as thermal sleeves, installed to protect the nozzles from thermal shock. That stressor could lead to fatigue failure of the thermal sleeve, with the possibility of the thermal sleeve breaking loose and moving through the piping. Some plants have analyzed the thermal shock loadings on the pressurizer surge nozzle and determined that the thermal sleeves are not needed; these plants are allowed to operate without them.

4.1.3. Thermal fatigue of other connected lines

Fatigue analyses of branch lines (safety injection, residual heat removal, and makeup lines, and other small diameter lines connected to main coolant piping) and nozzles generally show high cumulative usage factors resulting from thermal shock when cold water is suddenly injected. Transients such as safety injection initiation, initiation of shutdown cooling (residual or decay heat removal), or loss-of-letdown/loss-of-charging impose thermal shocks on the various branch nozzles.

The analysis of branch line thermal fatigue has been evaluated in different ways. Architect-engineering firms, utilities, and Westinghouse have typically used NB-3650 piping methods for fatigue analyses, whereas Combustion Engineering and B&W have typically used NB-3200 methods.

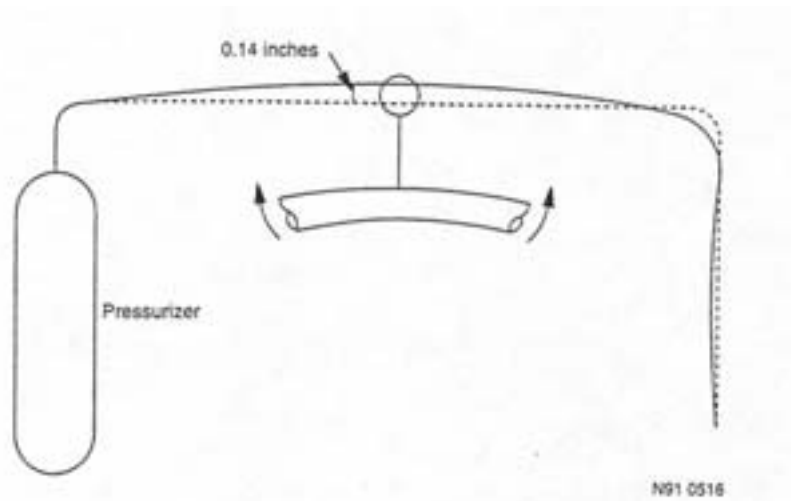


FIG. 4-5. Shape of spray line subject to stratified flow conditions.

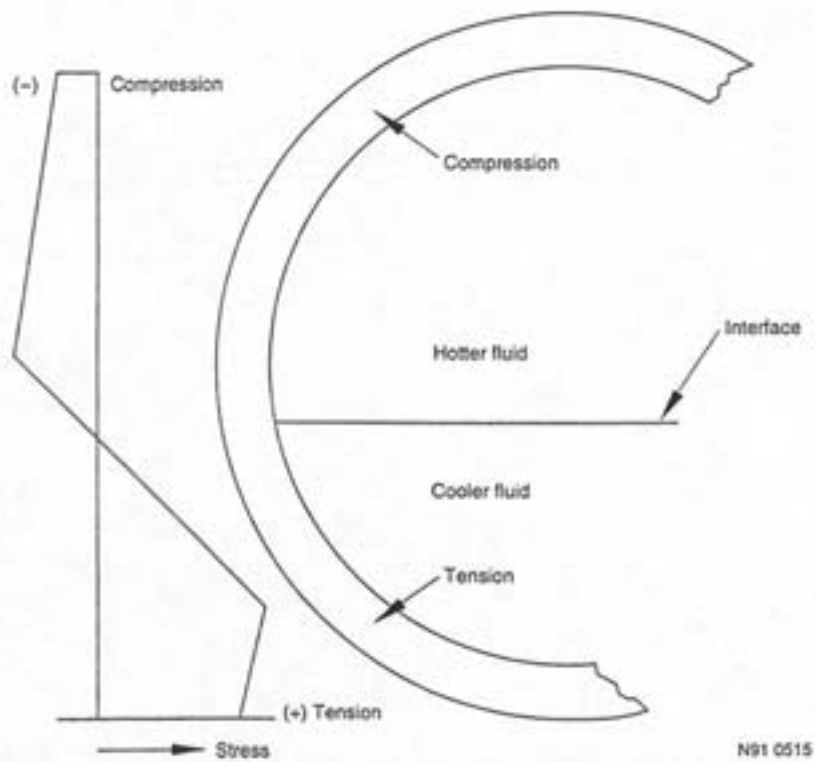


FIG. 40-6. Axial stress distribution in pipe caused by stratified flow loading.

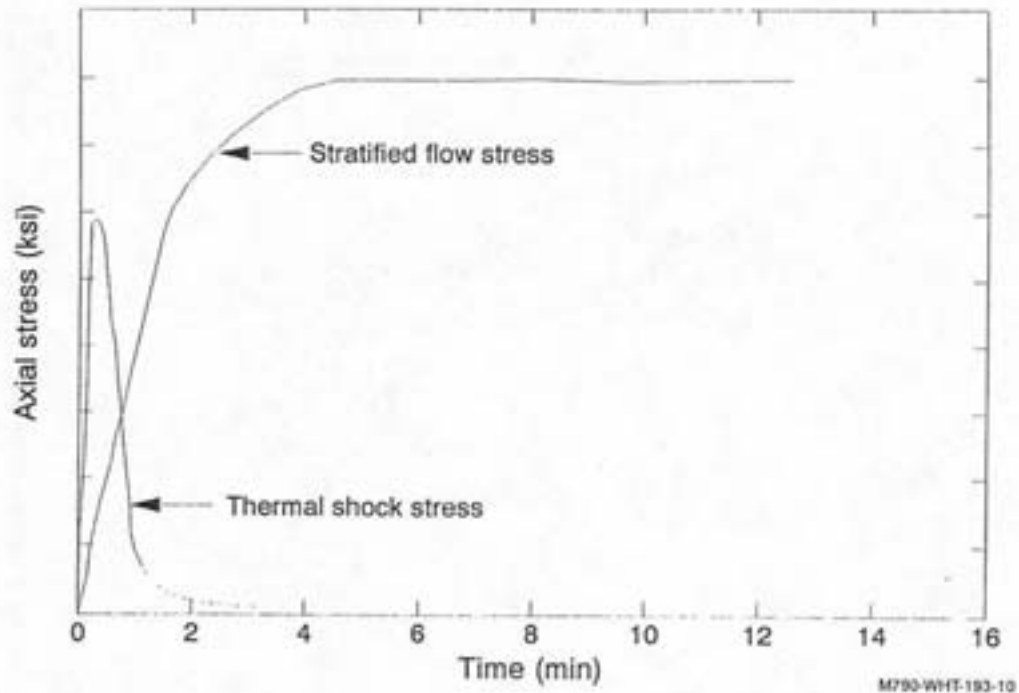


FIG. 4-7. Stress-versus-time profile for hypothetical thermal shock and stratified flow loadings for a given temperature difference, ΔT .

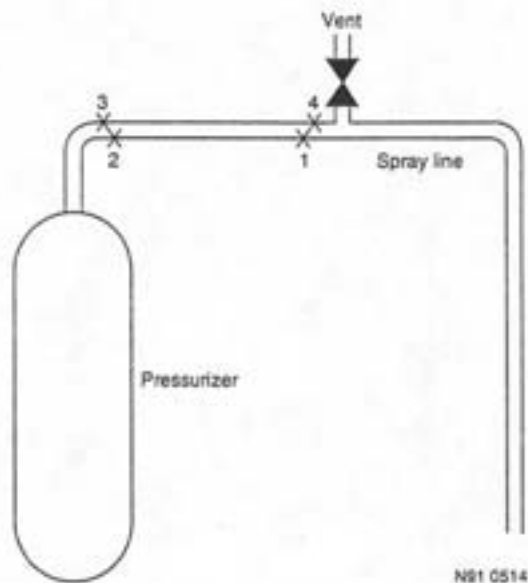


FIG. 4-8. Location on the pressurizer spray line of the fatigue analysis presented in Table XIX.

TABLE XIX. PRESSURIZER SPRAY LINE FATIGUE ANALYSIS

Loading description	Maximum allowable cycles			
	Location 1	Location 2	Location 3	Location 4 ^a
Stratified flow $\Delta T = 175F^c$	- ^b	4,000	6,000	56,000
Stratified flow $\Delta T = 300F$	1,500	170	6,500	170,000
Stratified flow $\Delta T = 360F$	400	80	3,500	75,000
Stratified flow $\Delta T = 600F$	180	25	500	4,700
Full flow ^d $\Delta T = 115F$	400,000	350,000	310,000	120,000
Full flow $\Delta T = 300F$	750	500	500	320
Full flow $\Delta T = 600F$	100	90	90	60

- a. Stress concentration effect resulting from vent line intersection is included.
- b. Alternating stress is below the endurance limit.
- c. ΔT is defined as the temperature difference between the spray fluid and the initial pipe and nozzle temperature.
- d. Full flow implies thermal shock conditions and no stratification.

Although the weld joining the nozzle to the reactor coolant piping can be located at different places and have different geometries as shown in, for example, Figures 2-23 and 2-24, the NB-3600 stress indices for axial gradients are assumed to be worst-case and independent of the weld location, so the actual fatigue usage from a thermal transient may be less than that calculated. The nozzles are welded to the main coolant piping in the shop and NB-3200 analyses typically do not include any fatigue strength reduction factors for these welds. However, stress indices are applied to the field welds joining the nozzle and the piping.

Industry experience has shown that unexpected thermal phenomena have caused fatigue cracking in several different branch lines: makeup, safety injection, and residual heat removal lines. Unlike surge lines for which the main phenomenon that has caused damage is thermal stratification, the phenomena that have caused damage in the branch lines are more complicated and termed these phenomena *turbulent penetration and thermal cycling*. Section 4.3.1 describes turbulent penetration and thermal cycling as it applies to branch lines. Then field experience with thermal fatigue failures of branch lines is summarized. Finally, the NRC Bulletin 88-08 and US utility responses to the bulletin are discussed.

Turbulent penetration and thermal cycling. Figure 4-9 illustrates how turbulence in a cold leg of the main reactor coolant piping penetrates into a connecting safety injection line. The turbulence intensity decays exponentially from the header pipe into the branch line, but the temperature remains fairly constant over the length of several diameters and then decays. The length of turbulent penetration is greater for a higher flow velocity in the main pipe. The length also depends on the layout of the branch line. The length of turbulent penetration in

typical PWR branch lines containing stagnant coolant is in the range of 15 to 25 branch-line inside diameters. Turbulent penetration may interact with stratified fluid layers, produce stratified fluid condition, or prevent the development of such conditions.

For a given operating condition, the length of turbulent penetration fluctuates about some average value by a small amount. If such fluctuations produce cyclic axial movement of an interface between hot and cold fluids, it is called *thermal cycling*. Such cycling takes place when a column of hot turbulent fluid from the main piping penetrates into a connecting branch line and interacts with thermally stratified flow. The cyclic changes in the length of turbulent penetration produce corresponding changes in the length of the stratified fluid layers. As a result, the pipe in contact with the interface between the turbulent column and stratified fluid layers experiences cyclic stresses causing fatigue damage. Thermal cycling has been suspected in fatigue cracking and leakage from safety injection lines (Farley 2, Tihange 2) and makeup/safety injection lines (Crystal River 3, Oconee 2), which are connected to the PWR primary coolant piping. These incidents are discussed later in this section.

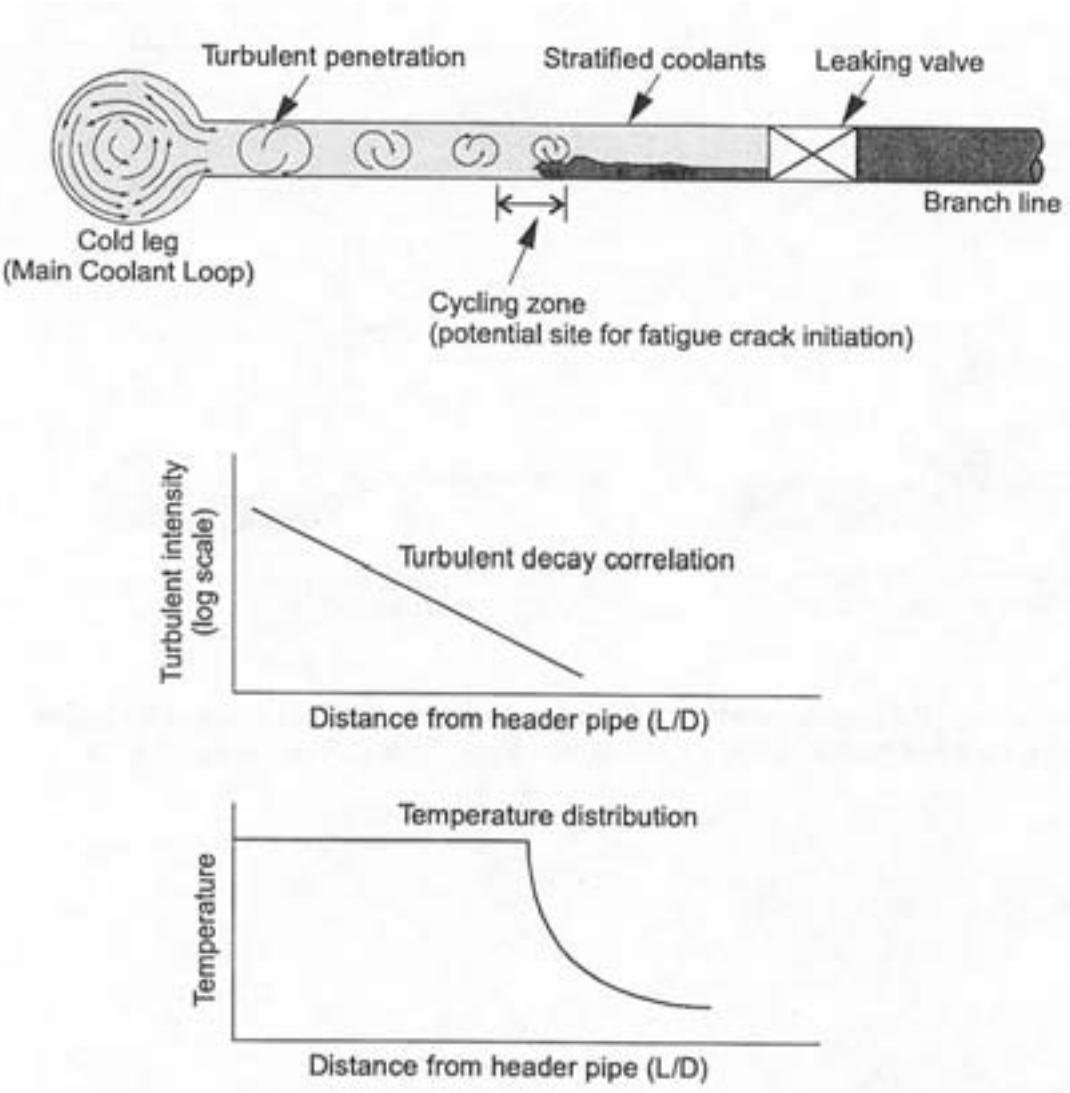


FIG. 4-9. Interaction between turbulent fluid from the main coolant loop and stratified coolants in a branch line, causing thermal fatigue damage.

In some branch lines containing hot stagnant fluid, such as safety injection lines, the stratified flow could be produced by a small leakage through the first upstream check valve (in-leakage). However, the temperature difference between the stratified layers can be sustained only for a short distance because of the small leak rate. The cold coolant leaking through the valve will heat up to the temperature of the hot coolant on the downstream side after it travels a short distance. So if the valve is at a sufficient distance away from the branch line connection with the main coolant piping, stratified fluids will not interact with the turbulent penetration column and thermal cycling will not take place.

It appears that turbulent penetration alone, under certain changes in operating conditions and with susceptible piping layouts, could produce thermal stratification in a branch line. However, the effects of plant operating conditions on the length of turbulent penetration are not well understood. The presence of thermally stratified fluids, in the absence of any valve leakage, has been detected in a branch line of a PWR plant, as illustrated in Figure 4-10. A plausible explanation for this presence of stratified fluids is as follows. The branch line containing stagnant fluid travels a certain distance vertically from the main coolant loop and then runs horizontally. The turbulent penetration initially developed in the vertical section of the branch line, as shown in Figure 4-10(a). Then, an operational transient such as a power change caused the turbulence to penetrate the full length of the vertical section and produce stratification in the elbow at the end and in the adjacent horizontal section of the branch line, as shown in Figure 4-10(b). With further changes in power, the length of the turbulent penetration receded and the stratified layer was no longer present. Thus, the base metal and welds of the elbow and the horizontal portion of the branch line experienced cyclic thermal stresses and fatigue damage.

There is another possible scenario in which turbulent penetration can produce thermal stratification in the branch line as shown in Figure 4-11. The stratification is driven by natural convection. For example, a top-to-bottom temperature difference of 78°C (140°F) at the upstream of the first check valve has been reported at one PWR plant [4.22].

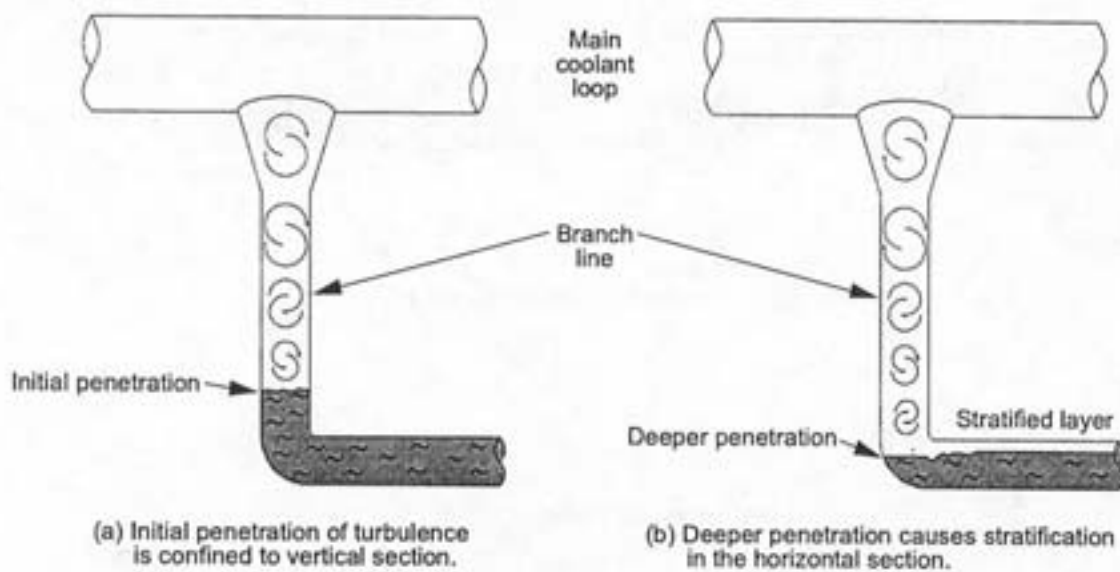


FIG. 4-10. A change in the penetration depth of turbulence from power variations can cause thermal stratification and cycling in a branch line.

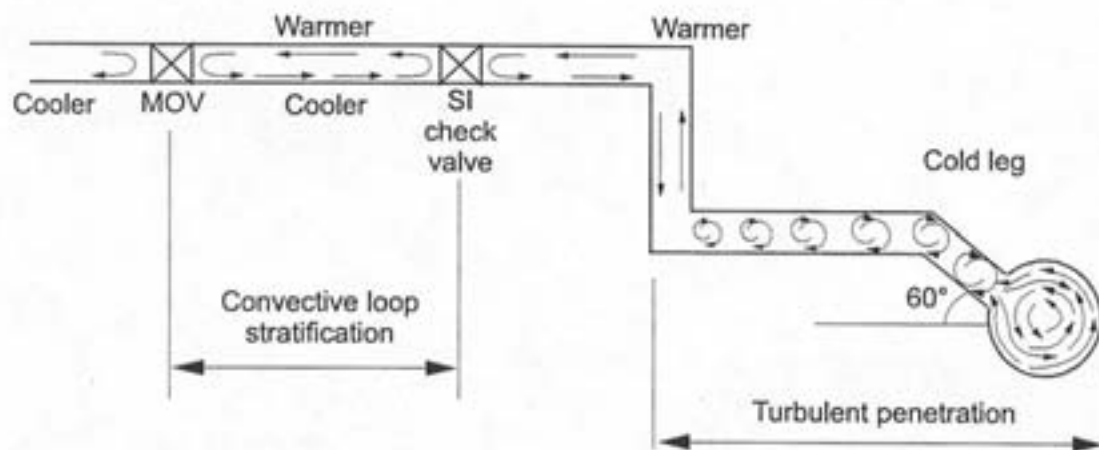


FIG. 4-11. Natural convection driven stratification in a safety injection line.

Turbulent penetration can prevent the development of a stratified fluid condition in some branch lines containing stagnant fluids, such as RHR lines, where out-leakage from the first isolation valve may take place. The out-leakage will produce a stratified fluid condition on the downstream side of the valve if the distance between the valve and the hot leg is large enough so that the temperature of the stagnant coolant in the vicinity of the valve is much lower than the hot-leg reactor coolant temperature. If the valve leak stops for some reason, the stratified fluid condition will also cease to exist after the layer of hot fluid cools down. Thus, on/off leakage from the valve will impose cyclic thermal stratification loads on the pipe. This phenomena has caused thermal fatigue cracking of a RHR line in Genkai 1, a Japanese PWR plant, which is described later in this section. If the isolation valve were within the turbulent penetration length, the coolant on the downstream side of the valve would have been at the hot-leg reactor coolant temperature and the stratified fluid condition would not have been developed.

The length of turbulent penetration in branch lines not containing stagnant fluid, such as a charging line, will depend on two factors: (a) the flow rate of the charging fluid and (b) the orientation of the charging line with respect to the main line. The length decreases as the flow rate increases.

Failures in branch lines. Thermal fatigue cracking leading to leakage is not widespread in the NPPs. Most of the reported leakage events have resulted from feedwater pipe cracking. Most of the failures have occurred because of the phenomena causing thermal fatigue cracking were not taken into account in the original design. The data related to through-wall fatigue cracking of the PWR branch lines are presented here.

Thirteen leak events caused by thermal fatigue cracking of PWR reactor coolant piping (branch lines) have been reported as of June 1998 [4.23]. The leak events are listed in Table XX along with the data related to piping system through which leakage occurred, through-wall crack location and size, leak rate, and the leak detection method³ for each event. These events took place in the USA, France, Belgium, Finland, Germany and Japan.

³ The description of different leak detection methods may be found in Section 6.3.

TABLE XX. PWR REACTOR COOLANT LEAK EVENTS CAUSED BY THERMAL FATIGUE

Plant	Event Date	Initial Criticality Date	NSSS Vendor	Piping System	Through-wall Crack		Leak Rate (L/min)	Leak Detection Method
					Location	Size		
Crystal River 3 ¹	1/82	1/77	B&W	Make-up/High Pressure Injection	Check valve body near the valve-to-safe end weld	140-degree circumferential crack; two crack initiation sites: one on the inside surface and one on the outside surface	3.8	RCS mass balance calculations
Obrigheim ²	/86	9/68	Siemens	Chemical and Volume Control	Weld between a 90-degree elbow and a nozzle	Crack extended 70 degrees circumferentially at the inside surface, 12-mm long at the outside surface	0.02	Visual observation (video monitor)
Farley 2 ³	12/87	5/81	W	Safety Injection	Heat affected zone of elbow-to-pipe weld	Crack extended 120 degrees circumferentially at the inside surface, 25-mm long at the outside surface	2.7	High containment cooler drain pot levels
Tihange 1 ⁴	6/88	2/75	ACLF	Safety Injection	Elbow base metal	89-mm long at the inside surface, 41-mm long at the outside surface	22	Airborne particulate and gaseous radioactivity monitors, RCS mass balance calculations
Genkai 1 ⁵	6/88	1/75	MHI	Residual Heat Removal	Heat-affected zone of elbow-to-pipe weld	Crack extended 97 mm circumferentially at the inside surface, 1.5-mm at the outside surface	0.8	Sump level and flow rate monitor

TABLE XX. PWR REACTOR COOLANT LEAK EVENTS CAUSED BY THERMAL FATIGUE (CONT'D)

Plant	Event Date	Initial Criticality Date	NSSS Vendor	Piping System	Through-wall Crack		Leak Rate (L/min)	Leak Detection Method
					Location	Size		
Dampierre 2 ⁶	9/92	12/80	Fra	Safety Injection	Check valve-to-pipe weld and base metal of straight portion of pipe	Crack extended 110 mm circumferentially at the inside surface, 25 mm at the outside surface	10	RCS mass balance calculations
Loviisa 2 ⁷	5/94	10/80	AEE	Spray Line	Pressurizer auxiliary spray line control valve body	Crack extended 80 mm along the horizontal surface and 25 mm along the vertical surface of the valve body	Few drops	Visual observation
Biblis-B ⁸	2/95	3/76	Siemens	Chemical and Volume Control System	Base metal of a straight portion of the pipe	Crack extended 50 mm axially at the inside surface, 20 mm at the outside surface	66.7	Visual observation (video monitor), condensate flow rate monitor
Three Mile Island 1 ⁹	9/95	6/74	B&W	Cold Leg Drain Line	Weld between a 90-degree elbow and a 51-mm diameter horizontal line	Crack extended 51 mm circumferentially at the inside surface, 14 mm at the outside surface	0.06	Airborne particulate radioactivity monitor
Dampierre 1 ¹⁰	12/96	3/80	Fra	Safety Injection	Base metal of a straight portion of the pipe	Crack extended 80 mm circumferentially at the inside surface, 22 mm at the outside surface	2.7	Sump level and flow rate monitor
Loviisa 2 ¹¹	1/97	10/80	AEE	Hot Leg Drain Line	Weld between a T-joint piece and a reducer	65-degree circumferential crack	0.5	Airborne particulate radioactivity monitor

TABLE XX. PWR REACTOR COOLANT LEAK EVENTS CAUSED BY THERMAL FATIGUE (CONT'D)

Plant	Event Date	Initial Criticality Date	NSSS Vendor	Piping System	Through-wall Crack		Leak Rate (L/min)	Leak Detection Method
					Location	Size		
Oconee 2 ¹²	4/97	11/73	B&W	Make-up/High Pressure Injection	Safe-end to pipe weld	Crack extended 360 degree circumferentially at the inside surface, about 77 degree circumferentially on the outside surface	45.6	Sump level and flow rate monitor, radiation monitor
Civaux 1 ¹³	5/98	Initial startup test phase	Fra	Residual Heat Removal	Longitudinal weld in an elbow	180-mm long through-wall crack	500	Drop in pressurizer level, fire alarm triggered by presence of steam

¹ Babcock & Wilcox 1983

² Junglaus et al. 1998

³ Farley 1987

⁴ Pirson and Roussel 1998

⁵ Shirahama 1998

⁶ Junglaus et al. 1998

⁷ Hytonen 1998

⁸ Junglaus et al. 1998

⁹ Three Mile Island 1995

¹⁰ Junglaus et al. 1998

¹¹ Hytonen 1998

¹² Duke Power 1997

¹³ MacLachlan 1998

One event took place during the plant initial startup test, two took place during the first 10-year operation, and 10 took place during the 10–25 year operation. For all of these events, through-wall cracking was in a unisolable portion of the small diameter (≤ 200 mm) reactor coolant piping. In seven of these events, the through-wall cracking was in the weld or its heat-affected zone. In the remaining four events the through-wall cracking was away from the weld and in the base metal of an elbow, straight pipes, and a valve body. The leak rate was ≤ 3.8 L/min. in nine events, and ≥ 3.8 L/min. in the remaining four events. The maximum leak rate was 500 L/min. during the May 1998 leak event at Civaux 1 plant (Class 2 piping). The analysis of the data presented in Table XX indicates that there is a statistically significant increasing trend in the number of leak events with plant age [4.22].

Recently, an additional leak event has been reported at Japan's Tsuruga-2 PWR. This is not included in Table XX. Leakage took place through a 47-mm long through-wall crack in base metal of a Type 316 stainless steel elbow (8.9-cm outside diameter with 1.1-cm thick wall) in the letdown system piping. In addition to these leak events, thermal fatigue cracks have been detected at two EDF plants during 1997: Dampierre 3 and Fessenheim 2.

The first leak event was reported in 1982 at Crystal River 3 which had been in operation for five yrs. The through-wall leakage occurred so early in the plant's operating life possibly because the through-wall crack was initiated at both the outside and inside surfaces. One of the recent leakages was reported in Oconee 2, which had been in operation for 23 years and is similar to Crystal River 3 in design. The through-wall crack in both Crystal River 3 and Oconee 2 were circumferential and at the same location (the weld at the upstream end of the MU/HPI nozzle safe end), but the Oconee 2 crack was initiated only at the inside surface. This may be the reason why the leakage event occurred much later in the plant's operating life.

Cracking of B&W MU/HPI nozzle thermal sleeves. Thermal shock has caused low-cycle fatigue damage to the circumferential and longitudinal welds in a 102-mm (4-in.) make-up-line thermal sleeve in a demonstration plant. The design of thermal sleeve and failure locations are shown in Figure 4-12. The thermal shocks were caused by the intermittent make-up coolant flow and the temperature differences between the make-up and cold-leg coolants, which might have been as high as 215°C (385°F). The design of the thermal sleeve and the failure locations are shown in Figure 4-12. In addition, turbulent mixing of the make-up and cold leg coolants caused high-cycle fatigue damage to the cold-leg piping. The damage resulted in about 40 surface cracks, up to 6.4-mm (0.25-in.) deep, on the inside surface of the cold leg piping downstream of the make-up line connection. Several steps were taken to resolve this problem. The minimum make-up flow was increased from 190 to 285 L/min. (50 to 75 gpm) to reduce the severity of the temperature transients and to promote better mixing of the make-up and cold leg coolants. A redesigned thermal sleeve, shown in Figure 4-13, was installed to reduce the fatigue damage. This sleeve was made from a solid forging with fewer welds and reduced stress concentrations; it was held in place by hard rolling, which gives it a tight fit inside the nozzle. In addition, the redesigned thermal sleeve was extended an additional 12-mm (0.5-in.) into the cold leg to improve the mixing of the make-up and cold leg coolants. The make-up line connection to the cold leg was also redesigned, as shown in Figure 4-13, to eliminate sharp corners.

Through-wall cracking of B&W MU/HPI lines. In 1982, an unidentified 0.9 to 1.0 gpm leak occurred through a crack in the safe end-to-check valve weld in the unisolable portion of the make-up line to the reactor coolant loop in a B&W 177 fuel assembly plant

[4.24]. Investigations showed an extensive network of cracking around the safe end inner surface. The most severe crack penetrated about 25% into the wall. As a result another utility initiated a radiographic examination of the makeup line inlet nozzle to the reactor coolant loop. The thermal sleeve in some nozzles were found to be loose, and subsequent liquid penetrant inspections revealed cracking on the inside surface of several nozzle safe ends. The cracks penetrated about 20% of the wall thickness. The inspection results implied that a loose thermal sleeve is a necessary condition for cracking of the safe end [4.25]. Corrective actions included redesign of the nozzle thermal sleeve.

In 1997, a similar leak event took place at Oconee 2. The leak was through a circumferential crack in the safe-end to MU/HPI line weld as shown in Figure 4-14. The leak was an unisolable pressure boundary leak and its magnitude was 45.6 L/min (12 gpm) [4.26]. In-depth evaluation of this leak event confirmed the earlier conclusion that a loose thermal sleeve is a necessary condition for cracking of the MU/HPI line safe end. Redmond [4.27] and Shah et al. [4.22] provide the details of this leak event including event description and root cause analysis.

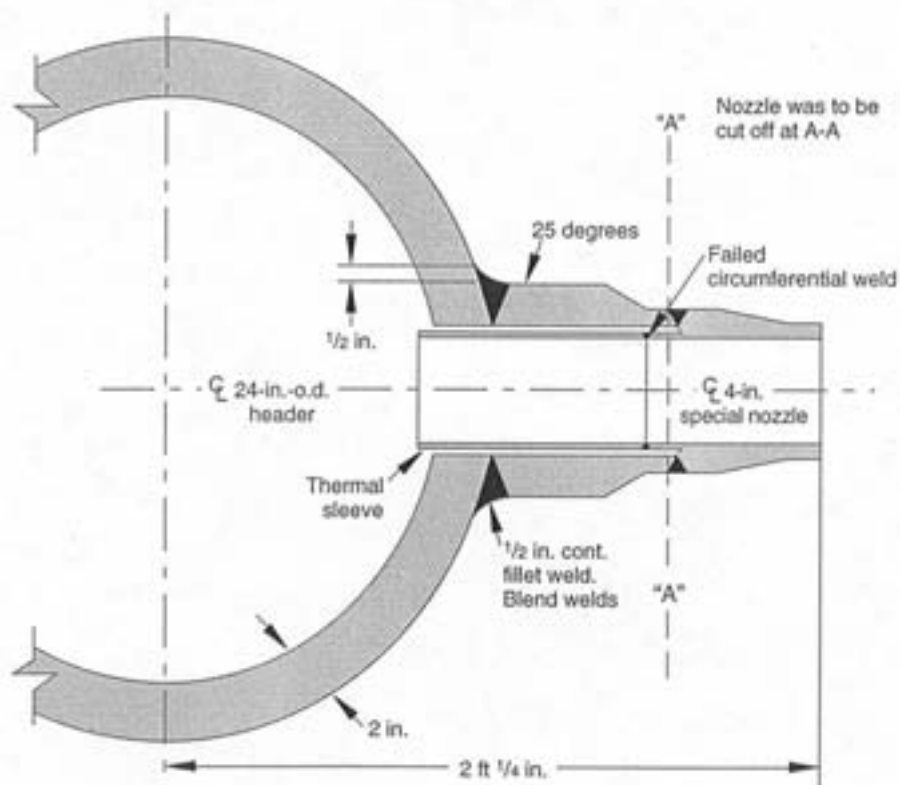


FIG. 4-12. Original makeup nozzle and thermal sleeve design in a demonstration PWR plant.

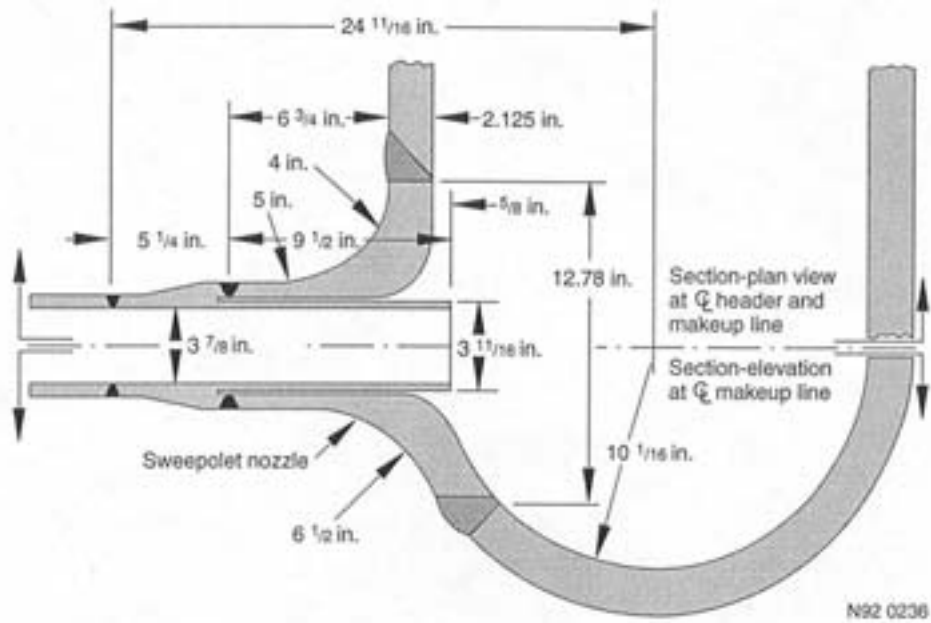


FIG. 4-13. Replacement makeup nozzle and thermal sleeve design in a demonstration PWR plant.

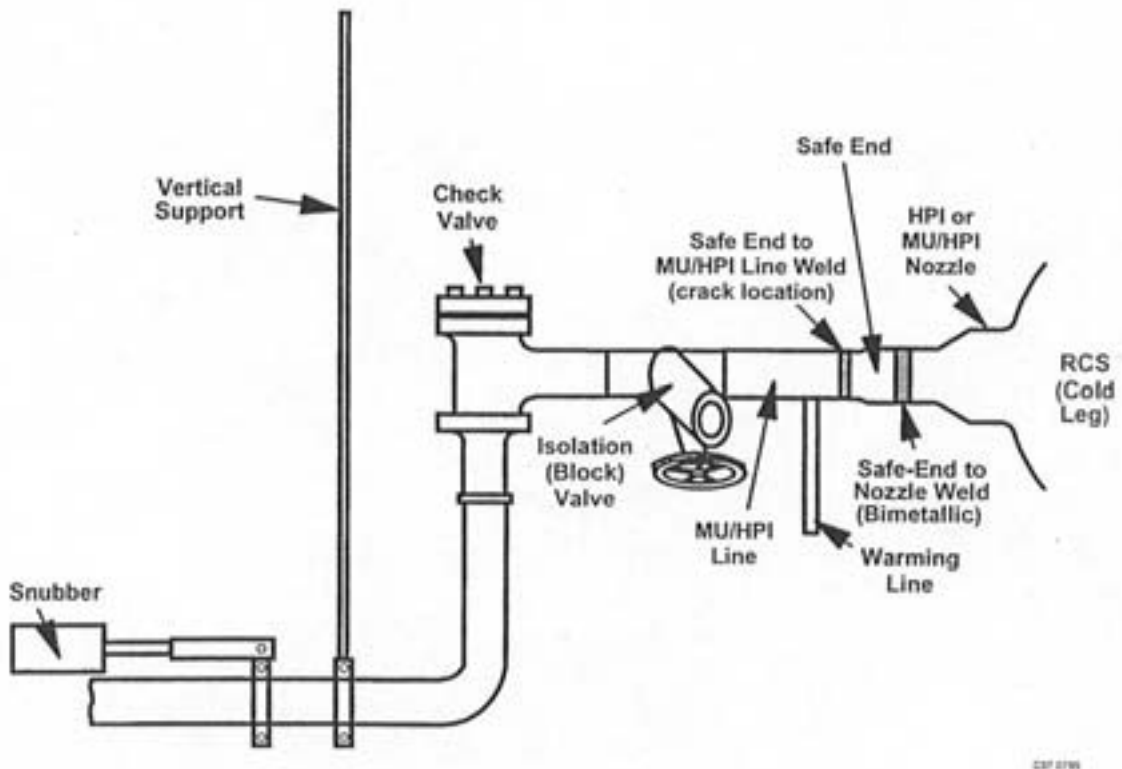


FIG. 4-14. Typical layout of Oconee 2 MU/HPI Line. Location of 1997 through-wall crack is shown.

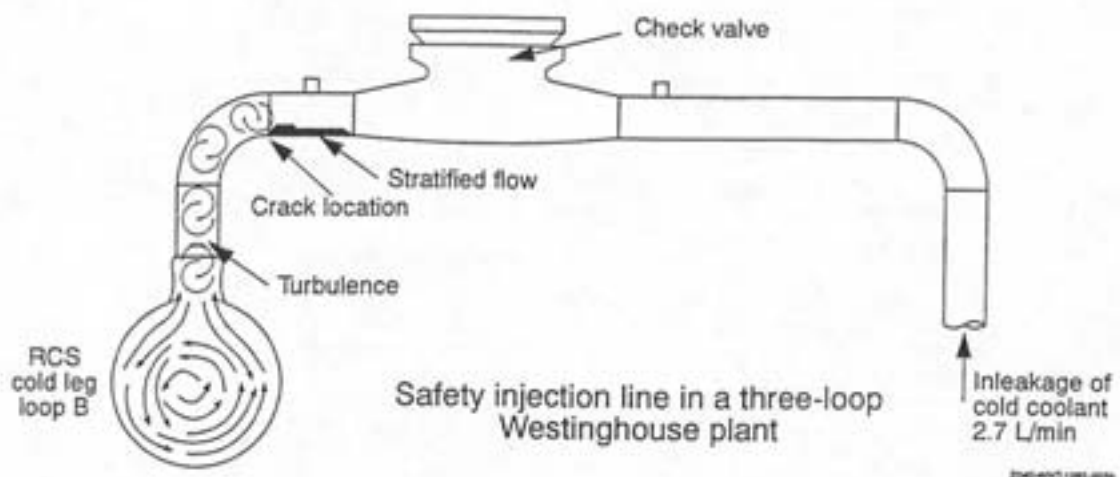


FIG. 4-15. High-cycle fatigue in safety injection line caused by valve leakage and turbulent penetration.

Through-wall cracking in the safety injection lines. In 1987, a leak occurred inside the containment of Farley 2 during normal power operation. The leak was found in the unisolable location of safety injection line as shown in Figure 4-15. The crack was on the inside surface of the weld and extended approximately 120 degrees circumferentially around the underside of the pipe. About 25 mm (1 in) of this crack was through-wall. The crack was caused by thermal fatigue and had developed slowly. The leak rate was 2.7 L/min (0.7 gpm). The monitoring of circumferential temperature distribution at the failed weld at Farley 2 carried out after the leak event showed spatial and temporal fluctuations in the temperature. The circumferential temperature difference at the weld varied from 3°C (5°F) to as high as 120°C (215°F). Based on this measurements, it was assumed that the temporal variations were because of intermittent action of the check valve. There were, however, no test results supporting this assumption.

Later, the experiments performed in Japan simulating the Farley event showed that the temperature fluctuation in the safety injection line was not caused by the intermittent action of the check valve (i.e. fluctuation in the flow rate) but by the mixing of low temperature leak flow with high temperature turbulent flow in the pipe downstream of the check valves [4.28]. The term *thermal cycling* describes this mixing phenomena and is discussed in Section 4.3.1. The Japanese test results also concluded that the thermal cycling is severe enough to cause high cycle fatigue failure of the piping material when the leak flow rate is equal to or larger than 100 kg/h as measured at Farley 2.

A similar occurrence caused cracking in both base metal and welds of Tihange 1 (1988) as shown in Figure 4-16 and Dampierre 1 and 2 (1992, 1996). All for plants Farley 2, Tihange 1, Dampierre 1 and 2 [4.29] are similarly designed Westinghouse-type 3-loop plants. The affected PWR plants have dual-purpose pumps used for both adding coolant during normal reactor operation and injecting emergency core coolant at high pressure following an accident. A schematic diagram of the high-pressure safety injection and RHR systems in a

three-loop Westinghouse plant with dual-purpose pumps is shown in Figure 2-17 [4.6]. The charging pumps supply the coolant to the safety injection system. The safety injection and RHR systems are connected to the RCS through the same nozzles, located one on each of the three cold legs. The charging system (not shown in Figure 2-17) is connected to the cold leg through a different nozzle. Accumulator tanks, also not shown in Figure 2-17, serve a function similar to that of the safety injection tanks but are connected to the primary system cold legs through separate nozzles. All valves in the safety injection system are closed during normal operation. Globe valve A, which leaked in Farley 2, is in a bypass line around the boron injection tank. Leakage of cold water through a closed globe valve continued down the line through the check valve and produced flow stratification [4.30–4.31].

The licensees undertook corrective actions to address these failures. These corrective actions included replacement of the elbow and the affected pipe spool and installation of an additional valve downstream from the check valve to prevent stratified flow.

Through-wall cracking in Japanese residual heat removal line. A 203 mm (about 8 in. nominal pipe size) Schedule 140, Type 316 stainless steel RHR line was found leaking in a Japanese plant. Figure 2-19 shows an isometric view of the RHR piping and includes the location of the through-wall crack [4.32]. The unisolatable leak was found in the RHR line weld joint between an elbow and a horizontal pipe section located between the hot leg and the first isolation valve.

The crack extended 97 mm (3.8 in.) circumferentially around the pipe on the inside surface of the weld. About 1.5 mm (0.06 in.) of this crack extended completely through the wall. The crack initiated on the inside surface at the weld metal-base metal interface and progressed through the weld toward the outside of the pipe wall. The leak rate was 0.8 L/min (0.2 gpm).

The crack was caused by high-cycle fatigue that resulted from cyclic thermal stratification in the horizontal pipe section. The stratified flow condition was caused by a small packing leak from the first isolation valve. The cyclic stresses may have been from intermittent valve leakage and turbulent penetration, which eventually caused the through-wall crack. An RTD previously installed on the valve gland leak-off line did not detect any temperature change because it was cooled by the ventilation system airflow. The effect of thermal cycling from turbulent penetration or valve leakage on piping was not considered in design analysis. The corrective actions taken as a result of this event included:

- The valve packing was replaced to stop the gland leak and the valve seat gap was increased to eliminate possible cyclic opening/closing of the gate.
- The elbow and horizontal pipe section were replaced.
- The RTD on the leak-off line was insulated to correct the ventilation cooling problem and temperature instrumentation was installed on the outside of the RHR line to monitor the top-to-bottom temperature differentials in the pipe.

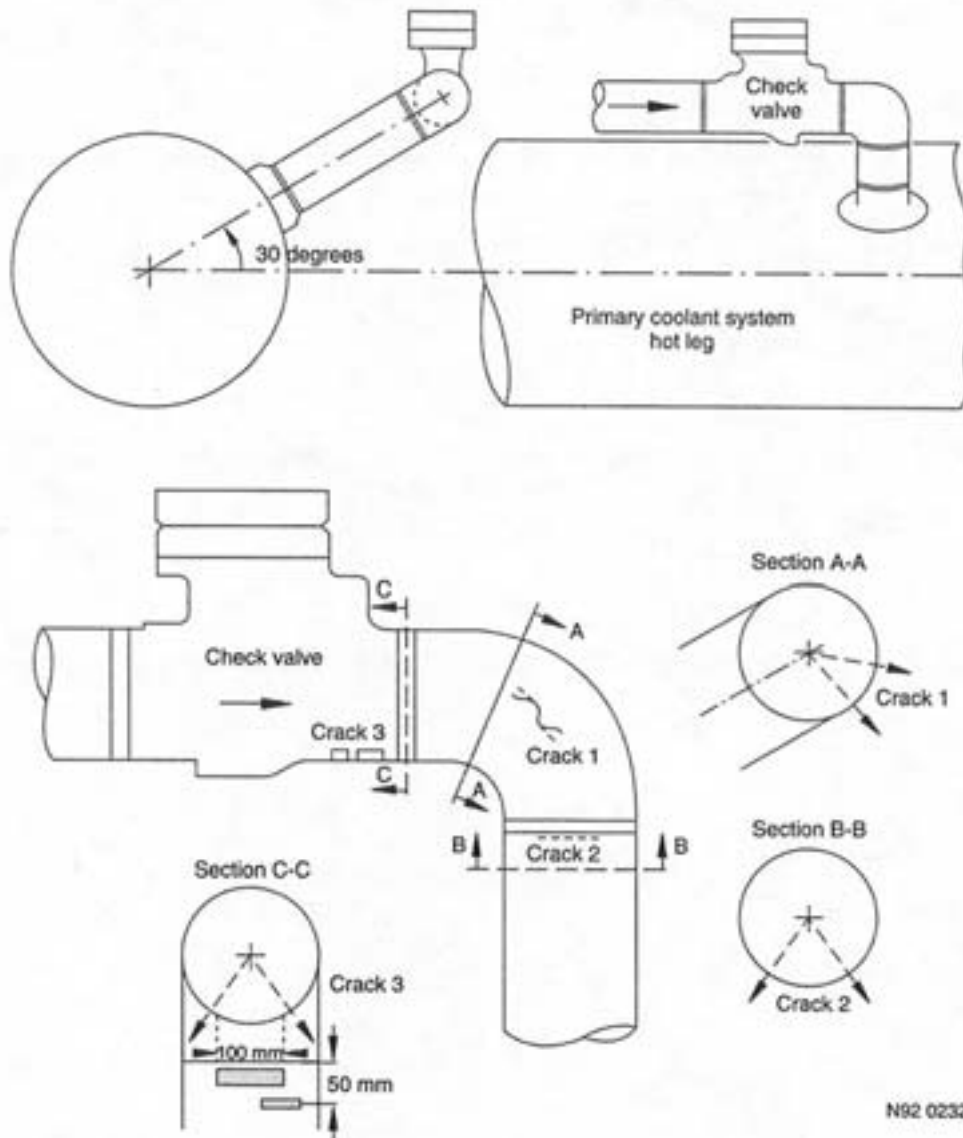


FIG. 4-16. Location of the cracks in the base metal and welds in the safety injection piping in Tihange Unit 1.

Through-wall cracking in French residual heat removal line. In May 1998 [4.32], a through-wall crack was discovered in CIVAUX 1 plant on an elbow of the RHR system (in the longitudinal weld, 10 in. diameter pipe, 10 mm thick), Class 2 part. The corresponding leak was around 6 m³/h. During detailed inspection of the inner surface of the elbows and all connected piping, different cracks were discovered in weld areas and ground areas. The root causes were attributed to high cycle thermal fatigue in mixing flow area with large temperature difference (up to 150°C) for an excessive length of time (more than 500 hours).

The corrective actions taken as result of this event are:

- limitation of time with high temperature difference in the mixing flow area
- improved piping layout for this area
- fabrication precautions on new pipes, like no longitudinal weld, good surface finish and low surface residual stress

- monitoring of the transients
- periodic qualified in-service inspection (detection performance around 1.5 mm).

Other actions following the event:

- check similar tees on similar plants, and other potential locations on RHR system
- check other RHR designs
- check other mixing tees on all safety class pipes
- review foreign practices
- develop a complementary R&D programme on load evaluation, material fatigue data and validation tests
- revise the RCC-M Code requirements.

Today, all the ISI results confirm that all similar tees have surface degradations and have to be replaced.

USNRC Bulletin 88-08. Based on the safety injection line cracking in the domestic plant (see Section 4.3.2), the NRC issued Bulletin 88-08 Thermal Stresses in Piping Connected to Reactor Coolant Systems in late December 1988 [4.33]. The Bulletin requested the following actions from licensees of operating PWRs:

- Action 1. Review and identify systems where unisolatable sections of piping connected to the reactor coolant system may be subjected to thermal stratification or temperature oscillations that could be induced by leaking valves and that were not evaluated in the design analysis of the piping
- Action 2. For susceptible locations, perform non-destructive examination of weld, heat-affected zones, and high-stress locations to assure that there are no existing flaws
- Action 3. Develop and implement a programme to provide continuing assurance that unisolatable sections of piping connected to the reactor coolant system will not be subjected to combined cycling and static stressors that could cause fatigue failure.

The assurance may be provided by:

- (a) redesigning and modifying these sections
- (b) instrumenting the piping to monitor for adverse temperature distributions and establishing appropriate limits on these distributions
- (c) providing means to ensure that pressure upstream of block valves which might leak is monitored and does not exceed reactor coolant system pressure.

Actions 2 and 3 apply only to systems that were identified in Action 1 as being susceptible to thermal stratification or temperature oscillations. Various time limits were included for the actions in the Bulletin, depending on whether the plant was in an extended outage.

Bulletin 88-08 was followed by three supplements: 24 June 1988 [4.34], 4 August, 1988 [4.35], and 11 April, 1989 [4.33]. Supplement 2 provided preliminary information on similar cracking in a European Westinghouse-type three-loop plant and noted that examinations of high stressed metal would include the base metal, but the reporting requirements of the Bulletin were not changed. Supplement 2 emphasized the need for

enhanced ultrasonic testing to detect fatigue cracks in stainless steel piping, but the reporting requirements in the Bulletin were not changed. Supplement 3 discussed the cracking event in the foreign plant RHR line (described in Section 4.3.2) and noted that periodic valve seat leakage through packing glands could result in unacceptable thermal stresses, but required no additional actions.

USNRC [4.36] provided following guidelines for identification of potentially susceptible piping. For sections of injection piping systems normally containing stagnant coolant, the susceptible piping, regardless of its pipe size, has the following characteristics: (a) the operating pressure is higher than the RCS pressure; (b) the piping sections contain long horizontal runs; (c) the piping systems are isolated by one or more check valves and a closed isolation valve in series; (d) water injection into the RCS is top or side entry; and (e) the first upstream check valve is located less than 25 pipe diameters from the RCS nozzle. Examples of such system in PWR are the safety injection and charging (make-up) lines between the reactor coolant loop and the first upstream check valve. Similar guidelines were presented for other piping systems, such as the RHR system, which normally contain stagnant coolant.

USNRC [4.36] also identified acceptable responses to Action 3 identified in Bulletin 88-08. The acceptable responses include revision of system operating conditions, relocation of the first upstream check valve, and installation of temperature and pressure monitoring instrumentation for detection of valve leakage imposing thermal cycling loads on piping. The guidelines for temperature monitoring included type and location of temperature sensors, determination of baseline temperature histories, monitoring time intervals, and acceptable top-to-bottom temperature difference. Mitigative actions such as reducing valve leakage were required if the acceptable temperatures were exceeded.

Responses to USNRC Bulletin 88-08. Licensees took differing approaches to the Bulletin requests. Some simply reviewed the branch lines according to Action 1, concluded that no stratification from valve leakage was possible, and left the matter there. At several other plants, potentially susceptible lines have been inspected [4.37], but no crack-like defects have been found. For example, on a Westinghouse two-unit facility, ten pipe lines including six 152-mm (6-in.) safety injection lines, one 102-mm (4-in.) auxiliary spray line, and three 51-mm (2-in.) reactor coolant fill lines were identified as having the potential for stratified flow, were instrumented, but no temperature oscillations that would cause a fatigue concern were identified [4.38].

One Westinghouse four-loop two-unit facility took a conservative approach for the RHR line. The analysts concluded that thermal cycling from valve leakage is unlikely because of two reasons: (1) the length of the RHR piping between its hot-leg nozzle and the valve was shorter than that in the Japanese plant where leakage took place in 1988, as discussed earlier. The distance was sufficiently shorter that it does not allow formation of a stratified layer when the valve is leaking, (2) the leakage path through the packing and valve leakoff does not exist since the leakoff is capped. Nevertheless, the licensee chose to have a fatigue analysis conducted with postulated valve leakage transients based on the incident at the Japanese plant. Even with the resulting fatigue usage added to the design basis CUF, the sum did not exceed the ASME Code limit of 1.0. Other actions taken by the licensee were using torque switches for isolation valve closure and inspection and testing of the isolation valves to ensure no leakage. Leakage monitoring guidelines were also developed.

Evidence of turbulent penetration thermal cycling was found in the shutdown cooling system of an older vintage Combustion Engineering plant. A fatigue analysis was conducted to demonstrate that, even with the additional fatigue usage contributed by the turbulent penetration thermal cycling transients, the cumulative usage factor would remain less than the ASME Code limit of 1.0 for the 40-year life. Actions taken by another licensee included installing redundant manual isolation valves on small lines [76-mm (3-in.) and smaller diameter lines], verifying valve integrity through an enhanced maintenance and leak testing programme, and a temporary temperature measuring programme on the RHR line.

With regard to Action 3 of the bulletin, several US utilities have based their response on an analytical methodology developed under a programme sponsored by the Electric Power Research Institute (EPRI) to investigate thermal stratification, cycling, and striping (TASCS). Application of this methodology is summarized in Section 5.3.

4.1.4. Thermal fatigue of dissimilar metal welds

The dissimilar metal welds in the PWR reactor coolant system piping (including the main coolant loop piping, spray and surge lines, branch lines, etc.) represent geometrical and metallurgical discontinuities that introduce high stress/strain concentrations and reduce the fatigue resistance. The geometrical discontinuities generally include inclusion and fabrication defects. As a result, in some cases, the weld geometry has an inherent built-in stress concentration similar to a crack. The metallurgical discontinuity is associated with dissimilar metal welds between stainless steel piping and low-alloy steel vessel, steam generator, or pressurizer nozzles. The metallurgical discontinuity and its impact on fatigue resistance is discussed in this section.

The severity of the metallurgical discontinuity depends upon the type of filler metal used in the dissimilar weld. As discussed in Section 2.6.3 and shown in Figure 2-44, the filler metal is either nickel-based Alloy 182 or Type 308 stainless steel with Type 309 stainless steel for buttering. The use of stainless steel as a filler metal has a slightly more detrimental influence on fatigue life of the dissimilar weld.

Thin layer of Type 309 stainless steel is applied to the end of the PWR reactor pressure vessel nozzles prior to post-weld heat treatment of the vessel. During post-weld heat treatment, carbon from the ferritic material, i.e. reactor pressure vessel steel (SA-508), migrates across the weld interface into the stainless steel butter material. The process of carbon migration involves decomposition of carbides in the vessel material, followed by diffusion of carbon from the vessel steel into the butter material. The driving force is the carbon activity gradient between the ferritic steel base metal and stainless steel weld metal. An example of carbon redistribution caused by carbon migration is shown in Figure 4-17(a) [4.39]. A dissimilar metal weld between the stainless steel spray line and a low alloy steel (A508-3) pressurizer nozzle is shown in this figure. Figure 4-17(b) shows a typical French spray line dissimilar metal weld.

The carbon migration from the ferritic material results in a narrow carbon-depleted *weak* zone in the heat affected zone, next to the hard zone of carbide precipitates in the stainless steel butter. These zones are immediately adjacent to each other and provide a significant properties change across a narrow region of about 0.25 mm width, which tend to localize the strains [4.40].

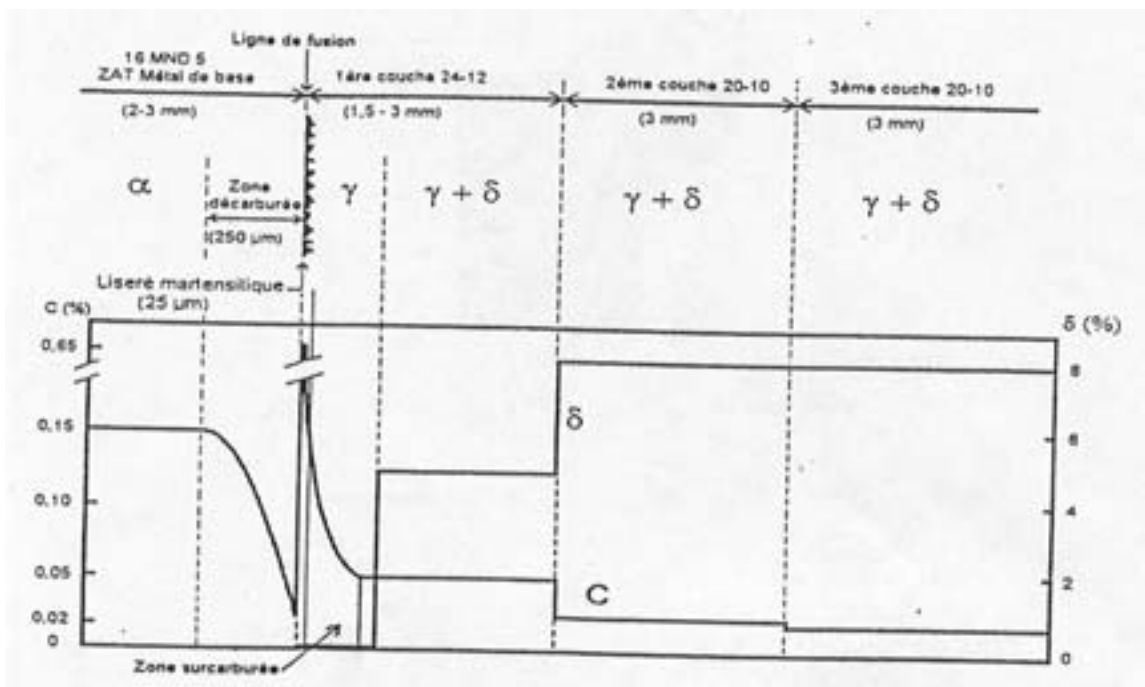


FIG. 4-17(a). Carbon distribution at the dissimilar metal weld between the stainless steel spray line and the low-alloy steel (A508-3) pressurizer nozzle.

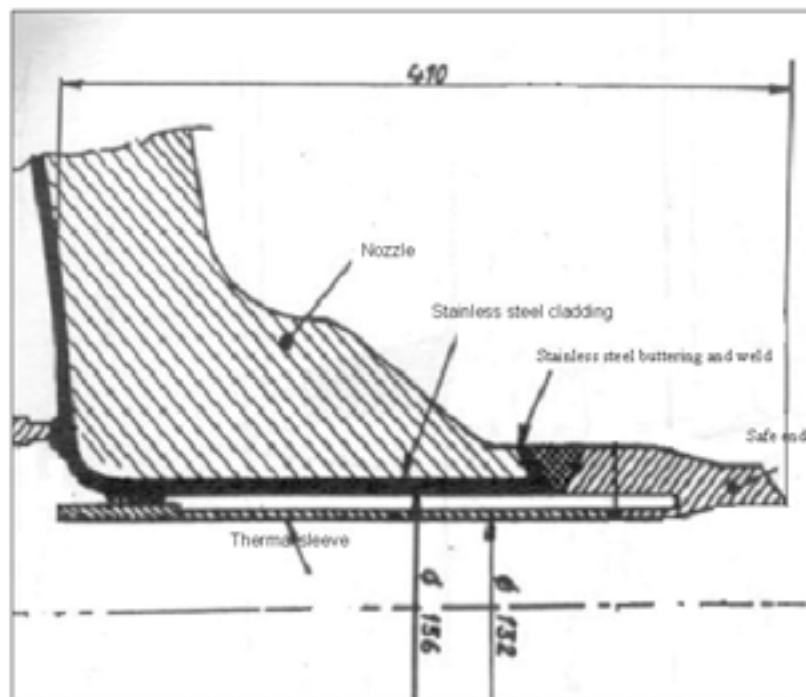


FIG. 4-17(b). Typical French spray line dissimilar metal weld.

The heat-up and cooldown cycles imposes thermal strains on the dissimilar metal weld having stainless steel as filler metal because the thermal expansion coefficients for the stainless steel is about 30% higher than that for ferritic steel. The thermal expansion coefficient for stainless steel is about $18 \mu\text{m/m-K}$ and that for ferritic steel is $14 \mu\text{m/m-K}$. The carbon-depleted soft zone in ferritic steel is restrained by the harder and stronger carbon-enriched zone in stainless steel butter material, which could introduce a complex stress state at

the weld interface. Thus, the mismatch of the thermal expansion coefficients and possibly carbon migration are more likely to shorten the fatigue life of a dissimilar weld having stainless steel as a filler metal.

The use of Ni-based Alloy 182 as a filler metal has a less adverse effect on the fatigue life of a dissimilar weld because of reduced carbon migration and significantly smaller mismatch in the thermal expansion coefficients between the filler metal and the vessel nozzle material. Carbon migration in a nickel-based weld metal has been found much smaller than that in the stainless steel weld metal. In addition, the coefficient of thermal expansion for Alloy 182 (14.4 $\mu\text{m}/\text{m}\cdot\text{K}$) is only about 6% greater than that for the ferritic steel. Thermal expansion for another nickel-based weld metal, Alloy 82, which is sometimes used for buttering, is about the same as that for the ferritic steel. However, there will be a significant mismatch in the thermal expansion coefficients between the Ni-based filler metal and the stainless steel piping.

Carbon migration in the dissimilar metal weld takes place only at postweld heat treatment temperature. It would not take place at lower LWR operating temperatures. So only those dissimilar metal welds which have stainless steel as filler metal and which were subject to postweld heat treatment are susceptible to have significant metallurgical discontinuity.

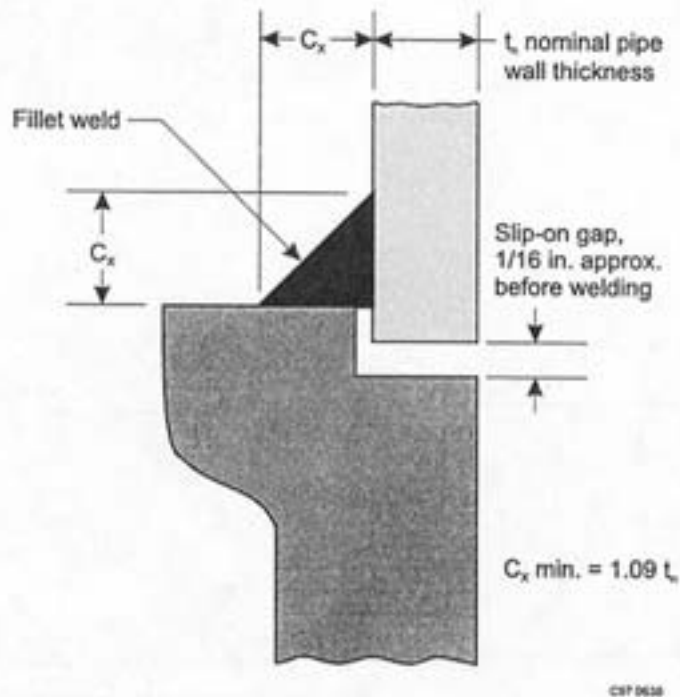
The welds that are subject to post weld heat treatment include those between the reactor pressure vessel and steam generator nozzles and the stainless steel main loop piping and between the pressurizer nozzles and the stainless steel surge and spray lines. These welds are present in the main loop piping of Westinghouse-type PWRs plants and surge and spray lines of all PWRs. Not all of these welds have stainless steel as a filler metal. For example, as discussed in Section 2.6.2, dissimilar metal welds with stainless steel filler metal are used at the ends of the main loop piping of only some Westinghouse plants, whereas Ni-based filler metal is used in the remaining Westinghouse plants. Stainless steel filler metal is used in most of the Framatome plants.

Fatigue analyses conducted using NB-3650 of Section III of the ASME Code [4.21] includes bimetallic welds using stress indices and the $\alpha_a T_a - \alpha_b T_b$ term, where α_a , α_b are the coefficients of thermal expansion on either side of the weld, and T_a , T_b are the corresponding temperatures. However, these analyses do not take into account the metallurgical changes introduced by the carbon migration.

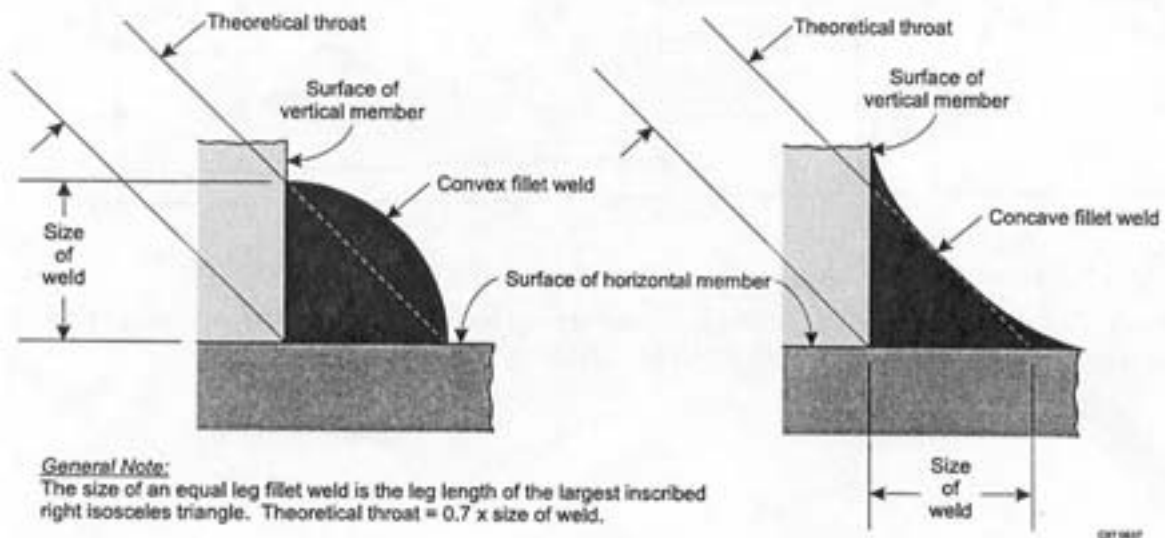
It seems that fatigue is not a real mechanism of initiation of dissimilar metal weld (DMW) degradations [4.41], but these DMW are more sensitive to stress corrosion cracking (SCC) (see Section 4.7) and fatigue with initial crack could be a potential mechanism, Alloy 182 welds being more sensitive than stainless steel welds to potential degradations by PWSCC.

4.2. Vibratory fatigue of small lines

Vibratory fatigue failures of small-diameter LWR piping have occurred worldwide. Review of the field experience indicate that these failures have been a significant source of problems in NPPs. The failures have occurred mainly at socket welds, shown in Figure 4-18, in small-diameter pipe lines. The failures have resulted from high-cycle mechanical fatigue accompanied by low-amplitude cyclic stress.



(a) Minimum welding dimensions for socket welding fittings.



(b) Equal leg fillet weld.

FIG. 4-18. Socket and fillet weld details and dimensions.

Three main contributing factors are (1) excitation mechanisms producing severe piping vibrations, (2) characteristics of socket weld making the weld susceptible to fatigue damage, and (3) inadequate piping supports that reduced natural frequency.

The excitation mechanisms that are responsible to cause vibratory fatigue failures are described first. Then the main characteristics of the socket weld that contribute to vibratory fatigue failures are described. Finally related field experience is presented.

4.2.1. Excitation mechanisms

The main excitation mechanisms for severe piping vibrations in NPPs are pump-induced pressure pulsations, cavitation and flashing. Pump-induced pressure pulsations occur at distinct frequencies, which are multiples of the pump speed. Pressure pulsations originate at the pump and are transmitted throughout the fluid the same way that sound is transmitted through air. In the case of positive displacement pumps, pulsations may be induced in both the suction and the discharge piping. When pressure pulsations coincide with a structural frequency of the piping system, severe vibratory fatigue damage may take place.

Cavitation occurs when the fluid pressure approaches its vapor pressure. Vapor pockets form and collapse in the low pressure region with extreme rapidity, generating intense shock waves. For example, it is estimated that two million cavities can collapse within one second over a small area [4.42].

The resulting broadband (a band with a wide range of frequencies) pressure pulsation can cause severe vibration of piping downstream of a cavitating component such as an orifice in the PWR letdown system. For example, vibration measurements in the vicinity of valves and orifices revealed high frequency, broadband vibration of an acceleration of hundreds of g's, with velocity at some points as high as hundreds of inches per second [4.43]. The frequency content of the excitation is one of the main differences between the cavitation- and pump-induced pressure pulsation. In addition to severe vibrations, the collapse of the cavities on a solid surface removes material by mechanical erosion, damaging piping and other components.

Flashing occurs when the temperature of water is higher than its saturation temperature at a given pressure and the water flashes into steam. This also results in broadband pressure pulsations causing vibration of piping downstream of the flashing component. Collapse of steam bubbles may also cause water hammer which may synergistically interact with vibratory fatigue in causing failure.

These excitation mechanisms generate high-frequency vibratory loads which were not considered in the design analysis because they cannot be predicted accurately. They can only be quantified during plant operation.

4.2.2. Characteristics of socket welds

Three characteristics of welded joints contribute to the vibratory fatigue failures: weld geometry, weld discontinuities, and residual stresses. Geometric discontinuities caused by a localized change in a section intensify the stresses in a very local area. The magnitude of the stresses decay rapidly to nominal stress values away from the discontinuity. The magnitude of the stress concentration depends on the geometry of the discontinuity; it is highest at the toe of the weld, if no crack-like discontinuities or weld imperfections are present.

Fatigue cracks in a weldment initiate where the localized stress range is maximum. This location may not correspond to a location with a geometric discontinuity where the stress concentration factor is maximum. This is so because, in addition to the geometric discontinuity, various imperfections and crack-like discontinuities (weld discontinuities) present in the weld metal or the heat-affected zone also act as stress raisers and drastically reduce the weld-joint fatigue strength (stress concentration factors as high as 15 have been estimated at the root of poor welds). Therefore, fatigue cracks may initiate either at surface

discontinuities such as at the weld toe, at embedded discontinuities such as inclusions, or at the weld root.

Markl and George [4.44] performed fatigue tests on socket-welded flanges. The results showed that fatigue cracking in a properly fabricated socket weld is usually associated with the weld toe in the case of a joint stressed in the transverse direction. In general, the crack initiates at the toe of the weld, propagates first through the weld metal, then through the heat affected zone, and finally through parent material as shown in Figure 4-19. None of the failures were attributed to the weld root defects, which are responsible for most of the socket weld failures reported in the nuclear industry. The fatigue strength reduction factor in the ASME Code for a socket weld is based on these data. Recent review of these data reveal that the corresponding tests represent relatively high-stress, low-cycle fatigue testing and do not represent the typical high-cycle vibratory fatigue conditions present in the field [4.45].

Vibratory fatigue failures of socket welds, as mentioned, have occurred predominately at weld roots. If the weld is incorrectly proportioned, either through bad design or through faulty fabrication, the stress across the weld throat may be sufficient to initiate a crack at the weld root. Usually, such a crack propagates through the weld metal and breaks the surface near the center of the weld face as shown in Figure 4-20. The presence of a discontinuity such as a lack of penetration at the weld root, degrades the fatigue strength greatly.

However, it should be noted that the mere existence of a discontinuity does not make a weldment defective or unsuitable for a given application. Discontinuities are designated as defects only when their size, orientation, and distribution exceed specification limits and their presence affects the integrity of a component. The presence of radially oriented root defects can significantly reduce fatigue strength of the socket weld [4.45].

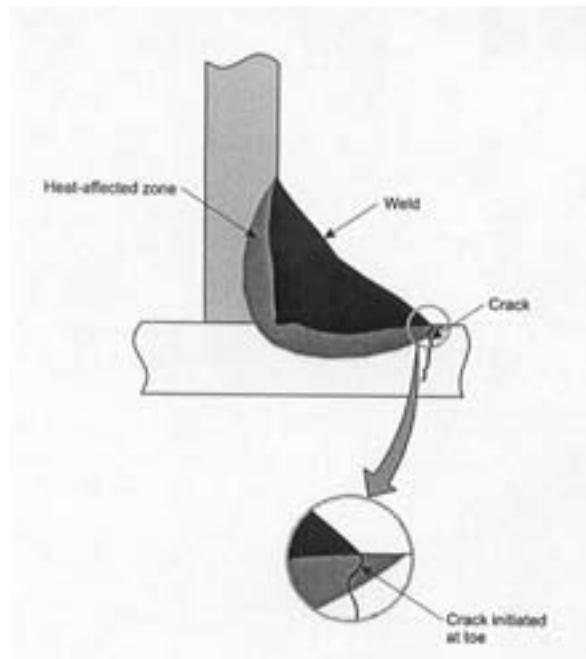


FIG. 4-19. Socket weld failure initiating at toe of fillet weld.

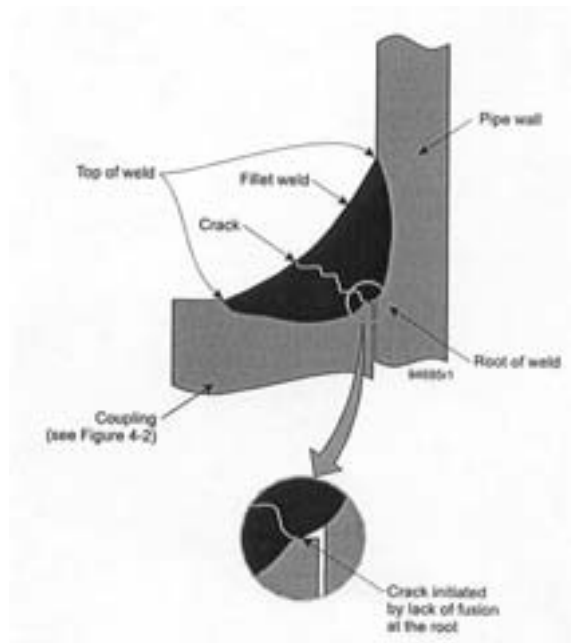


FIG. 4-20. Socket weld failure initiating at root of fillet weld.

Residual stresses are introduced in a weldment because of the inability of the deposited molten weld metal to shrink freely as it cools and solidifies. The magnitude of the residual stresses depends on several factors such as the size of the deposited weld beads, weld sequence, total volume of deposited weld metal, weld geometry, strength of deposited weld metal and of the adjoining base metal, and cooling rate. The concave shape of the weld, shown in Figure 4-20, obtained by placement of one last bead on the toe yields higher fatigue strength than the convex shape. This is attributed to the changes in the residual stresses at the weld root from highly tensile to compressive resulting from the placement of the last bead [4.45].

Mean stresses, which include residual stresses, play a significant role in crack initiation caused by high-cycle fatigue because the amplitude of the alternating stress is below the yield stress. As a result, the presence of a mean stress lowers the fatigue life. In contrast, mean stresses do not play a significant role in crack initiation by low-cycle fatigue where the amplitude of the alternating stresses is greater than the yield strength, so that the material shakes down to elastic action and the mean stress becomes zero. For high-cycle fatigue, the greater the mean stress, the greater the effect on lowering the fatigue life. ASME Section III has accounted for this by conservatively decreasing the fatigue design curves in the high-cycle region (at alternating stresses below the yield stress) to include the maximum effect of mean stress. The Code conservatively assumes that the alternating stress for a given life decreases linearly with mean stress. As the crack propagates, the residual stress will redistribute. The magnitude and orientation of the residual stresses play a part in determining the direction of crack propagation and its rate. The mean stress will change if the residual stresses relax during cyclic loading.

4.2.3. Experience in the USA

Table XXI lists several instances of fatigue failures of small lines connecting to the reactor coolant systems of PWRs over the past 20 years [4.46]. The predominant failure location is in socket welds. In some cases the weld was simply repaired by welding, and failure reoccurred in only a matter of days.

TABLE XXI. EXAMPLES OF FATIGUE FAILURES IN SMALL (<2 IN.) LWR LINES CONNECTING TO THE REACTOR COOLANT SYSTEM (STOLLER CORPORATION)

Year	Plant	Line	Diameter	Location	Comments
1994	Diablo Canyon 2 (W)	Accumulator vent	3/4	Socket weld	Fatigue, originated at weld defect
1992	Vogtle 1 (W)	Drain	1	Socket weld	Fatigue
1991	Nine Mile Pt. 2 (GE)	Flex hose	3/4	Socket weld	Fatigue
1991	North Anna 1 (W)	Valve pressurization	3/4	Weld	Fatigue, from external source
1989	Vogtle 1 (W)	Safety valve drain	3/4	Socket weld	Fatigue, drain manifold vibration
1989	Yankee Rowe (W)	Loop bypass vent	3/4	Weld	Fatigue
1989	Robinson 2 (W)	Thermowell	0.777	Threads in joint	Fatigue
1987	Hatch 2	Instrument	1	Socket weld	Fatigue
1987	Monticello (GE)	Decontamination	2	Fillet weld toe	Fatigue
1985	Rancho Seco (B&W)	OTSG vent	1	Pipe	Fatigue, lack of support
1984	Palisades (CE)	dp sensing	3/4	Socket weld	Fatigue, cantilever design, lack of weld penetration

TABLE XXI. EXAMPLES OF FATIGUE FAILURES IN SMALL (<2 IN.) LWR LINES CONNECTING TO THE REACTOR COOLANT SYSTEM (STOLLER CORPORATION) (CONT'D)

Year	Plant	Line	Diameter	Location	Comments
1983	Calvert Cliffs (CE)	Pump seal bleedoff	1	Weld	Fatigue
1981	Dresden 2 (GE)	Leakoff	3/4	Socket weld	Fatigue
1981	Beaver Valley 1 (W)	Instrument		Weld	Corrosion fatigue
1979	Brunswick 2 (GE)	Test connection	3/4	Pipe-to-elbow weld	Fatigue
1977	Brunswick 2 (GE)	Test connection	3/4	Socket weld	Fatigue, unsupported
1977	Millstone 2 (CE)	dp pressure tap	1	Socket weld	Fatigue, occurred at rewelded joint
1976	Millstone 2 (CE)	dp pressure tap	1	Socket weld	Fatigue
1975	Millstone 2 (CE)	3 dp pressure taps	1	Socket weld	Fatigue, vibration from RCPs
1975	Millstone 2 (GE)	Instrument	3/4	Longitudinal weld	Fatigue, corrugated tubing
1974	Browns Ferry 1 (GE)	Flow sensing	1	Fillet weld toe	Fatigue, improper support
1974	Browns Ferry 2 (GE)	Valve bypass	2	Fillet weld toe	Fatigue, at connection to valve

Shah et al. [4.22] have statistically investigated the trends of vibratory fatigue-related leak events (29 events in total), took place during the 1985–1996 time period, in calendar time and plant age. The effect of calendar time reflects the evolving body of regulations, design improvements, and industry wide learning, whereas the effect of plant age reflects the learning of the plant personnel and the ageing of the hardware. The results revealed no statistically significant trend in calendar time, but a decreasing trend with age. Apparently, the decreasing trend implies that the vibratory fatigue failures are caused by premature ageing because of inadequacy of the initial design and fabrication. In other words, the decreasing trend implies that the vibratory fatigue failures are not caused by ageing damage resulting from long term operation.

Suitable resolution of the vibratory fatigue problems generally required design changes such as adding additional supports, changing the mass of the line (such as by installing a loop seal), or rerouting the line. Another design change is to replace the socket welds with butt welds.

In several cases, vibration monitoring was used to assist in identifying the magnitude, frequency, and source of vibration. This was generally accomplished by strapping accelerometers to the affected pipe, sometimes supplemented by displacement measuring devices such as linear potentiometers. Strain gages have been used to determine the stresses in the vicinity of the failure.

While the failures of the small lines in Table XXI have been attributed to mechanical fatigue, these lines can also have high CUFs to which thermal transients are major contributors. For example, a CUF of 0.993 was calculated for the inside diameter of a liquid sample line attached to the surge line of a newer vintage Combustion Engineering plant [4.47]. The line branches from the vertical run of the surge line directly beneath the pressurizer. In one of the failures noted in Table XXI, the vibrational fatigue may have been accompanied by cold water from another source dripping on the line and causing thermal fatigue.

4.2.4. French experience

In the early 1990s, some leaks were discovered on small connecting piping in 4-loop plants. The destructive examinations performed identified high cycle thermal fatigue in the weld, not necessary on the socket-weld joint. The excitation sources are presented in paragraph 4.5.1; they are difficult to be precisely evaluated for analysis, and they are generally amplified by the design of these small lines (with a valve far from the tee junction without adequate support for this type of load). All the identified cracks were initiated in the outer surface heat affected zone of the weld, following the weld joint on an angle greater than 90° (up to 360°) for socket weld type and maximum of 70° followed by axial crack propagation for the other type of welds.

4.3. Thermal ageing of cast stainless steel piping and welds

Cast stainless steel piping and weldments are susceptible to reduction in toughness and tensile ductility because of long term exposure to LWR operating temperatures. This type of ageing is termed as thermal ageing. As discussed in Section 2.6.2, stainless steel piping material includes both wrought and cast stainless steels. However, ferrite is not present as a metallurgical constituent in the wrought stainless steel, whereas it is present in cast stainless

steel and also in the stainless steel weld metal. Since presence of ferrite is necessary to cause thermal ageing, wrought stainless steel piping does not experience this damage, whereas cast stainless steel piping and fittings and stainless steel weldments do experience it. We first discuss thermal ageing of cast stainless steel piping and then that of stainless steel weldments.

4.3.1. Thermal ageing of cast stainless steel piping

Cast austenitic-ferritic (duplex) stainless steels experience a reduction of toughness when aged at elevated temperatures. Ageing causes the ductile-to-brittle transition temperature increase, and both room-temperature and operating temperature toughnesses decrease. The maximum effect occurs at 475°C (885°F), and the general phenomenon is often identified as 475°C embrittlement. This temperature is well above the maximum temperatures of PWR main coolant piping (~320°C); nevertheless, a reduction of toughness does take place at the PWR operating temperatures over longer times.

This section first describes the physical metallurgy of the cast stainless steels and then qualitatively describes the basic mechanisms causing thermal ageing. Finally, it discusses effect of thermal ageing on mechanical properties of cast stainless steels.

Physical Metallurgy of Cast Stainless Steels. The required chemical compositions of the cast stainless steel Grades CF-8, CF-8A, and CF-8M are listed in Table XXII. Niobium may be present as a trace element. The compositions of Grades CF-8 and CF-8M are similar to those of the wrought stainless steel grades Type 304 and Type 316, respectively. The wrought grades have microstructures that are usually fully austenitic, whereas the cast grades typically have microstructures consisting of about 5 to 25% (volume) ferrite phase and the balance austenite [4.48]. (The ferrite phase in cast stainless steels and stainless steel welds is sometimes referred to as delta ferrite because it forms at high temperatures, where the ferrite field of the phase diagram is known as the delta phase to distinguish it from low-temperature ferrite known as the alpha phase.) The primary factor controlling the ferrite-austenite balance is bulk chemical composition. Chromium, silicon, molybdenum, and niobium (if present) promote the formation of ferrite, whereas nickel, carbon, manganese, and nitrogen promote the formation of austenite [4.48].

TABLE XXII. REQUIRED CHEMICAL COMPOSITIONS OF CAST STAINLESS STEELS^a

Element	Chemical composition (percent by weight ^b)	
	CF-8 CF-8A	CF-8M
Carbon	0.08	0.08
Manganese	1.50	1.50
Silicon	2.00	1.50
Sulfur	0.040	0.040
Phosphorus	0.040	0.040
Chromium	18.0 to 21.0	18.0 to 21.0
Nickel	8.0 to 11.0	8.0 to 11.0
Molybdenum	0.50	2.0-3.0

a. From Section II — material Specifications, Part A — Ferrous Materials, 1983 ASME Boiler and Pressure Vessel Code.

b. Maximum except where range is indicated.

The nitrogen is introduced during the casting process, but its percentage is not specified. Typical values of nitrogen in cast stainless steels vary from 0.03 to 0.08%. Empirical relationships have been developed for estimating the ferrite content from the chemical composition.

The size, distribution, and morphology of the ferrite within the austenite matrix also depends on the solidification conditions during the casting process. Cast stainless steels may solidify with a columnar or an equiaxed grain structure or a mixture of both structures. Researchers at the Argonne National Laboratory (ANL) have observed that in steels of similar chemical composition, the average grain size and the spacing between the ferrite islands generally tend to increase with larger section sizes and corresponding slower heat removal rates. Therefore, there can be considerable variations in microstructure across heavy wall castings. In castings with complex geometries such as an elbow, there can also be considerable variation in microstructure along the wall. The complex nature of metal solidification during casting makes it difficult to predict the finer details of the actual microstructure in cast stainless steel piping.

Grade CF-8A has controlled ferrite-austenite ratios to increase the minimum strength levels listed in Table XXIII [4.48]. This controlled-ferrite grade can have the same chemical composition as CF-8; with the ferrite and the strength controlled by adjusting the chemical composition within the limits for Grade CF-8 shown in Table XXIII. An increased ferrite content increases the yield and tensile strength of the cast stainless steels. Experience has shown that castings made from the alloys listed in Table XXIII may contain up to 30% ferrite when control of the amount of ferrite is not specified, though ferrite levels near 30% are not usual for castings made in accordance with ASTM specifications (e.g., A-743 and A-744).

Examples of austenitic-ferritic microstructures observed in cast stainless steel are shown in Figure 4-21. These samples were obtained from centrifugal castings. The ferrite phase (darkened networks and/or islands) is contained within a matrix of the austenite phase. The sample shown in Figure 4-21(a) had about 16% ferrite; the sample shown in Figure 4-21(b) had about 30% ferrite.

TABLE XXIII. REQUIRED ROOM-TEMPERATURE TENSILE PROPERTIES OF CAST STAINLESS STEELS^a

Property (minimum)	CF-8	CF-8A	CF-8M
Tensile strength MPa (ksi)	485 (7)	530 (77)	485 (70)
0.2% offset yield strength, MPa (ksi)	205 (30)	240 (35)	205 (30)
Elongation in 50 mm or in 2 in.	35.0%	35.0%	30.0%

a. From Section II – Material Specifications, Part A – Ferrous Materials, 1983 ASME Boiler and Pressure Vessel Code.

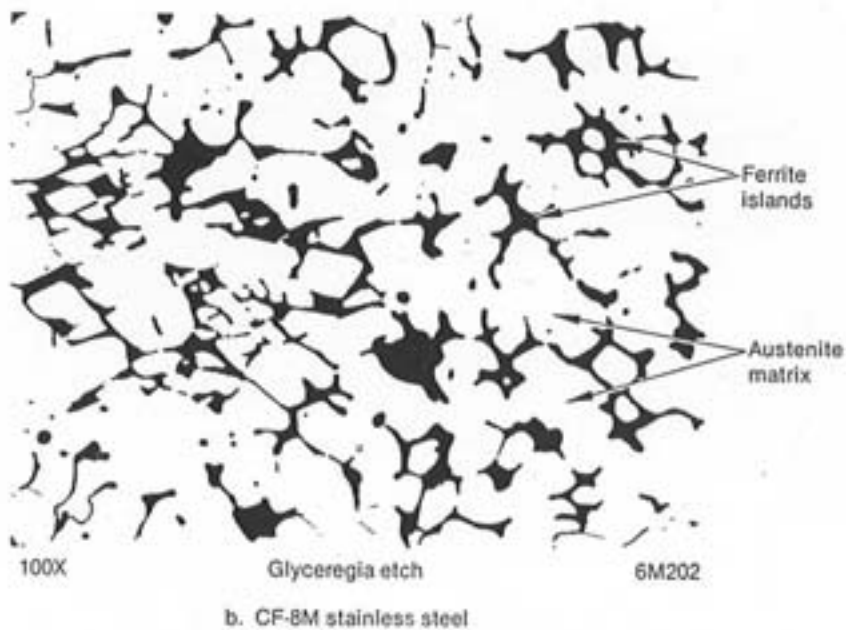
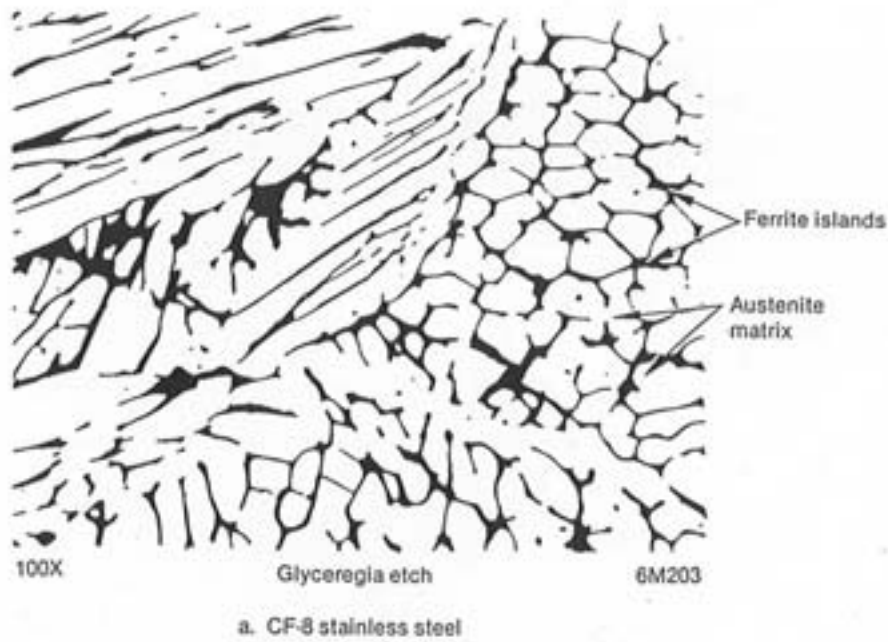


FIG. 4-21. Typical microstructures of centrifugally cast austenitic-ferritic stainless steels, with islands of ferrite in an austenite matrix. (a) Grade CF-8 stainless steel (16% ferrite), (b) Grade CF-8M stainless steel (30% ferrite).

The loss of toughness caused by thermal ageing of the cast stainless steels during elevated-temperature operation is related to (a) the formation of a Cr-rich alpha-prime phase and a Ni-rich and Si-rich G phase in the ferrite and (b) precipitation of carbides or nitrides in high-nitrogen steels at the austenite-ferrite phase boundaries. The formation of the alpha-prime phase in the ferrite is the primary factor involved in the thermal embrittlement of cast stainless steel at PWR operating temperatures. The phase-boundary carbides play a significant role in thermal embrittlement at temperatures greater than 400°C (750°F), but have less effect on the embrittlement at exposure temperatures less than 400°C. Also, the kinetics

of the formation of the alpha-prime and G phases appear to be different at PWR temperatures (temperatures less than 400°C (750°F)). Because of these differences in formation and precipitation behavior, the results of tests on material subjected to accelerated ageing at temperatures greater than 400°C should not be extrapolated to the lower PWR operating temperatures [4.49].

The alpha-prime phase typically forms by the process of spinodal decomposition [4.50–4.51]. Spinodal decomposition refers to a reaction whereby two phases of the same crystal lattice type, but different compositions and properties, form because a miscibility gap exists in the alloy system. In the iron-chromium system, these immiscible phases are known as the iron-rich alpha phase and the chromium-rich alpha-prime phase. This phase separation process occurs at a very fine scale (on the order of only a few nanometers) in the ferrite regions of cast stainless steel, and use of an atom probe field ion microscope is required to detect the presence of the alpha-prime phase [4.51]. There are indications that after extensive (many years) ageing at PWR operating temperatures the alpha-prime phase can also form by means of a nucleation and growth process, as well as by spinodal decomposition [4.50]. Depending on the composition of the ferrite (mainly Chromium content) and the exposure temperature, either or both of these processes may be involved in the formation of the alpha-prime phase [4.49].

The G phase forms in the ferrite by a nucleation and growth process, and its rate of formation increases with increased levels of carbon and molybdenum. The G phase has little direct effect on the degree of thermal embrittlement, as demonstrated by a laboratory experiment in which a thermally aged cast stainless steel pump cover was annealed at 550°C (1020°F) for one hour followed by water quenching. The annealing dissolved the alpha-prime phase and restored the Charpy-impact resistance to the level expected for unaged material, but the annealing had no effect on the G phase [4.50]. However, the presence of the G phase may indirectly affect the degree of thermal embrittlement in cast stainless steel components; cast stainless steel materials with significant G phase precipitation show low activation energies of embrittlement that may permit embrittlement to occur at PWR operating temperatures.

Because only the ferrite phase is embrittled by long term service at PWR operating temperatures, the overall thermal ageing of cast stainless steel piping depends on the amount and morphology of the ferrite present. For light water reactor applications, the traditional guideline has been that low-temperature embrittlement is a major concern only when the volume fraction of the ferrite exceeds approximately 15 to 20% [4.52]. The reasoning behind this guideline is that the ferrite phase tends to form in isolated pools contained within the austenite when ferrite levels are less than or equal to 15%. In this case, the overall toughness of the stainless steel casting is not greatly affected even if the ferrite were embrittled. However, where ferrite levels are greater than 15%, there is a greater tendency for a continuous path of embrittled material to exist through the thickness of the cast component, which would greatly reduce its toughness if the ferrite regions were embrittled [4.50].

There is more recent evidence that thick-walled (typically greater than 100-mm) Grade CF-8M cast stainless steel castings with ferrite levels in the range of 10 to 15% may also be subject to significant thermal embrittlement [4.50]. The grain size tends to be large, and the ferrite spacing (average distance between ferrite islands) is increased in heavy-section castings. With increasing ferrite spacing at a constant ferrite content, the size of the ferrite island increases and the probability of a continuous path of ferrite through the thickness of the

cast component increases. Bonnet et al. [4.53] selectively dissolved the austenite phase from samples of CF-8M and found that the ferrite phase remains continuous at ferrite volume fractions as low as 5%. Therefore, the thermal ageing of Grade CF-8M with such a ferrite distribution needs to be evaluated.

Mechanical Properties. Thermal ageing of cast stainless steels results in an increase in the tensile ultimate and yield strengths and a slight decrease in the tensile ductility [4.54–4.56]. The increase in the ultimate strength is much greater than the increase in the yield strength. Chopra [4.57–4.58] has presented empirical correlations to estimate the tensile properties of thermally aged cast stainless steel components. Thermal ageing also increases the ductile-to-brittle transition temperature of cast stainless steels. The effect of thermal ageing, for example, on the ductile-to-brittle transition behavior of Grade CF-8M cast stainless steel with 18% ferrite content is shown in Figure 4-22 [4.59].

Thermal ageing also decreases the lower and upper shelf Charpy energy (typically >100 ft-lb CVN initially) of cast stainless steels. The extent of the low-temperature embrittlement is most often quantified by measuring the room-temperature Charpy impact energy after ageing at temperatures in the range of 300 to 400°C (570–750°F), but not exceeding 400°C because of the potential for phase-boundary carbide formation and the kinetics of alpha-prime and G phase formation are likely to be different. An increased ageing temperature is often employed to accelerate the rate of thermal embrittlement compared with that occurs at normal PWR operating temperatures near 288°C (550°F). Chopra has developed two different approaches to determine the extent of the thermal embrittlement of cast stainless steel. The first approach provides a means for estimating the lower bound fracture toughness after long term thermal embrittlement, whereas the second approach provides means for estimating fracture toughness at a given service time and temperature. These approaches are discussed in Section 5.6.

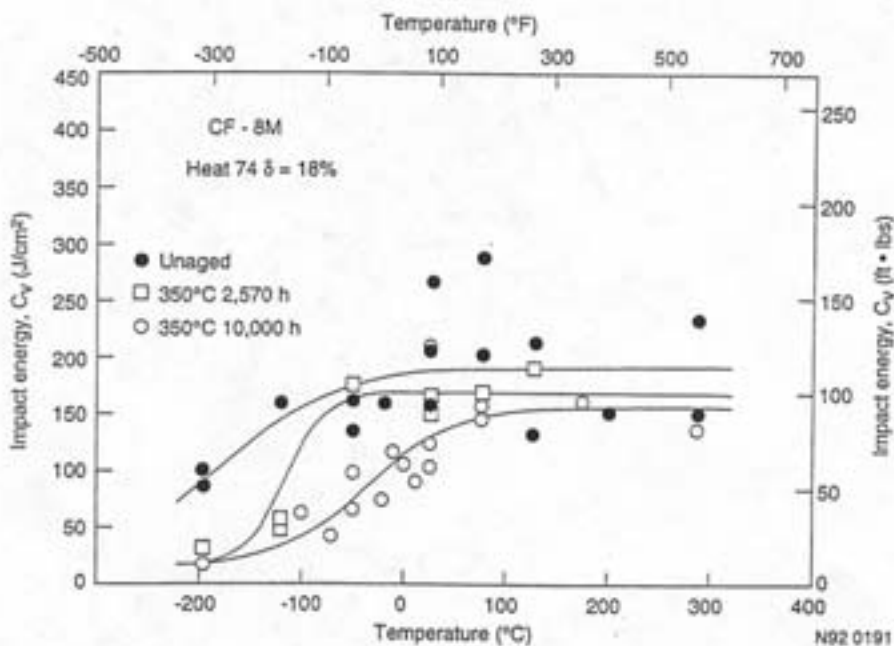


FIG. 4-22. Effect of ageing time on the ductile-to-brittle transition curves for Grade CF-8M stainless steel aged at 350°C [4.59].

EDF [4.60] has done complementary analysis on the effect of fabrication and test parameters on the toughness of aged cast stainless steel. In an elbow, the toughness is sensitive to the direction to location through the thickness and to location in the elbow, in connection with the elbow manufacturing process.

4.3.2. Thermal ageing of austenitic stainless steel welds

The stainless steel welds in older plants were made using shielded metal arc welding (SMAW) (or submerged arc welding) process, whereas in newer plants the welds were made using gas-tungsten arc welding (GTAW) process. The fracture behavior of the stainless steel welds is affected by the welding process used. Welds fabricated using a SMAW process have a lower fracture toughness than those made using a GTAW process, probably because the SMAW welds are likely to have a higher inclusion content and dendritic grain structure.

Initial room temperature CVN for the SMAW weld metal is in the range of 70 to 100 J (52–74 ft-lb), which is lower than that for wrought and cast stainless steel materials. Because of the presence of delta ferrite, the SMAW weld metal exhibit transition behaviour in which the CVN increases with test temperature resembling the behavior of ferritic steels. The room temperature CVN value for the unaged SMAW weld metal is at the upper shelf of the transition range. The unaged GTAW weld metal can have much higher upper shelf CVN values than does unaged SMAW; the upper shelf values for the GTAW are comparable to those for wrought stainless steel piping. The unaged SMAW weld metal has a significantly lower resistance to stable crack growth than unaged cast stainless steels [4.61].

Thermal ageing of stainless steel welds has been investigated by several researchers. Research results show that thermal ageing may cause a reduction in both the impact energy and fracture toughness of SMAW welds but not GTAW welds. Hale and Garwood [4.61] investigated the thermal ageing of Type 19-9-L austenitic welds made by SMAW. The ferrite content of the weld metal was in the range of 5 to 9 FN. Their results show that ageing at 400°C (752°F) for 10 000 to 20 000 h had little effect on the room temperature tensile properties and Charpy impact energy of these welds but resulted in a significant increase in the ductile-to-brittle transition temperature measured at the 27-J energy level, which was increased from –158 to –75°C, an increase of 83°C (150°F).

Alexander et al. [4.62] also investigated the thermal ageing of Type 308 stainless steel welds fabricated using the shielded metal-arc welding process. The ferrite content of these welds was 12%. Their results show that ageing of these welds at 343°C (650°F) for 20 000 h has a minimal effect on the room temperature tensile properties but caused a significant increase in the ductile-to-brittle transition temperature measured at the 68-J energy level, an increase from –25 to 60°C or 85°C (153°F). It appears that there may be a synergistic interaction between the embrittled ferrite phase and inclusions in the shielded metal-arc welds.

The results from Hale and Garwood [4.61] also show that thermal ageing at 400°C for up to 10 000 h reduces the elastic-plastic fracture toughness of the SMAW weld metal. The lower bound fracture toughness, J_{IC} , measured at 300°C (572°F) was reduced from 67 to 32 kJ/m². Most of this reduction in fracture toughness took place in the first 1000 h. Test results for thermally aged cast stainless steels and stainless steel weld metal show that the higher room temperature CVN energy is associated with higher elastic-plastic fracture toughness.

Mills [4.63] investigated the thermal ageing of Type 308 stainless steel welds fabricated using the gas-tungsten-arc welding process. The ferrite content of the weld metal was about 10 FN. Mills' results indicate that the fracture toughness of his welds was not affected by ageing at 427°C (800°F) for 10 000 h.

Further investigation is needed of the thermal ageing behaviour of shielded metal-arc welds having a ferrite contents representative of those in production welds. Significant embrittlement of welds, if confirmed by test results, could become a major problem because welds generally have a lower initial fracture toughness before thermal exposure than does the base metal.

4.4. Primary water stress corrosion cracking of alloy 600

Alloy 600 components such as steam generator tubes, pressurizer instrument penetrations and heater sleeves, control rod drive mechanisms (CRDM) nozzles, and hot leg penetrations have experienced primary water stress corrosion cracking (PWSCC) during the last 25 years. As a result, significant research and development efforts have been expended to determine the factors affecting the PWSCC. A mechanistic understanding of PWSCC is not yet established, but an empirical relationship based on field experience and research results has been developed. The results show that PWSCC of Alloy 600 components occurs when high tensile stress, an aggressive environment, and a susceptible microstructure are simultaneously present. This section discusses the effects of these parameters on PWSCC initiation time in Alloy 600 base metal. Then it discusses the factors affecting PWSCC growth rates.

4.4.1. Initiation key parameters

Effect of stress. The PWSCC damage rate increases as a function of stress to an exponent. Test results have shown this exponent to be in the range of 4 to 7 [4.64–4.65]. An exponent of 4 is typically used, i.e. damage rate $\propto \sigma^4$ where σ is the maximum principal tensile stress, which includes both applied and residual stresses. This correlation suggests that a 50% reduction in the effective stress will result in a sixteen-fold decrease in the damage rate and a corresponding increase in PWSCC initiation time. The correlation was developed using tensile specimen data and is widely used. A threshold stress, a stress below which PWSCC does not initiate, is not determined experimentally for Alloy 600. However, use of the strain rate damage model, which is based on slow strain rate test data, leads to an estimated threshold stress of about 241 MPa (35 ksi) at the operating temperature of about 315°C (600°F) [4.66].

All the PWSCC failures reported in the field, including hot leg penetrations cracking, resulted from high residual tensile stresses. High residual stresses are generally introduced during fabrication or installation of the Alloy 600 components. Cold work increases the residual stresses on the inside surface and thereby reduces the resistance to PWSCC.

Effect of operating temperature. PWSCC is a thermally activated process that can be described by an Arrhenius relationship of the form damage rate $\propto e^{-Q/RT}$ where:

- Q = activation energy
- R = universal gas constant
= 1.1×10^{-3} kcal/°R (mole)
- T = temperature in degrees Rankine.

Various estimates for the activation energy, Q, of Alloy 600 tube materials have been derived from laboratory studies and field experience. The estimates range from 163 to 272 kJ/mole (39 to 65 kcal/mole), with a best-estimate value of 209 kJ/mole (50 kcal/mole) [4.65], [4.67–4.68]. Estimates for activation energy for Alloy 600 components fabricated from bar materials may be different than those fabricated from tube materials.

PWSCC initiation is sensitive to temperature. For example, in any affected steam generator, the PWSCC has been first reported in the tubes on the hot-leg side, not on the cold-leg side. Similarly, PWSCC has been first reported in Alloy 600 penetrations in the hot leg and not in the cold leg. For activation energy equal to 209 kJ/mole, a temperature reduction of 10°C (from 320 to 310°C (608–590°F)) will reduce the PWSCC initiation time by a factor of two.

Effect of microstructure. Field experience and research results show that the PWSCC resistance of Alloy 600 is highest when the grain boundaries are covered with continuous or semicontinuous carbides [4.65]. The PWSCC resistance is lower when the grain boundaries are covered with widely spaced, discrete carbides. The PWSCC initiation time increases by a factor of five as the grain boundary carbide coverage increases from 0 to 100% [4.41]. The reasons for this beneficial effect of the intergranular carbides are not yet fully understood. According to Bruemmer, Charlot, and Henager [4.69], the intergranular carbides act as a source of dislocations, resulting in plastic strains that cause crack tip blunting and, thus, reduce PWSCC susceptibility. Another possible explanation, according to Smialowska of the Ohio State University, is that the Alloy 600 material passivates more readily in the presence of intergranular carbides [4.64].

The percentage of the grain boundary covered with intergranular carbides depends on the heat treatment temperature and time, carbon content, and grain size. During the heat treatment, if the temperature is high enough (>925°C (1700°F)), the Alloy 600 material recrystallizes, and new grain boundaries are formed [4.70]. If all the carbides are dissolved during the heat treatment, then carbon is in solution. The carbides will reprecipitate at the new grain boundaries during subsequent cooldown. As a result, the grain boundaries may be fully covered with carbides and the material becomes resistant to PWSCC. If all the carbides are not dissolved, the undissolved carbides remain as intragranular carbides (at old grain boundaries), and during subsequent cooldown the additional carbides will preferentially precipitate at the sites of these intragranular carbides. As a result, the grain boundaries are not fully covered with carbides, and the material is less resistant to PWSCC.

The solubility of carbon in Alloy 600 is fairly low and depends on its carbon content. The temperature at which all the carbides are dissolved increases as the carbon content increases [4.71]. For example, all the carbides will be dissolved at a heat treatment temperature of 980°C (1800°F) for a carbon content of 0.03 wt%. The corresponding temperature is 1204°C (2200°F) for a carbon content of 0.15%. So, if the heat treatment temperature is not high enough or the carbon content is too large, such that all the carbides are

not dissolved, the resulting microstructure will be less resistant to PWSCC. A review of several PWSCC failures supports this observation [4.72].

Alloy 600 material is more resistant to PWSCC if its grains are larger. This occurs because a larger grain size is associated with a lower yield strength and also with a smaller total grain boundary, requiring a smaller amount of carbide for complete coverage. When recrystallization takes place, the final grain size depends on the heat treatment temperature and time [4.70]. Higher heat treatment temperature and longer heat treatment time result in a larger grain size. The size of the recrystallized grains also depends on the amount of cold working of the material before the heat treatment. The greater the amount of cold work will result in finer post-heat treatment grain size.

Effect of coolant chemistry. Tests over the range of pH values from 6.9 to 7.4 at high temperatures show that the primary coolant chemistry has a secondary effect on PWSCC initiation in Alloy 600 material [4.73]. Some preliminary results show that PWSCC initiation is sometimes accelerated when the lithium content is high. For example, PWSCC initiation time was reduced (PWSCC susceptibility increased) by about a factor of two when the lithium concentration was increased from 2.2 ppm to 3.5 ppm at a constant boron concentration of 1200 ppm. Some tests are being performed to determine the lithium concentration above which the PWSCC risk begins to decrease [4.74]. A study in Japan shows that PWSCC damage is minimized at 2-ppm lithium, compared to 1 ppm and 3.5 ppm [4.75]. EPRI-sponsored studies indicate that increasing the hydrogen concentration in the primary coolant increases the rate of PWSCC. Consequently, EPRI PWR Primary Water Chemistry Guidelines (Rev. 2) recommend that utilities maintain lower hydrogen concentrations in the range of 25 to 35 cm³/kg, which is near the lower end of the typically used range of 25 to 50 cm³/kg [4.76–4.77]). A study at PWRs in France shows that minimum hydrogen concentration can be reduced from 25 to 15 cm³/kg [4.75].

4.4.2. Crack growth rate key parameters

PWSCC crack growth rates depend on the stress distribution in the penetration wall, operating temperature, and primary coolant chemistry. The growth rates are higher at those sites where the tensile stresses are higher. Cold work also promotes crack propagation [4.78]. The results from the crack growth rates in a 360°C (680°F) primary coolant are as follows. The measured rates were between 6 and 8.5 μm/h (0.2 and 0.3 mil/h) for 5% prestrained specimens and 0.8 μm/h (0.03 mil/h) for the as-received specimens.

EDF has developed crack growth rate based on plant measurements and laboratory tests [4.79]; The sensitivity to SCC seemed to depend mainly on the yield stress, cold work and temperature and can be expressed as follows:

$$da/dt=4.75 \cdot 10^{-9} \cdot \alpha(H_2, T) [\beta(GBC) \exp(0.0077YS)] [-5 \cdot 10^{-13} (\%CW)^2 + 4 \cdot 10^{-10} (\%CW) + 3 \cdot 10^{-10}] \cdot (K-9)^{0.1} \exp(-130000/RT)$$

with: da/dt in m/s; YS yield strength in MPa; K in MPa√m; % CW cold work percentage and; alpha which account for H2 and Temperature; beta for GBC Grain Boundary Coverage and YS interactions; R ratio to take into account the cycling effect of stresses.

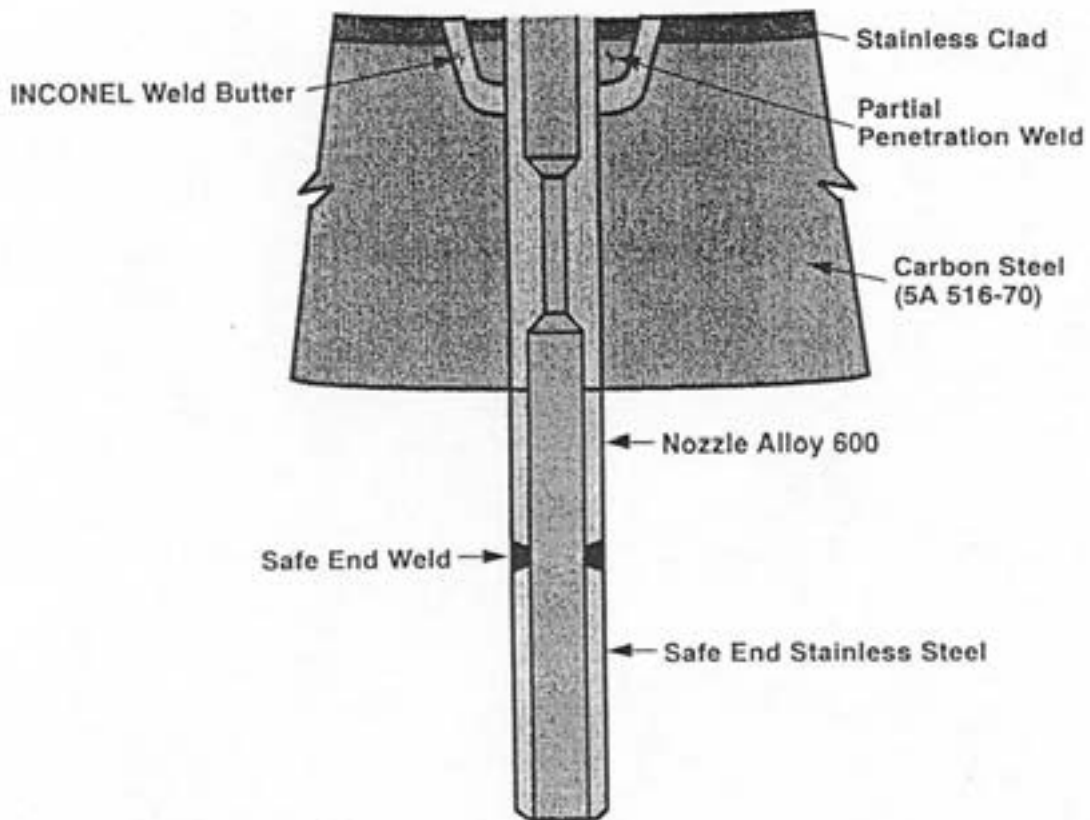


FIG. 4-23. As constructed configuration of the main loop instrumentation nozzles at Palo Verde Unit 2 [4.80].

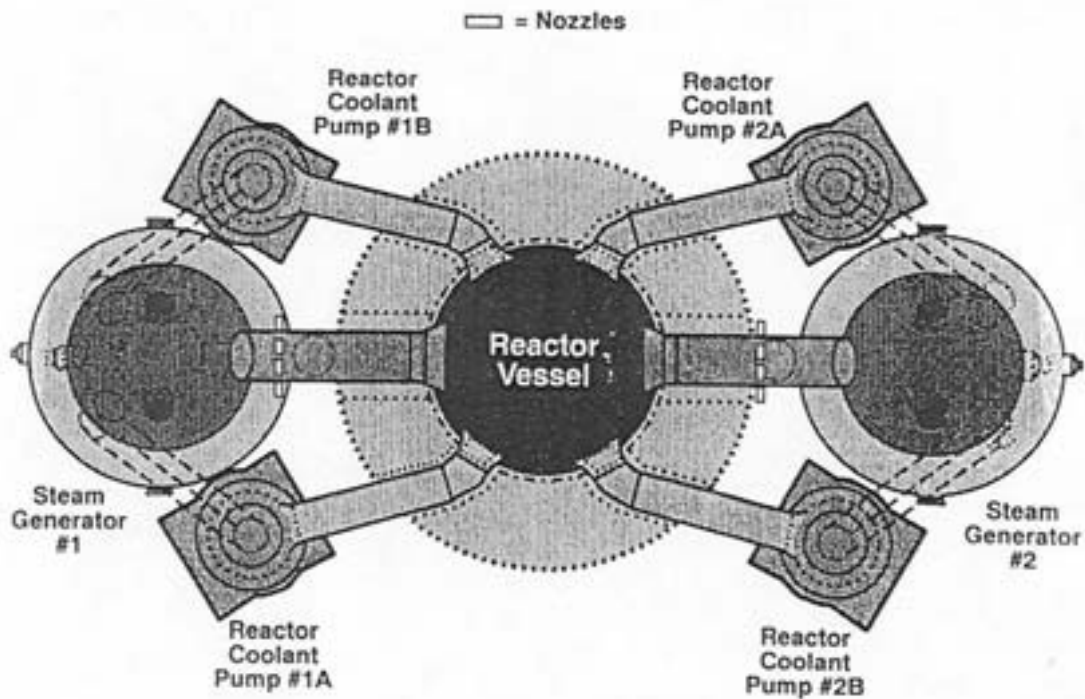


FIG. 4-24. Locations of Alloy 600 pressure/sampling instrumentation nozzles shown in the plan view of the reactor coolant system of Palo Verde Unit 2 [4.80].

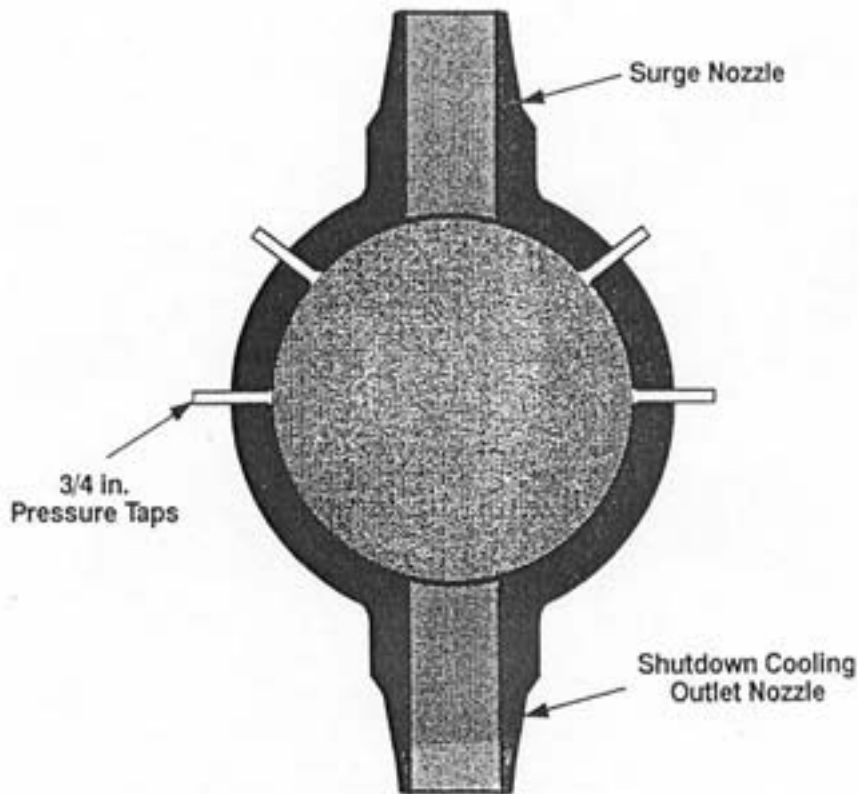


FIG. 4-25. Locations of Alloy 600 pressure/sampling instrumentation nozzles in hot leg A of Palo Verde Unit 2 [4.80].

4.4.3. Primary water stress corrosion cracking — operating experience

Arizona Public Service, a US utility operating Combustion-Engineering designed PWRs, evaluated the PWSCC susceptibility of Alloy 600 primary loop penetrations in the three Palo Verde units in response to PWSCC in other Combustion Engineering units. These penetrations are attached to the inside surface of the piping by a partial penetration weld as shown in Figure 4-23. The susceptibility ranking was based primarily on material yield strength (as determined from material certifications) and operating temperature. The analysis showed that the highest susceptibility parts were hot leg piping penetrations (8 penetrations) in Palo Verde Unit 2 with a yield strength of 499 MPa (72.3 ksi) and operating temperature of 327°C (621°F). The locations of these penetrations (nozzles) are shown in Figure 4-24, which is a plan view of the reactor coolant system, and Figure 4-25, which is a cross of the hot leg. A decision was made to preventively replace the Unit 2 hot leg nozzles during the 1991 refueling outage to avoid a forced outage during the summer months if a leak were to develop. (These penetrations are difficult to inspect because of the presence of the flow restrictors, which are located within the pipe wall thickness.) Penetration with moderate PWSCC susceptibility were to be inspected for boric acid deposit during each outage. The hot leg instrument nozzles (7 nozzles) in Palo Verde Unit 1 were also determined to have some PWSCC susceptibility. These nozzles were also to be inspected during each refueling outage. Replacement of these nozzles in 1993 was to be considered [4.80].

When the hot leg penetrations on Unit 2 were replaced in December 1991, it was discovered that two of the eight penetrations had axial cracks in the area adjacent to the partial

penetration weld. This is the same location as cracks discovered in pressurizer instrument nozzles [4.81]. The replacement of these penetrations is discussed in Section 7.

In January 1992, a leak was discovered in one of the pressurizer instrument nozzles in Palo Verde Unit 1 and a decision was made to replace all of the Alloy 600 pressurizer instrument nozzles in the Palo Verde units. Thus, PWSCC was discovered at the nozzles and penetrations at the Palo Verde units that were determined to have the highest susceptibility. Therefore, the susceptibility ranking may be one part of an effective strategy for managing PWSCC damage.

However, it should be noted that the ranking Alloy 600 by microstructure or using Arrhenius relationship has not been successful in several cases. For example, mechanical plugs for Westinghouse steam generator tubes have failed in the “best” condition and at lower temperatures. Similarly, the ranking has not been successful for instrument nozzles in pressurizers.

In October 2000, an axial through-wall crack along with a small circumferential crack were discovered on the 'A' hot leg nozzle of V. C. Summer Nuclear Station (VCSNS) at the beginning of Refuel Outage 12, when boric acid was found on the floor of the containment building. The axial crack was located in the weld between the RCS piping and the vessel nozzle, on the nozzle side of the weld, as shown in Figure 4-26. The circumferential crack was shallow and located at the inside surface of the weld. The UT inspections detected the axial through-wall crack but did not detect other shallow axial or circumferential indications in “A” hot leg nozzle. The eddy current inspections were able to detect the shallower indications, which were later confirmed during a destructive examination of the cracked weldment [4.82].

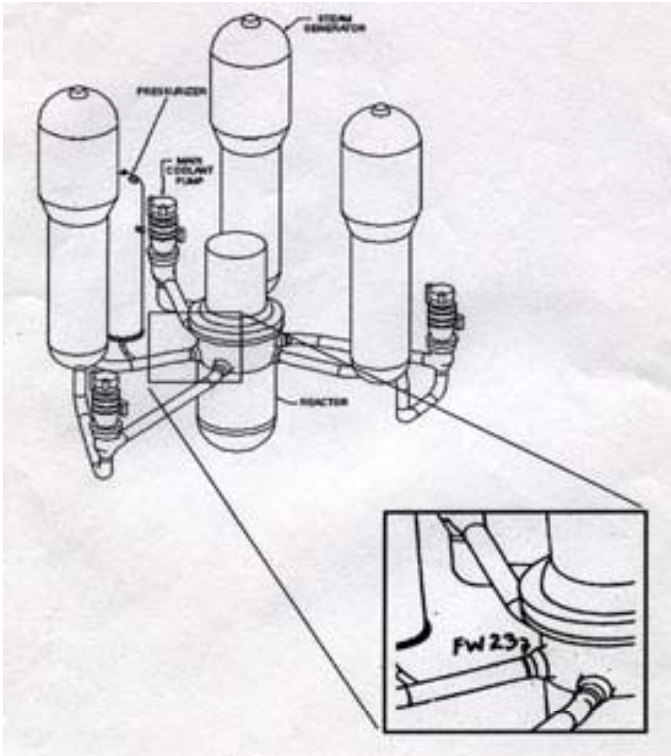


FIG. 4-26. Location of through-wall crack at V. C. Summer hot leg nozzle weld. FW23 shows the approximate location of the weld.

The RCS piping is Type 304 stainless steel. The vessel nozzle is SA-508 material clad with austenitic stainless steel. The weld used Inconel 182 butter between the weld piece and the vessel nozzle as shown in Figure 4-27. Figure 4-28 shows the location of the cracks in the nozzle-to-RCS piping weld. The VCSNS crack was the subject of NRC Information Notice 2000-17, *Crack in Weld Area of Reactor Coolant System Hot Leg Piping at V. C. Summer*. The investigation into the crack concluded that the cause was indirectly attributed to PWSCC. The weld at the nozzle was determined to be subjected to high tensile stresses as a result of extensive weld repairs performed during the original construction. The operating temperature for the weld was 326°C. A number of smaller PWSCC cracks were subsequently identified when the weld was cut out and destructively tested. A spool piece was used to replace the affected weld and was installed utilizing Inconel 52 and 152 weld materials, which are more resistant to PWSCC. The welding was performed in a manner which minimized residual stresses.

Further eddy current inspections of the other VCSNS RCS nozzle-to-pipe welds of the B and C hot leg nozzles detected minor indications of cracking. The UT examinations did not detect these indications. During the next fueling outage, VCSNS took mitigative actions by applying the Mechanical Stress Improvement Process (MSIP) to these other nozzles. MSIP contracts the pipe on one side of the weldment, placing the inside diameter of the weld into compression. This is an effective means to prevent and mitigate PWSCC. MSIP has been used extensively on piping in boiling water reactor (BWR) plants to successfully prevent and mitigate SCC. This includes reactor vessel nozzle piping over 30-inch diameter with 2.3 inch wall thickness similar in both size and materials to piping in pressurized water reactor (PWR) plants such as VCSNS.

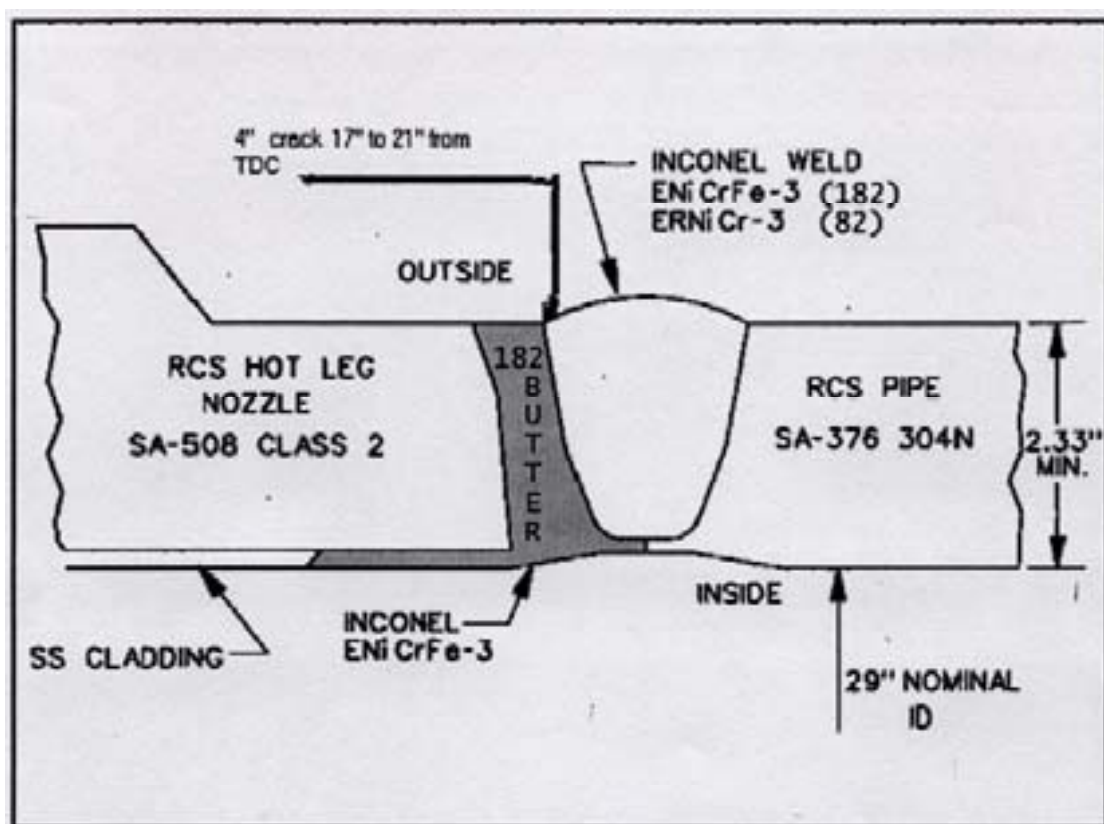


FIG. 4-27. Geometry of V. C. Summer RCS "A" hot leg nozzle-to-pipe weld region [4.83].

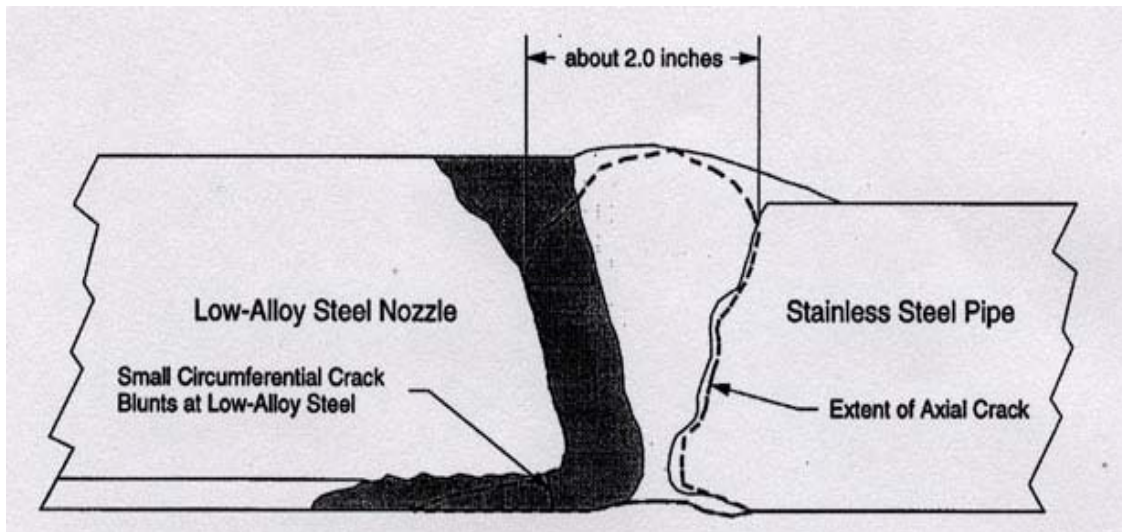


FIG. 4-28. Location of axial and circumferential cracks in V.C. Summer hot leg nozzle to primary coolant pipe weld [4.84].

In May 2002, using a newly designed 34-inch clamp, MSIP was successfully applied to the two hot-leg nozzle weldments. The pre- and post-MSIP NDE results were highly favorable. Analyses were performed to determine the redistribution of residual stresses, amount of strain in the region of application, reactor coolant piping loads and stresses, and effect on equipment supports.

During a regularly scheduled inservice inspection of Ringhal Units 3 in the summer of 1999, two shallow axial surface flaws were discovered in the Alloy 182 outlet nozzle to safe end weld region. These flaws were all in a single weld, and were evaluated and allowed to remain in service.

During a regularly scheduled inservice inspection of Ringhal Units 4 in the summer of 2000, four axial surface flaws were found in one of the outlet nozzle-to-safe end weld regions. The deepest of these flaws was approximately 28 mm deep, and all four were removed by taking contoured boat samples. No weld repairs were made.

4.5. Boric acid corrosion

Leakage of primary coolant may cause boric acid corrosion (wastage) of main coolant loop piping components made from carbon steel or low-alloy steel materials and lead to loss of material. The primary coolant contains boric acid and some lithium hydroxide in solution, and its pH at 25°C (77°F) varies over the range of 4.2 to 10.5. The boric acid in the leaking primary coolant may cause wastage or general dissolution corrosion of carbon steel and low-alloy steel components. The corrosion rate appears to depend upon the pH of the solution, the solution temperature, and the boric acid concentration in the solution. Some studies have shown that the corrosion rates of the steel at pH values of 8 to 9.5 are six times those at pH values of 10.5 to 11.5 [4.85]. As temperatures increase to the boiling point of water, the water evaporates, the solution concentrates, and the corrosion rate increases at much faster rates. Concentrated boric acid is highly corrosive at ~95°C (~200°F).

Field experience and test results indicate that the corrosion rates for carbon steels and low-alloy steels exposed to primary coolant leakage are greater than previously estimated and

could be unacceptably high. The field experience is mainly associated with the carbon steel and low-alloy steel pressure boundary components such as closure bolting and carbon steel safety valve bonnets. The related field experience with reactor pressure vessel head and closure studs for reactor coolant pump is summarized here. In one incident, leakage from the CRDM housing penetrated the reactor vessel head insulation at Salem Unit 2 and ran down along one side of the reactor vessel head. Three reactor vessel head bolts were severely corroded and had to be replaced [4.86]. In addition, nine corrosion pits of 25 to 76-mm (1 to 3-in.) diameter and 9 to 10-mm (0.36 to 0.4-in.) deep were found in the reactor vessel head [4.82]. Turkey Point Unit 4 personnel discovered more than 227 kg (500 lb) of boric acid crystals on the reactor vessel head in 1987. The cause was a leak from a lower instrument tube seal (Conoseal) of one of the in-core instrument tubes [4.88–4.89]. (About 0.028 m³ (one cubic foot) of boric acid crystals had been removed from the same area in 1986). Vapors containing water-soluble boric acid had been borne into the upper CRDM area, and into the CRDM cooling coils and ducts. The CRDM cooling shroud support was severely corroded and required replacement.

PWR pump closure studs are susceptible to corrosion wastage caused by primary coolant leakage across the pump body-to-cover gaskets. Leakage and then evaporation of the boron containing primary coolant water on the outside surface leaves a concentrated boric acid solution in contact with the closure studs. Concentrated boric acid solution corrode ferritic steel easily. Boric acid corrosion in one PWR plant reduced seven reactor coolant pump studs from a nominal diameter of 90 mm (3.5 in.) to between 25 to 37 mm (1.0 and 1.5 in.) [4.90–4.91]. The corrosion occurred in the region of the studs adjacent to the top surface of the lower flange, and caused an hour-glass appearance. Inspection of closure studs at other PWR plants have revealed that the studs in all pump designs are susceptible to boric acid corrosion.

The observed boric acid corrosion rates are relatively high. Therefore, it is important to ensure that adequate monitoring procedures are in place to detect boric acid leakage before it results in significant ageing of the reactor coolant pressure boundary, such as wastage of carbon steel and low-alloy steel base metal.

4.6. Atmospheric corrosion

The French Dissimilar Metal Welds (DMW) are described in Paragraph 2.6.3, they used stainless steel buttering and stainless steel weld. In 1997 more than 1000 DMW inspection results have been analysed and 50 of them are affected by intergranular degradation on the outer surface (few mm deep) in the buttering and close to the ferritic to stainless steel interface. Different complementary investigations have been done (replica, optical surveillance, laboratory test). The degradations are in the austenitic zone of the first layer of the buttering; in many case, in the same time corrosion pitting are discovered in the same area in the ferritic steel; all the degradations are filled up by oxyde. No growth and no new degradations have appeared on 4 DMW periodically inspected [4.92].

Laboratory tests confirmed absence of hot cracking and three other mechanisms have been studied [4.39]: high temperature oxydation, stress corrosion cracking and intercrystalline corrosion (atmospheric type). Finally, the degradations were attributed to intercrystalline corrosion after reproduction in laboratory on small specimen and on a 10 cm scale 1 DMW with good representativity of the major parameters: metallurgical state, oxyde environment and mechanical loads followed by high temperature regime (operating temperature).

REFERENCES TO SECTION 4

- [4.1] LEE, S., and KUO, P.T., Ageing Management of Reactor Coolant System Piping for License Renewal, presented at the 14th International Conference on Structural Mechanics in Reactor Technology (SMiRT-14), Lyon, France, 17–22 August 1997 (1997).
- [4.2] BUCKTHORPE, D., ESCARAVAGE, C., NERI, P., PIERANTOZZI, P., SCHMIDT, D., “Study Contract on Bi-Metallic Weldments”; EC Report C9731/TR002, Issue V02, April 1997.
- [4.3] American Society of Mechanical Engineers, Boiler and Pressure Vessel Code, Section III, Rules for Construction of NPP Components, Division 1, Subsection NB, Class 1 Components, ASME, New York (1989).
- [4.4] WEC (Westinghouse Electric Corporation), Application of the Leak-Before-Break Approach to Westinghouse PWR Piping, EPRI NP-4971, Electrical Power Research Institute, Palo Alto, CA (1986).
- [4.5] RICCARDELLA, P.C., Application of Fatigue Monitoring to the Evaluation of Pressurizer Surge Lines, EPRI TR-100273, Electric Power Research Institute, Palo Alto, CA (1992).
- [4.6] SU, N.T., Special Study Report — Review of Thermal Stratification Operating Experience, AEOD/S902, USNRC Office of Analytical and Evaluation of Operational Data (1990).
- [4.7] MUKHERJEE, S.K., et al., Beaver Valley Unit 2 Pressurizer Surge Line Stratification, Duquesne Light Company (1988).
- [4.8] USNRC, Pressurizer Surge Line Thermal Stratification, USNRC Bulletin 88-11 (1988).
- [4.9] HAFNER, W., SPURK, J.H., Formation of Waves in Thermal Stratified Flow, presented at the International Conference on Physical Modeling of Transport and Dispersion, MIT, Cambridge, MA, 7–10 August 1990.
- [4.10] WOLF, L., Results of Thermal Mixing Tests at the HDR-Facility and Comparisons with Best-Estimate and Simple Codes, Nuclear Engineering and Design, **99** (1987) 287–304.
- [4.11] DEARDORFF, A.F., et al., Development of a Thermal Striping Spectrum for Use in Evaluating Pressurizer Surge Line Fatigue, Advances in Dynamics of Piping and Structural Components, PVP Vol. 198, American Society of Mechanical Engineers, New York (1990) 23–28.
- [4.12] TURNER, J.S., Buoyancy Effects in Fluids, Cambridge University Press, Cambridge, MA (1973).
- [4.13] MASSON J.C., STEPHAN, J.M., “Fatigue Induced by Thermal Stratification: Results of Tests and Calculations of the COUFAST model”, NEA/CSNI Specialist Meeting on Experience with Thermal Fatigue in LWR piping caused by Mixing and Stratification”, Paris, June 1998.
- [4.14] GRIESBACH, T., (Electric Power Research Institute), Private communication with E.A. Siegel (Combustion Engineering) (1988).
- [4.15] United States Nuclear Regulatory Commission, Safety Injection Pipe Failure, USNRC Information Notice 88-01, 27 January 1988.
- [4.16] COCKFIELD, D.W., (Portland General Electric), Letter to USNRC (27 April 1988).
- [4.17] BRICE-NASH, R.L., et al., Evaluation of Thermal Stratification for the South Texas Units 1 and 2 Pressurizer Surge Line, WCAP-12087, Revision 1, Westinghouse Electric, Pittsburgh, PA (1989).

- [4.18] ENSEL, C., COLAS, A., BARTHEZ, M., “Stress Analysis of a 900 MW Pressuriser Surgeline including Stratification Effects”, Nuclear Engineering and Design, Vol. 153, January 1995.
- [4.19] MATTHEWS, M.T., et al., Final Submittal in Response to Nuclear Regulatory Commission Bulletin 88-11 “Pressurizer Surge Line Thermal Stratification”, BAW-2127, Babcock & Wilcox, Lynchburg (1990).
- [4.20] BABCOCK & WILCOX, Pressurizer Surge Line Thermal Stratification for the B&W-177 Fuel Assembly Nuclear Plant, B&W-2127, Supplement 2, 177 Fuel Assembly Nuclear Plans, Summary Report (1992).
- [4.21] American Society of Mechanical Engineers, Boiler and Pressure Vessel Code, Section III, Rules for Construction of NPP Components, Division 1, Subsection NB, Class 1 Components, ASME, New York (1989).
- [4.22] SHAH, V.N., et al., Assessment of Pressurized Water Reactor Primary System Leaks, NUREG/CR-6582, INEEL/EXT-97-01068 (1998).
- [4.23] JUNGCLAUS, D., et al., “Common IPSN/GRS Safety Assessment of Primary Coolant Unisolable Leak Incidents Caused by Stress Cycling”, presented at the NEA/CSNI Specialists’ Meeting on Experience with Thermal Fatigue in LWR Piping Caused by Mixing and Stratification, OECD Nuclear Energy Agency, 7–12 June 1998, Paris, France.
- [4.24] United States Nuclear Regulatory Commission, Cracking in Piping of Makeup Coolant Lines at B&W Plants, USNRC Information Notice 82-09 (1982).
- [4.25] BABCOCK & WILCOX, 177 Fuel Assembly Owner’s Group Safe End Task Force Report on Generic Investigation of HPI/MU Nozzle Component Cracking, B&W Document 77-1140611-00, Babcock & Wilcox, Lynchburg.
- [4.26] United States Nuclear Regulatory Commission, Unisolable Crack in High-Pressure Injection Piping, USNRC Information Notice 97-46 (1997).
- [4.27] REDMOND, K., ONS 2 & # HPI/MU Nozzle Components, Metallurgical Analysis Report, Report 2181, Duke Power Company (1997).
- [4.28] NAKAMORI, N., HANZAWA, K., Valve Maintenance Guideline to Prevent Thermal Fatigue Damage of the Reactor Pressure Boundary Piping, PVP Vol. 313-2, ASME (1995) 95–102.
- [4.29] THEBAUT, Y., GRANDJEAN, Y., GAUTHIER, V., LAMBERT B., CEBUSTCHER, B., “Contrôles et Examens Métallurgiques sur Tuyauteries de Circuit RIS”, Contribution des expertises sur matériaux à la résolution des problèmes rencontrés dans les réacteurs à eau pressurisée, Colloque International Fontevraud IV, Fontevraud, France, Septembre 1998.
- [4.30] USNRC, Safety Injection Piping Failure, USNRC Information Notice 88-01 (1988).
- [4.31] USNRC, Pressurizer Surge Line Thermal Stratification, USNRC Bulletin 88-11, (1988).
- [4.32] FAIDY, C., LE COURTOIS, T., DE FRAGUIER, E., DECHELOTTE, J., LEDUFF, J.A., LEFRANÇOIS, A., “Thermal Fatigue in French RHR system”, International Conference on Fatigue of Reactor Components, Napa, CA, July 31– August 2 2000.
- [4.33] USNRC, Thermal Stresses in Piping Connected to Reactor Coolant Systems, USNRC Bulletin 88-08, Supplement 3 (1989).
- [4.34] USNRC, Thermal Stresses in Piping Connected to Reactor Coolant Systems, USNRC Bulletin 88-08, Supplement 1 (1988).
- [4.35] USNRC, Thermal Stresses in Piping Connected to Reactor Coolant Systems, USNRC Bulletin 88-08, Supplement 2 (1988).

- [4.36] United States Nuclear Regulatory Commission, Thermal Stresses in Piping for McGuire and Catawba, Letter from R.E. Martin to M.S. Tuckman, USNRC Bulletin 88-08, 31 October 1991.
- [4.37] STRAUCH, P.L., et al., “Stratification Issues and Experience in Operating Power Plants”, High Pressure Technology, Fracture Mechanics, and Service Experience in Operating Power Plants, ASME Pressure Vessels and Piping Conference, Nashville, TN, PVP Vol. 192 (1990) 85–92.
- [4.38] BAIN, R.A., et al., A Long term Programme to Address NRC Bulletin 88-08 Thermal Stratification Concerns, PVP-Vol. 264, ASME (1993) 21–28.
- [4.39] CATTANT, F., DE BOUVIER, O., ECONOMOU, J., TEISSIER, A., YRIEX, B., “Examens et Études Métallurgiques de Liaisons, Bimétalliques de Circuit Primaire Principal”, Contribution des expertises sur matériaux à la résolution des problèmes rencontrés dans les réacteurs à eau pressurisée, Colloque International Fontevraud III, Fontevraud, France, Septembre 1994.
- [4.40] LUNDIN, C.D., Dissimilar Metal Welds — Transition Joints Literature Review, Welding Journal, **61** 2 (1982) 58–63.
- [4.41] RAO, G.V., “Methodologies to Assess PWSCC Susceptibility of Primary Component Alloy 600 Locations in Pressurized Water Reactors”, Sixth International Symposium on Environmental Degradations of Materials in Nuclear Power Systems - Water Reactors, San Diego, CA (1994) 871–882.
- [4.42] SEDRIKS, A.J., Corrosion of Stainless Steels, John Wiley, New York (1979) 208.
- [4.43] KELLY, M.W., DAVIS, J.M., Vibration Issues and Examples, presented at the Electric Power Research Institute (EPRI) Seminar on Operating Power Plant Fatigue Damage Assessment, Burlington, VT, 9–11 August 1995.
- [4.44] MARKL, A., GEORGE, M., Fatigue Tests on Flanged Assemblies, Transactions of the ASME, January 1950.
- [4.45] Structural Integrity Associates, Vibration Fatigue of Small Bore Socket-Welded Pipe Joints, EPRI TR-107455, Electric Power Research Institute, Palo Alto, CA (1997).
- [4.46] STOLLER, S.M., 1974–1994 Nuclear Power Experience, PWR-2, V.B., S.M. Stoller Corporation, Lafayette, CO (1994).
- [4.47] WARE, A.G., Fatigue Monitoring for Ageing Assessment of Major LWR Components, NUREG/CT-5824, EGG-2668, Draft (1994).
- [4.48] PECKNER, D., BERNSTEIN, I., Handbook of Stainless Steels, McGraw-Hill Book Company, New York (1977).
- [4.49] BETHMONT, M., et al., Properties of Cast Austenitic Materials for Light Water Reactors, International Journal of Pressure Vessels and Piping, **65** (1996) 221–229.
- [4.50] CHOPRA, O.K., CHUNG, H.M., Investigations of the Mechanics of Thermal ageing of Cast Stainless Steels, presented at the Metal Component Subcommittee of the Advisory Committee on Reactor Safeguards Meetings, Columbus, OH, 1–2 July 1986, transcript available from the NRC Public Document Room.
- [4.51] SASSEN, J.M., et al., Kinetics of Spinodal Decomposition in the Ferrite Phase of a Duplex Stainless Steel, Properties of Stainless Steels in Elevated Temperature Service, MPC-Vol. 26, PVP Vol. 132, American Society of Mechanical Engineers, New York (1987) 65–78.
- [4.52] COPELAND, J.F., GIANNUZZI, A.J., Long term Integrity of Nuclear Power Plant Components, EPRI NP-3673-LD, Electric Power Research Institute, Palo Alto, CA (1984).
- [4.53] BONNET, S., et al., Relationship between Evolution of Mechanical Properties of Various Cast Stainless Steels and Metallurgical and Ageing Parameters: Outline of Current EDF Programmes, Materials and Science Technology, **6** (1990) 221–229.

- [4.54] LANDERMAN, E.L., BAMFORD, W.H., “Fracture Toughness and Fatigue Characteristics of Centrifugally Cast Type 316 Stainless Steel Pipe after Simulated Thermal Service Conditions”, in *Ductility and Toughness Considerations in Elevated Temperature Service*, MPC-8, The American Society of Mechanical Engineers, New York (1978) 99–127.
- [4.55] CHOPRA, O.K., CHUNG, H.M., Long term Embrittlement of Case Duplex Stainless Steels in LWR Systems: Semiannual Report April–September 1986, NUREG/CR-4744 Vol. 1, No. 2, ANL-87-16.
- [4.56] SLAMA, G., et al., Effect of Ageing on Mechanical Properties of Austenitic Stainless Steel Castings and Welds, SMiRT Post Conference Seminar 6, Monterey, CA (1983).
- [4.57] CHOPRA, O.K., Estimation of Mechanical Properties of Cast Stainless Steels During Thermal Ageing in LWR Systems, Proceedings of the US Nuclear Regulatory Commission Nineteenth Water Reactor Safety Information Meeting, NUREG/CP-0119, Vol. 1 (1992) 151–178.
- [4.58] CHOPRA, O.K., Thermal Ageing of Cast Stainless Steels in LWR Systems: Estimation of Mechanical Properties, Nuclear Plant System/Components Ageing Management and Life Extension, PVP Vol. 228, American Society of Mechanical Engineers, New York (1992) 79–92.
- [4.59] CHOPRA, O.K., SATHER, A., Initial Assessment of the Mechanisms and Significance of Low-Temperature Embrittlement of Cast Stainless Steels in LWR Systems, NUREG/CR-5385, ANL-89/17 (1990).
- [4.60] MASSOUD, J.P., BOVEYRON, C., OULD, P., BAZDIKIAN, G., CHURIER-BOSSENE, H., “Effect of the Manufacture Process on Thermal Ageing of PWR Duplex Stainless Steel Components”, ICONE-6, International Conference on Nuclear Engineering, paper 6085, San Diego, CA, May 1998.
- [4.61] HALE, G.E., GARWOOD, S.J., Effect of Ageing on Fracture Behaviour of Cast Stainless and Weldments, *Material Science and Technology*, 6, March (1990) 230–235.
- [4.62] ALEXANDER, K.B. et al., Microscopical Evaluation of Low Temperature ageing of Type 308 Stainless Steel Weldments, *Material Science and Technology*, 6, March (1990) 314–320.
- [4.63] MILLS, W.J., Fracture Toughness of Aged Stainless Steel Primary Piping and Reactor Vessel Materials, *Journal of Pressure Vessel Technology*, **109** (November 1987) 440–448.
- [4.64] HUNT, E.S., GROSS, D.J., PWSCC of Alloy 600 Materials in PWR Primary System Penetrations, EPRI TR-103696, EPRI TR-103345, Electric Power Research Institute, Palo Alto, CA (1994).
- [4.65] BOURSIER, J.M., ROUILLON, Y., LE HONG, S., AMZALLAG, C., “Expertises métallurgiques et essais de corrosion sous contrainte en milieu primaire des alliages Ni-Cr-Fe”, Contribution des expertises sur matériaux à la résolution des problèmes rencontrés dans les réacteurs à eau pressurisée, Colloque International Fontevraud IV, Fontevraud, France, Septembre 1998.
- [4.66] BEGLEY, J., Application of the Gerber-Garud Strain Rate Damage Model to PWSCC, Proceedings: 1987 EPRI Workshop on Mechanisms of Primary Water Intergranular Stress Corrosion Cracking, EPRI NP-5987SP, Electric Power Research Institute, September (1988) D6-1–D6-11.
- [4.67] GORMAN, J.A., et al., Statistical Analysis of Steam Generator Tube Degradation, EPRI-NP-7493, Electric Power Research Institute, Palo Alto, CA (1991).

- [4.68] STEIN, A.A., McILREE, A.R., Relationship of Annealing Temperature and Microstructure to Primary-Side Cracking of Alloy 600 Steam Generator Tubing and the Prediction of Stress Corrosion Cracking in Primary Water, Proceedings of the Second International Symposium on Environmental Degradation of Materials in Nuclear Power Systems — Water Reactors, American Nuclear Society, La Grange Park, IL (1986) 47.
- [4.69] BRUEMMER, S.M., CHARLOT, L.A., HENAGER Jr, C.H., Microstructure and Microdeformation Effects on IGSCC of Alloy 600 Steam Generator Tubing, Proceedings: 1987 EPRI Workshop on Mechanisms of Primary Water Intergranular Stress Corrosion Cracking, EPRI NP-5987SP, Electric Power Research Institute, Palo Alto, CA (1988) C3-1–C3-31.
- [4.70] TILLACK, D.J., FERNSLER, E.B., Heat Treating of Nickel and Nickel Alloys, Metals Handbook Ninth Edition, Volume 4, Heat Treating, American Society for Metals, Metals Park, OH (1981) 754–759.
- [4.71] SCARBERRY, R.C., PEARMAN, S.C., CRUM, J.R., Precipitation Reactions in Inconel Alloy 600 and Their Effect on Corrosion Behaviour, Corrosion-NACE, **32** 10 (1976) 401–406.
- [4.72] CAMPBELL, C.A., FYFITCH, S., PWSCC Ranking Model for Alloy 600 Components, Sixth International Symposium on Environmental Degradations of Materials in Nuclear Power Systems — Water Reactors, San Diego, CA (1994) 863–870.
- [4.73] LOTT, R.G., et al., Primary Water Stress Corrosion Crack Growth Rates in Alloy 600 Steam Generator Tubing, Proceedings of the Fifth International Symposium on Environmental Degradation of Materials in Nuclear Power Systems - Water Reactors, Monterey, CA, 25–29 August 1991, American Nuclear Society, La Grange Park, IL (1992).
- [4.74] BERGE, P., et al., The Effects of Chemical Factors on Stress Corrosion of Alloy 600 Exposed to the Cooling Medium in Pressurized Water Reactors, Proceedings of the Fifth International Symposium on Environmental Degradation of Materials in Nuclear Power Systems — Water Reactors, Monterey, CA, 25–29 August 1991, American Nuclear Society, La Grange Park, IL (1992) 533–538.
- [4.75] MILLETT, P.J., WOOD, C.J., Mediterranean Reflections — Recent Development in Water Chemistry, Nuclear Engineering International, August (1994) 14–15.
- [4.76] EPRI, PWR Primary Water Chemistry Guidelines: Revision 2, EPRI NP-7077, Electric Power Research Institute, Palo Alto, CA (1990).
- [4.77] GORMAN, J.A., Survey of PWR Water Chemistry, NUREG/CR-5116, ANL-88-43 (1989).
- [4.78] CASSAGNE, T.B., GELPI, A., Crack Growth Rate Measurements on Alloy 600 Steam Generator Tubes in Steam and Primary Water, Proceedings of the Fifth International Symposium on Environmental Degradation of Materials in Nuclear Power Systems — Water Reactors, Monterey, CA, 25–29 August 1991, (1992) 518–524.
- [4.79] VAILLANT, F., LE HONG, S., AMZALLAG, C., BOSCH, C., “Crack Growth Rates on Vessel Penetrations in Alloy 600 in Primary Water”, Contribution des Expertises sur Matériaux à la résolution des problèmes rencontrés dans les réacteurs à eau pressurisée, Colloque International Fontevraud IV, Fontevraud, France, Septembre 1998.
- [4.80] SACHS, D., Replacement of the Unit 2 Inconel-600 Hot-Leg Nozzles, Proceedings: 1991 EPRI Workshop on PWSCC of Alloy 600 in PWRs, EPRI TR-100852, Electric Power Research Institute, Palo Alto, CA (1992) 3–3 to 3-6 and B2-1–B2-18.

- [4.81] SHAH, V.N., MACDONALD, P.E., (Editors/Authors), Ageing and Life Extension of Major Light Water Reactor Components, Elsevier Science Publishers B.V., Amsterdam, June 1993.
- [4.82] MOFFAT, G., et al., 2001. Development of the Technical Basis for Plant Startup for the V. C. Summer Nuclear Plant; Service Experience, Fabrication, Residual Stresses and Performance, PVP Vol. 427, ASME (2001) 33–39.
- [4.83] USNRC, Crack in Weld Area of Reactor Coolant System Hot Leg Piping at V. C. Summer, USNRC Information Notice 2000-17 (including Supplement 1) (2000).
- [4.84] EPRI, PWR Materials Reliability Project Interim Alloy 600 Safety Assessments for US PWR Plants (MRP-44NP), Part 1: Alloy 82/182 Pipe Butt Welds, TP-1001491-NP, Part 1, Interim Report, April 2001. (Non-Proprietary Information).
- [4.85] BERRY, W.E., Corrosion in Nuclear Applications, Jon Wiley and Sons, Inc., New York (1971) 173–174.
- [4.86] USNRC, Degradation of Reactor Coolant System Pressure Boundary Resulting from Boric Acid Corrosion, USNRC Information Notice 86-108, Supplement 1 (1987).
- [4.87] USNRC, Degradation of Reactor Coolant System Pressure Boundary Resulting from Boric Acid Corrosion, USNRC Information Notice 86-108, Supplement 2 (1987).
- [4.88] O’NEILL, A.S., HALL, J.F., Boric Acid Corrosion of Carbon and Low-Alloy Steel Pressure-Boundary Components in PWRs, EPRI NP-5985, Electric Power Research Institute, Palo Alto, CA (1988).
- [4.89] STOLLER, S.M., (S.M. Stoller Corporation), Boric Acid Corrosion of Carbon Steel Components — Weakness in Conoseal Installation Maintenance Procedures, Nuclear Power Experience, PWR-2, VII, A, 568 (1988) 176.
- [4.90] STOLLER, S.M., RCP Gasket Leaked-Closure Studs Corroded, Nuclear Power Experience, PWR-2, V, A, 89, S.M. Stoller Corporation (1980).
- [4.91] United States Nuclear Regulatory Commission, Degradation of Reactor Coolant Pump Studs, USNRC IE Information Notice 80-27 (1980).
- [4.92] DE BOUVIER, O., GALLET, S., TEISSIER, A., YRIEX, B., MEYZAUD, Y., “Origine des Défauts Intergranulaires en Surface Externe des Soudures Bimétalliques du Circuit Primaire Principal”, Contribution des expertises sur matériaux à la résolution des problèmes rencontrés dans les réacteurs à eau pressurisée, Colloque International Fontevraud IV, Fontevraud, France, Septembre 1998.

5. ASSESSMENT METHODS

Assessment of ageing degradation is required for designing a new component, estimating the remaining life of a component, evaluating acceptability of a flaw, and evaluating a component repair. Thus, ageing assessment plays an important role in evaluating structural integrity of PWR components. This section presents methods for assessing ageing degradation of PWR piping caused by the following ageing mechanisms: thermal fatigue, vibratory fatigue of welded piping connections, thermal ageing of cast stainless steel piping, PWSCC of Alloy 600 instrument penetrations, boric acid corrosion, and atmospheric corrosion. In addition, the approaches taken in the USA, France, and Germany for LBB analyses are described. However, these analyses are often not applicable if significant ageing mechanisms are present.

5.1. Assessment of thermal fatigue

Thermal (low-cycle) fatigue may be divided in two parts: crack initiation and crack propagation. Fatigue analysis of piping by ASME code method is discussed first. (This analysis is performed during piping design and during operation for fatigue damage assessment in piping). The assessment methods for thermal fatigue in surge and branch lines are summarized next.

5.1.1. Fatigue analysis of piping by ASME code method

5.1.1.1. Crack initiation based on S-N curves

ASME Code methods: Fatigue analysis method in the B31.1, B31.7, and ASME Codes that have been used for nuclear piping and branch nozzles. The past analysis practices are summarized first and then the present ASME Code analysis techniques are summarized.

Past fatigue analysis practices. Prior to 1969, nuclear piping was designed using United States of America Standard (USAS) B31.1, from 1969 to 1971 plants were designed with USAS B31.7-1969 as the standard, and the ASME Code has been used thereafter. Piping systems purchased for NPPs prior to July 1, 1971, generally used the rules set forth in B31.7. Those purchased after July 1, 1971, generally used the rules of ASME Code, Section III. The rules of B31.7 were incorporated in Subarticle NB-3600 of the 1971 edition of Section III.

USAS B31. The Piping Code of the United States of America Standards Institute [formerly the American Standards Association (ASA)] was originally published in 1935 as the *American Tentative Standard Code for Pressure Piping* (ASA B31.1). It was focused on satisfying primary stress limits, and did not specifically address fatigue, which was assumed to be covered by design safety factors on primary stresses. The 1955 issue of ASA B31.1 is particularly noteworthy in that it introduced several new concepts into the piping code. Standard equations for piping design were included; fatigue failures caused by thermal expansion stresses were considered; and the concepts of stress range and maximum shear stress, as pertinent to the fatigue of piping systems, were used. The quantitative evaluation of local expansion stresses was introduced through stress intensification factors. Fatigue was addressed by stating that the expansion stress S_E could not exceed the allowable stress range S_A , which included a stress reduction factor f , as follows:

$$S_A = f(1.25 S_C + 0.25 S_h) \quad (1)$$

where:

S_c = the basic material allowable stress at the minimum cold temperature

S_h = the basic material allowable stress at the maximum hot temperature

$f = 1.0$ for ≤ 7000 cycles, gradually reducing to 0.5 at $\geq 100,000$ cycles

This equation is still used by the chemical, petroleum, and power industries, with minor modifications.

When the first generation NPPs were designed in the mid-1950s, the only basis for design and fabrication of piping was the ASA B31.1-1955 *Code for Pressure Piping*. The critical nature of NPP piping demanded something beyond the minimum requirements of ASA B31.1-1955. Designers specified many requirements themselves, such as ordering materials to existing ASTM specifications. As time went on, starting in about 1962, many of these supplemental, but necessary, requirements were eventually incorporated into the *Nuclear Code Cases*. Much of this experience was later consolidated in the USAS B31.1-1967 *Power Piping Code*, which was commonly referenced for early nuclear plants.

Piping designed to B31.1 is generally thicker than piping designed to the present ASME Code. This results in pressure and moment stresses tending to be lower in B31.1 piping, but stresses caused by local thermal gradients can be more severe. A number of PWRs have had their surge lines originally designed to B31.1 reanalyzed (most to the 1986 ASME Section III edition) to include thermal stratification transients. Cumulative usage factors (CUFs) were calculated to meet the ASME Code allowable value in all cases. Ware et al. [5.1] have analyzed two B31.1 piping systems and two B31.1 branch nozzles to the 1992 ASME Code edition and found that all four would meet the ASME CUF allowable value based on representative transients.

In 1969, USAS B31.7, *Nuclear Power Piping*, was issued specifically for nuclear piping. USAS B31.7-1969 provided design rules for three classes of piping. This included a set of rigorous design rules for Class 1 piping, whereas the design of Classes 2 and 3 piping were performed in accordance with USAS B31.1 (1967 or earlier edition), with slight modifications. USAS B31.7-1969 introduced three fatigue curves to the B31 piping standards: curves for carbon and alloy steels with metal temperatures not exceeding 370°C (700°F) (one for UTS 551 MPa (≤ 80 ksi) and one for UTS 793 to 896 MPa (115 to 130 ksi); one for austenitic stainless steels, nickel-iron-chromium, nickel-chrome-iron, and nickel-copper alloys with metal temperatures not exceeding 426°C (800°F); and curves for steel bolting.

The USAS B31.7-1969 requirements were very similar to the existing ASME Code Section III requirements for nuclear vessels. The piping for some currently operating nuclear plants were designed using USAS B31.7-1969. Piping analysis requirements were incorporated into Section III of the ASME Code in 1971.

ASME Code. The ASME set up a committee in 1911 for the purpose of formulating standard rules for the construction of steam boilers and other pressure vessels. In the early 1960s, the rules and philosophy of ASME Code Section VIII closely paralleled that of the power piping sections of B31. A few early plants (for example, Yankee Rowe, SONGS1, and Haddam Neck) were built to Section VIII. As with piping, there grew the realization that more rigorous requirements were needed for nuclear vessels; consequently, Section III, *Nuclear*

- Environment
- Residual stress

while Porowski et al. [5.5] credit the 2 and 20 factors weighing equally to the following four factors:

- Scatter in data
- Surface finish
- Size
- Environmental

Large-scale vessel fatigue tests performed at room temperature for the express purpose of checking the ASME Code fatigue design curves [5.6] showed that fatigue cracks may initiate below the ASME Code design curves, but that wall penetration is not expected until the fatigue cycles exceed the ASME Code design curves by about a factor of 3 [5.7].

A correction for the maximum effects of mean stress, S_m , was made when the fatigue curve drops below the cyclic yield stress as follows:

$$S' = \frac{(S_u - S_m)}{(S_u - S)} S \quad S < S_m \quad (3)$$

$$S' = \frac{(S_u - S_y)}{(S_u - S)} S \quad S < S_y \quad (4)$$

$$S = S \quad S \geq S_y \quad (5)$$

where S' is the corrected alternating stress, S is the completely reversed amplitude at the same fatigue life as S' , S_u is the ultimate strength, and S_y is the actual stress amplitude under cyclic conditions (usually approximated by the cyclic yield strength). The mean stress corrections were used to modify the best-fit curves before the 2 and 20 reduction factors were applied. The mean stress correction occurs at about 10^4 cycles for ferritic steels and about 10^6 cycles for austenitic steels. No correction is necessary if the fatigue curve is above the yield stress because the component, undergoing plastic cycling, has shaken down to elastic action, and thus the mean stress is zero. The high-cycle fatigue curves are partially based on load-controlled data, rather than strain controlled data.

Piping. For Class 1 piping, the ASME Code (Article NB-3600 of Section III) provides for protection against two types of fatigue failure, those caused by (1) elastic cycling and (2) plastic cycling. To determine if the piping cycles elastically, the requirement of Equation 10 of NB-3650 must be satisfied [5.8]. The stress in Equation 10 of NB-3650 is comprised of pressure, moment, and axial temperature gradient terms, but excludes radial temperature gradient terms. The shakedown requirement states that the maximum primary plus secondary stress intensity range, which excludes local stress concentration effects, must be $\leq 3 S_m$. The purpose of this criterion is to ensure that after a few stress cycles, the piping will cycle within the range of the tensile yield strength and the compressive yield strength. (The yield strength in the ASME Code is the minimum specified yield strength, which should

represent the cyclic yield strength for the material.) Using the $3 S_m$ criterion, no incremental distortion, other plastic cycling, or ratcheting will occur. The peak stress intensity range S_p , which includes the effects of stress concentrations including radial thermal gradients, is then calculated using Equation 11 of NB-3650, and the alternating stress intensity for each pair of load sets ($S_{alt} = 1/2 S_p$) is computed using Equation 14 of NB-3650.

If the shakedown criterion cannot be met, the Code allows for a penalty factor to be applied to the stress for fatigue calculations. The procedure is briefly summarized as follows:

- (a) ensure the stress intensity range caused by moments, thermal expansion, and thermal anchor movements is $\leq 3 S_m$ (Equation 12 of NB-3650)
- (b) ensure the thermal stress ratchet criterion is met (NB-3653.7)
- (c) ensure the primary plus secondary membrane plus bending stress intensity, excluding thermal bending and thermal expansion stress, is $\leq 3 S_m$ (Equation 13 of NB-3650)
- (d) increase the peak stress intensity value by a factor K_e , based on material parameters m and n (specified in Table NB-3228.5(b)-1 of the ASME Code), and calculate the allowable cycles based on the appropriate fatigue curve.

Nozzles. In some cases, designers and utilities treat nozzles as branch connections and use the ASME Code NB-3650 piping rules for fatigue analyses. In other cases, ASME Code NB-3200 (design by analysis) fatigue analysis methods have been chosen. This type of analysis generally includes finite element thermal and stress analysis methods and has been used by NSSS vendors (B&W and Combustion Engineering).

To determine a cumulative usage factor, an approach consisting of the following steps can be taken by an analyst. (Auxiliary analyses such as thermal stress ratchet and simplified elastic-plastic are not included in this discussion.)

Step 1 First, the analyst must obtain a set of service loadings for the component. This is generally in the form of a set of design transients in the Design Specification. Examples of design transients are discussed in Section 3. These service loadings define the temperature and pressure changes that the component must undergo during its lifetime.

Step 2 Next, the analyst needs to determine the stress distribution at the most highly stressed locations in the component. This includes the thermal and pressure stresses, and sometimes the preload stresses. Closed form solutions are available for some geometries, but often more detailed finite element analyses are performed. For older plants interaction analyses of connected shells were used. The temperature distribution is necessary to determine the stress distribution. A conservative one-dimensional heat transfer analysis is generally performed. Two sources of inaccuracy in determining the highest stresses are (1) during a heatup or cooldown, the temperatures and therefore the thermal stresses are changing with time, and (2) the analyst must use judgment to determine the locations of maximum stress. Both of these sources of inaccuracy have one thing in common: it is impractical to investigate each point in time and each location of the component. While the thermal analysis can generate a time temperature relationship for selected points, no comparative method is available to generate stress-history plots without considerable effort. The process generally involves selecting representative points in time during the heatup or cooldown to compute the stresses, and using the analyst's judgment, to estimate the time of maximum stress. Similarly,

it is unreasonable in many calculations to determine the stresses at each unique point, and again the analyst's judgment is used to determine the locations of highest stress. A stress determination is required for each load set.

Step 3 The three principal primary plus secondary stresses (S_1 , S_2 , and S_3) for each load set are determined. This often involves separating the peak stress from the total stress, such as by linearizing the thermal stress distribution.

Step 4 From the results of step 3, three stress intensities are calculated by subtracting the principal stresses.

$$\begin{aligned} S_{12} &= S_1 - S_2 \\ S_{23} &= S_2 - S_3 \\ S_{13} &= S_1 - S_3 \end{aligned} \tag{6}$$

The maximum primary plus secondary stress intensity range is the largest difference between the S_{12} , S_{23} , or S_{13} values, determined by comparing the stress intensities of all the load sets. This maximum stress intensity range must meet the $3S_m$ limit.

Step 5 Using the stress values determined in step 2, the primary plus secondary plus peak stresses are calculated. This may involve the use of stress indices, stress concentration factors, experimental stress analysis, etc. The six components of stress for each time and location of interest are determined for each load set.

Step 6 For each pair of load sets, the six components of stress are subtracted and the three principal stress ranges are computed. The peak stress intensity range for each pair is computed by subtracting the principal stresses as shown in step 4, and choosing the largest. Thus the anticipated cycles n_i for the i^{th} load set pair are determined.

Step 7 The S_{alt} for each load set pair is one-half the peak stress intensity range. To adjust for temperature and material, S_{alt} is multiplied by the ratio of the elastic modulus on the appropriate fatigue curve to the elastic modulus used in the analysis. The allowable cycles N_i for each load set pair are read from the appropriate design fatigue curve.

Step 8 The individual fatigue usage factor U_i at each location is determined by the ratio of the anticipated to the allowable cycles for each pair of load sets.

$$U_i = \frac{n_i}{N_i} \tag{7}$$

The CUF is the sum of the individual usage factors.

$$U = U_1 + U_2 + U_3 + \dots + U_n \tag{8}$$

The CUF factor at each location must not exceed 1.0.

Ware et al. [5.1] have analyzed two nozzles with thermal sleeves designed to B31.1, using both NB-3200 and NB-3600 methods. The stresses from pressure, moments, and radial (through-wall) temperature gradients were not significantly different using the two approaches. However, the portion of the CUF calculated from stresses caused by axial thermal

gradients was significantly higher using the stress indices and temperature differences in NB-3600 as opposed to the finite element results and the NB-3200 method.

RCC-M methods: Since 1974 the French Design and Construction Code (RCC-M) group has improved the fatigue analysis methods on different aspects:

- optimization of the K_e formula for Class 1 materials,
- specific rules for crack like defects, as thermal sleeve attachments,
- B3600 S_{alt} evaluation using range versus time of pressure, bending, and thermal loads
- coupling of B3600 beam approach with B3200 finite element approach for pipe fittings and discontinuity, as nozzles and thickness variation pipe fittings
- revision of some stress indices.

5.1.1.2. Crack propagation in piping

ASME Code method for carbon steel piping. Cyclic crack growth rates are typically depicted by a relationship involving (a) the maximum stress intensity factor K_{max} (where the stress intensity factor K defines the applied stress field in the vicinity of the crack tip), and (b) the cyclic stress intensity range ΔK , [which is the difference between the maximum and minimum stress intensity factors ($K_{max} - K_{min}$) during a given cycle]. In other words,

$$\text{cyclic crack growth rate: } da/dN = f(K_{max}, \Delta K) = f(R, \Delta K) = C_o (\Delta K)^n \quad (9)$$

where variables a and N in da/dN are crack length and number of cycles, respectively, C_o is a scaling factor, and R is the load ratio (K_{min} / K_{max}). Typical example of fatigue crack growth rates for subsurface flaws (air environment) in low-alloy steel is as follows [5.9]. The relationship between the crack growth rate and ΔK , for a given ratio R , is linear on a log-log scale:

$$da/dN = (1.99 \times 10^{-10}) S (\Delta K)^{3.726} \text{ in./cycle} \quad (10)$$

where S is a scaling parameter to account for the R ratio.

For $0 \leq R \leq 1$, $S = 25.72(2.88 - R)^{-3.07}$. ASME [5.9] provides expressions for S for other values of the ratio R . The applied stress intensity factor K is in $\text{ksi}\cdot\text{in}^{0.5}$. Reference fatigue crack growth rate curves given by Equations (9) and (10) are presented in Figure 5-1.

Crack growth rates are also influenced by the environment. For surface flaws in a light water reactor environment, the relationship is bilinear on a log-log scale.

For high ΔK ,

$$da/dN = (1.01 \times 10^{-7}) S (\Delta K)^{1.95} \text{ in./cycle}, \quad (11)$$

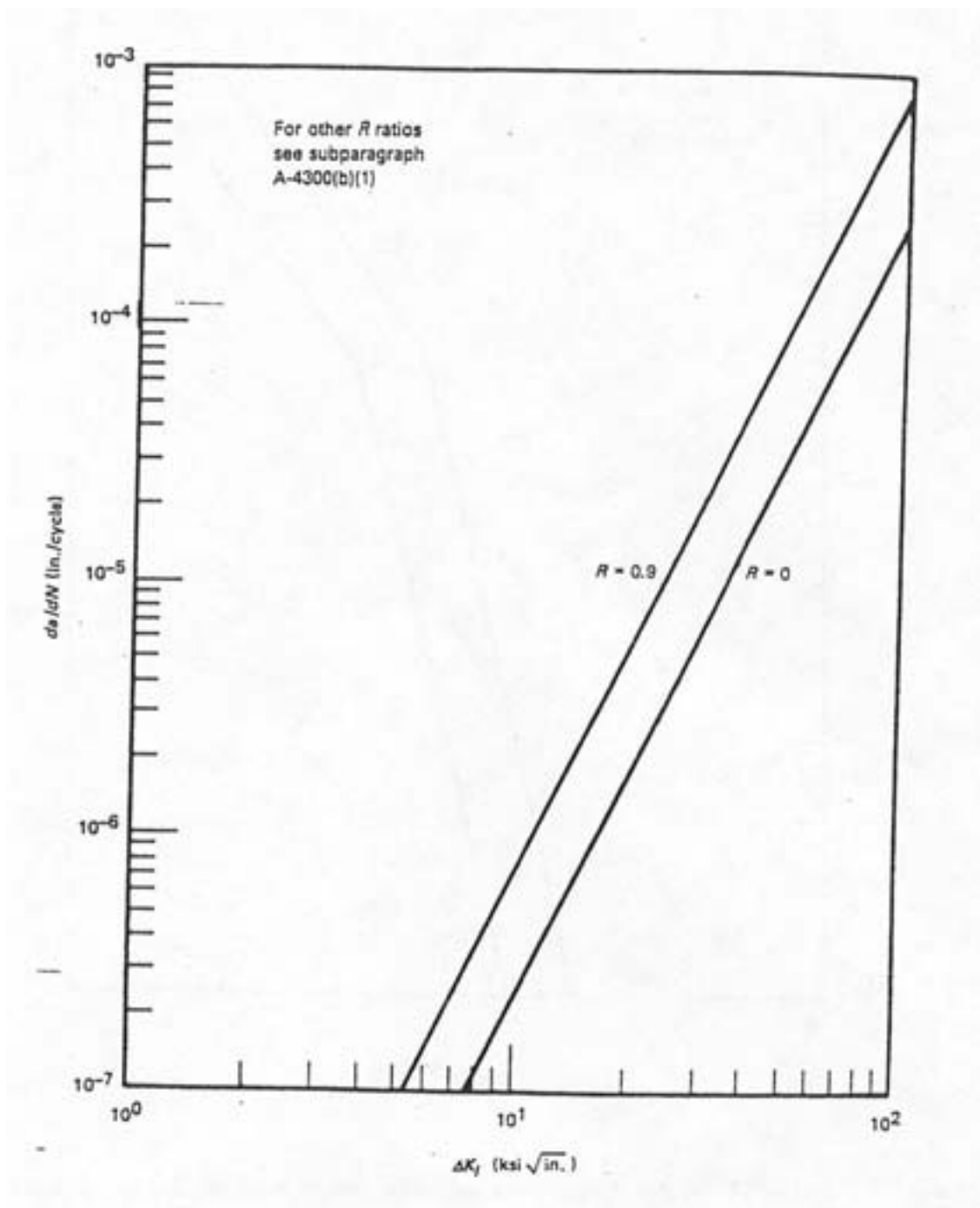


FIG. 5.1. Reference fatigue crack growth curves for carbon and low alloy ferritic steels exposed to air environment (subsurface flaws) [5.9].

where the parameter S is given by

$$\begin{aligned}
 S &= 1.0(0.0 \leq R \leq 0.25) \\
 &= 3.75R + 0.06(0.25 \leq R \leq 0.65) \\
 &= 2.5(0.65 \leq R \leq 1.0)
 \end{aligned}$$

and for low ΔK ,

$$da/dN = (1.02 \times 10^{-6}) S (\Delta K)^{5.95} \text{ in./cycle}, \quad (12)$$

where the parameter S is given by

$$\begin{aligned} S &= 1.0(0.0 \leq R \leq 0.25) \\ &= 26.9R - 5.725(0.25 \leq R \leq 0.65) \\ &= 11.76(0.65 \leq R \leq 1.0) \end{aligned}$$

Equation (11) is applied when ΔK is greater than the corresponding value at the intersection of the curves given by Equations (11) and (12), and Equation (12) is applied for smaller ΔK s. Reference fatigue crack growth rate curves given by Equations (11) and (12) are presented in Figure 5-2.

ASME Code method for austenitic stainless steel piping: The fatigue crack growth model presented here is based on the EPRI Database for Environmentally Assisted Cracking (EDEAC) [5.10]. This database includes data from tests conducted at various load ratios, cyclic frequencies, environments, temperatures and neutron irradiation levels. The model presented here can be used for predicting the extension of existing flaws in pressure vessel and piping components exposed to air environments. This model is in the current ASME Code [5.9]. The crack growth behavior in the LWR water environment is currently being evaluated.

There are several parameters that may potentially affect fatigue crack growth behavior of austenitic stainless steels in an air environment: heat-to-heat variations, carbon content, grain size, product form, cold work, thermal ageing, neutron irradiation, weld metal and weldments, frequency, R-ratio (mean stress), temperature, and cyclic stress intensity range. However, evaluation of the EDEAC data show that the first three of these parameters (heat-to-heat variations, carbon content, grain size) have little or no influence on the fatigue crack growth behavior of the austenitic stainless steels in an air environment.

Little information is available for the effect of product form on fatigue crack growth behavior of austenitic stainless steels. Based on the limited information, it is assumed that the crack growth behaviors of different product forms of the same wrought alloy do not differ significantly. Thermal ageing of austenitic stainless steel components at the operating LWR temperature generally has no detrimental effect on the fatigue crack growth rates in an air environment. This holds true for both base metal and weldments. Often the crack growth rates for the thermally aged components are lower. The fatigue crack growth model presented later in the section may be used when data from actual product form are not available.

Fatigue crack growth rates in Grade CF-8 (the cast version of wrought Type 304 SS) have been shown to be equivalent to or slightly lower than growth rates in wrought Type 304 SS. However, the fatigue crack growth rates in aged Grade CF-8M (the cast version of wrought Type 316 SS) increased by as much as a factor of 10 when tested in a simulated PWR water environment, compared to testing in air at 320°C, but did not exceed the upper bound design fatigue-crack-growth-rate curve for stainless steels [5.11–5.12].

Small amount of cold work that might be introduced incidentally into the structure by machining, fabrication, or installation procedures has a little effect on the crack growth rate and it is conservatively represented by the crack growth rate in the air environment. Large amount of cold work (20–25%) is known to produce a small reduction in the fatigue crack growth rate, but such a amount of cold work is generally not present in the LWR pressure vessel and piping components.

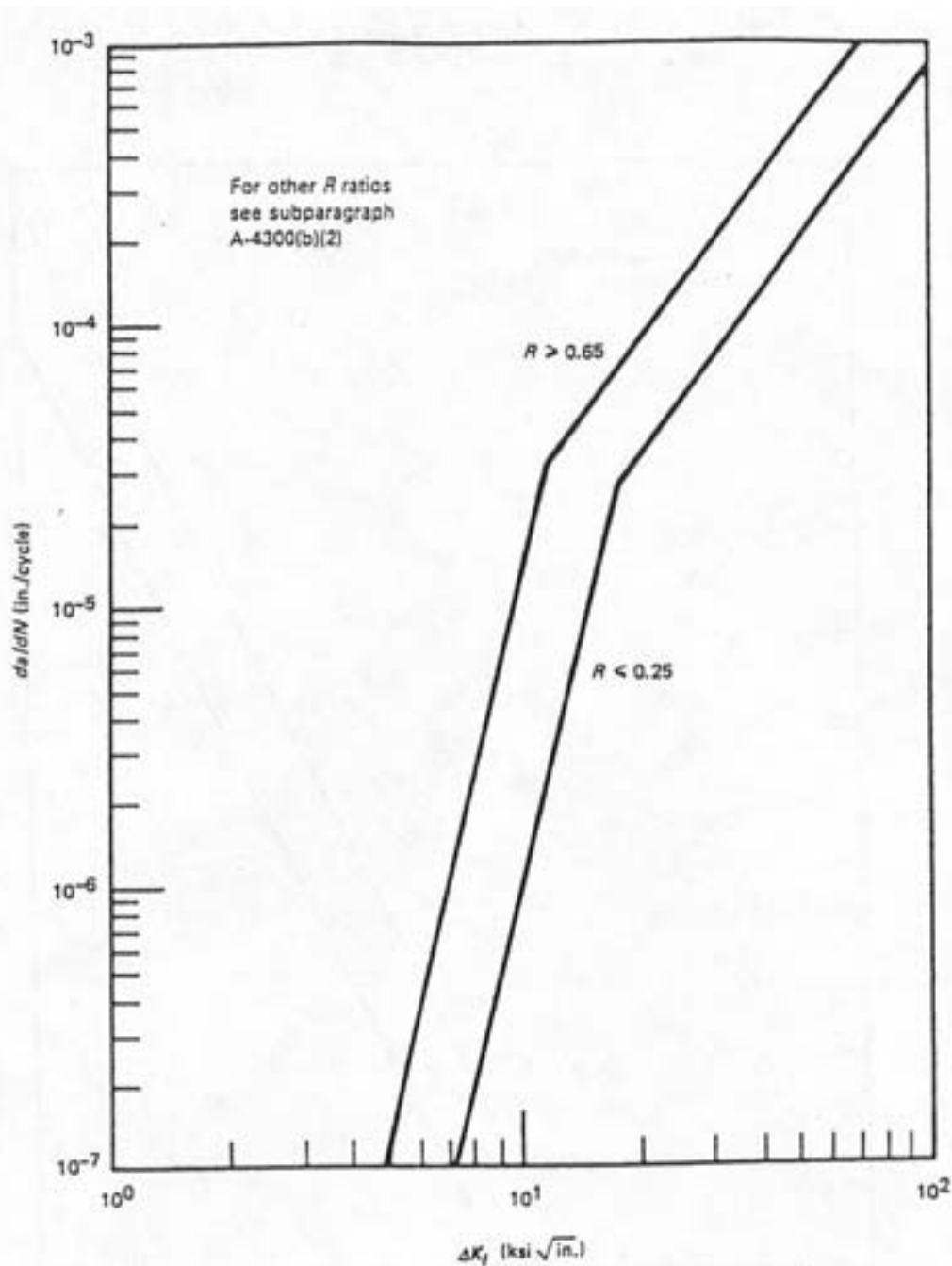


FIG. 5-2. Reference fatigue crack growth curves for carbon and low alloy ferritic steels exposed to water environments.

Neutron irradiation does not produce higher fatigue crack growth rates in austenitic stainless steel base metal and weldments for neutron fluences up to about 1×10^{22} n/cm² ($E > 0.1$ MeV) and irradiation temperatures below 480°C (900°F).

A significant percentage of actual defects encountered in structural components are at or in the vicinity of welds. Austenitic stainless steel welds have different microstructures than wrought stainless steels. These variations along with several welding variables (weld process, delta ferrite level, flux and filler rods, residual stresses, etc.) can produce variation in the fatigue crack growth behavior. However, in spite of these differences, fatigue crack growth

rates in austenitic steel weldments, in the absence of residual stresses are generally equal to or lower than the rates in the wrought austenitic stainless steels under similar conditions. These differences do not justify development of separate model for weldments. Therefore, the weldment data were combined with the data for wrought and cast materials to develop the model.

The main parameters affecting the fatigue crack growth rate in the austenitic stainless steel in the air environment are cyclic frequency, cyclic stress ratio (R-ratio or mean stress effect), temperature, and cyclic stress intensity range. Cyclic frequency effects can be significant for austenitic stainless steel tested in aggressive environment (e.g. air, water, etc.) at elevated temperature. The crack growth per cycle increases with the decreasing cyclic frequency. Loading wave forms generally do not have a significant effect upon fatigue crack growth behavior of stainless steel in the air environment at LWR operating temperatures; however, at high temperature $>590^{\circ}\text{C}$ ($>1100^{\circ}\text{F}$) the creep-fatigue interactions should be considered.

The fatigue crack growth model applicable to austenitic stainless steels in air is

$$da/dN = C F S [\Delta K]^{3.3} \quad (13)$$

where:

da/dN = crack growth rate per cycle (in./cycle)

C = correction factor for temperature

F = correction factor for frequency

S = correction factor for R-ratio

R = K_{\min}/K_{\max}

K = stress intensity factor (ksi $\sqrt{\text{in.}}$)

ΔK = $K_{\max} - K_{\min}$ (ksi $\sqrt{\text{in.}}$)

The correction factors for temperature and frequency are given by third degree polynomials as shown in Figures 5-3 and 5-4, respectively. Use of a correction factor for frequency is only recommended for applications equal to or greater than 480°C (800°F) where time-dependent effects in air become more pronounced; use of this correction factor below 480°C could lead to overly conservative estimates of time-dependent effects.

The correction factor for R-ratio is given in Figure 5-5. When both K_{\min} and K_{\max} are negative, the correction factor S should be taken as unity. The correction factor S is based on R-ratio data for the temperature in the vicinity of 290°C to 315°C (550°F to 600°F). Therefore, the correction factor S should be applied to that temperature range.

The crack growth model presented by Equation (13) is validated by the results of some fatigue crack growth experiments that were not used in developing the model. The validation results show that the model presented by Equation (13) provides estimates for crack extension in stainless steel in an air environment that are both conservative and reasonably accurate.

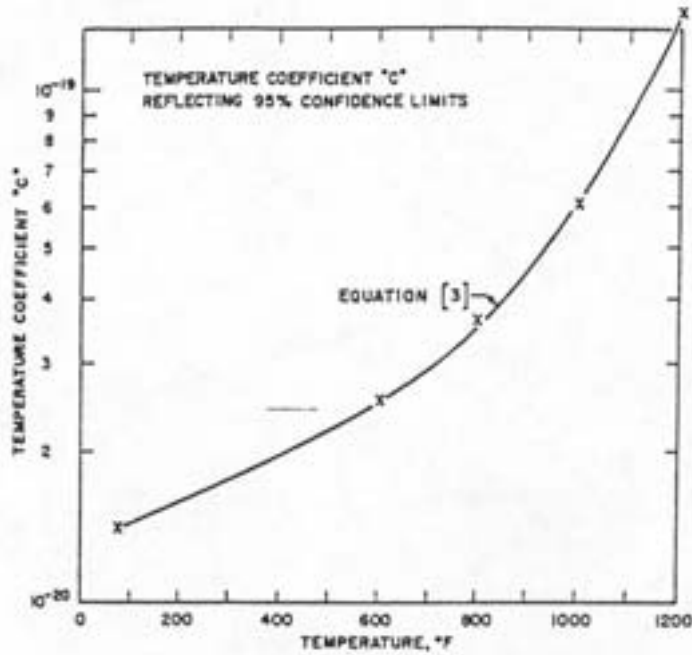


FIG. 5-3. Coefficient C in Equation (13) as a function of temperature.

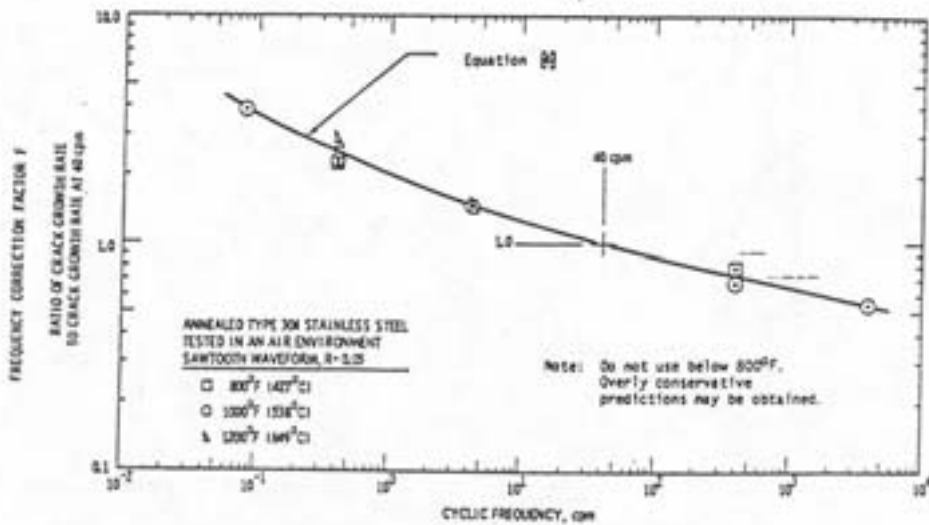


FIG. 5-4. Frequency correction factor F as a function of cyclic frequency in the range 800 to 1000 $^{\circ}F$.

This model has been adopted by the ASME Code Section XI. The reference fatigue crack growth curves for austenitic stainless steels in air environments are presented in Figure 5-6. Equations (13) may be used to estimate the cumulative growth of a detected flaw during a specified period of normal operation. This involves identifying design basis transients during the period and estimating incremental flaw growth for each of the transients in a chronological order. Flaw length and depth are updated at the end of each transient by the incremental flaw growth estimated during the transient. The allowable sizes for flaws oriented either in circumferential or axial direction are defined in the nonmandatory Appendix C of ASME Code Section XI [5.9].

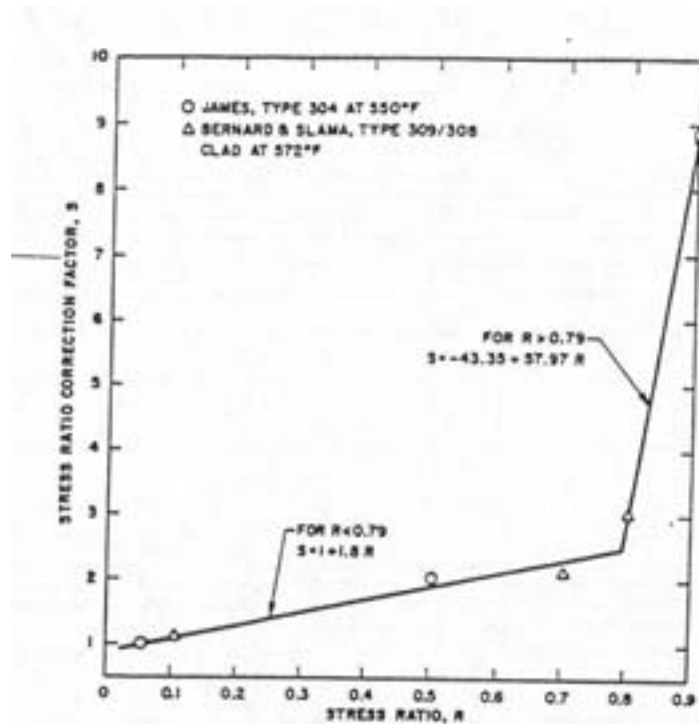


FIG. 5-5. R-ratio correction factor S as a function of stress ratio.

Environmental effects. The fatigue crack growth curves for austenitic stainless steels in PWR environment are steeper than those in an air environment shown in Figure 5-6. But the effect of R-ratio and temperature on the fatigue crack growth rate are very similar. The fatigue crack growth curves for PWR environment are being developed. The fatigue crack growth curves for BWR environment will be developed later [5.13].

ASME Code method for crack growth analyses. The behavior of a flaw in the pressure-retaining wall of components subject to cyclic stress (crack growth in depth and length direction) can be predicted by calculation, using Paris Law (i.e. Equations (11), (12) or (13)). Furthermore it is possible to determine the length at which the crack will have penetrated the pressure-retaining wall. Environmental conditions (current and projected) have to be regarded when selecting the crack propagation rate. After penetration of the wall a leakage occurs. If this leakage crack size is smaller than the critical through-wall crack length, LBB behavior is given (Fail Safe Principle).

As shown in Figure 5-7, initial defects (or reference defects) are used in the Fatigue Crack growth (FCG) analysis and in the LBB fatigue crack growth demonstration. Reference defects are circumferential surface defects. They are postulated in highly stressed welds. The geometry of a reference defect is elliptical, defined by the depth a and the total length in surface $2c$. The size is an envelope of the allowable defects for in-shop examination and in-service inspection. Performance of inspection technologies and accumulated experience are taken into account to define the reference defects.

Fatigue crack growth computation of a surface defect is normally performed under normal and upset transients using Equations (11), (12) or (13). The computation is performed simultaneously at the deepest point on the crack and at the surface. Consequently it is needed to compute stress intensity factor, K , at these two points on the crack.

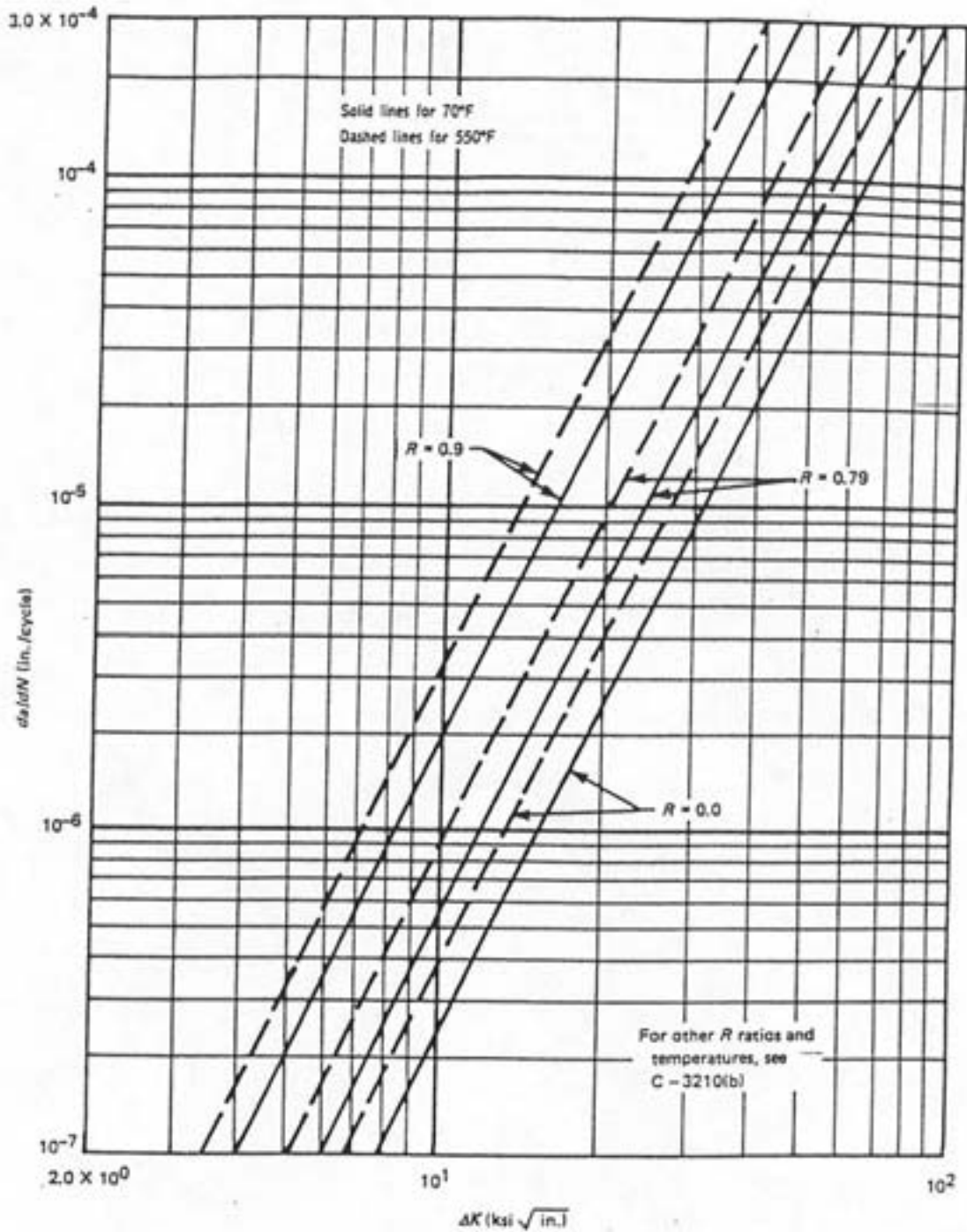


FIG. 5-6. Reference fatigue crack growth curves for austenitic stainless steels in air environments.

It is shown that an elliptical crack remains elliptical with growth determined by PARIS law applied at the surface and at the deepest point. Thus a new ratio of crack length to its depth (c/a) is obtained after every increment of crack growth. A conservative crack growth curve is used taking into account environmental effects. The criterion is to demonstrate small fatigue crack growth of the initial defects during one specified load collective of the plant.

A similar analysis as the previous one described is additionally performed in Germany with unlimited specified plant load collectives in order to show the fundamental tendency of the growth of the considered crack, with respect to its shape development (see Figure 5-7) [5.14].

- (1) If the crack grows through the wall by fatigue or the ligament breaks without instability in the circumferential direction, than the LBB fatigue crack growth condition is demonstrated (“leak-before-break”).
- (2) If the crack becomes critical before it goes through the wall, than there is the condition of “break-before-leak”; in this case equivalent safety measures (e.g., extended ISI) have to be taken into account to ensure break preclusion.

In a further analysis it is shown that the fatigue crack growth of the reference defect during the whole life (one life) of the plant is limited and that there is no risk of break of the remaining End of Life (EOL) crack ligament under Safe Shutdown Earthquake (SSE) + normal operation. Elasto-plastic concepts (including Flow Stress Concept and/or Plastic Limit Load concept, see Section 5.8.2) are used for defect assessment. To perform this analysis, one needs the corresponding material data at the appropriate temperature. The criterion is that no plastic instability can occur.

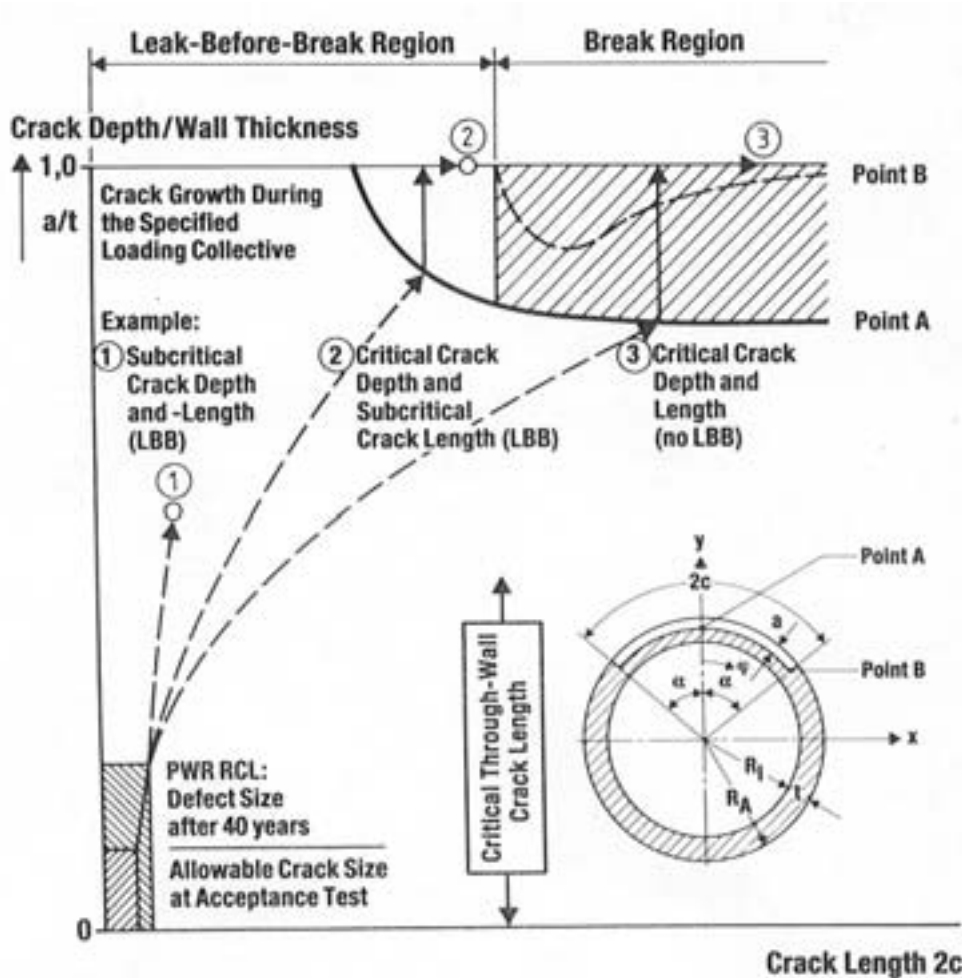


FIG. 5-7. Procedure for fatigue crack growth analysis and LBB fatigue crack growth demonstration.

The stability of a through-wall crack under maximum loads (i.e. SSE + normal transients) is analyzed by computing the size of the critical through-wall crack at full power operation. The critical through-wall crack is the crack size which leads to instability under the maximum load, considering pressure, thermal expansion loads, and dead weight. Calculation methods are the same as mentioned above.

A most essential precondition for all analyses is the completeness of loads used for determining the fatigue crack growth and crack stability. Basic principle is that all failure modes are identified and ruled out either by previous experience or predictability of margins against such failure modes. This principle implies that the operating conditions are known with confidence at the design stage. Particular care is given to

- high external loads of erratic nature (seismic loads, water hammer, unstable flow conditions)
- operating thermal transients (stratification potential, two phase flow, unstable flow conditions)
- vibrations (induced by high flow velocity or rotating machinery) lines with potential for corrosion or erosion (stagnant water, high fluid velocity).

RSE-M Code method for crack growth analyses. The French Operation and Surveillance Code (RSE-M) group has developed similar methods for flaw evaluation [5.15]. The major improvements are:

- the plasticity effect of different type of loads (thermal gradient through the wall and residual stresses)
- the evaluation of the fracture mechanic parameters in mixed mode situation
- the material properties with different environments and different R ratio
- the crack growth and ductile tearing interaction.

5.1.2. Thermal fatigue assessment of surge line

US experience. After the issuance of Bulletin 88-11, research projects were initiated to understand and mitigate the effects of surge line thermal stratification. Measurements were conducted on operating reactors. Laboratory tests were conducted to simulate the field behavior. Analytical models, both thermal and stress, were developed to predict surge line behavior under stratification conditions.

Several PWR plants in the United States subsequently instrumented their surge lines to monitor coolant temperatures and flow rates and piping outside-surface temperature distributions. Then, the piping inside-surface temperature distributions were calculated using finite element heat transfer techniques. For example, measured surge line outside-surface temperatures at a representative Westinghouse plant are plotted in Figure 5-8a as a function of time during an operational transient caused by a reactor coolant pump trip. The temperatures were measured at five circumferential locations on the surge line cross section [5.16]. Two-dimensional finite element heat transfer analysis was used to calculate the coolant temperature distribution that caused the observed surge line outside-surface temperatures at the time of the maximum temperature difference between the top and bottom of the piping (approximately 15 minutes into the transient). The surge line inside-surface temperature

distribution assumed in the analysis and the resulting calculated outside-surface temperature distribution are plotted, respectively, in Figures 5-8b and 5-8c (solid lines) as a function of relative location around the pipe circumference (where 0 degrees is at the top of the pipe). The measured surge line outside-surface temperature distribution at 15 minutes into the pump trip transient is also plotted in Figure 5-8c. The data compares well with the calculated temperature distribution, suggesting that the assumed surge line inside-surface temperature distribution plotted in Figure 5-8b closely approximates the actual temperature distribution, and the flow at 15 minutes into the pump trip transient is highly stratified with a cold/hot interface at approximately 22.5 degrees. These temperature distributions were then used to perform appropriate stress and fatigue analyses. The updated stress and fatigue analyses have shown that the calculated usage factors are less than 1.0; however, factors greater than 0.4 have been reported for several base metal and weld sites at Babcock & Wilcox plants [5.17]. Examples of surge line components with high fatigue usage factors are the elbows and the hot-leg surge nozzle safe ends.

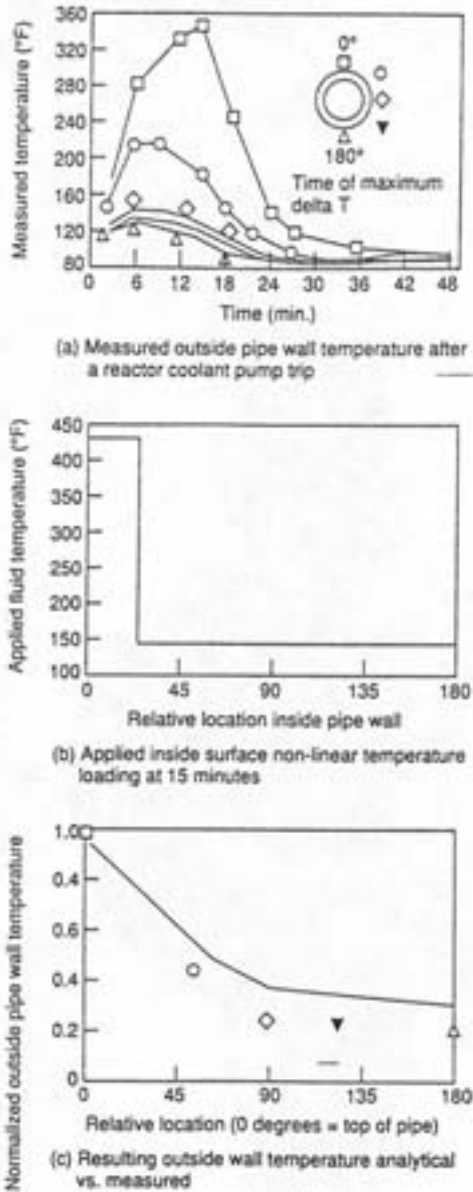


FIG. 5-8. Comparison of calculated and measured temperatures on the outside wall of a surge line subject to thermal stratification [5.16].

Detailed monitoring of surge lines has been conducted on two B&W plants (one raised loop and one lowered loop), three Combustion Engineering plants, several Westinghouse plants, as well as overseas (primarily French) plants. The results of the monitoring programmes confirmed the presence of thermal stratification, and have been used extensively in the licensee responses to Bulletin 88-11 (See Section 4.1.6).

The EPRI Thermal Stratification, Cycling and Striping (TASCS) Programme is also funding testing and development of analytical methods to develop the needed methodology. While thermal stratification can be measured by thermocouples or RTDs mounted on the exterior of the piping, thermal striping cannot be measured in this manner. Rather it must be accounted for indirectly. One method would be to use spectra generated from laboratory tests to approximate the thermal striping stresses. The amplitude of the temperature swing could be used to determine the magnitude of the corresponding stress cycling on the inside surface of the pipe wall. Such data could then be used to generate a spectra of stress versus frequency for periods of thermal striping. By combining this with the time that the thermal striping would be occurring, the total cycles and fatigue usage from the thermal striping could be estimated.

Deardorff et al. [5.18] have used data from the German HDR⁴ test facility to produce curves that the authors have proposed for use in evaluating thermal striping in pressurizer surge lines. The pipe surface temperature fluctuation spectra was determined from HDR test data. (B&W also used HDR test results to estimate the fatigue caused by thermal striping in the B&W Owners Group response to Bulletin 88-11.) Then, stress analyses were conducted using ASME Code methods to determine the fatigue usage that would result from the developed curves. The German data were specifically developed for PWR and BWR feedwater nozzles. The results were applied to a pressurizer surge line configuration, and minimal fatigue usage was predicted. However, results from a number of confirmatory tests using various pipe sizes and thermal-hydraulic conditions may be needed to develop thermal striping curves for general use.

The approach used was to determine the alternating stress for use in the ASME Code fatigue equation as:

$$S_{\text{alt}} = \frac{E\alpha\Delta T_{p-p}}{2(1-\nu)} \quad (14)$$

where:

- S_{alt} = alternating stress
- E = modulus of elasticity
- α = coefficient of thermal expansion
- ΔT = temperature gradient in wall
- ν = Poisson's ratio.

A spectrum for ranges of peak-to-peak temperature differences ΔT_{p-p} was determined by counting the number of cycles of different ranges of temperature fluctuations for a given time period in the various HDR tests. Then the fatigue usage for each of the

⁴ Tests at the decommissioned German nuclear plant Heissdampfreaktor (HDR) have been conducted for a number of years.

temperature ranges was computed based on the number of cycles for that temperature range, and the results added to compute the total fatigue usage per hour. Since the temperature difference was judged to be flow-rate dependent, fatigue usages were calculated for several flow rates.

In practice, an application of this method to estimate thermal striping damage includes determination of the flow velocity in the surge line using the pressurizer spray flow rate and the rate of change of pressurizer level, determination of the temperature difference between the coolants in the pressurizer and the hot leg, and then calculation of the fatigue usage using an appropriate spectrum for the number of hours over which the thermal striping is judged to have occurred. It appears that such spectra could be generated by developing sufficient data for various temperatures, flow rates, geometry, and materials.

Cranford et al. [5.16] have investigated the additional analyses needed to properly account for thermal stratification of pressurizer surge lines. Their conclusions were that it is important to determine as accurately as possible the local temperature, pressure, and flow conditions in the pressurizer surge line. They concluded that simple correlations based on gross parameter changes such as pressurizer level are too crude for accurate calculation, since the surge line volume is small when compared to the water space volume of the pressurizer itself. Westinghouse developed a rather extensive database by monitoring the transients taking place in the pressurizer surge line [5.19]. While at power, when the difference in temperature between the pressurizer and the hot leg were 10°C (50°F), the extent and effects of stratification were observed to be small. However, during certain modes of plant heatup and cooldown, the temperature difference can be as large as 160°C (320°F), and significant stratification occurs. All three US PWR NSSS vendors have used such modeling, combined with monitoring results, in their responses to Bulletin 88-11.

French experience. EDF has monitored for surge line thermal stratification on operating plants and developed with FRAMATOME a plexiglass model of a surge lines [5.20]. Stratification during steady-state and low flow rate conditions was confirmed on a 900 MW plant (Cruas 2). During heatup (in the steam bubble mode) and cooldown, the temperature difference between the pressurizer and the hot leg was 110°C (about 200°F). Tests conducted by EDF and Framatome on a half-scale plexiglass model that measured temperatures with thermocouples located around different cross-sections of the model agree with the fluid temperature profiles measured at Cruas 2. These tests revealed that the fluid temperature profile can be correlated to the Froude number, depending on the flow rate in the line and the temperature difference between the pressurizer and the hot leg. A Froude number threshold is determined by experiments; that is, above the threshold (at higher velocities), stratification vanishes. Stress analyses concluded that a maximum alternating stress intensity of 750 MPa (109 ksi) can occur in the upper half of the elbow directly underneath the pressurizer. This value is comparable to the maximum alternating stress intensity computed for US plants in response to Bulletin 88-11 [5.1].

Research. A brief mention will be made to related research projects that the reader may refer for further information. Other analytical investigations include use of simplified model in computer programmes by Framatome [5.21–5.22] for Belgian units. Other experimental investigations include French studies to characterize flow regimes for different operating conditions using the EXPRESS experimental facility which represents the surge line of a French PWR. A numerical simulation using the CEA TRIO computer code was used to achieve a good prediction of the thermal loadings. Morgan et al. (1989) report on experiments

conducted on a scale model (7.6 cm versus 22.2 cm in actual PWR) of a B&W surge line using stratified fluid dyed different colors in a clear plastic pipe.

The loads are now well known, for different designs and operating conditions through mock ups results, computations and plant instrumentation. The classical rules for plastic shakedown and fatigue analysis (ASME or RCC-M) can be easily adapted to take into account stratification loads in surge lines.

5.1.3. Thermal fatigue assessment of branch lines and connections

PWR branch lines are subject to thermal fatigue loading mainly caused by turbulent penetration and thermal cycling. Efforts made to assess this damage are summarized here. Other phenomena, thermal stratification and striping, thermal shock, and operational transients might contribute to this damage, and their assessment is summarized in Sections 5.1.1 and 5.1.2. Basic phenomena of turbulent penetration and thermal cycling are presented in Section 4.13.

US experience. In response to Action 3 of the USNRC Bulletin 88-08 (see Section 4.3.3), several utilities have based their response on an analytical methodology developed under a programme sponsored by the Electric Power Research Institute (EPRI) to investigate thermal stratification, cycling, and striping (TASCS). A method to estimate fatigue damage caused by turbulent penetration thermal cycling is developed by Roarty (1994) under the TASCS programme (EPRI, 1993e). A heat transfer model was developed and the results benchmarked against available data. It appears that a reasonable estimate of the turbulent penetration depth for reactor coolant system branch lines is 15 to 25 pipe diameters. The data indicates that the random turbulent fluctuations cause a complex loading spectrum, consisting of both high- and low-frequency content. This makes selecting a reasonable estimate of applied cycles difficult.

The TASCS methodology, for example, was used to evaluate the temperature monitoring results for the South Texas 1 and 2 normal charging, alternate charging, and auxiliary spray piping. The conclusion of the evaluation was that the piping integrity would not be jeopardized, should inleakage of cold water through a valve into the RCS occur over the life of the units. Subsequently Houston Lighting & Power (HL&P) informed the USNRC that temperature monitoring of these lines will be discontinued (HL&P 1996). The decision to remove the temperature monitoring instrumentation, however, may have been premature because, as explained next, the cause of fatigue cracking at Farley and Tihange is not yet well established.

It appears that the mechanism of turbulent penetration has not been fully investigated under the TASCS programme and its significance in the failures at Farley 2 and Tihange 1 has not been clearly established. The TASCS experimental programme and analytical methodology do not predict the locations of these failures correctly. The TASCS methodology predicts higher cyclic stresses at the end of the turbulent penetration column where thermal cycling may take place if valve inleakage is present, and lower stresses at locations within the turbulent penetration column where temperature differences approach zero. But when the TASCS methodology is applied to the Farley 2 safety injection line fatigue failure, the through-wall crack location is within the calculated length of the turbulent penetration column and not at the end of the column where the cyclic stresses are expected to be higher and a fatigue failure is more likely to occur. Because the Tihange 1 failure is similar to the Farley

2 failure, the TASCs methodology is not likely to predict correctly the through-wall crack location in the Tihange 1 safety injection line. This discrepancy between the calculated and actual location of cracking implies that the thermodynamic phenomena that caused these failures are not well understood. Therefore, at present, pressure and temperature monitoring of the unisolable piping susceptible to thermal cycling is the most reliable method to ensure its structural integrity [5.23–5.25].

There is not a great deal of test data on fatigue of branch connections. Rodabaugh, Moore, and Gwaltney [5.26] have collected the available data and have made recommendations for further testing. They also have reviewed the ASME Code NB-3600 fatigue procedure for branch connections and tees under internal pressure and moment loadings. However, they did not address fatigue for thermal shock loadings which contribute most of the CUF for tees and branch connections. Some of their conclusions for internal pressure loading are:

- The cyclic pressure test data indicate that the Code Class 1 failure evaluation method, using K_e , is unconservative for $S_n/3S_y$ less than about 1.2.
- A thorough review of the Code Class 1 fatigue evaluation procedure is urgently needed.
- Development of design guidance is needed for locations other than the inside corner.

Some of the conclusions for moment loading are:

- The Code Class 1 fatigue evaluation procedure appears to be inaccurate on the conservative side for high-amplitude cycles and inaccurate on the unconservative side for low-amplitude cycles.
- The Code equations for the stress indices may be unconservative where the branch or nozzle wall thickness is much smaller than the run pipe thickness.

French experience. Following to major degradations in Dampierre, similar to Farley and Tihange, different actions have been engaged between EDF, FRAMATOME and CEA in order to approach the loads in these connected lines through mock-ups, computations and plant instrumentation. The conclusions of all these actions are:

- the loads in the nozzle areas are very complex on a larger distance than initially envisaged, up to 20 to 30 diameters for certain designs
- these loads are very sensitive to the piping layout
- the potential damage is high cycle fatigue that is very difficult to assess accurately
- surface state (finish and residual stresses) and welds are limited situations, but crack in the base metal has been discovered in some situations (DAMPIERRE or TSURUGA plants)
- the potential damage increase if you are close to a leaking cold water valve
- some situations can be diphasic with steam bubbles than can lead to local corrosion at the water–steam interface, impossible to assess through analytical models
- some particular loads, not defined at the design stage, can happen between the two isolation valves of the primary circuit.

5.1.4. Consequences of fatigue damage on dynamic load carrying capacity of pipings

Safety margins and energy absorption levels demonstrated by experimental and numerical investigations of non-linear response of piping systems subjected to intense dynamic loads are becoming part of the design basis for qualification and optimized backfitting of operating nuclear power stations. In this connection the plant-specific assessment of the applicability of leak before break concepts is also expected to become increasingly useful [5.19]. For instance experimentally a failure of a flexible piping system subjected to a simulated earthquake has been impossible to achieve under realistic conditions. Fictitious dynamic loadings (such as periodic excitation or extremely high accelerations) and degraded piping (such as due to sequential loadings or intentionally cracked test specimens) were necessary for bringing about progressive damage, leaks, and breaks. Dynamic elasto-plastic analyses of a three-dimensional piping system for which experimental results are known are being performed in order to interpret these findings. The analyses are expected to provide the theoretical justification for simplifying current rules of seismic design. Concerning seismic qualification of existing systems, these results are most useful in the case of facilities with no seismic design, or plants designed for a lower level of seismic loading than currently required.

Blowdown and valve closure experiments with unflawed lines and one weakened by a circumferential crack have resulted in considerable plastic deformation and leakage, respectively. Concerning qualification of existing piping systems for pressure wave loadings, these results, for example, are most useful in justifying avoidance of snubbers, while exhibiting leak before break for loads of short duration.

Postulated pipe ruptures in high-energy systems of nuclear power stations are being simulated by means of computer codes which take various non-linear effects into account: plastic response of piping, as well as gaps and plastic deformation of pipe whip restraints. Time history of plastic strains in three-dimensional piping systems, including ovalization with possible dynamic hinge formation, help determine the type and number of restraints for optimum protection.

5.2. Assessment of vibratory fatigue of piping connections

Situation in the USA. There are two approaches for high-cycle vibratory fatigue life evaluation of socket-welded small-diameter piping connections and fillet welded attachments: (1) ASME Section III fatigue design, an analysis-based approach, and (2) American Association of State Highway Transportation Officers (AASHTO) fatigue design, an empirical approach. These two approaches are discussed here and their advantages and limitations have been identified.

ASME Section III Fatigue Design. The ASME Code Class 1 piping is subject to ASME Section III fatigue analysis procedures. However, the socket welds of small diameter piping were not subject to analysis by the ASME Section III Code because of their size and/or location. These procedures are most frequently applied to low-cycle fatigue loading conditions such as those occurring during plant heat-up, cool down and other thermal transients rather than high-cycle vibratory conditions. In addition, the fatigue design curves in ASME Section III are based on small, smooth specimen data rather than actual weldment fatigue data. Therefore, the detrimental effects of weldments on fatigue life are accounted for by the use of fatigue strength reduction factors along with detailed stress analyses of component [5.27].

The difficulty with the analytically based approach of ASME Section III is the development of a sufficiently accurate assessment of local peak stresses including the effects of stress concentrations introduced by weld geometry such as a toe-undercut and fabrication defects such as incomplete penetration. The stress analysis may not accurately estimate the peak stress. If these stress concentrations are present, the fatigue life of a socket-welded piping connection may be significantly reduced or eliminated. Since the ASME Section III fatigue curves include fatigue crack initiation as a significant portion of the total fatigue life, particularly in the high-cycle regime, loss of fatigue crack initiation portion of the total life can result in non-conservative life estimate. The laboratory test results supports this assessment. The results show that the fatigue strength reduction factors for socket welds are much larger than the ASME Code values, and therefore, the ASME Section III Code does not always ensure a conservative design for socket-welded piping connections subject to vibratory fatigue [5.28]. However, it is worth to note at this point that, in general, the ASME Section III procedures (NB-3200 and NB-3650) yield conservative lives for vessels and piping subject to low-cycle fatigue [5.1], [5.6].

AASHTO fatigue design. In contrast to analysis based approach such as ASME Section III fatigue design approach, this empirically based approach does not depend on complex stress analysis. Instead, this approach relies on statistically significant data from the fatigue tests of actual or full-sized weldments. With the use of statistical data, the design curves can be specified with known confidence levels with respect to mean. In addition, this approach requires an estimate of nominal or net applied stress instead of highly complex local stresses. The effects of stress concentrations caused by weld geometry and defects, which cannot be easily characterized by the stress analysis, are incorporated in the fatigue design curves.

The National Cooperative Highway Research Programme (NCHRP) studies showed that the two important parameters affecting the fatigue life estimated by this approach are the weld type and the nominal applied stress range. The mean stress and material strength had only secondary effects on weldment fatigue life. The mean stress effects are accounted for in the design fatigue curves by virtue of the fact that the welded fatigue test specimens used for developing the design curves contained high tensile residual stresses. These studies also demonstrated that fatigue damage could also occur at weld details located in relatively low stress fields which were subjected to high-cycle loading in excess of 2×10^6 cycles. The AASHTO design curves were modified in 1974 to incorporate the NCHRP results. Fatigue analysis of socket-welded connection using appropriate AASHTO fatigue curve has provided results that compare well with the full-size test results [5.27].

Situation in France. Following a number of leaks and breaks on different small connected lines, EDF has established an R&D project to:

- review the design and fabrication rules (RCC-M does not consider vibration loads but requires a pre-operating test to assure a negligible level of vibrations)
- review the pre-operating test criteria (ANSI) because they do not cover all relevant cases
- to identify and characterize vibration excitation sources (using plant instrumentation) in order to include it in a specific piping computer code to analyse the corresponding stress level
- define criteria for ranking the sensitivity of piping connections to vibration fatigue
- analyse and propose modifications of piping support and layout in sensitive locations.

5.3. Assessment of thermal ageing

5.3.1. Cast stainless

Situation in the USA. Two different approaches to determine the extent of the thermal ageing of cast stainless steel are described below. These approaches quantify the extent of low-temperature ageing by measuring the room-temperature Charpy impact energy after ageing at temperatures in the range of 300 to 400°C (570 to 750°F). The higher ageing temperature (400°C) is often employed to accelerate the rate of thermal ageing compared with normal PWR operating temperatures (288°C (550°F)). The first approach provides a means for estimating the lower bound fracture toughness after long term thermal ageing, whereas the second approach provides means for estimating fracture toughness at a given service time and temperature.

Long term thermal ageing: Chopra [5.29–5.30] has developed empirical correlations for calculating the minimum room temperature Charpy V-notch impact energy after long term ageing (also called the saturation value of the room-temperature Charpy V-notch energy, CV_{sat}) from the chemical composition and ferrite content of a cast stainless steel. Two different empirical correlations were developed for each of the Grades CF-8 and CF-8M cast stainless steels. To ensure that the estimated values are either accurate or conservative for all heats, the saturation impact energy for a specific cast stainless steel is determined using both correlations, and the lower value is used for assessing the long term thermal ageing. These correlations account for degradation in the mechanical properties caused by thermal ageing but do not explicitly account for initial properties of unaged material. If the saturation properties are higher than the minimum initial properties, then the initial properties are used as the saturation properties.

Correlation for Grade CF-8

$$\log_{10}CV_{sat} = 1.15 + 1.364\exp(-0.035\Phi) \quad (15)$$

where

$$\Phi = \delta_c(\text{Cr} + \text{Si})(\text{C} + 0.4\text{N})$$

and the chemical composition is in weight % (wt%). δ_c is the ferrite content and is calculated in terms of Hull's equivalent factors Cr_{eq} and Ni_{eq} , using the following equation.

$$\delta_c = 100.3(Cr_{eq}/Ni_{eq})^2 - 170.72(Cr_{eq}/Ni_{eq}) + 74.22 \quad (16)$$

where

$$\begin{aligned} Cr_{eq} &= \text{Cr} + 1.21(\text{Mo}) + 0.48(\text{Si}) - 4.99 \\ Ni_{eq} &= \text{Ni} + 0.11(\text{Mn}) - 0.0086(\text{Mn})^2 + 18.4(\text{N}) + 24.5(\text{C}) + 2.77 \end{aligned}$$

Also,

$$\begin{aligned} \log_{10}CV_{sat} &= 5.64 - 0.006\delta_c - 0.185C_r + 0.273\text{Mo} - 0.204\text{Si} \\ &\quad + 0.044\text{Ni} - 2.12(\text{C}+0.4\text{N}) \end{aligned} \quad (17)$$

and the chemical composition is again in wt%. The nitrogen content is assumed to be 0.04wt% if not known.

Correlation for Grade CF-8M

$$\log_{10}C_{Vsat} = 1.10 + 2.12\exp(-0.041\Phi) \quad \text{for Ni} < 10 \text{ wt\%} \quad (18a)$$

or,

$$\log_{10}C_{Vsat} = 1.10 + 2.64\exp(-0.064\Phi) \quad \text{for Ni} > 10 \text{ wt\%}. \quad (18b)$$

where

$$\Phi = \delta_c(C+0.4N)(Ni+Si+Mn)^2/5$$

Also,

$$\begin{aligned} \log_{10}C_{Vsat} = & 7.28 - 0.011\delta_c - 0.185C_r - 0.369Mo - 0.451Si \\ & - 0.007Ni - 4.71(C+0.4N) \end{aligned} \quad (19)$$

Grade CF-8M steel with a Ni content greater than 10 wt% is found to have large variations in its δ_c ferrite content (2). Equation (18b) attempts to account for such variations in the ferrite content. The difference between experimentally observed and predicted saturation values for the room-temperature impact energy, C_{Vsat} , for Grade CF-8 stainless steels is typically less than $\pm 15\%$; the difference is larger for the Grade CF-8M steels. Correlations based on ferrite content and ferrite spacing also have been developed to estimate the room temperature Charpy V-notch impact energy at saturation; these correlations are based on limited data and need to be optimized and validated.

The fracture toughness J-R curve can be conservatively determined from the estimated room-temperature Charpy V-notch impact energy. This curve defines the resistance of thermally aged cast stainless steel material to ductile, stable crack growth. The J-R curve is expressed by the power law relation $J = C\ddot{A}an$, where J is determined according to ASTM Specifications E 813-85 and E 1152, $\ddot{A}a$ is the crack extension, and C and n are constants. Chopra [5.29–5.30] has developed correlations between these constants and the estimated Charpy V-notch impact energy to determine the lower bound J-R curve at PWR operating temperatures; these correlations account for differences between statically and centrifugally cast materials. The degree of conservatism in this J-R curve is low if both the estimated room temperature and operating temperature Charpy V-notch impact energies are on the upper shelf (greater than about 80 J/cm²), but the degree of conservatism is higher if the room temperature impact energy is on the lower shelf. These correlations and the calculated values of C_{Vsat} can be used to estimate lower bound fracture toughnesses after long term thermal ageing.

Example estimates of the lower bound fracture toughness of Grade CF-8 and Grade CF-8M cast stainless steel that are within ASTM Specification A 351 and have a ferrite content greater than 15% are presented in Table XXIV. The corresponding values of C_{Vsat} , the constants C and n for the J-R curves at 290°C, and the lower bound fracture toughness, J_{Ic} (J at crack extension of 0.2 mm), for both statically and centrifugally cast materials are also presented in Table XXIV [5.30]. The lower bound fracture toughness of Grade CF-8M

stainless steel is lower than that of Grade CF-8 stainless steel. In addition, the lower bound fracture toughness of statically cast material is lower than that of centrifugally cast material. These lower bound toughnesses are for steels with ferrite content greater than 15%, which is higher than the typical average ferrite content in the US nuclear industry.

TABLE XXIV. ESTIMATES OF OPERATING TEMPERATURE (290°C) LOWER BOUND FRACTURE TOUGHNESS OF GRADE CF-8 AND GRADE CF-8M CAST STAINLESS STEEL WITH FERRITE CONTENT GREATER THAN 15%

Cast stainless steel grade	Saturation room temperature impact energy C_{Vsat} (J/cm ²)	Statically cast stainless steel			Centrifugally cast stainless steel		
		C	n	J_{Ic} (kJ/cm ²)	C	n	J_{Ic} (kJ/cm ²)
CF-8	25	251	0.32	150	330	0.32	197
CF-8M	20	167	0.30	103	195	0.30	120

Thermal Ageing at Time and Temperature: The fracture toughness of cast stainless steel at time and temperature of service and the corresponding room temperature Charpy V-notch impact energy, C_V , can be estimated using the kinetics of the thermal ageing process, described by the following hyperbolic tangent relationship developed by Chopra [5.29]:

$$\log_{10}C_V = \log_{10}C_{Vsat} + \beta \{1 - \tanh[(P - \theta)/\alpha]\} . \quad (20)$$

The constant β is half the maximum possible change in $\log_{10}C_V$, i.e.

$$\beta = (\log_{10}C_{Vint} - \log_{10}C_{Vsat})/2$$

where C_{Vint} is the Charpy V-notch energy of the unaged material and C_{Vsat} is the saturation value of the Charpy V-notch energy discussed above. A typical value for the initial Charpy V-notch energy is 200 ± 20 J/cm²; however, it can be as low as 60 J/cm² for some steels. The constant θ is the log of the time at 400°C required to achieve a reduction in impact energy equal to $\hat{\alpha}$. A lower value of θ implies a faster ageing rate at 400°C. Test results have shown that the value of the constant θ can vary over a wide range for different heats of the same steel with a similar chemical composition. The constant α is a shape factor; it defines the shape of the curve of the Charpy V-notch energy versus ageing time in the temperature range of 290 to 400°C (550 to 750°F) as follows:

$$\alpha = -0.585 + 0.795 \log_{10}C_{Vsat} \quad (21)$$

the parameter P is an ageing parameter defined by the following expression:

$$P = \log_{10}(t) - [1000Q/19.143 \times (1/T - 1/673)]$$

where t is time in hours, Q is an activation energy (kJ/mole), and T is the absolute service temperature in degrees Kelvin. The variable P is defined such that it is equivalent to the logarithm (base 10) of the number of hours of ageing at 400°C (750°F). The activation energy is a function of the chemical composition of the material and may be affected by the initial heat treatment of the material. Correlations for the activation energy Q have been developed

using Charpy V-notch impact test results for about 50 different experimental and commercial heats of cast stainless steel aged for up to 50 000 h at temperatures in the range of 290 to 400°C (550 to 750°F). The activation energy for Grade CF-8 is given by

$$Q = 10[74.52 - 7.20\theta - 3.46\text{Si} - 1.78\text{Cr} + 148\text{N} - 147\text{C}] \quad (22)$$

and for Grade CF-8M,

$$Q = 10[74.52 - 7.20\theta - 3.46\text{Si} - 1.78\text{Cr} - 4.35\text{Mn} + 23\text{N}] \quad (23)$$

where the constant θ is the same as the one in Equation (20) and appears to account for the effects of the heat treatment and casting process on the kinetics of the thermal ageing. The activation energy is higher for a lower value of θ , which represents a higher ageing rate at 400°C (750°F) as discussed earlier, and is lower for a higher value of θ .

Equations (15) to (23) are empirical correlations and should not be applied outside the database from which they were derived. These correlations may not be applied to some statically cast components such as an elbow because the correlations are based on testing of components whose geometry differ substantially from that of the elbow. Otherwise, the database for these correlations appears to be broad enough to address thermal ageing concerns associated with many of the PWR cast stainless steel main coolant loop piping. The correlations are based on test results for Grades CF-8 and CF-8M steel specimens thermally aged at temperatures between 290 and 400°C (550 to 750°F) for up to 58 000 h. [These equations are somewhat different than earlier correlations that were based on test results for Grades CF-8 and CF-8M cast stainless steel specimens thermally aged up to 30 000 h [5.31]. The specimens included several experimental and commercial heats with chemical compositions that satisfied the ASTM specifications, and the equations also take into account the variation in ferrite content in specimens with certain chemical compositions.

The above correlations were used for estimating the material properties of aged, Grade CF-8 cast stainless steel components from the Shippingport reactor and also a recirculation pump cover from the KRB reactor in Germany [5.32]. The material from the Shippingport reactor included two hot-leg main shutoff valves along with other components. The extent of thermal ageing damage in these components was likely to be small because they were in service at temperatures less than 290°C for 13 years or less. Therefore, the samples from the naturally aged components were further aged in the laboratory, and the laboratory ageing times were adjusted to account for the ageing at the reactor temperatures. The data required for the estimation included the chemical composition, the impact energy of the unaged material, and the constant θ . Two different values of θ , the assumed value of 2.9 and an experimental value, were used to estimate the material properties. The experimental values of θ were determined from accelerated ageing tests at 350 and 400°C (660 and 750°F) on the component materials. The comparisons between the estimated and the measured material properties for one hot-leg valve from the Shippingport reactor and the pump cover from the KRB reactor are as follows. The valve was in service for about 13 years at 281°C (538°F), and the calculated ferrite content in the valve material was about 5.2%. The impact energies estimated with the assumed value of θ compared well with the measured ones for ageing temperatures $\leq 320^\circ\text{C}$ (610°F); those estimated with the experimental value ($\theta = 3.4$) compared well at all temperatures. The estimated and measured fracture toughness J-R curves for the valve material at room temperature and at 290°C (553°F) also compared well. The KRB pump cover was in service for about 8 years at 284°C (543°F), and the calculated ferrite

content in the cover material was about 28%. The impact energies for the pump cover material estimated with the assumed value of θ compared well with the measured ones for ageing temperatures $\leq 320^{\circ}\text{C}$ (610°F), but the estimated values were nonconservative at higher temperatures. It appears that the assumed value of $\theta = 2.9$ provides a reasonable estimate for ageing temperatures $\leq 320^{\circ}\text{C}$ (610°F). The estimated fracture toughness J-R curves for the pump cover material were conservative; these curves are 40% below the average measured ones. This conservatism in the estimated curves possibly results from uncertainty in the material temperature during service and uncertainty in the ferrite content.

Significant spatial variations in the ferrite level may be present in statically cast stainless components. Such variations are caused by the solidification process, which depends on the particular casting technique used. Recently, two cast stainless steel elbows (Grade CF-8M, Ni in the range of 9 to 12 wt%), one from a hot leg and one from a crossover leg, were removed from Ringhals Unit 2 after 15 years of service. The service temperatures for these two elbows were 325 and 291°C (615 and 555°F), respectively. The estimated values of ferrite content in hot-leg and crossover leg elbows were 13% and 8%, respectively. These values were within $\pm 3\%$ of the bulk average values. Examination of these elbow materials led to a disturbing observation about a significant variation in their ferrite content. The ferrite in the hot-leg elbow varied from about 3 to 23%, whereas the ferrite in the crossover leg elbow varied from about 1 to 15% [5.33]. The elbow regions containing low ferrite level ($< 5\%$) are susceptible to stress corrosion cracking if located at the surface and, therefore, exposed to PWR environment.

Chopra [5.32] applied his correlations (presented in this section) to estimate the Charpy V-notch impact energy for the Ringhals elbows. The estimated Charpy V-notch impact energy for the crossover leg elbow of 112 J/cm^2 agrees well with the measured value of 107 J/cm^2 equivalent Charpy V-notch energy, which was converted from a measured Charpy U-notch impact energy, but the estimated value is significantly lower than another measured value of 177 J/cm^2 obtained from a Charpy V-notch specimen. The difference between these two measured values of Charpy energies is most likely the result of variation in the ferrite content in the crossover leg elbow. The estimate for the hot-leg elbow is higher than the measured value of the Charpy V-notch energy; the estimated value is 67 J/cm^2 , whereas the measured one is 50 J/cm^2 . The correlations need to be further optimized to account for large variations in ferrite content in statically cast stainless steel components.

Procedure for estimating mechanical properties of PWR cast stainless steel components: Chopra and Shack [5.34] have developed a procedure for estimating mechanical properties, i.e. CVN and elastic-plastic fracture toughness, of thermally aged cast stainless steel piping components. The procedure is divided into three parts:

- estimation of lower-bound material properties of steels with unknown chemical composition,
- estimation of saturation material properties of steels with known chemical composition but unknown service history,
- estimation of material properties at time and temperature for steels having known chemical composition and service history.

The estimation of lower-bound material properties, required by the first part of the procedure, is based on the worst-case chemical composition ($> 15\%$ ferrite), which is very

conservative for most steels. A more realistic lower bound can be developed if the ferrite content is known.

For the second part of the procedure, the estimation of the saturation (long-term) mechanical properties does not explicitly use the initial properties. So, as discussed, the saturation properties need to be compared with an estimate of the initial mechanical properties. If the initial properties are lower than the saturation properties, then the initial properties are treated as the saturation properties. If the initial properties are not available, the lower-bound initial properties based on the chemical composition may be used.

For the third part of the procedure, the estimation of the material properties at time and temperature require that the initial properties of the unaged material are known. If the estimated fracture toughness is higher than the minimum initial fracture toughness of the unaged material, the later is used as the estimated fracture toughness at time and temperature.

Suzuki et al. [5.35] investigated mechanical properties and metallurgical structure using Grade CF8M and CF8 materials aged at 290 to 400°C for up to 30 000 hours, and identified effects of thermal ageing on mechanical properties and metallurgical behavior and, in addition, established prediction method for Charpy absorbed energy and fracture toughness.

Flaw acceptance criteria for thermally aged cast stainless steels: No flaw acceptance criteria for Class 1 cast stainless steel components are available in the ASME Code Section XI. But such criteria are available for austenitic stainless steel weldments, in particular submerged arc welds (SAWs). Chopra and Shack [5.34] have shown that the lower bound crack growth resistance curves for thermally aged, statically cast Grade CF-8M material at operating temperature (290°C) are comparable to those for SAW [5.36]. Therefore, the crack growth resistance curves for SAW can be used as the basis for flaw acceptance for cast stainless steel components during current and renewed license period.

Situation in France. A set of actions has been agreed between EDF and FRAMATOME to assess the changes in material properties (toughness and fatigue) due to thermal ageing of French CF8 and CF8M. The second (CF8M) is more sensitive and a lot of effort has been done on:

- chemistry composition and local change in metallography of the material at different temperature and different ageing duration and temperature
- comparison of different manufacture procedures
- fatigue tests for different materials
- toughness and Charpy values for different level of ageing
- predictive formula for toughness of aged CF8M
- validation on removed elbows and valves in France and in Sweden with steam generator replacement operation, and on large scale artificially aged elbows
- generic assessment of cast stainless steel components (pipes, elbows, inclined nozzles and valves)
- large scale demonstration tests on scale 1 and 2/3 elbows.

The prediction formula for toughness is based on:

- KCU (20°C) or KCV (320°C) estimation with the chromium, silicium and molibdenum contents

- use of experimental results of different materials, different ageing levels (duration and temperature) to interpolate the J values; a specific activation energy formula has been developed for the ageing temperature:

$$Q = -194 + 14(\%Si + \%Cr + \%Mb) \text{ kJ/mole}$$

- the predicted minimum values at end of life (40 years) are for hot leg CF8M:
 - KCV 320°C = 18 J/cm²
 - J_{0.2mm} 320°C = 16 kJ/m²
- new results obtained from direct measurements on CT specimen from aged ingots confirm the conservatism of the prediction for very similar conditions:
 - J_{0.2mm} 320°C = 35 kJ/m² instead of 16 kJ/m²
- a detail fracture mechanic assessment based on J and the RSE-M flaw evaluation methodology applied to all ISI results confirms that all the French elbows are in accordance with RSE-M criteria [5.15] for 40 years of life.

5.3.2. Stainless steel welds

To date, a limited work relating to thermal ageing of stainless steel welds has been done on the assessment and quantification of margins. In France, the RSE-M flaw evaluation procedure suggests to use a lower value (28 kJ/m²) of toughness for ageing of submerged arc welds.

ASME Code uses different values for the assessment of thermal ageing that are included in the Z-factor: a maximum reduction of maximum moment in a cracked stainless steel weld of piping.

5.4. Primary water stress corrosion cracking of Alloy 600

The approach in the USA. Primary water stress corrosion cracking (PWSCC) initiation and growth models have been initially developed for Alloy 600 steam generator tubes. These models cannot be directly applied to other Alloy 600 components without some modifications to account for differences in fabrication of these components. A steam generator tube is a thin-walled component and has a significant amount of cold work, whereas the CRDM nozzles and instrument penetrations are thick-wall components having a very small amount of cold work.

5.4.1. Crack initiation

Based on the stress and temperature dependencies as described in Section 4.7.1, the damage rate for PWSCC of Alloy 600 components can be described by an equation of the form:

$$\text{damage rate} \propto \sigma^4 \exp(-Q/RT) \quad (24)$$

The time to crack initiation, t_i , is given by:

$$t_i \propto (\text{damage rate})^{-1} = A\sigma^{-4} \exp(-Q/RT) \quad (25)$$

where the constant A is a scaling factor determined by using some standard stress level and reference temperature. The value of A will change whenever there is a systematic change in the material characteristics, the average stress level at the location of interest, or other conditions that may depend on type of component and differ from plant to plant. The constant A for steam generator tube, tube plugs, CRDM nozzles, and instrument penetrations is likely to be different because different fabrication and installation procedures are used.

5.4.2. Crack growth

PWSCC growth rates in thick-wall components such as CRDM nozzles and instrument penetrations may be performed using the model developed by P. M. Scott of Framatome [5.37]. The model is based on the test results for steam generator tube materials and then modified for CRDM nozzles and other thick-wall components. The Scott model is based on PWSCC growth rate data obtained by Smialowska et al. [5.37] of Ohio State University. The data were developed at 330°C and include the effects of several different water chemistries. Only those data associated with standard primary water chemistry of 2 ppm Li, 1200 ppm B, and pH = 7.3 were considered in developing the model. The equation fitted to these data is

$$da/dt = 2.8 \cdot 10^{-11} (K_I - 9)^{1.16} \text{ m/sec} \quad (26)$$

where da/dt is a PWSCC growth rate and K is a crack tip stress intensity factor in MPa.m^{0.5}. The model presents the PWSCC crack growth rate at 330°C as a function of the applied crack tip stress intensity factor K_I. The equation implies a threshold value of K_ISCC = 9 MPa.m^{0.5}; no crack growth takes place when the applied crack tip intensity factor is less than K_ISCC. This value of K_ISCC appears to be reasonable because some other test results also indicate that K_ISCC for Alloy 600 in primary water would be in the range of 5 to 10 MPa.m^{0.5} [5.38].

The specimens used by Smialowska et al. for crack growth tests were machined from flattened halves of a short length of steam generator tubing. These specimens are likely to have a significantly higher degree of cold work than that found in steam generator tube roll transition regions (maximum of 2%). Some stress corrosion crack growth rate tests for Alloy 600 performed in 400°C hydrogenated steam environments and in 360°C primary water environments have shown that 5% prior cold work leads to growth rates between 5 to 10 times faster than those observed in materials without cold work [5.39]. Another factor affecting the crack growth rate is test temperature; crack growth rate is higher for a higher test temperature. Scott made corrections to the above crack growth equation (26), by dividing it by 10, to take into account the absence of cold work or a presence of a small amount of cold work. So the PWSCC growth rates for Alloy 600 components at 330°C and no cold work is

$$da/dt = 2.8 \times 10^{-12} (K_I - 9)^{1.16} \text{ m/sec.} \quad (27)$$

This equation may be used for predicting crack growth in the CRDM nozzle material, because in the CRDM nozzles cold work is present only in a thin layer of material on the inside surface of the nozzle, whereas the remaining subsurface material has little cold work. The effects of temperature were added to the Scott model using available Alloy 600 primary water SCC crack growth rates estimated from laboratory test results and field data for steam generator tubes. The estimated activation energy for PWSCC growth in CRDM nozzle materials is 33 kcal/mole. The modified crack growth model is

$$da/dt = 2.56 e^{-(33,000/RT)} (K_I - 9)^{1.16} \quad (28)$$

The available crack growth data for Alloy 600 was for thin steam generator tubes on which the modified model is based. No crack growth data for thick Alloy 600 components, such as CRDM nozzles and instrument penetrations, were available at the time the modified model was developed. Therefore, the Westinghouse Owners Group initiated a project in 1992 to obtain crack growth rate data for the CRDM nozzle materials. The test materials were obtained from six fabricators of the CRDM nozzles. The test results show that the measured crack growth rates for the materials with high grain boundary carbides fall at or below those predicted by the modified Scott model as shown in Figure 5-9a, whereas the measured growth rates for materials with low grain boundary carbide coverage fall at or above the modified model as shown in Figure 5-9b [5.40]. The higher PWSCC growth rates for materials with low grain boundary carbides are being further evaluated. The PWSCC growth rate data presented in Figure 5-9 are based on the laboratory test data and need to be validated in the field. The PWSCC growth rates in Alloy 182 weld metal has been found to be about one order higher than those for Alloy 600 for comparable load and PWR environmental conditions [5.41]. But the changes in the crack growth rate with the applied stress intensity (KI) have been found to be the same for both Alloy 600 base metal and Alloy 182 weld metal.

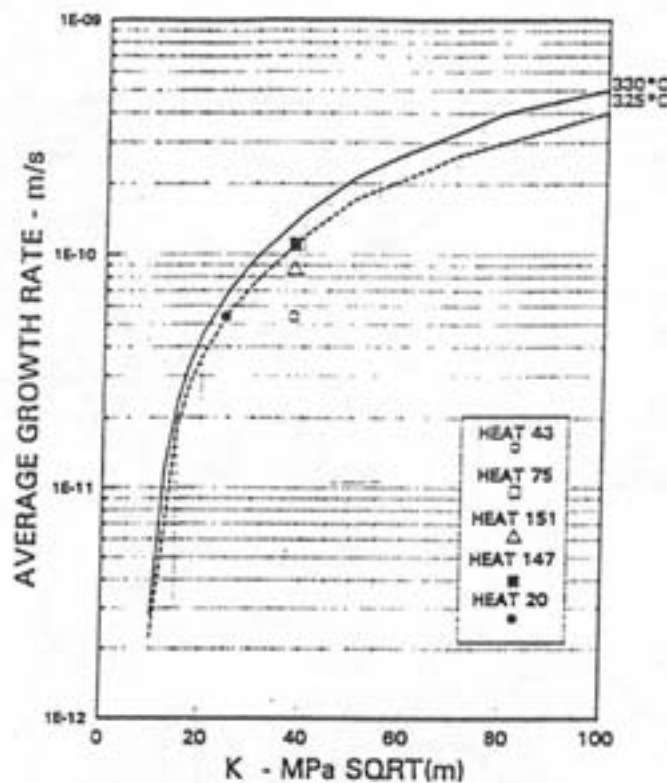


FIG. 5-9(a). Comparison of average PWSCC growth rates with the modified Scott model. High grain boundary carbide coverage materials (>40%).

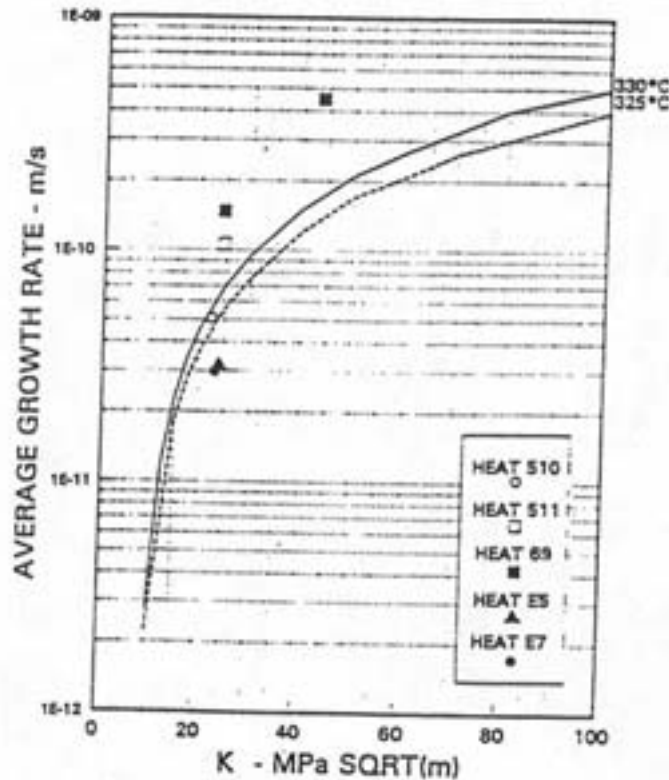


FIG. 5-9(b). Comparison of average PWSCC growth rates with the modified Scott model. Low grain boundary carbide coverage materials (<20%).

If the percentage of grain boundary carbides is not known, a recently developed field surface replication technique for the microstructural characterization of Alloy 600 components could be used to accurately determine the percentage of intergranular carbides [5.42]. This technique has been successfully demonstrated by determining the intergranular carbides in outer CRDM nozzles at one European plant.

Crack growth rate for Alloy 182 weld metal: Moffat et al. [5.43] reports the crack growth results for Alloy 182. The results show that there is more scatter in the crack growth results for welds than for the Alloy 600 base metal. Crack orientation has a very important effect on crack growth rate in the weld metal. The growth rate parallel to dendrite is five to ten times that for flaws propagating through the dendrites. The effects of temperature and stress intensity factor are similar to those observed for Alloy 600 base metal, but the crack growth rate is higher. The crack growth rate for Alloy 82 is likely to be similar to that for Alloy 182. A model of the crack growth rate for Alloy 182 has been developed by applying a factor of 5 to the Scott Model [Equation (27)]. The equation for this model at 325°C is

$$da/dt = 1.4 \times 10^{-11} (K - 9)^{1.16} \quad (29)$$

The model, along with the available data to support it, is shown in Figure 5-10.

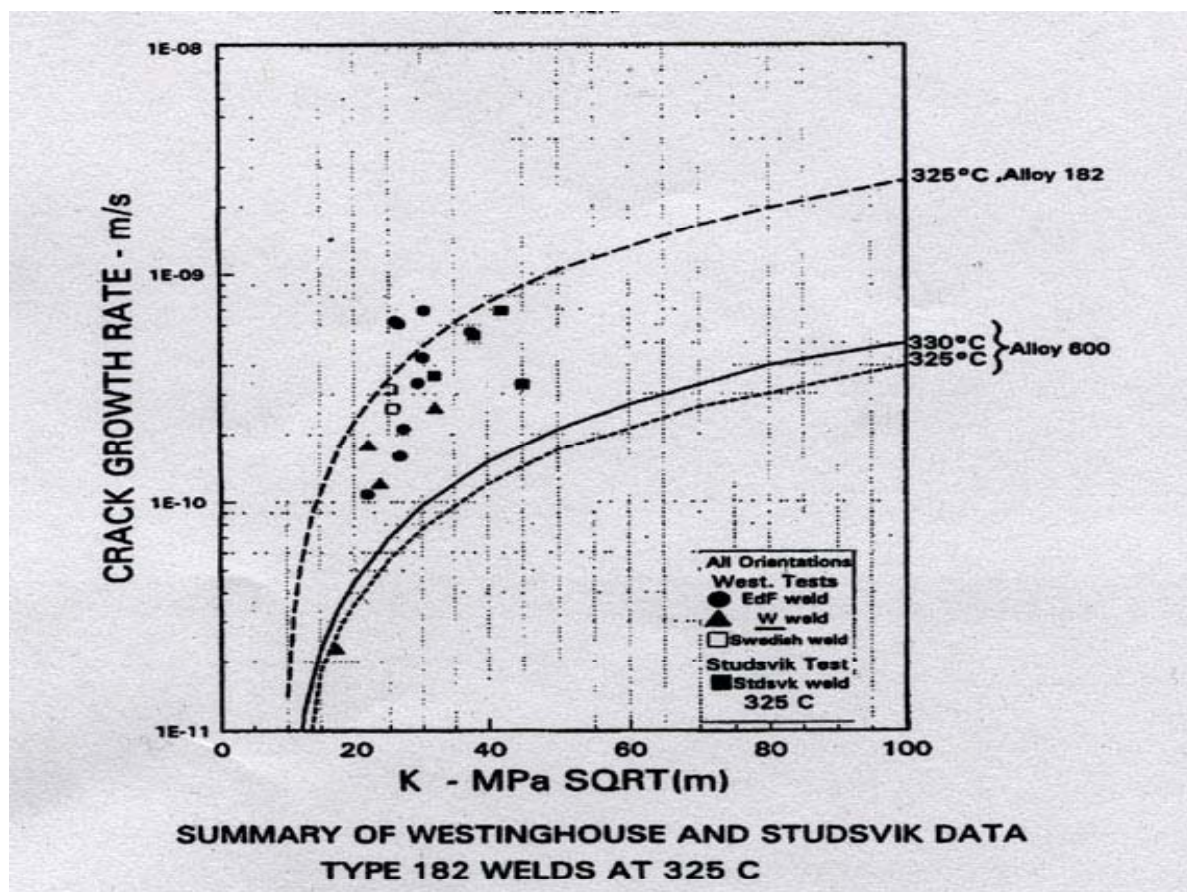


FIG. 5-10. Crack growth model for Alloy 182 in PWR environment with available data. Note that majority of the results are for cracks oriented along the dendrites [5.43].

The approach in France. After an extensive research programme on this material (Alloy 600), its corresponding welds (Alloys 82 and 182) and the alternative material and welds (Alloys 690, 52 and 152) for steam generator and penetration applications, a general criteria has been developed [5.44]. PWSCC is not considered to be a significant degradation mechanism in EDF primary piping except for 3 dissimilar metal welds in the latest plants (Alloys 52). Degradation of these welds is not expected in 40 years of operation based on a simple evaluation of Alloy 52 susceptibility using existing data.

5.5. Assessment of boric acid corrosion

The assessment of boric acid corrosion of carbon steel and low alloy steel components may be performed by visual examination during surveillance walkdown inspections as required by the USNRC Generic Letter 88-05, *Boric Acid Corrosion of Carbon Steel Reactor Pressure Boundary Components in PWR Plants*. This is further discussed in Section 6.1.3.

5.6. Assessment of atmospheric corrosion of dissimilar metal welds

No specific assessment has been developed for this degradation mechanism. The major degradations have been removed by grinding operation.

5.7. Leak-before-break analysis

Leak-before-break (LBB) is an analysis procedure for the evaluation of PWR primary piping system integrity in the absence of active degradation mechanisms and unpredictable dynamic loadings. The basic philosophy of LBB is to demonstrate that a substantial margin exists between the through-wall flaw size which is detectable by the installed leakage detection systems and the critical flaw size which could lead to piping rupture. This analysis includes fracture mechanics and/or limit load analysis of critical crack length in comparison to the stable through-wall crack based on actual (plant specific) material properties and operational and emergency conditions.

The LBB approach cannot be applied to piping that is subject to active degradation mechanisms such as any type of stress corrosion cracking, erosion, corrosion, erosion/corrosion, fatigue, creep, etc. The rationale is that these degradation mechanisms challenge the assumption in the LBB acceptance criteria. For example, fatigue crack growth may introduce flaws whose geometry may not be bounded by the discrete postulated through-wall flaw in the LBB analysis. In addition, piping which is subject to dynamic loading mechanisms (such as water hammer) whose severity cannot be accurately predicted, and thus cannot be bounded by the analysis assumptions, is not a candidate for LBB. To demonstrate that the candidate piping is not susceptible to failure from active degradation mechanisms and unanalyzed dynamic loads, the operating history and measures to prevent their occurrence or mitigate their effects must be reviewed.

5.7.1. The approach in the USA

The application of LBB analysis methodology represents an important change to some US Nuclear Regulatory Commission requirements. The initial application of the LBB approach was proposed to the NRC in 1981 by a Westinghouse owners group. The NRC accepted the approach in Generic Letter 84-04, but limited it to the disposition of Unresolved Safety Issue (USI) A-2 on axisymmetric blowdown loads, and the removal of pipe rupture restraints and jet impingement shields [5.45]. LBB technology was approved in general in 1987 in a change to General Design Criterion 4 (GDC-4) of Appendix A to 10 CFR Part 50 and became effective November 27, 1987. Specific limitations on the use of the LBB methodology (e.g. it is not be used to modify the break spectrum to be considered for emergency core cooling system sizing or for environmental qualification of components) were published in the *Federal Register* as a Nuclear Regulatory Commission Policy Statement on May 2, 1989. The technical procedures and criteria for LBB are defined in NUREG/CR-1061, Volume 3 [5.46]. A brief history of LBB may be found in Wichman and Lee [5.47].

In most cases, generic requests and approvals have been made for Westinghouse [5.45], Combustion Engineering [5.48], and Babcock & Wilcox [5.49] plants. The Ft. Calhoun plant (Combustion Engineering design) was included in the Generic Letter 84-04 review because Ft. Calhoun has stainless steel primary coolant piping as do Westinghouse plants rather than carbon steel piping found in other Combustion Engineering plants. Fifteen Westinghouse plants were included in the Generic Letter 84-04 review and others applied for LBB individually. Although, Generic Letter 84-04 accepted the technical basis for LBB, it stipulated that licensees had to demonstrate that an adequate leakage detection system was operational for their facility. The bases of the Generic Letter 84-04 required that this be a leakage detection system with a sensitivity capable of detecting a 1 gallon per minute leak (gpm) in 4 hour (1 gpm = 3.8 L/min).

A summary of the NRC methodology for LBB application follows. Note that this procedure should be applied to a bounding location(s) (i.e. a cast SS elbow, a section of wrought SS cold leg piping, etc.) to demonstrate that the required margins are met for every location to which LBB is to be applied. Details of this procedure are available in NRC NUREG/CR-1061, Volume 3, Chapter 5.0 [5.46].

Step 1 - Establish initial conditions and properties, demonstrate fatigue resistance.

- (1) Establish the conditions of normal operation (i.e. normal operating pressure, normal operating temperature, etc.) under which this flaw should be detected.
- (2) Determine the as-built dimensions and layout of the system being analyzed. Determine the appropriate material properties (i.e. stress-strain behavior, fracture toughness, etc.) at the operating temperature for the material being analyzed from certified material test reports, if possible.
- (3) From the conditions and material properties above, determine the stresses present at the analysis location during normal operations.
- (4) Demonstrate that the largest flaw permissible under ASME Code Section XI criteria will not grow significantly during service due to fatigue.

Step 2 - Establish a detectable, through-wall, "leakage crack" size.

- (1) Postulate a through-wall flaw at the analysis location and determine the leakage rate through the flaw based on the information from (1.) through (3.) In Step 1 above and an assumed crack morphology.
- (2) The "leakage crack" size is taken to be the flaw size which provides a leakage rate 10 times greater than that which should be detectable by the facility's leakage detection system.
- (3) Demonstrate that the "leakage crack" is stable under safe-shutdown earthquake (SSE) loads with appropriate margins.

Step 3 - Determination of the through-wall "critical flaw" size.

- (1) Using the same material properties, system geometry, and SSE loading conditions as in Step 1 above, determine the largest stable through-wall crack size which can exist at the given location. This maximum stable crack size is the "critical flaw" size.
- (2) Demonstrate that a factor of 2 exists between the size of the "leakage crack" and the "critical flaw" size.

In reference to the description given above, it should be noted that three primary margins of factors of safety are introduced into the LBB analysis:

- (1) A margin on leak detection of 10 on the minimum leakage detectability limit of 0.5 to 1.0 gpm (32 to 63 cm³/s).
- (2) A margin on crack size of 2 for comparing the detectable leakage flaw to the critical crack size.
- (3) A margin on loads of 1.414 if the normal operating and SSE load are combined in a square-root-of-the-sum-of-the-squares fashion. A margin of 1.0 is applied if the absolute values are summed.

The criteria noted in the methodology above can be verified in different ways for different materials. Due to the inherent toughness of wrought stainless steel piping, its failure analysis is controlled by limit load/net-section collapse behavior.

A typical licensing request requires an evaluation of the leakage detection system to demonstrate conformance to NRC Regulatory Guide 1.45, in addition to the loading analysis. The leakage detection system must be capable of detecting leakage through the postulated primary system through-wall crack by one or more methods (humidity monitoring, sump level, activity monitoring, etc.). Leakage detection is discussed further in Section 6.3.

Although LBB can be readily applied to the main reactor coolant loop piping, application to smaller branch lines may present difficulties. While all operating PWRs in the United States have received approval for the application of LBB to the reactor coolant system main loop piping, fewer have received approval of LBB for their auxiliary lines (pressurizer surge, accumulator, and residual heat removal), and for safety injection and the reactor coolant loop bypass lines.

Several difficulties arise with the application of LBB to branch lines. Because of the thermal stratification in pressurizer surge lines, demonstrating acceptance of LBB to these lines became more challenging. A compounding factor in this problem is that stresses resulting from thermal stratification increase as shutdown occurs. Therefore, to ensure a plant can be safely shut down in the event of leakage from a surge line, a stability analysis must be performed which evaluates the effect of the developing stresses on the postulated leakage crack. Vibration-induced fatigue cracking of small lines which use socket welds removes these small-bore piping lines as candidates for LBB. Furthermore, the LBB concept might not apply for pipes with inside diameter 102 mm (4 in.) or less because of the comparatively large flaw size associated with the 38 L/min. (10 gpm) leak rate [5.50]. The circumferential length of the resulting flaw becomes large for a small pipe, leaving a small uncracked ligament, resulting in a large uncertainty in the analysis due to pressure-induced bending.

The NRC has taken the position that cast stainless steel materials will be evaluated on a case-by case basis for the application of LBB. Although “Z” correction factors have been developed to compensate for the lower toughness of flux welds, unfortunately no “Z” correction factors have been developed for thermally aged cast stainless steel [5.51].

Ageing management and mitigation are important parts of the LBB methodology in that they assist in assuring that the various forms of degradation such as fatigue, which can produce cracks in piping walls, are well understood, properly analyzed for, and inspected and monitored adequately. Although the LBB concept has been accepted in general, there remains considerable analysis work [5.52–5.54] and benchmarking theory with experiments [5.55–5.56] to be conducted to further establish this notion.

5.7.2. The approach in Germany

The preclusion of piping breaks (catastrophic failure) in German PWRs is based on the basic safety concept, overview of which is given in Figure 5-11. The concept is based on five principles: (1) optimized design, material, and manufacturing, and defect characterization with non-destructive testing as summarized in Figures 5-12 to 5-15; (2) multiple parties preservice testing for independent quality assurance; (3) research and development including full scale component tests, and failure investigation; (4) continuous in-service monitoring and surveillance and repeated in-service inspection; and (5) verification and validation with Codes, fracture mechanics analysis, and non-destructive evaluation. The safety concept, i.e. the LBB concept, when fulfilled, provides several benefits such as eliminating or reducing the number of pipe whip restraints and a possible reduction of in-service inspection.

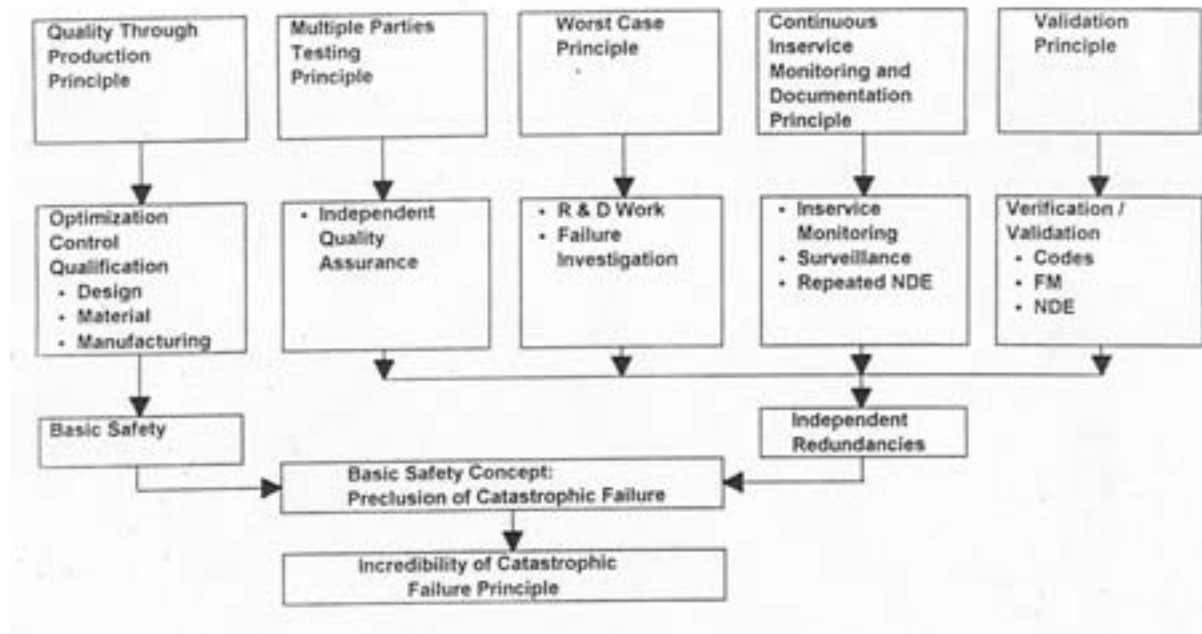


FIG. 5-11. General concept of break preclusion

DESIGN	MATERIAL	MANUFACTURE
Stress calculation	High purity	Optim. welding procedures
Testability	Optim. properties	- optim. properties
Red. No. of weldments	- strength	- low defect quotas
- straight pipe	- toughness	- well known defect types
- elbow	- property gradient	- parameters of procedure defined
- nozzle	- isotropy	- favorable repair possibility
Type of weld	- long time behaviour	- low residual stresses
Avoiding stress concentration	- weldability	- low property gradients
Nozzle cutout reinforcement	Material selection	Qualification
Accessibility for inservice inspection	Component / function-related selection	Qualified welding material
Consideration of water chemistry	Consideration of water chemistry	Optim. non destructive test methods
Quality control	Qualification	Quality control
	Quality control	

FIG. 5-12. Basic safety criteria.

DESIGN	KWU-STANDARD	NON DISPENSABLE FOR BP
Stress calculation	fulfilling KTA-rules equivalent to ASME-Code	fulfilling ASME-Code
Testability	UT + radiography + MP / PT	UT / radiography + MP / PT
Red. No. of weldments	seamless forged or "Erhard"	seamless no cast
- straight pipe (forged, "Erhard", cast)		
- elbow (forged, inductive bending, cast, pressed, welded)	bendings or forged elbows integrated nozzles	no cast good testability
- nozzle (forged, inserted, abutting)		
Type of weld	narrow gap as far as possible	good testability
Avoiding stress concentration	specif. fillets	specif. fillets
Nozzle cutout reinforcement	integrated nozzles	nozzle cutout reinforcement in shell
Location of welds	in low stress areas	in low stress areas
Accessibility for inservice inspection	pipe whip restraint not necessary, simple dismantling/ mantling of isolation,	non destructive testing
Consideration of water chemistry	stabilized, stainless steel cladding	corrosion resistance ID-surface
Quality control	QAM	QA-system

FIG. 5-13. Main coolant loop – requirements on design.

MATERIAL	KWU-STANDARD	NON DISPENSABLE FOR BP
High purity	spec. trace elements	specif. trace elements
Optim. properties	lower and upper limit	lower and upper limit
- strength	> 68 J at lowest service temp.	> 68 J (SS:>60J) at lowest service
- toughness	no gradient in requirements	temp. no gradient in requirements
- property gradient	z > 35 %	z > 35 % (C-steel)
- isotropy	Av, da/dN, N, properties confirmed	Av, da/dN, N, properties confirmed
- long time behaviour		
- weldability	"limit conditions" confirmed	"limit conditions" confirmed
Material selection	only one material	only few materials optimized and approved
Component / function- related selection	20 MnMoNi 5 5 / 1.4551	fixing: low alloyed C-steel / cladded with stainless steel
Consideration of water chemistry	corrosion resistance approved	evidence of resistance
Qualification	unlimited suitability admission	suitability admission
Quality control	QAM of suppliers	QA-system

FIG. 5-14. Main coolant loop – requirements on material.

MANUFACTURE	KWU-STANDARD	NON DISPENSABLE FOR BP
Optim. welding procedure - optim. properties - C-steel-connection - C-steel-stainless steel-connection - low defect quotas - well known defect types - parameters of procedure defined - favorable repair possibility - low residual stresses - low property gradients	limited, optim. welding procedure - specif. requirements BM / HAZ / WM: > 68 J BM (C-steel) / HAZ: > 68 J FL / Butter / WM: > 56 J BM (SS) / HAZ: > 60 J - mechaniz. proced. as far as possib. - experience - relev. welding energy confirmed - repair qualification performed - low residual stresses confirmed or stress relief heat treatment - low gradients in HAZ	optim. welding procedure - specif. requirements BM / HAZ / WM: > 68 J BM (C-steel) / HAZ: > 68 J FL / Butter / WM: > 56 J BM (SS) / HAZ: > 60 J - experience in nucl. manufact. - experience - rel. welding energy confirm. - experience - experience - experience
Qualification	procedure qualific. valid for 2 years, production weld tests	procedure qualification test time dependent
Qualified welding material	welding material test	suitability test, quality assured transport / storage
Optim. non destructive test methods (C-steel-connections and C-steel-stainless steel-connection)	radiography (indicat. length) acc. to UT UT (sensitivity // max. indication length): t < 40 / C-steel: CRR2 // 1 x 40 mm t < 40 / C-steel: CRR3 // 1 x 50 mm SS-ID-surface: PT, alternatively UT	radiography : Indication length see KWU-standard
Quality control	QAM	QA-system

FIG. 5-15. Main coolant loop – requirements on fabrication.

If some of the prerequisites for LBB concept are missing, they can be compensated by other suitable measures such as in-service inspection at higher frequency. The break preclusion based on the safety concept has been implemented at all German PWRs since the late 1970s.

The LBB behavior of NPP piping system is based on analytical fracture mechanics approaches for the evaluation of ductile failure. Siemens uses engineering concepts based on simplified elastic-plastic fracture mechanics concepts to calculate the critical through-wall crack lengths in circumferential direction: flow stress concept (FSC) and plastic limit load (PLL) concept.

The allowable bending moment in the pipe with circumferential through-wall as well as part-through cracks is calculated either by FSC comparing the relevant stress at the crack tip with the flow stress or by PLL assuming yielding over the whole ligament as shown in Figure 5-16. The influence of the axial loading is also taken into account. The FSC concept provides a local LBB criteria whereas the PLL concept provides a global LBB criteria. The flow stress for FSC is dependent on the material, whereas the specified threshold flow stress for PLL is the 0.2% yield strength. The validity of the methods is ensured by the requirement of a minimum Charpy V-notch energy of 45 J and by the use of the material properties of the base metal instead of those of the weld and heat affected zone.

A comprehensive and exhaustive literature review for information on tests of real components was done to verify these two approaches. All available data were evaluated in respect to the influence of material properties, loading conditions, geometry of components, and cracks on the calculated values for the failure stress. Approximately 200 experiments have been analyzed. It is shown that the Siemens procedures FSC and PLL always give

conservative predictions of these tests with circumferential through-wall cracks, i.e. the experimental failure stress is larger than the theoretical one as shown in Figures 5-17 and 5-18.

The LBB analysis as performed by one nuclear steam supplier for German plants aims at four goals: (1) assuring integrity of main coolant piping including piping systems that have experienced high fatigue usage factors, (2) definition of weak points with respect to material properties, ISI, and loadings. This is a specific advantage of the application of the approach in Germany as compared to the approach in the USA based on NUREG-1061 where a crack length is only assumed with respect to the leak detection system capacity. The approach in Germany includes a specific consideration of crack growth behavior under given conditions (material, loading, etc.); (3) definition of deficiencies in support structure; and 4) qualification of leak detection system. The approach in Germany is also used for LBB analysis for various WWER 440-NPP in the eastern European countries.

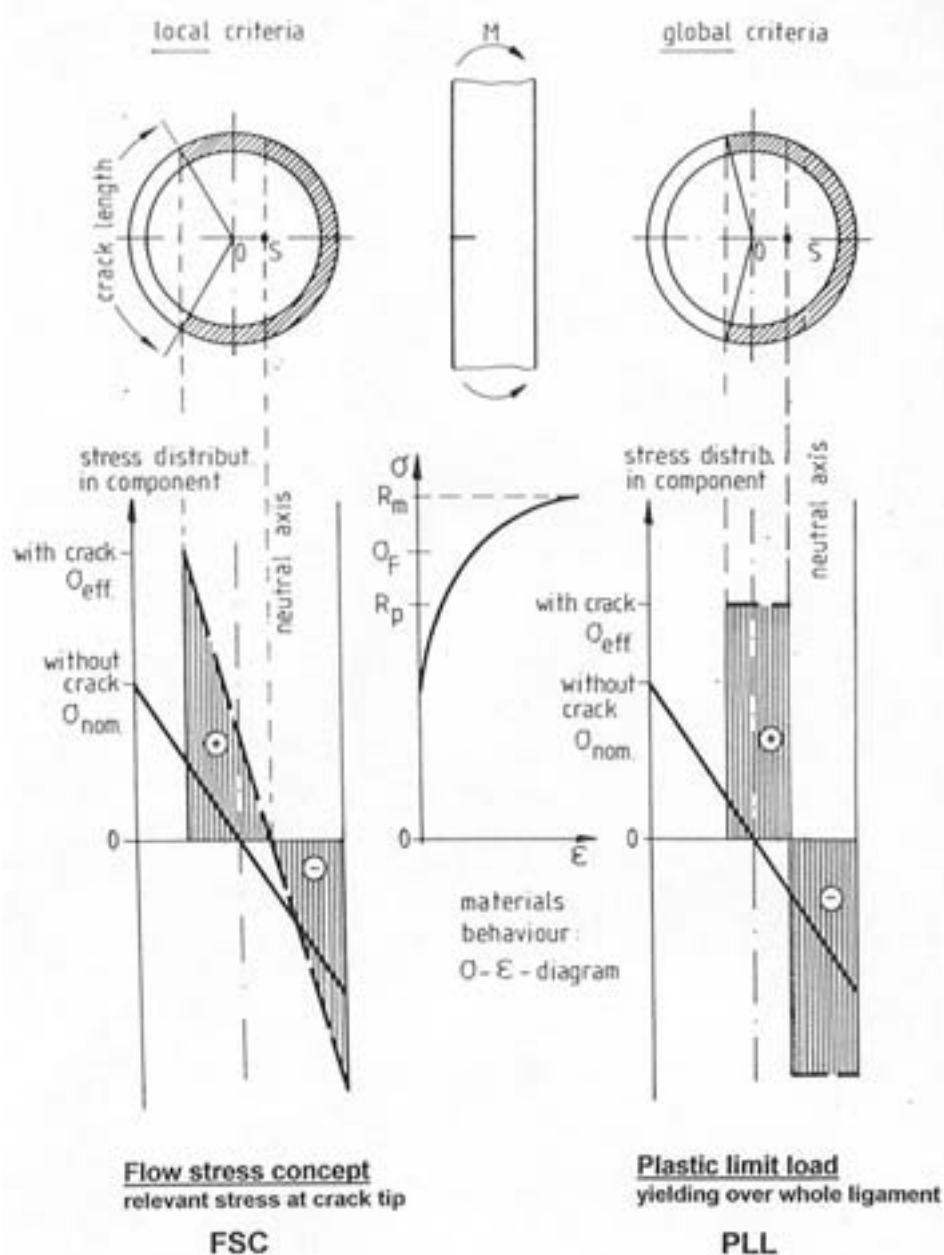


FIG. 5-16. Models for ductile failure (only bending moments).

The application of the approach in Germany on a typical main coolant loop of a Siemens-built NPP provides critical through-wall circumferential crack lengths between 500 and 800 mm; therefore, a great margin exists between the critical crack length and the acceptable indication length (the acceptable indication length is 30 mm for preservice inspection, and 20 mm for in-service inspection). The indication length for acceptable sensitivity of leak-detection system ranges from 70 to 100 mm and higher.

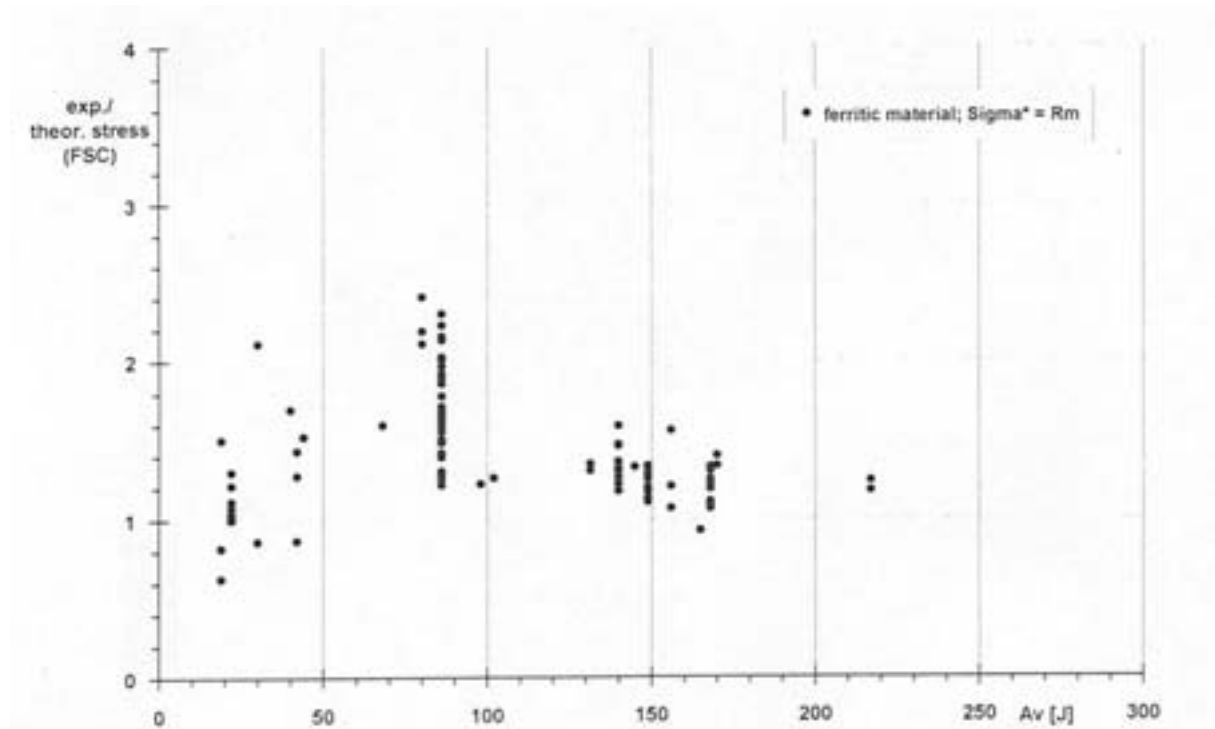


FIG. 5-17. Ratio of experimental and calculated stress versus Charpy energy for through-wall circumferential cracks in weld and heat-affected zone. Stresses are calculated using flow stress concept.

5.7.3. The approach in France

The major difference with other countries in the French approach [5.57] is that a crack is considered in all the piping welds, including dissimilar metal welds, and also in any location in the elbows (they are not covered by elbow to pipe weld).

The French assessment procedure is based on the J integral concept. The validation of the J integral concept has been performed in the Degrading Piping Programme, the IPIRG programme, and national programmes with FRAMATOME and CEA. In France, the J integral concept has been proven to be conservative: the experimental results are found to be higher than the calculated moments.

The dimensional relation between the stress intensity factor, K, which characterize the singular stress and strain fields along a crack front, and the J value, which characterize the elasto-plastic material behavior, appears through their relation in linear elasticity:

$$J = K^2/E'$$

where E' is a corrected Young's modulus; and J , called crack driving force, has the unit of a force per unit length of crack front. The criterion for ductile tearing initiation is $J_{app} > J_{0.2}$, where J_{app} is computed for the considered crack in the loaded structure and $J_{0.2mm}$ represents the crack driving force obtained from tests on small standardized specimens with 0.2mm deep crack. A correlation between $J_{0.2mm}$ and Charpy U-notch energy (KCU) at 20°C is used to estimate $J_{0.2mm}$. This correlation is shown in Figure 5-19. A correlation between $(dJ/da)_{appl.}$ and KCU at 20°C is shown in Figure 5-20 where $(dJ/da)_{appl.}$ represents the derivative of J with respect to the crack length a in the crack extension direction. For stable ductile crack growth, $(dJ/da)_{appl.}$ has to be less or equal to $(dJ/da)_{mat.}$, representing the slope of the $J - a$ resistance curve of the material (or of a connection in the area of poorest toughness within the joint) obtained through experiments performed on standardized specimens. The application of the criterion is shown in Figure 5-21.

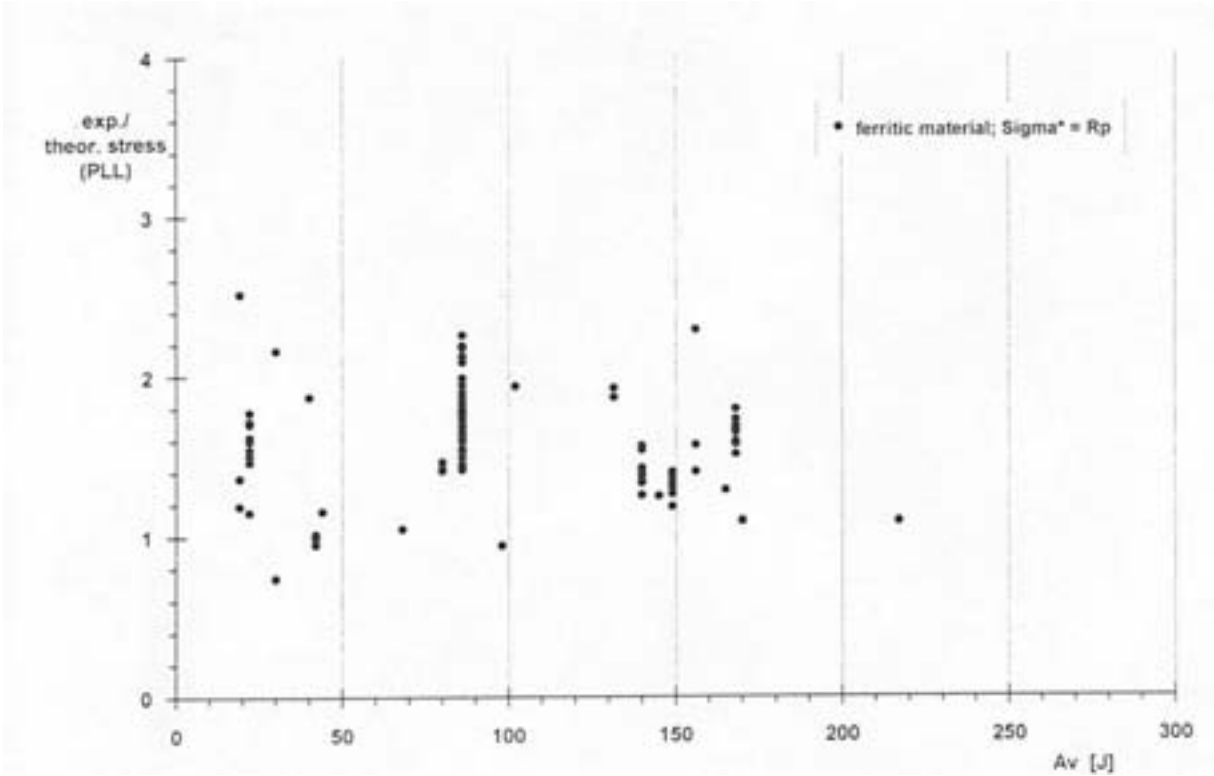


FIG. 5-18. Ratio of experimental and calculated stress versus Charpy energy for through-wall circumferential cracks in weld and heat-affected zone. Stresses are calculated using plastic limit load concept.

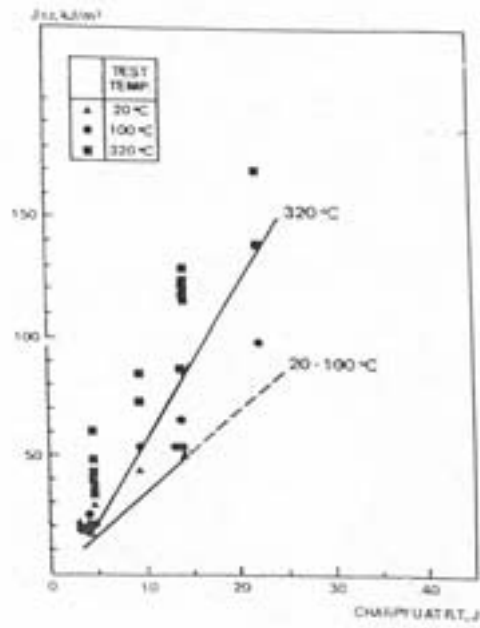


FIG. 5-19. Correlation between $J_{0.2}$ and KCU at 20 °C.

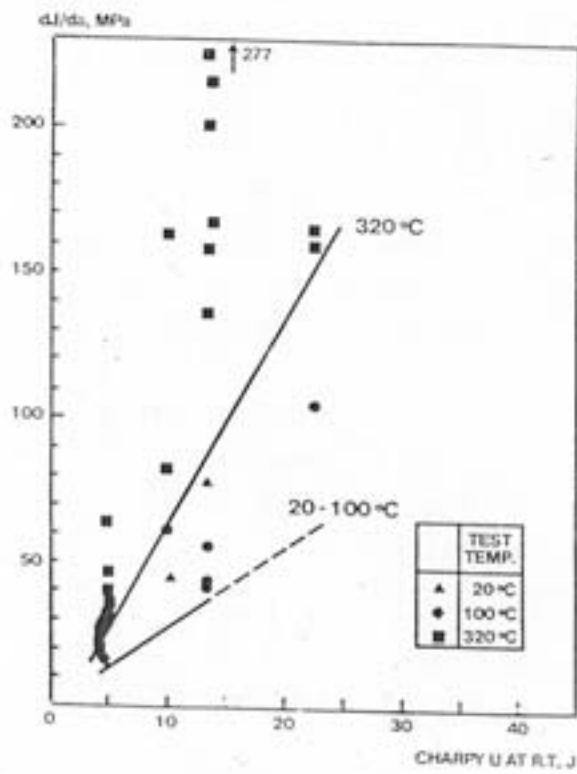


FIG. 5-20. Correlation between dJ/da and KCU at 20 °C.

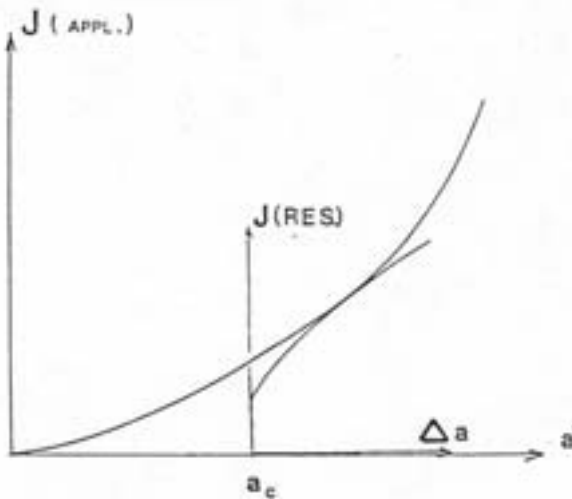


FIG. 5-21. Applied $J - a$ curve and resistance $J - \Delta a$ curve at the instability condition.

It has to be pointed out that for most of the materials, the $J_{0.2\text{mm}}$ and $J - \Delta a$ curve measurements are sensitive to the specimen size and the type of loading; but CT results are conservative to predict cracked pipe behaviour. ASTM standards and ESIS European standards give recommendations for safe and representative measurements of $J_{0.2\text{mm}}$.

5.7.4. The approach in Japan

In Japan, the concept of LBB has been applied to the protective design standard against pipe break for stainless steel piping in RCPB. The premise condition of LBB is as follows:

- I. Selection of piping material, standards for structure, design production, testing and examination, etc., have to be achieved based on the technical standard and PSI (pre-service-inspection) requirements.
- II. The ISI is to be implemented according to the existing standards.
- III. Since SCC and the fluctuation phenomena in the thermal stratification are events beyond expectation in the strength design, the measure against these damage factors is to be taken as a premise.

The assumed crack is to be determined as a larger one by comparing the crack length based on the crack propagation analysis with the crack length bringing about a 19 L/min leak.

- Crack length based on the crack propagation analysis. A single initial defect with a margin to the detection limit of the UT is to be assumed on the inner surface of the pipping as an allowable defect of PSI. The fatigue crack propagation analysis should be continued without specifying the load cycles until the crack grows to a full wall thickness in order to make it possible to deal with an event having probability beyond the design assumption.
- Crack length bringing about a 5 gpm leak. Although the leak detection system in the PWRs has a capability of detecting a 3.8 L/min leakage within an hour, the size of a leak detectable crack is defined to have a margin of 5 times.

The crack stability analysis is based on the net stress concept for stainless steel piping and based on EPFM (elastic-plastic fracture mechanics) analysis for carbon steel, low-alloy steel and thermally aged cast stainless steel piping. (The LBB standardization for carbon steel piping, low alloy steel piping and thermally aged cast stainless steel piping are in the stage of preparation.)

5.7.5. Russian approach

LBB conception can be applied for WWER type reactors if it is demonstrated that a margin exists between the through-wall flaw which size is reliable detectable by the leakage detection systems and the flaw of critical size, which could result to piping rupture. Kiselev et al. (1994) Presents an example of application of the LBB concept to integrity and safety of PWR primary piping for WWER 1000.

For this approach, it is necessary to demonstrate that the required margins are met for every location to which LBB is to be applied. A short description of the procedure is given below.

- Determine that the component is fabricated and inspected according to standards, determine the appropriate material properties, determine the stresses during normal operation condition (NOC) and safe shutdown earthquake (SSE). All possible operating transients and combination of loads, including NOC + SSE should be taken into account.
- Determine detectable crack size, Minimum leakage detectability is 3.8 L/min, taking into account the safety margin 10 to leak detection the crack size that yields 38 L/min is postulated.
- Determine postulated crack size. The in-service inspection data indicate that there are no cases of defects significantly exceeding the sizes specified for welded joint. Therefore the postulated surface flow (semi-elliptic crack) of 0.1 t deep and 0.5 t long was adopted conservatively, where t is wall thickness.
- Perform crack growth analysis to demonstrate that the postulated defect will not grow significantly during service.
- Perform fracture mechanics analysis. And demonstrate that safety margin exists between the size of the detectable crack size and critical crack size. To validate the adequacy of applied methods test of the full scale pipes was performed. The test showed that at 1.4 (NOC + SSE) loads no crack initiation was observed.

5.7.6. Calibration of leak detection system (LDS)

LBB behavior can be proven if a leak, which occurs after a crack has penetrated the wall, can be safely detected by a leak detection system long time before a critical crack size is reached. For the efficiency of leakage detection systems, the knowledge of the correlation between leakage detection signals (temperature, condensate, humidity, acoustic parameters) and leakage rates, leakage areas and through-wall crack lengths is required.

The leakage area is computed with a fracture mechanics model using the integration of the crack opening along the crack front, considering plasticity and geometrical effects. The calculation of the leak rate from a through-wall crack in a component is based on a thermal hydraulics model taking into account the effects of pressure, temperature, crack length, crack width, leakage area, crack depth (wall thickness), roughness, and hydraulic coefficient of

resistance. These analytical approaches, both fracture mechanics and thermal hydraulics, are used to quantify the availability and safety margins of components in connection with plant life extension studies.

All parameters such as crack length, leakage area, leakage rate and leak detection system parameters can be correlated in nomograms as shown, for example, in Figure 5-22. These nomograms allow to calibrate the leak detection system if safety margins are demanded, to assess the safety margins of the component if a leak detection system is installed, to estimate the influence of parameters (geometry, load, material) on the scatter band of detectability, or to optimize the leak detection system in respect to detectability, safety, availability and economy. The nomograms have to be calculated for each individual part of a system to establish the relevant calibration requirements of the leak detection system.

5.7.7. Check of leak/break reaction forces

In the event of a through-wall opening in a pipe the reaction forces resulting from the leakage (quantity and velocity of fluid discharged) can be analyzed by thermal hydraulic analysis. Blowdown into the surroundings from the opening in a fluid reservoir under pressure is mainly governed by the pressure and temperature levels in the reservoir and by the hydraulic resistance given by the flow path and the discharge opening. If pressure in the piping relative to pressure of the surroundings exceeds a certain level, critical discharge takes place. Here the fluid attains sonic velocity. The pressure reduction in the discharge opening can also result in a phase change (steam formation). The varying conditions can be considered by a calculation concept where the discharged rates are derived sections-wise as a function of the change in state of the medium. A procedure of this type was published by the GRS [5.58–5.59]). The four most essential calculation steps are: (1) determination of the critical crack length, (2) calculation of the (minimal and realistic) crack opening and crack areas, (3) determination of the leakage rates considering the hydraulic resistant coefficient and a friction factor for the fluid discharging through the opening, and (4) calculation of the reaction forces.

5.7.8. LBB safety margins

Safety margins are determined by comparing (1) the calculated crack length and depth, including crack propagation, with the reference crack length and depth, respectively (demonstration of exclusion of leaks); (2) the calculated crack length with the critical crack length and calculated crack depth with the wall thickness (demonstration of stability of end-of-life surface crack), (3) the critical crack length with the calculated crack length considering combined normal operating and safe shutdown earthquake loads (demonstration of leak before break behavior, see Figures 5-23 and 5-24), and (4) the opening of the critical crack with the leak cross section. Figure 5-25 gives examples of safety margins obtained by a LBB-analysis of the main coolant loop for a Siemens Konvoi plant. Practically all countries use the safety factors of 2 on critical crack size and 10 on flow rate, as proposed by USNRC in NUREG 1061.

5.7.9. Toughness assessment

Determination of the critical transition temperature (for piping) is performed in some Western countries on the basis of Charpy impact testing layed down in ASME Code Section III/NB 2300 or KTA 3201.1 and 3201.3, V-notches for ferritic material (preferably in USA and Germany also for austenitic material) or U-notches are used. A test shall consist of a set, of three full-size 10 mm × 10 mm specimens oriented in defined direction, according to

ASME specimens from material for pipe shall be oriented in the axial direction, according to KTA in transverse direction. Normally absorbed energy (the requirement for the transition temperature is at least 68 J), lateral expansion (the requirement for the transition temperature is at least 1.0 mm (0.040 in.) for axial direction and 0.9 mm in transverse direction) and sometimes the percentage of brittle/ductile fracture (Germany) are measured.

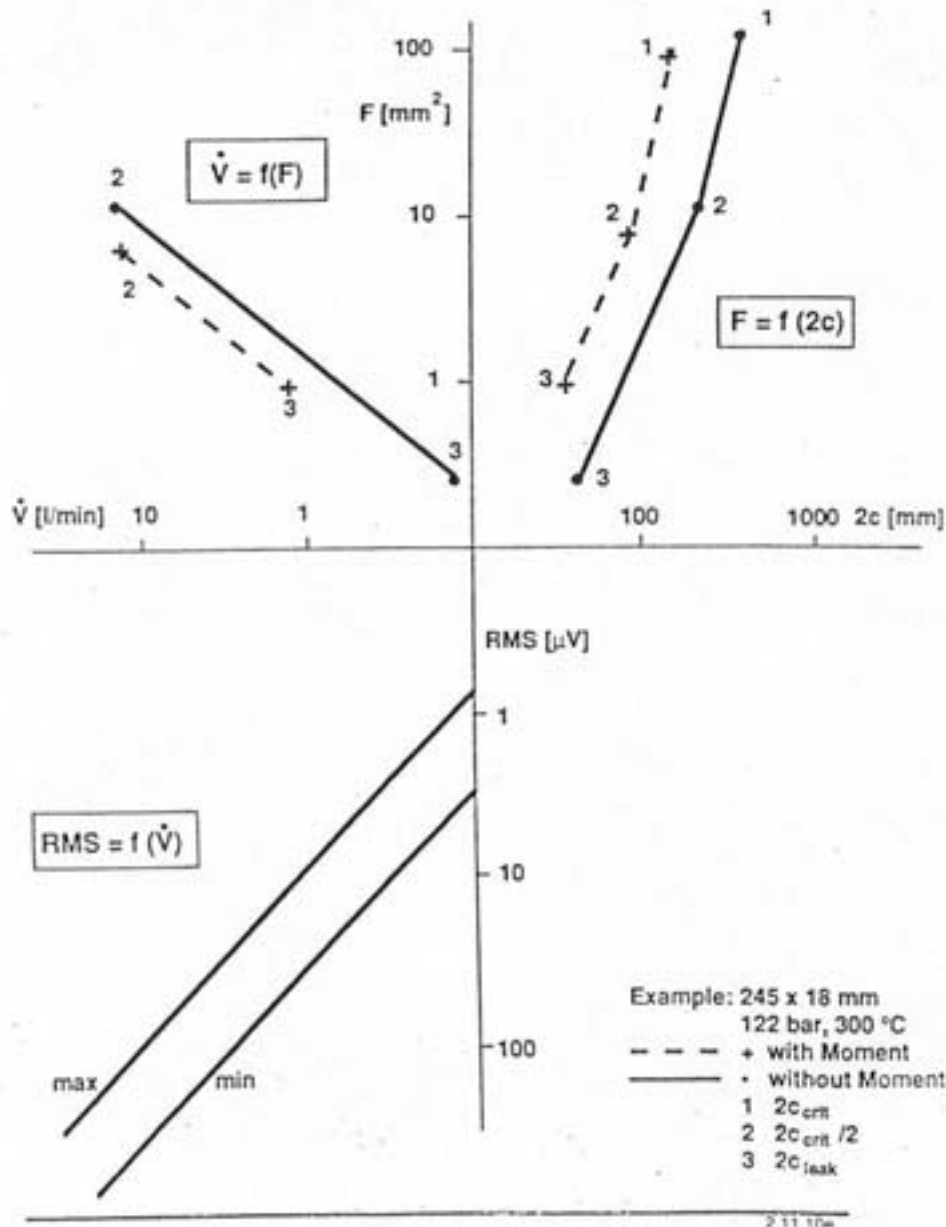


FIG. 5-22. Correlations between crack length ($2c$), leakage area (F_{leak}), leak rate (V), and RMS signal (RMS).

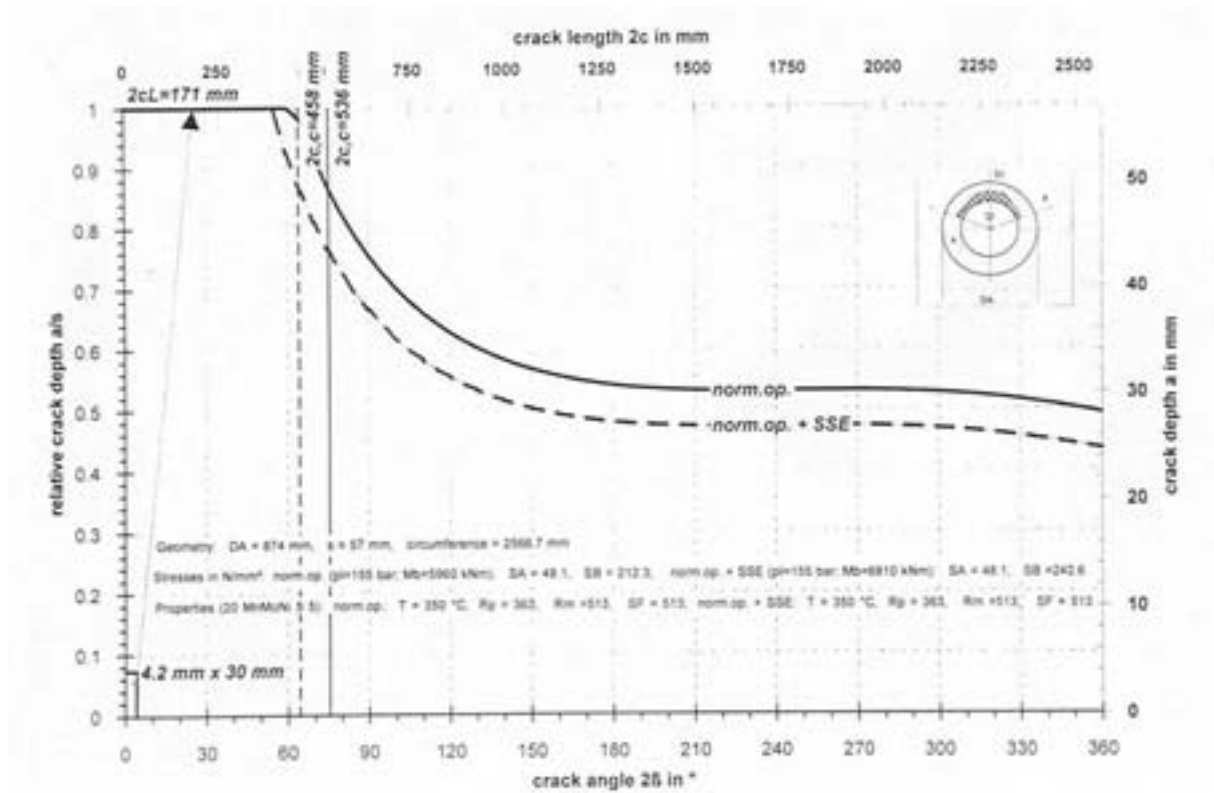


FIG. 5-23. Critical lengths of circumferential cracks for Konvoi plant. Calculated using flow stress concept.

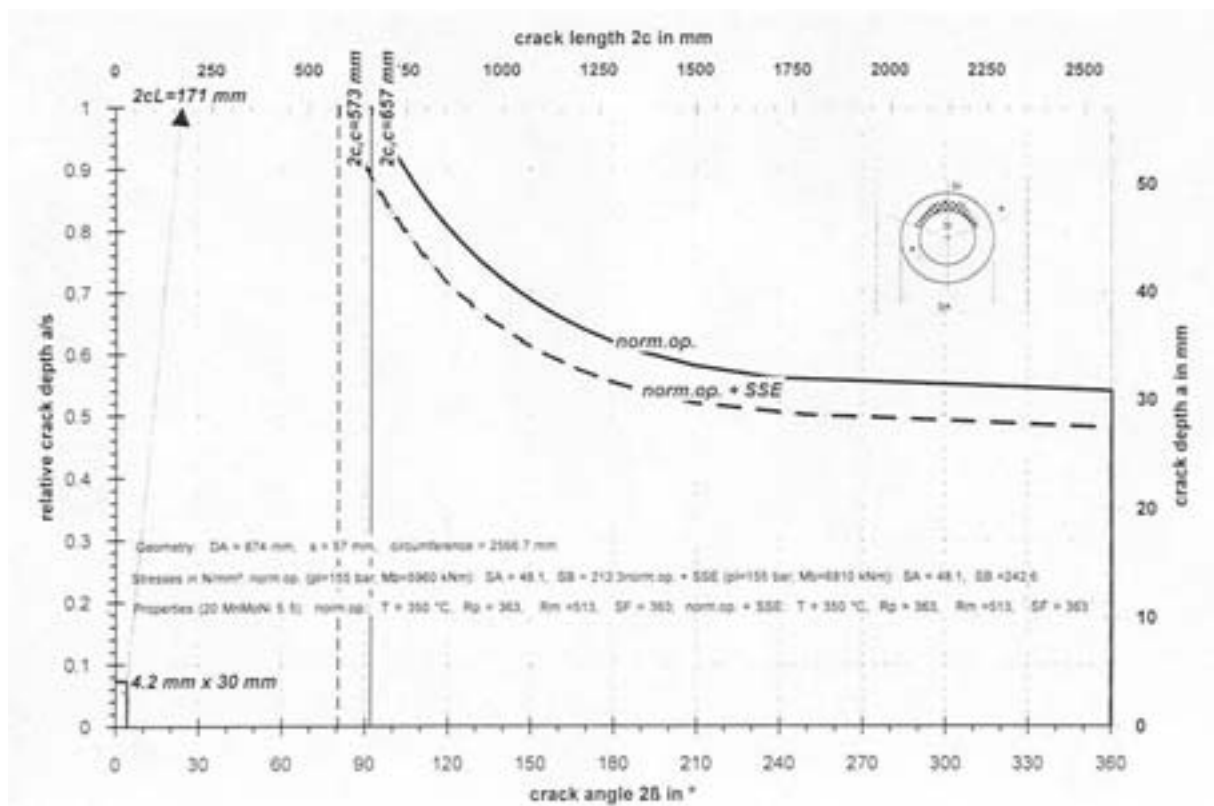


FIG. 5-24. Critical lengths of circumferential cracks for Konvoi plant. Calculated using plastic limit load concept.

			Depth	Length	Safety	Leak Cross	Safety
			a	2c	Margin	Section	Margin
			mm	mm	$S_c = 2c_c / 2c$	mm ²	$S_f = F_c / F$
Surface Crack Examination	$2c_g$	KTA 3201	0 1.5	0 6	- -	- -	- -
UT Examination (Acceptance tests)		KTA 3201	6 4.2	10 30	50 17	- -	- -
UT Examination (Inservice Inspection)		KTA 3201.4	3	20	25	-	-
Leakage Crack Length	$2c_l$			171	3.4		
Leakage Monitoring System: • Condensate, Moisture • Condensate, Moisture	$2c_d$	min. max.	57 57	70 130	8.2 4.4	3 10	720 217
Crit. Through-Wall Crack Length $2c_c$, Cross-Section F_c	$2c_c$		57	573	1	2170	1

FIG. 5-25. LBB analysis of main coolant loop of Siemens-PWR (Konvoi plant).

Additional NDT drop weight tests are required in Germany for class 1 piping made of ferritic steel in order to fulfil the RT_{NDT} concept; this shall be done as follows:

- Determine a temperature T_{NDT} that is at or above the nil-ductility transition temperature by drop weight tests.
- At a temperature not greater than $T_{NDT} + 33$ K, each specimen shall exhibit at least 0.9 mm lateral expansion and not less than 68 J absorbed energy. When these requirements are met, T_{NDT} is the reference temperature RT_{NDT} .
- In the event the above requirements are not met, additional Charpy-tests have to be conducted to determine the temperature T_{CV} at which they are met. In this case the reference temperature $RT_{NDT} = T_{CV} - 33$ K. Thus, the reference temperature is the higher of T_{NDT} and $(T_{CV} - 33$ K).

The critical transition temperature according to the Russian concept is that temperature, which meets the following requirements:

- the mean notch toughness determined in transverse specimens at a temperature T_k or greater shall not be below 32 J (for yield strength 300 to 400 MPa)
- the single value of notch toughness at a temperature T_k shall not be below 70% of the mean value
- the mean notch toughness determined at a temperature $T_k + 30$ K and higher shall be at least 1.5 times the mean value at T_k
- the percent ductile fracture of each specimen shall not be less than 50% at $T_k + 30$ K.

Conclusions with respect to LBB behaviour of the piping system being considered are based on the assumption that toughness properties of base metal and welds (including bimetallic welds, if present) are adequate enough to ensure ductile failure mode. German investigations on specimens and components with different toughness properties have confirmed that Charpy-V energy of 45 J (instead of commonly used higher value of 68 J) at lowest service temperature is sufficient to guarantee ductile failure (see Section 5.7.2). Consideration of environmental conditions during the service life of the component need to be done as a part of any assessment of toughness.

REFERENCES TO SECTION 5

- [5.1] WARE, A.G., MORTON, D.K., NITZEL, M.E., Application of NUREG/CR-5999 Interim Fatigue Curves to Selected NPP Components, NUREG/CR-6260, INEL-95/0045 (1995).
- [5.2] JASKE, C.E., O'DONNELL, W.J., Fatigue Design Criteria for Pressure Vessel Alloys, *Journal of Pressure Vessel Technology*, November 1977, 584–592.
- [5.3] HARVEY, J.E., *Pressure Component Construction*, Van Nostrand Reinhold Company, New York, NY (1980)
- [5.4] MANJOINE, M.J., TOME, R.E., Proposed Design Criteria for High Cycle Fatigue of Austenitic Stainless Steel, ASME Pressure Vessel and Piping Conference, Portland (1988) or ASME H00255, 51–57.
- [5.5] POROWSKI, J.S., et al., Fatigue Criteria for Remaining Life Assessment of Shell Structures Programme Plan, Submitted to the Subcommittee on Shells and Ligaments of the Pressure Vessel Research Committee, May (1988).
- [5.6] KOOISTRA, L.F., LANGE, E.A., and PICKETT, A.C., Full Size Pressure Vessel Testing and Its Approach to Fatigue, *Journal of Engineering for Power*, Transactions of the American Society of Mechanical Engineers, 86, 4, (1961) 419–428.
- [5.7] COOPER, W.E., The Initial Scope and Intent of the Section III Fatigue Design Procedures, presented as the Pressure Vessel Research Council Workshop on Environmental Effects on Fatigue Performance, Clearwater Beach, Florida, 20 January (1992).
- [5.8] ASME 1989a , ASME Boiler and Pressure Vessel Code, Section XI, Rules for In-service Inspection, American Society of Mechanical Engineers, New York (1989).
- [5.9] ASME, ASME Boiler and Pressure Vessel Code, Section XI, Appendix C: Evaluation of Flaws in Austenitic Piping, American Society of Mechanical Engineers, New York (1995) 381–394.
- [5.10] JAMES, L.A., JONES, D.P., Fatigue Crack Growth Correlations for Austenitic Stainless Steels in Air, Predictive Capabilities in Environmentally Assisted Cracking, *PVP Vol. 99* (1985) 363–414.
- [5.11] SLAMA, G., et al., Effect of ageing on Mechanical Properties of Austenitic Stainless Steel Castings and Welds, SMiRT Post Conference Seminar 6, Monterey, CA (1983).
- [5.12] BUCHALET, C., et al., Effect of Long Term Embrittlement on the Critical Defect Sizes in Primary Piping Cast Stainless Elbows, Proceedings of the Second International Symposium on Environmental Degradation of Materials in Nuclear Power Systems — Water Reactors, Monterey, CA, 9–12 September 1985, American Nuclear Society, La Grange Park, IL (1986) 477–484.
- [5.13] BAMFORD, W.H., JONES, D.P., JAMES, L.A., Flaw Tolerance in Engineering Structures: An Assessment of Current Approaches and Future Needs for Predicting Subcritical Crack Growth, Proceedings of the Fourth International Symposium on Environmental Degradation of Materials in Nuclear Power Systems — Water Reactors (1989) 8-1–8-27.
- [5.14] BARTHOLOME, G., ERVE, M., Evaluation of Operating Plants with Respect to Structural Integrity of Components and Systems, First International Conference on Problems of Material Science in Manufacturing and Service of NPP Equipment, Leningrad, 17–21 June (1991).
- [5.15] RSE-M Code, “Surveillance and in-service inspection rules for mechanical components of PWR nuclear islands”, AFCEN Paris, 1997 edition + addenda 1998 and 2000.

- [5.16] CRANFORD, E.L., et al., Considerations in Pressurizer Surge Line Stratification Stress Analysis; Damage Assessment, Reliability, and Life Prediction of Power Plant Components, PVP Vol. 193, NDE Vol. 8, American Society of Mechanical Engineers, New York (1990) 21-26.
- [5.17] MATTHEWS, M.T., et al., Final Submittal in Response to Nuclear Regulatory Commission Bulletin 88-11, Pressurizer Surge Line Thermal Stratification, BAW-2127, Babcock & Wilcox, Lynchburg (1990).
- [5.18] DEARDORFF, A.F., et al., Development of a Thermal Striping Spectrum for use in Evaluating Pressurizer Surge Line Fatigue, Advances in Dynamics of Piping and Structural Components, PVP Vol. 198, American Society of Mechanical Engineers, New York (1990) 23–28.
- [5.19] BRICE-NASH, R.L., et al., Evaluation of Thermal Stratification for the South Texas Units 1 and 2 Pressurizer Surge Line, WCAP-12087, Revision 1, Westinghouse Electric, Pittsburgh, January 1989.
- [5.20] ENSEL, C., COLAS, A., BARTHEZ, M., “Stress Analysis of a 900 MW Pressuriser Surgeline including Stratification Effects”, Nuclear Engineering and Design, Vol. 153, January 1995.
- [5.21] THOMAS-SOLGADI, E., TAUPIN, P., ENSEL, C., “Analysis of Stratification Effects on Mechanical Integrity of Pressuriser Surge Line”, ASME Pressure Vessel and Piping Conference, Vol. 233, New Orleans, June 1992.
- [5.22] KUO, A.Y., TANG, S.S., RICCARDELLA, P.C., An On-Line Fatigue Monitoring System for Power Plants: Part I — Direct Calculation of Transient Peak Stress Through Transfer Matrices and Green’s Functions, Pressure Vessel and Piping Conference, Chicago, IL, July 1986.
- [5.23] USNRC 1996a, Letter from T.W. Alexion to W.T. Cottle, Resolution of NRC Bulletin 88-08, Thermal Stresses in Piping Connected to Reactor Coolant Systems, South Texas Project, Units 1 and 2 (STP).
- [5.24] USNRC 1997a, Unisolable Crack in High-Pressure Injection Piping, USNRC Information Notice 97–46 (1997).
- [5.25] LUND, A.L., HARTZMAN, M., USNRC Regulatory Perspective on Unanticipated Thermal Fatigue in LWR Piping, presented at the NEA/CSNI Specialists’ Meeting on Experience with Thermal Fatigue in LWR Piping Caused by Mixing and Stratification, OECD Nuclear Energy Agency, Paris, 7–12 June (1998).
- [5.26] RODABAUGH, R.C., MOORE, R.C., GWALTNEY, S.E., Review of Elastic Stress and Fatigue-To-Failure Data for Branch Connections and Tees in Relation to ASME Design Criteria for Nuclear Power Piping Systems, NUREG/CR-5359, Nuclear Regulatory Commission, Washington, DC (United States). Office of Nuclear Regulatory Research (1994).
- [5.27] VECCHIO, R.S., Fatigue Evaluation of Socket Welded Piping in a Nuclear Power Plant, ASME Pressure Vessels and Piping Conference, Montreal, Canada, July 1996, PVP Vol. 338 (1996) 25–42.
- [5.28] HIGUCHI, M., IIDA, K., Fatigue Strength Data of LWR Structural Materials in Japan (Effects of LWR Water Environment on Fatigue Strength), Technical Information from Workshop on Cyclic Life on Environmental Effects in Nuclear Applications, PVRC Volume 2, Clearwater Beach, Florida, January 20–21 1992, Welding Research Council, Inc., New York (1992).
- [5.29] CHOPRA, O.K., Estimation of Mechanical Properties of Cast Stainless Steels During Thermal ageing in LWR Systems, Proceedings of the US Nuclear Regulatory Commission Nineteenth Water Reactor Safety Information Meeting, NUREG/CP-0119, Vol. 1, (1997) 151–178.

- [5.30] CHOPRA, O.K., Thermal ageing of Cast Stainless Steels in LWR Systems: Estimation of Mechanical Properties, Nuclear Plant System/Components Ageing Management and Life Extension, PVP Vol. 228, American Society for Mechanical Engineers, New York (1992) 79–92.
- [5.31] CHOPRA, O.K., Estimation of Fracture Toughness of Cast Stainless Steels During Thermal ageing in LWR Systems, NUREG/CR-4513, ANL-90/42 (1991).
- [5.32] CHOPRA, O.K., Mechanical-Property Degradation of Cast Stainless Steel Components from the Shippingport Reactor, Proceedings of the U.S. Nuclear Regulatory Commission Nineteenth Water Reactor Safety Information Meeting, NUREG/CP-0119, Vol. 1 (1992) 179–195.
- [5.33] BOGIE, K.D., et al., Ageing of Cast Stainless Steel Components, International Journal of Pressure Vessel & Piping, 50 (1992) 161–177.
- [5.34] CHOPRA, O.K., SHACK, W.J., Assessment of Thermal Embrittlement of Cast Stainless Steels, NUREG/CR-6177, ANL-94/2 (1994)
- [5.35] SUZUKI, I., et al., Long term Thermal Ageing of Cast Duplex Stainless Steels, International Conference on Nuclear Engineering, Volume 5, ASME (1996) 253–257.
- [5.36] LANDES, J.D., McCABE, D.E., Toughness of Austenitic Stainless Steel Pipe Welds, EPRI NP-4768, Electric Power Research Institute, Palo Alto, CA (1986).
- [5.37] SCOTT, P., An Analysis of Primary Water Stress Corrosion Cracking in PWR Steam Generators, Proc. of the Specialists Meeting on Operating Experience with Steam Generators, Brussels, Belgium (1991) 5–6.
- [5.38] REBAK, R.B., MCILREE, A.R., SZKLARSKA-SMIALOWSKA, Effects of pH and Stress Intensity on Crack Growth Rate in Alloy 600 in Lithiated and Borated Water at High Temperatures, Proc. of the 5th International Symposium on Environmental Degradation of Materials in Nuclear Power Systems-Water Reactors, American Nuclear Society, La Grange Park, IL (1992) 511–517.
- [5.39] CASSAGNE, T.B., GELPI, A., Crack Growth Rate Measurements on Alloy 600 Steam Generator Tubes in Steam and Primary Water, Proceedings of the Fifth International Symposium on Environmental Degradation of Materials in Nuclear Power Systems - Water Reactors, Monterey, California, 25–29 August 1991, (1992) 518–524.
- [5.40] FOSTER, J.P., BAMFORD, W.H., PATHANIA, R.S., Initial Results of Alloy 600 Crack Growth Rate Testing in a PWR Environment, Proceedings of the Seventh International Symposium on Environmental Degradation of Materials in Nuclear Power Systems – Water Reactors, NACE International, 7–10 August 1995, 25–40.
- [5.41] LINDSTROM, R., et al., Crack Growth of Alloy 182 in a Simulated Primary Side PWR Environment, Proceedings of the Eighth International Symposium on Environmental Degradation of Materials in Nuclear Power Systems — Water Reactors, Vol. 1, 10–14 August 1997, Amelia Island, Florida, American Nuclear Society, La Grange Park, IL (1997) 422–428.
- [5.42] RAO, G.V., “Methodologies to Assess PWSCC Susceptibility of Primary Component Alloy 600 Locations in Pressurized Water Reactors”, Sixth International Symposium on Environmental Degradations of Materials in Nuclear Power Systems — Water Reactors, San Diego (1994) 871–882.
- [5.43] MOFFAT, G., et al., Development of the Technical Basis for Plant Startup for the V. C. Summer Nuclear Plant, Service Experience, Fabrication, Residual Stresses and Performance, PVP Vol. 427, ASME (2001) 33–39.
- [5.44] AMZALLAG, C., LE HONG, S., BENHAMOU, C., GELPI, A., “3 Methodology used to rank the stress corrosion susceptibility of alloy 600 components”, ASME Pressure Vessel and Piping Conference, Seattle, July 2000.

- [5.45] USNRC 1984b, Safety Evaluation Of Westinghouse Topical Reports Dealing With Elimination Of Postulated Pipe Breaks In PWR Primary Main Loops, USNRC Generic Letter 84-04, February 1 1984.
- [5.46] USNRC 1984a, Investigation and Evaluation of Stress Corrosion Cracking in Piping of Boiling Water Reactor Plants, Report of the U.S. Regulatory Commission Piping Review Committee, Volume 1, NUREG-1061.
- [5.47] WICHMAN, K., LEE, S., Development of NRC Standard Review Plan 3.6.3 for Leak-Before-Break Applications to NPPs, International Journal of Pressure Vessels and Piping 43 (1990) 57–65.
- [5.48] RICHARDSON, J.E., (NRC) letter to E.C. Sterling (CEOG), Acceptance for Referencing of Topical Report CEN-367, Leak-Before-Break Evaluation of Primary Coolant Loop Piping in Combustion Engineering Designed Nuclear Steam Supply Systems”, 30 October 1990.
- [5.49] CRUTCHFIELD, D.M., (NRC) letter to L.C. Oakes (B&W Owners Group), Safety Evaluation of B&W Owners Group Reports Dealing with Elimination of Postulated Pipe Breaks in PWR Primary Main Loops, 12 December 1985.
- [5.50] MAXHAM, W.D., YOON, K.K., Application of Leak-Before-Break Approach to PWR Piping Designed by Babcock and Wilcox, EPRI NP-4972 (1987).
- [5.51] QUINONES, D.F. HARDIN, T.C., Recent Developments in Leak-Before-Break Technology, ASME Pressure Vessels and Piping Conference, Denver, CO, PVP Vol. 261 (1993) 79–87.
- [5.52] WILKOWSKI, G., et al., Pipe Fracture Evaluations for Leak-Rate Detection: Deterministic Models, ASME Pressure Vessels and Piping Conference, Denver, CO, PVP, Vol. 266 (1993) , 243–254.
- [5.53] RAHMAN, S., WILKOWSKI, G., GHADIALI, H., Pipe Fracture Evaluations for Leak-Rate Detection: Deterministic Models, ASME Pressure Vessels and Piping Conference, Denver, CO, PVP Vol. 266 (1993) 269–286.
- [5.54] RAHMAN, S., WILKOWSKI, G., GHADIALI, H., Pipe Fracture Evaluations for Leak-Rate Detection: Applications to BWR and PWR Piping, ASME Pressure Vessels and Piping Conference, Denver, CO, PVP Vol. 266 (1993) 269–286.
- [5.55] GREBNER, H., HÖFLER, A., HUNGER, H., Comparison of Leak Opening and Leak Rate Calculations to HDR Experimental Results, ASME Pressure Vessels and Piping Conference, Denver, CO, PVP Vol. 266 (1993) 217–229.
- [5.56] MOULIN, D., AGUILAR, J., Influence of Crack Opening Displacement on Water Flow Rates Through Cracked Plates Under Tension, ASME Pressure Vessels and Piping Conference, Denver, CO, PVP Vol. 266 (1993) 231–242.
- [5.57] FAIDY, C., “LBB application on French PWR plants under Operation”, LBB95 Conference, Report OCDE/GD (96) 11, Lyon, France, June 1995.
- [5.58] PANA, P., CSNI-Paper, Paris, 16–17 May 1974.
- [5.59] PANA, P., MÜLLER, M., Nuclear Engineering Design 45 (1978) 117–125.

6. INSPECTION, MONITORING AND LEAK DETECTION

Effective ageing management of PWR primary coolant piping requires, among other things, timely detection and characterization of any significant ageing degradation of the piping. In-service inspection plays an important role in detecting a crack early enough so that appropriate mitigation/repair steps can be taken before it grows beyond allowable size. Monitoring of stressors causing ageing degradation, especially fatigue damage aids in more accurate assessment of the damage and in identification of the most damaging pressure and temperature transients. Detection of reactor coolant leakage representing breach of primary pressure boundary, and loose part monitoring for detection of any broken part inside the primary coolant system can alert the plant operators if a failure has occurred.

6.1. Inspections of PWR primary piping

The principal means for ensuring the integrity of the PWR primary piping pressure boundary is through non-destructive testing (NDT) of piping welds. These non-destructive inspection methods are broadly classified as either volumetric or surface inspection methods. The non-destructive examination method generally used for volumetric in-service inspection of Class 1 piping welds is ultrasonic testing. This section first summarizes the US current in-service inspection requirements for piping welds and corresponding French and WWER practices. Then, it discusses the inspection difficulties associated with different piping materials and with dissimilar metal welds. Finally, emerging inspection techniques are discussed, along with a brief description of ASME Mandatory Appendix VIII, which was developed to qualify new and existing techniques and improve the overall reliability of ultrasonic examinations.

6.1.1. Inspection requirements

6.1.1.1. Practices in the USA

NPP Class 1, 2, and 3 components in the United States are subject to the requirements of Section XI of the ASME Code [6.1] as required by the Federal Regulations [10 CFR 50.55a(g)(4)]. Section XI contains the minimum in-service inspection requirements for those components. PWR in-service inspection requirements are typically written around four 10-year inspection intervals (Inspection Programme B of Section XI) to cover the 40-year operating life. This requirement includes a preservice inspection (PSI) and four in-service inspections (ISI) at 10-year intervals during the 40-year operating life of a nuclear plant. The specific edition of Section XI required by the Regulations is based on the start of each 10-year inspection interval. In accordance with the Regulations, the examination of components must comply with the latest edition and addenda incorporated by reference in 10 CFR 50.55a(b) on the date 12 months prior to the start of the 10-year inspection interval.

Preservice inspection requirements. Preservice examination is performed to establish baseline examinations of welds that may be examined during ISI. The preservice and in-service inspection requirements for the Class 1 piping systems are specified in Subsection IWB of Section XI of the ASME Code. These requirements include examination of the Class 1 Reactor Coolant System piping welds as specified in Table IWB-2500-1, Examination Categories B-F and B-J. The examination requirements and methods are identical for both the preservice and in-service inspections, and only differ by the extent of the examination. For the

preservice inspection, the extent of examination extends to 100% of the non-exempt⁵ pressure retaining welds. In accordance with Section XI, preservice examinations are to be conducted with techniques and equipment, and under conditions equivalent to those expected during subsequent ISI examinations. The same preservice examination requirements are also applicable for components repaired or replaced during the service lifetime prior to the components return to service. The examination requirements are the same for both PSI and ISI, and the details will be discussed in the next section.

In-service inspection requirements. The examination requirements for Class 1 piping welds are generally categorized as Examination Category B-J, “Pressure Retaining Welds in Piping”. During ISI, examination is required for 25% of all the butt and socket welds in the Class 1 piping⁶, and includes volumetric and/or surface examination. In accordance with Examination Category B-J, Note (1), the examination sample shall include

- (a) all terminal ends in pipe runs connected to vessels,
- (b) *all* weld locations where the calculated design-basis stress intensity exceeds $2.4 S_m$ (S_m is the maximum allowable general primary membrane stress intensity as defined in Section III of the ASME Code) or where the calculated design-basis cumulative fatigue usage factor exceeds 0.4,
- (c) *all* dissimilar metal welds, and
- (d) an additional number of welds to bring the examination sample to 25% of the weld population.

In a recent Code Interpretation [6.2], it is stated that an examination sample of more than 25% is not required. Consequently, for licensees applying this interpretation, it is conceivable that certain high stress, high usage factor, or dissimilar metal welds may not be included in the examination sample once the 25% sample is reached. However, Code Interpretations are not endorsed by the NRC, and a conservative interpretation of the Code requirements would result in examination of *all* of the welds specified in Note (1), parts (a), (b), and (c) regardless of sample size.

Volumetric examination is performed on the inner one-third of the weld volume and adjacent base metal, and the surface examination includes inspection of the external surface of the weld and the adjacent base metal⁷. Section XI [6.3] recognized that the inner weld surface is the most likely site for initiation of a service-induced flaw; thus, examination of the full weld volume is not required. For pressure retaining welds in piping less than NPS (nominal pipe size) 4 and socket welds, only a surface examination of the exterior surface of the weld is required.

The other category of piping welds included in IWB are the dissimilar metal welds (Examination Category B-F). Prior to the 1989 Addenda of the 1989 Edition of ASME Section XI, dissimilar metal piping welds could fall under either B-J or B-F. In the 1989 Addenda of Section XI, Examination Category B-F was reorganized and retitled to “Pressure Retaining Dissimilar Metal Welds in Vessel Nozzles”. This revised category includes the dissimilar nozzle-to-safe end butt welds of the reactor vessel, pressurizer, steam generator and

⁵ Generally, Class 1 components that are exempt from examination are piping systems NPS 1 and smaller. (NPS 1 means nominal pipe size of 1 in.)

⁶ Excluding those welds already classified as Examination Category B-F welds.

⁷ For volumetric and surface examination purposes, the adjacent base metal extends $\frac{1}{2}$ of the nominal wall thickness from the weld.

Class 1 heat exchangers, but removed all piping welds from the Category to eliminate the redundancy in the Code. Under Examination Category B-F, 100% of the dissimilar metal welds to vessel nozzles are examined. The examination requirements are similar to those of Examination Category B-J; that is volumetric of the inner 1/3 volume and/or surface examination of the external surface, depending on size. As will be discussed in a later section, dissimilar metal welds create unique inspection problems that affect the reliability of ultrasonic examination.

Section XI does not require any in-service inspection of the elbow base metal, which can be susceptible to fatigue damage. The inside surfaces of the flanks of thin-wall elbows (ratio of the outside to the inside diameter less than 1.2) subject to inplane bending are most susceptible to fatigue cracking in the transverse direction. The outside surfaces of the intrados of thick-wall elbows (ratio of the outside to inside diameter greater than 1.2) subject to inplane bending are most susceptible to fatigue cracking in the circumferential direction. In addition, statically cast stainless steel elbows are known to have shrinkage flaws in the intrados regions where fatigue cracks may initiate and the cumulative usage factor for some surge line elbows has been calculated to be greater than 0.4 [6.4]. Therefore, there is a potential need to examine the susceptible elbow base metal during in-service inspection. Such an examination of the elbow base metal is required for the highest loaded region of the base material of one representative elbow in each loop in German plants. The outside and inside surfaces with the near-surface region have to be tested by magnetic particle or ultrasonic testing method.

The “Generic Ageing Lessons Learned” (GALL) report, which the Nuclear Regulatory Commission (NRC) published in June of 2001, evaluated existing plant programmes generically to document the basis for determining when existing programmes are adequate without change and when existing programmes should be augmented for license renewal. Many of the existing programmes are based on the ASME Section XI Code requirements. In some cases, the Code did not directly or explicitly address the ageing management as required by 10 CFR Part 54, the license renewal rule. In some cases, there was no existing programme to mitigate or prevent the ageing effects expected during the period of extended operation. The GALL report identifies the areas where the ASME Code needs to be enhanced to be credited as an effective ageing management programme [6.5—6.6]

6.1.1.2. Practices in France

All the French pre-service and in-service inspection programme is presented in the French RSE-M In-service Code for Nuclear PWR [6.7], with corresponding techniques, performance demonstration procedure and flaw evaluation procedure. The main difference with the US practice is the location and the performance objectives for the Class 1 piping ISI programme. All the locations are connected to the potentiality of mechanical degradation (like fatigue and stress corrosion cracking) and flaw tolerance of the specific location. If some location has a low toughness level compared to the maximum load in a location, the utility has to assure no defect in this location through specific ISI and complementary flaw evaluation procedure. It is the reason why all the cast elbows of the primary system have been inspected on all the French plants (base metal and weld areas), due to existing cast defects and low toughness value of aged CF8M elbows. It is the first step of a risk-informed process (without any sampling requirements) on class 1 piping. For class 2 and 3 piping systems, different risk informed pilot studies are in progress [6.8]. This process has to take into account feedback of the national and international experience to revise the corresponding ISI programme.

Stratification, dead legs and mixing areas will be included in the recent revised ISI programmes.

6.1.1.3. WWER practices

Aged material testing requirements for WWER Plants. The mechanical properties of piping for NPS with WWER reactors after 100 000 hours of operation was defined by Point 7.4.10 of the old rules [6.9]. In accordance with these rules, it is necessary to investigate the metal structure and mechanical properties of piping by testing specimens which took out of the controlling piping including both base metal and welds.

In accordance with the recent rules PNAE-G-7-008-89 (Point 7.6.3), the mechanical properties control of piping after 100 000 hours of operation must be estimated by destructive and/or non-destructive methods [6.10]. This alternate replacement of the control technology (destructive *or* non-destructive) is became possible only after the complex investigations of specimens of the real piping material (after 100 000 hours of operation):

- Units 1-4 with VVWER-210, VVWER-365, VVWER-440 reactors (Novovoronezh)
- Units 1-4 with reactors VVWER (Kola NPS)

The test results have not shown any significant difference in material properties. The investigations have revealed that the NPPs piping material maintain high properties after 100 000 hours of operation and gave possibility to create new effective methods of non-destructive estimation of piping mechanical properties (without removing specimens). It is elaborated in a typical programme on the piping material after 100 000 hours of operation.

This programme includes:

- experimental/analytical estimation of the control places by the maximum operating damage principle
- measurement of the material mechanical properties at chosen places of piping by the non-destructive method of uniform local deformation (kinetic hardness)
- microstructure analysis by the replication
- ultrasonic and radiographic inspection.

The complex investigations (without specimens) of the main coolant loop base metal and weld metal of the Novovoronezh unit 5 were carried out. The structure and mechanical properties were investigated. The comparative analysis of the metal in initial state (certificate data) and after control (control data) was carried out. As a result, the base and weld metal properties after 100 000 hours of operation were found acceptable for the regulatory documents requirements. No significant difference in material properties was found.

6.1.2. Material considerations

The three principal material types found in PWR main coolant piping, listed in the order of increasing inspection difficulties, are ferritic, austenitic stainless, and duplex austenitic-ferritic stainless steels. Inspection considerations for each will be discussed in the following sections.

Ferritic steels. Ferritic steel is the easiest to examine ultrasonically, and standard ASME Code procedures have performed well. Ferritic steels have randomly oriented grains, which are generally smaller than 1 mm in size. Hence, for commonly used test frequencies of 2 to 5 MHz, with wavelengths somewhat longer than the grain size (1-3 mm), ferritic steels appear acoustically homogeneous and isotropic (with low attenuation and noise levels). The only complication associated with the primary piping arises from the austenitic cladding on the inside surface of the ferritic piping, which produces a local increase in noise level called clad roll. Clad roll is caused by the internal acoustic interface at the stainless steel clad-to-ferritic pipe interface and by clad surface irregularities. Because the increased noise is located in the same vicinity (on the ultrasonic A-scan) as any flaw indication signals from the piping inside surface, the potential for noise interference with the flaw detection exists. However, this has not caused major problems in the past.

Austenitic stainless steels. Austenitic stainless steels, on the other hand, can solidify in much larger grains (e.g., >1mm) depending on processing history, making inspection far more difficult than for ferritic steels [6.11]. Inspectability can vary from difficult in the weld metal to good in the surrounding heat-affected zone and base material, depending on the type of parent material (wrought, forged), and the welding process used, all of which influence the size and shape of the grain structure. Figure 6-1 depicts a possible grain structure in a wrought stainless steel butt weld. Dendritic grains are typical within the weld, with coarse equi-axed grains directly adjacent to the weld that become finer with increasing distance. These regions can possess different acoustic properties that can create acoustic interfaces, cause beam redirection, false calls, and a general loss of confidence and reliability. With grain sizes larger or equal to the commonly used wavelengths of 1 to 3 mm, each grain can influence the sound beam, causing scattering and attenuation of ultrasonic energy, and creating high levels of background noise.

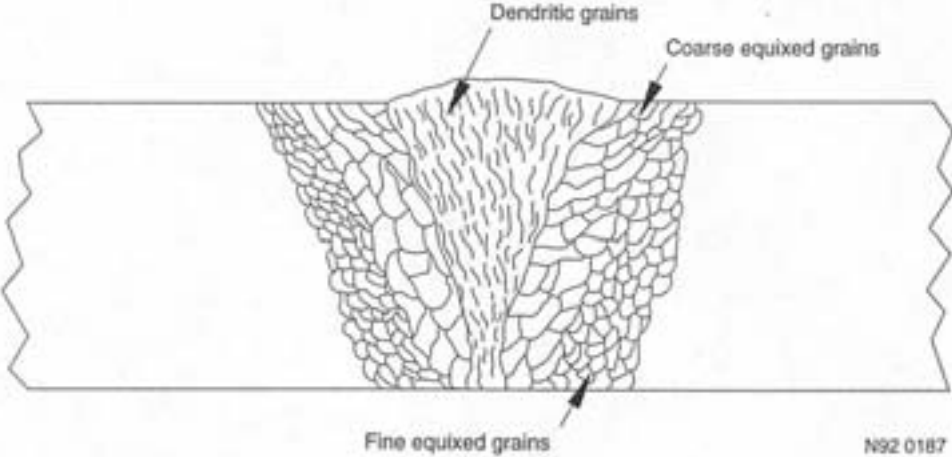


FIG. 6-1. Typical wrought austenitic weld joint showing possible grain structure.

Cast stainless steel. Compared to wrought austenitic piping, which has inspectability that ranges from good in the fine grained parent material to poor in the large grained weld metal, inspection problems are further magnified for the cast variety of austenitic stainless steel material. Inspectability ranges from poor in the large grained parent material to nearly impossible in the large dendritic grains (up to several centimeters) within the weld material. Figure 6-2 shows a typical weld joint containing a columnar-dendritic grain structure of a

statically cast elbow on the right, and a coarse equi-axed grain structure of centrifugally cast piping on the left [6.12]. In cast austenitic materials, where grains can be as large as cracks, the ultrasonic beam is severely attenuated, scattered, and redirected to the point that only cracks greater than 30% through-wall are reliably detected, and sizing is often impossible, even with specially developed techniques [6.13].

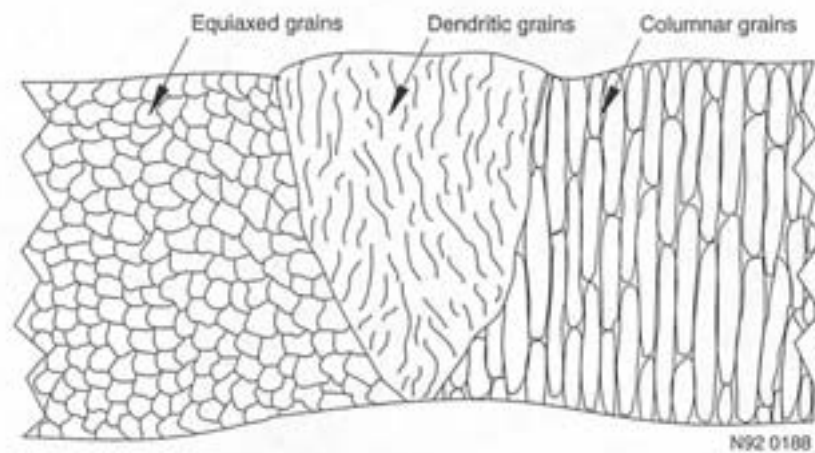


FIG. 6-2. Typical cast stainless steel pipe-to-elbow weld joint showing possible grain structure. Centrifugally cast pipe has equiaxed grains and statically cast elbow has columnar grains [6.10].

Dissimilar metal welds. The final and perhaps the most important welds to consider in the primary piping system are the dissimilar metal welds, sometimes called bi-metallic or tri-metallic welds. Dissimilar metal welds are defined by Section XI as:

- (a) carbon or low-alloy steel to high- alloy steel welds,
- (b) carbon or low-alloy steel to high-nickel alloy welds, and
- (c) high-alloy steel to high-nickel alloy welds.

These three types of weld material are commonly known as carbon steel (carbon or low-alloy steels), stainless steel (high-alloy steels), and Inconel or Alloy 600 (high-nickel alloys), respectively. In addition, buttering material is often used to act as a transition between dissimilar metals. Figure 6-3 shows nozzle to safe-end and safe-end to pipe welds containing a combination of all of the above discussed materials [6.14]. From left to right in the figure is a centrifugally cast stainless steel pipe, a stainless steel weld, a forged stainless steel safe-end, an Alloy 600 weld, Alloy 600 buttering, and a clad low-alloy steel nozzle. In addition to the inspection problems that exist for each of the individual materials contained in the weld joint, the combination of materials further complicates ultrasonic examination due to differences in materials acoustic properties (i.e. velocity, attenuation). The large, often columnar grain structure typical for austenitic welds leads to anisotropic acoustic properties, and the size and arrangement of the grains, along with the differences in the elastic properties of the materials cause scattering, mode conversions, beam distortions, and velocity variations that vary with position and scanning direction [6.15]. These variations in material properties that the ultrasonic beam must traverse can significantly reduce examination reliability through attenuation or redirection of the sound beam in an unpredictable manner, that interferes with crack detectability and characterization of both cracks and weld geometry.

6.1.3. Past experience/augmented examinations

The ASME Section XI Code was written to address generic in-service degradation and intended to provide the minimum in-service inspection requirements. As such, Section XI examinations are only performed on a portion of critical components for degradation mechanisms postulated in the design basis (i.e. primarily thermal fatigue). Thus, the Code does not address every location or type of degradation that could occur or are found during plant operation. In these cases, the NRC may impose augmented examination requirements to supplement Code requirements, enter into agreements (e.g., IGSCC Coordination Plan) or accept licensees' commitment (e.g., commitment to follow RG 1.150). In accordance with the Code of Federal Regulations [10 CFR 50.55a(g)(6)(ii)], the NRC may imposed augmented inspection programmes for systems and components where added assurance of the structural integrity is deemed necessary. As will be discussed below, this can apply to inspection methodologies, as well as systems and locations susceptible to certain types of degradation.

For license renewal, applicants may also have to address ageing management beyond the requirements of ASME Section XI. The "Generic Ageing Lessons Learned" (GALL) report evaluated the existing Inservice Inspection Programmes generically and found that the Inservice Inspection Programme needed to be augmented to be credited as an effective ageing management programme for license renewal [6.5–6.6].

Examination for thermal fatigue. Fatigue occurring at several operating plants prompted the NRC to issue several documents to inform licensees and in some cases, to recommend certain actions to address this phenomena. Documents addressing the thermal fatigue issue were Information Notice 88-01 [6.16], Bulletin 88-11 [6.17] and three supplements of Bulletin 88-08 [6.18]. In some cases, enhanced inspection procedures were recommended.

As a result of the 1982 fatigue cracking at Crystal River 3, the B&W Owner's Group Safe End Task Force performed generic investigation and recommended an augmented, periodic ISI programme for MU/HPI nozzles. As discussed earlier, the augmented programme included radiographic and ultrasonic examinations. USNRC Generic Letter 85-20 endorsed the Task Force recommendations. All B&W-designed plants implemented the augmented inspection programme.

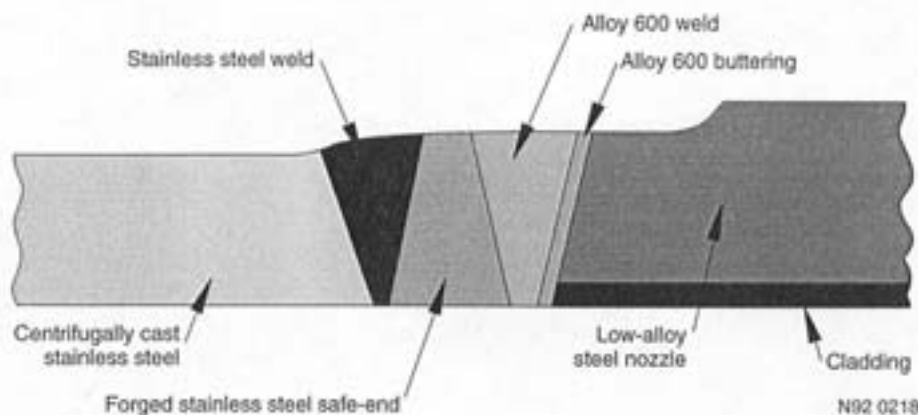


FIG. 6-3. Reactor vessel outlet nozzle-to-safe end-to-cast pipe weld joint [6.14].

As a result of the fatigue failure at Farley Unit 2, the use of special techniques, higher instrument gain, and examination personnel with demonstrated ability to detect and evaluate cracks in stainless steel welds was recommended by the USNRC in Bulletin 88-08, Supplement 2. In this case, conventional amplitude-based ultrasonic examination procedures specified in ASME Section XI could not reliably detect or accurately size tight thermal fatigue cracks. In December 1987, Farley Unit 2 had to shut down when a leak was discovered in a weld in the stainless steel safety injection line. The through-wall crack was determined to be caused by thermal fatigue. No reportable indications were found when the weld was examined as part of the normal in-service inspection programme during a 1986 outage. Ultrasonic testing with a 45-degree transducer and a gain of 6 dB above the reference level, as required by ASME Section XI, was used in this examination. The weld was reexamined using the same procedure after the leakage was discovered, but still no reportable indications were found. Supplemental techniques using a 60-degree shear wave transducer, and an additional 8 dB of gain with the 45-degree transducer were needed to identify the crack. In a similar situation, an additional 24 dB (16 times) above the ASME Code sensitivity was needed to detect a through-wall crack at Tihange Unit 1 in Belgium. In the latter case, the crack was discovered in the base metal of an elbow, which is not included in the ASME Section XI required in-service inspections, and was only detected because of the leakage.

In response to USNRC Bulletin 88-08 and its three supplements, PWR utilities in the United States have performed non-destructive examinations of the critical sites in the charging and safety injection lines and nozzles [6.19]. The critical sites include the welds and the base metal sites with high stresses. No crack-like defects have been found. On-line temperature and pressure monitoring has also been implemented to detect and estimate the thermal stratification loads. These measurements indicate that some thermal stratification and cycling do take place; however, the magnitude is small and no significant actions are required. Some experimental flow tests have also been carried out to assess the effect of valve leakage, and some utilities have added or removed valves in the various piping systems to reduce the potential for valve leakage problems.

Stratified flows are likely to cause significant fatigue damage to both welds and base metal in the surge and spray lines. As the result of thermal stratification in the pressurizer surge line at the Trojan Plant, the NRC issue Bulletin 88-11, suggesting that licensees of operating PWRs perform a visual examination (VT-3) of the piping, supports, whip restraints and anchor bolts of the entire pressure surge line. Furthermore, Bulletin 88-11 requested that licensees update their stress and fatigue analysis to ensure compliance with applicable Code requirements. In accordance with Section XI, welds exceeding the fatigue usage factor of 0.4 should be examined as part of the in-service inspection programme. Augmented examination of base metal sites with fatigue usage factors greater than 0.4 is also worth consideration. The ASME Section XI Task Group on Fatigue in Operating Plants has recommended that the need for in-service inspection of the base metal sites that are susceptible to significant fatigue damage be evaluated [6.2]. Such base metal sites, as discussed earlier, are in the surge line elbows and pipe bends.

Use of reliable ISI techniques is effective in detecting fatigue cracks in a timely manner provided the crack growth rate is low, that is, a small undetectable crack takes longer than an operating cycle to become a through-wall crack. This was the case for the 1982 Crystal River 3 and the 1997 Oconee 2 cracking of MU/HPI safe-end weld. However, effectiveness of the ISI techniques is reduced if a small defect, nondetectable during regular in-service inspection, becomes a through-wall crack within an operating cycle. Such a rapid

crack growth occurred at Dampierre 1 in 1997. A portion of the safety injection line was replaced during the repair for the 1996 leakage event (see Table XX). A crack initiated and propagated to 67% through-wall depth in the replaced piping within 8 months after the replacement. This results contradicted the fatigue analysis results for the replaced piping, which indicated that the crack should not initiate for years, even when taking into account local thermal loads revealed by temperature monitoring of the piping. One of the concern of the French safety authority is that the stability of a through-wall crack under seismic conditions is not well assessed by the analysis [6.20]. The leakage rate can be enhanced by an earthquake. Experiments need to be performed to demonstrate the stability of a through-wall crack in piping exposed to valve leakage of cold coolant and to seismic conditions.

Use of reliable ISI techniques is effective in detecting fatigue cracks provided all the susceptible locations, both welds and base metal, are inspected. Generally, for branch lines with diameter greater than 102 mm (4 in.), welds and adjacent base metal are inspected during in-service inspection, but base metal away from the welds are not inspected [6.21]. For piping with diameter smaller than 102 mm, the ASME Section XI Code does not require volumetric inspection of either weld or base metal. Through-wall thermal fatigue cracks in base metal away from the welds, however, have been reported at two PWRs: Tihange 1 in 1988 and Dampierre 1 in 1996. Figure 6-4 is an isometric view of Dampierre 1 safety injection piping showing the location of through-wall cracking in the straight portion of the piping. As a result of this cracking, EDF has revised its ISI programme. The revised programme includes the inspection of base metal as shown in Figure 6-5 [6.22].

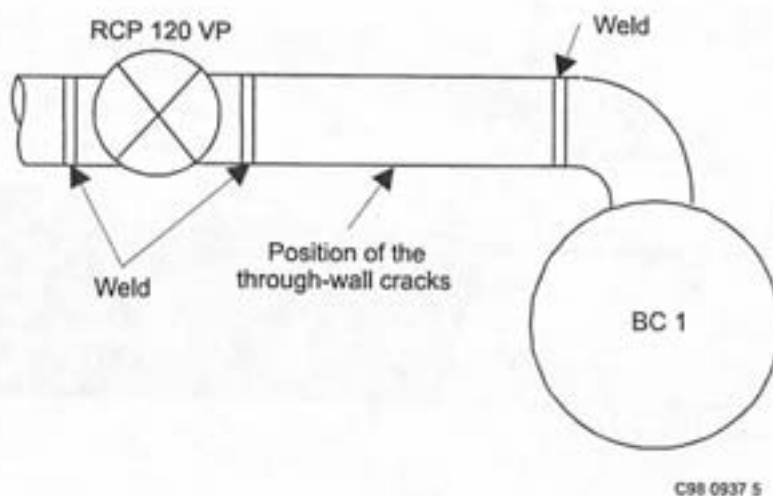


FIG. 6-4. Thermal fatigue cracking in the straight portion of the safety injection piping, Dampierre 1 [6.22].

Merle [6.20] has identified another limitation of in-service inspection methods as one of the difficulties in managing fatigue damage to the branch lines. For example, 33% to 66% through-wall cracks were not detected during in-service inspections.

Examination of dissimilar metal welds. During NRC inspections of ISI activities at a number of operating facilities, the NRC noted that shear wave transducers were commonly used to examine dissimilar metal welds containing Inconel filler and weld butter materials. As a result of intergranular stress corrosion cracking (IGSCC) problems identified in piping in boiling water reactor (BWR) plants, it was concluded that shear wave techniques could not reliably detect cracking in dissimilar metal welds. As a direct result, the NRC issued

Information Notice No. 90-30, Ultrasonic Inspection Techniques for Dissimilar Metal Welds [6.23]. In this bulletin, the use refracted longitudinal waves for inspection of these welds was strongly recommended. Longitudinal waves are less susceptible to beam redirection and attenuation due to metallurgical features (i.e. anisotropic and dendritic grain structure) than shear waves. This notice was issued as a result of inspection experience associated with IGSCC cracking at BWR plants. However, dissimilar metal welds in PWR plants have similar metallurgical characteristics (i.e. anisotropic grain structure and properties); therefore, the recommendations of NRC Information Notice No. 90-30 should be considered applicable to the ultrasonic examination of dissimilar metal welds for all operating plants.

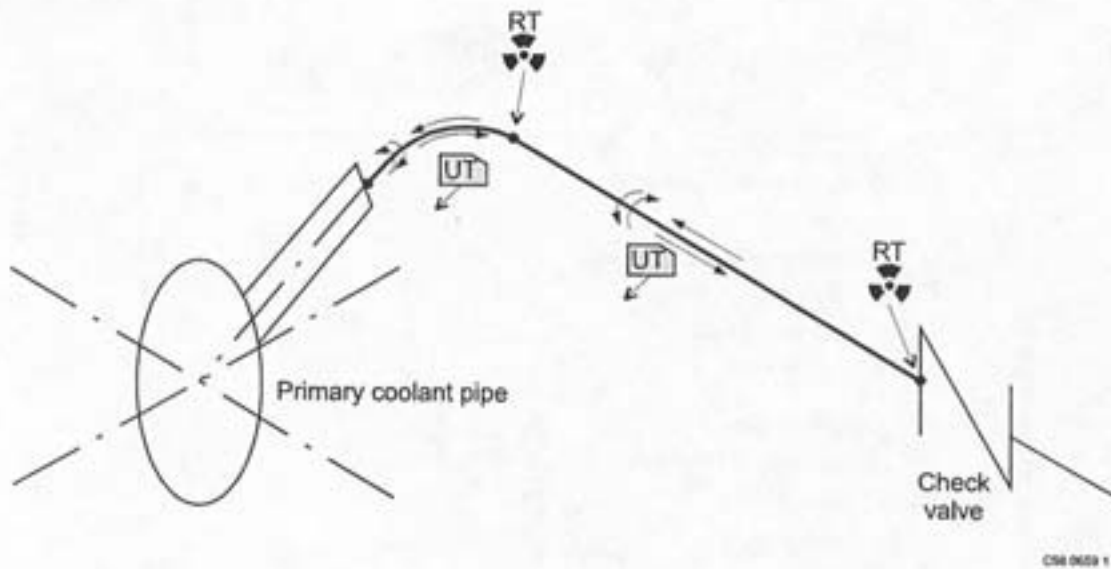


FIG. 6-5. Details of 1997 in-service inspection program for the French PWR safety injection piping [6.22].

A significant difference in the examination of the RPV dissimilar metal safe-end welds for BWRs and PWRs is an access consideration. For BWRs, the examinations are typically performed from the OD surface of the weld. For PWRs, the RPV dissimilar metal safe-end welds are located between the vessel and biological shield wall and are, therefore, impractical to access from the OD surface for performance of the Code-required surface and volumetric examinations. Thus, the RPV dissimilar metal vessel safe end welds in PWRs usually receive a full volume examination from the inside surface with remote reactor vessel inspection systems in lieu of the surface examination and volumetric examination of the inner 1/3T. Examination from the inside is typically performed using immersion techniques and has demonstrated high inspection capability as indicated by the PISC III work for nozzles and dissimilar metal welds [6.24]. The subject PISC studies indicate the importance of recording level. Techniques employing a recording level of 50% distance amplitude correction (DAC) did poorly, whereas, procedures using recording levels of 10–25% or that used noise level recording criteria performed best. The PISC III studies also indicate that flaw indications <2 mm (0.080") are beyond the reach of today's common technology.

Examination for boric acid corrosion. Utilities in the USA perform visual examination during surveillance walkdown inspection to detect any boric acid leakage. A small [0.38 L/min (<0.1 gpm)] primary system leak through pressure boundary can be detected during the walkdown; such a small leak is generally not detected by the plant leak detection systems. The utilities perform this inspection in response to the USNRC Generic

Letter 88-05, Boric Acid Corrosion of Carbon Steel Reactor Pressure Boundary Components in PWR Plants. This letter required the following:

- Determination of the locations where leaks smaller than the allowable technical specifications can cause boric acid corrosion of the primary pressure boundary
- Procedures for locating small leaks
- Evaluation of the primary pressure boundary integrity when leakage is located
- Corrective actions to prevent recurrence of the type of corrosion

In 1990, USNRC audited 10 PWR licensees and found that they all have addressed the above four requirements [6.25]. Similar visual inspections are performed in other countries, e.g. France and Germany.

6.1.4. In-service inspection methods/reliability

The Code requirements and associated non-destructive inspection methods continues to evolve. These changes are the result of inspection failures and improvements in technology. In the following sections, the primary volumetric inspection methods will be discussed, along with some of the notable weaknesses of the Code.

Volumetric examination methods. Section XI recognizes two volumetric inspection methods, ultrasonic testing (UT) and radiographic testing (RT). Of the two methods, ultrasonic testing is the preferred volumetric method for in-service inspection because of its lower cost and better sensitivity for detecting and sizing service-induced defects. The disadvantages of UT have been the lack of a permanent record and the dependance on operator judgement. The inherent advantage of radiography is that testing can be performed through insulation and can provide a permanent examination record which can be used to compare future examinations to. The resulting image can also be used to characterize weld geometry. Most of the disadvantages for RT stem from convenience factors. These include radiological controls that may interfere with critical path activities, interference from contaminated and irradiated components, and access to the inside surface. Because there is rarely access to the inside of the pipe, double wall techniques must be used which reduce sensitivity. The final consideration is that RT is arguably a less sensitive method for crack detection as compared to other NDE methods. Although RT is sensitive to defects that are volumetric in nature (e.g., erosion-corrosion, slag inclusions, etc.), the density differences caused by a crack may not be sufficient for detection if the orientation of the crack is not parallel to the gamma or X ray. In addition, the crack may be filled with oxides which further reduces the density difference [6.26].

Crack detection. Ultrasonic examination of piping welds is addressed in a Mandatory Appendix III of Section XI. The criteria used by Appendix III regarding detection of flaws is based on a comparison of the reflected amplitude from a flaw to that of a reference reflector, typically a notch. The current Appendix III recording levels are a direct result of the Programme for the Inspection of Steel Components II (PISC II) trials [6.27]. The PISC II results indicated that a recording level of 50% DAC used by earlier editions of Section XI was unreliable for flaw detection. Hence, the 1985 Addenda of the 1983 Edition reduced the recording level such that flaw indications exceeding 20% of the calibrated reference level had to be recorded and investigated. The reference level is determined by the reflected amplitude from calibration notches (side-drilled holes are also used in some situations), which decreases as metal path distance increases. The resulting curve is called a distance-amplitude correction or DAC curve.

Crack sizing. Guidelines for flaw sizing have long been a weak spot of Section XI (flaw sizing sections are currently in the course of preparation in Appendices I and III). Hence, Section V requirements are commonly used for flaw sizing. Section V of the ASME Code specifies the “6 dB drop” method for determining both the through-wall size (depth) and the lateral extent of any planar flaw. In this method, the edges of the defect are established by moving the transducer forward, backward, and side to side from the point of maximum signal amplitude until the reflected amplitude is reduced to 50% (or other fractions) of the maximum amplitude.

Although the dB drop method is effective in determining crack length, it has been shown to be an ineffective method for determining the depth of planar reflectors such as cracks [6.28]. As demonstrated by the PISC II trials and shown in Figure 6-6, time-based sizing methods (i.e. crack-tip diffraction techniques) using time-of-flight to determine crack depth are far superior to the amplitude-based sizing methods. The amplitude-based methods tend to undersize flaws, especially the deeper ones, as indicated by the flat response shown in Figure 6-6, while measurements made with the time-based methods (i.e. crack-tip diffraction techniques) correlate well with actual flaw depth.

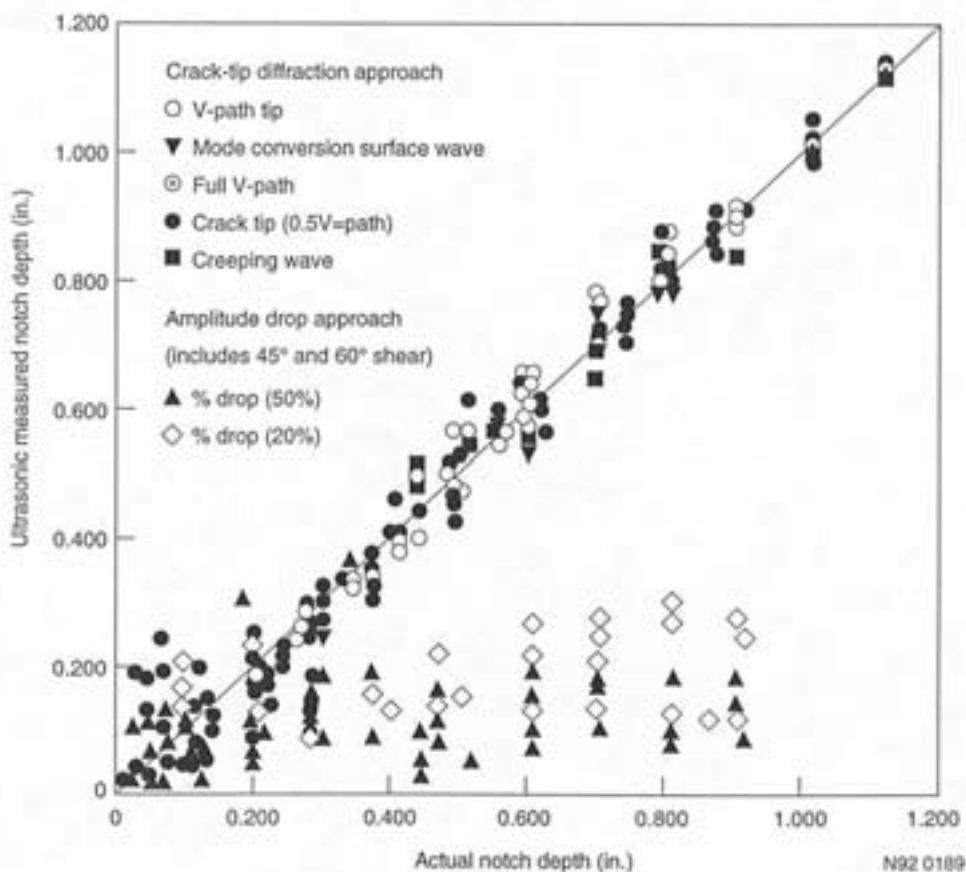


FIG. 6-6. Assessment of UT flaw-sizing techniques showing the poor performance of amplitude-based sizing techniques compared to crack-tip diffraction techniques [6.28].

Crack-tip diffraction techniques depend on a time measurement from the transducer to the signal that is emitted from the crack tip. When an ultrasonic wave impinges upon a crack, the sound energy is reflected in a specular fashion from the crack face (no surface roughness), texture reflections from the rough flaw surface, and diffracted at the end or tip of the crack as shown in Figure 6-7. This diffracted energy acts as a point source and radiates in all directions, thus, can be detected using a backscatter approach (i.e. transmitter and receiver are on the same side of the crack) or a forward scattering approach (transmitter and receiver are on opposite sides of the crack). Using the transducer angle and sonic velocity in the material (both known quantities), the distance to the crack tip and the crack depth are easily calculated. It is worth noting that there are numerous approaches that can be used for tip diffraction sizing of cracks. These techniques often are high resolution to maximize signal separation, and come in a variety of configurations to optimize the tip response for the applicable condition (i.e. depth in material, weld configuration). These include single element “backscatter” techniques such as “PATT” (Pulse Arrival Time Technique) and “SPOT” (Satellite Pulse Observation Technique) and dual element approaches using tandem arrangements and side by side arrangements. Double element techniques are often preferable because they can be modified to focus energy at various depths, and they tend to have better signal-to-noise ratio due to the separate transmitter and receiver. As will be discussed later, forward scattering techniques (i.e. “TOFD”) are also possible.

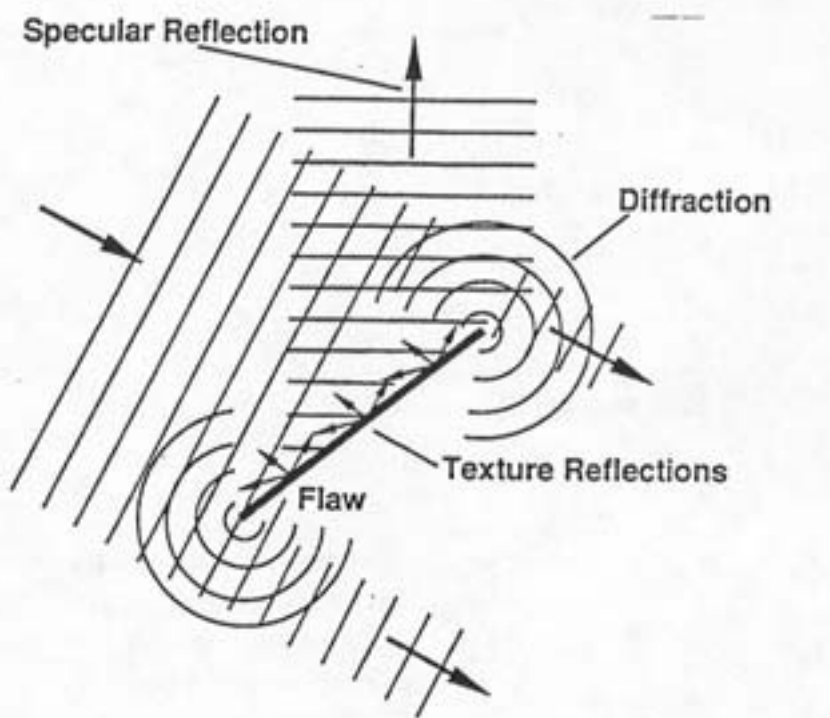


FIG. 6-7. Three major centers of ultrasonic radiation from a planar flaw.

Appendix VIII qualifications. Due to the inadequacies of Section XI examination procedures for detecting and sizing IGSCC, qualification of inspection personnel and procedures was mandated in Generic Letter 88-01 [6.29] to ensure effective examinations were performed. Similarly, publication of Mandatory Appendix VIII, Performance Demonstrations for Ultrasonic Examination Systems was intended to improve the effectiveness and reliability of UT in general. Appendix VIII, published in the 1989 Addenda of ASME Section XI [6.1], provides requirements for the performance demonstration of

ultrasonic examination personnel, procedures, and equipment used to detect and size flaws. The intent of Appendix VIII is to establish a minimum level of skill and effectiveness for ultrasonic inspection systems. It will be a requirement for the in-service inspection of piping welds, vessels, vessel nozzles, and bolts and studs. Although the implementation schedule is still uncertain, the US industry is in the process of preparing the necessary mockups for the performance demonstrations [6.30–6.31]). In order to minimize the number of samples needed and eliminate the need for site-specific qualifications, test blocks are being prepared to cover a range of pipe sizes and thicknesses rather than one block for each specific size. Appendix VIII does not dictate any specific ultrasonic testing methods. Rather, it is meant to encourage industry to develop and use reliable techniques and procedures.

Appendix VIII currently addresses piping welds, vessel welds, vessel base metal-to-clad interface, vessel nozzle welds and inside radius sections, and bolts and studs. As specified by the 1989 Addenda, performance demonstrations will be performed on mockups with weld preparation, geometry, and access conditions representing those encountered during in-service inspection. The blocks must also contain a certain number of realistic defects to confirm inspection technique reliability. For wrought austenitic piping welds, all flaws must be cracks with at least 75% of the defects be either thermal fatigue or IGSCC cracks. For ferritic piping welds, all flaws must be cracks with at least 75% of the defects be either mechanical or thermal fatigue cracks. Requirements for dissimilar metal welds and cast stainless steel are in the course of preparation [6.32] and will appear in a future edition or addenda of the ASME Code. Similar approach is presented in the French RSE-M code, with two types of performance demonstration and qualification: one generic (for all general application) and one specific (for focused application).

6.1.5. Emerging in-service inspection techniques

Ultrasonic inspection is capable of detecting many types, sizes and orientations of cracking. However, as mentioned previously, manual UT examinations have had two inherent disadvantages. The reliance on the inspectors ability and judgement, and the lack of a permanent record. This has resulted in inconsistent results, miscalls of both cracks and weld geometry, and a general lack of confidence in UT. Additionally, because of inconsistencies and miscalls, the inadequacy of Code prescribed techniques have also been recognized. Failure in Code procedures to detect and size certain types of degradation have emphasized the need to move beyond the minimum requirements of the Code to provide a more reliable examination, and have driven industry to develop more reliable inspection techniques.

Lessons learned from inspection of IGSCC in stainless steel piping have provided improvements in three areas that should be considered for all examinations of piping welds. With minor adjustments in frequency⁸ to optimize for the material differences, the same angles, modes and configurations should also be effective for thermal fatigue in carbon steel. The areas of improvement are:

- (1) improved search units that employ a variety of angles, modes and configurations,
- (2) proactive procedures that rely on several different ultrasonic techniques to verify and discriminate in-service degradation from weld geometry, and
- (3) the use of automated inspection equipment to improve reliability and repeatability, and to provide a permanent record of the examination results.

⁸ Typically, frequencies used to examine carbon steel (2–5 Mhz) are higher than those used to examine austenitic stainless steel materials (1–2.25 Mhz).

Improvements in search unit technology has moved far beyond the 45° shear wave approach prescribed by the Code. As discussed briefly in previous sections, manufacturers now build numerous types of search units incorporating different wave modes (shear, longitudinal and multimodes), angles, and configurations (single, dual element, tandem, phased arrays), all designed to enhance sensitivity to cracks. Supplementing Code techniques with these enhanced inspection techniques and using a proactive approach to examining components is far more effective than the Code prescribed techniques alone.

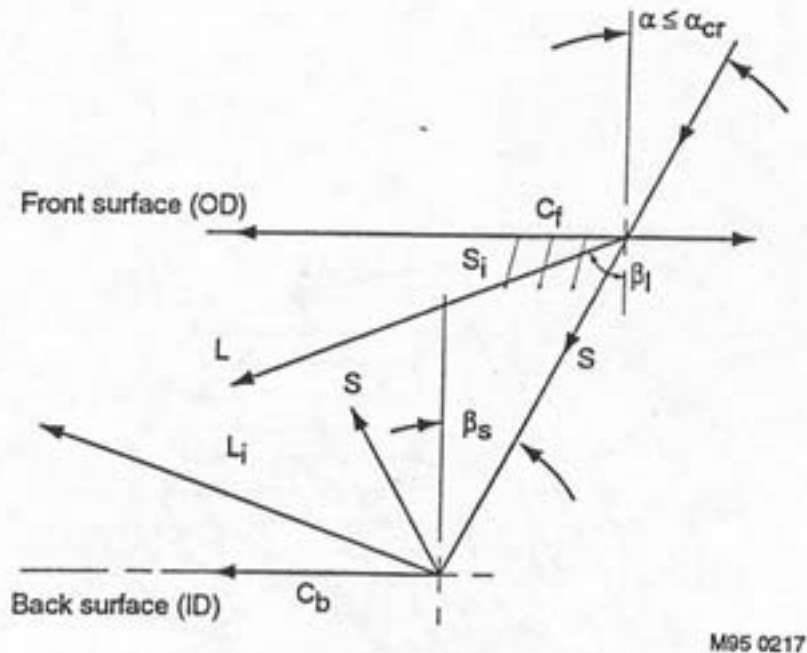
An inspection approach developed for IGSCC inspection that can be effective for the inspection of thermal fatigue is the use of “ID creeping waves” and related mode conversion techniques to detect and size cracks. This family of techniques has gained wide acceptance in the nuclear industry because of the high sensitivity to inside diameter (ID) connected flaws. Creeping waves are generated as a result of a high angle refracted longitudinal wave and corresponding shear wave (Figure 6-8). When the shear wave strikes the ID surface, mode conversion phenomena creates an indirect longitudinal wave (Li) and the ID creeping wave (Cb) which propagates along the ID surface of the pipe. Since a similar event is occurring at the outside diameter surface to induce a front surface creeping wave (Cf), this technique is capable of detecting cracking at the OD and ID simultaneously⁹. In addition to the creeping wave, the multiple modes and high angle longitudinal wave make it possible to size cracks with the same search unit [6.33–6.34]. These possibilities are shown in Figure 6-9. The disadvantages of this approach are the complexity of signal interpretation and potential interference from non-parallel ID and OD component surfaces that may cause redirection of the reflected and mode converted waves.

An enhanced technique with potential for detection and sizing of cracks in piping systems is the time-of-flight diffraction (TOFD) method [6.35], which has been used effectively to size cracks in control rod drive penetrations [6.36]. TOFD is a forward-scattering crack tip diffraction method that employs opposing elements as shown in Figure 6-10. As shown in 6-10(a), two signals are present in the absence of a crack, a direct lateral wave signal and a backwall reflection signal from the ID surface. Diffraction occurs when the incoming sound beam impinges upon a finite planar reflector such as a crack. The diffracted sound energy from the crack tip acts as a point source and radiates a sound wave to the receiving transducer. The time of arrival of this signal can then be used to pinpoint the tip of the crack and determine crack depth. Figure 6-10(b) illustrates such a diffracted signal produced by the tip of a crack; note the presence of a backwall reflection signal and the absence of a lateral wave signal. A through-wall signal would of course eliminate all signals as shown in Figure 6-10(c). This approach provides a means of both sizing and verifying the extent of the crack, but could be hindered by weld geometry on the OD and ID surface (i.e. weld crown or weld root) that could cause a loss of transducer contact and/or the loss of the backwall signal or the lateral wave signal for reasons other than the presence of a crack.

Another powerful ultrasonic inspection approach is the use of phased-array technology that has been employed successfully in a number of applications including boiling water reactor feedwater nozzles [6.37], and for detection of IGSCC [6.38]. As shown in Figure 6-11, a phased-array transducer consists of multiple elements that can be controlled

⁹ Under certain conditions, it is conceivable that this approach could eliminate the need for performing the surface examination on the OD surface. However, reliability would be inadequate in many cases depending on crack depth, orientation, and surface conditions. Therefore, this is not recommended.

individually to create a variety of beam patterns. Through the use of multiplexer circuits, the pulse sequence can be controlled to alter the inclination angle or focus the beam. The FATS or Focused Array Transducer System, is a phased array technique that allows the beam to be focused electronically to the area of interest and has been used to enhance examination of PWR feedwater pipe-to-nozzle welds [6.39]. This technique reduces beam spread and allows the beam to focus in on the crack opening to enhance detection, or focus in on the crack tip to improve sizing accuracy. A technique using a divergent transducer with computer focusing is the synthetic aperture focusing technique (SAFT) described in NUREG CR-6344.



- C_f Front surface creeping wave
- C_b Back surface creeping wave
- L Direct longitudinal wave
- L_i Indirect longitudinal wave
- S Shear wave
- S_i Indirect shear wave
- α Incident angle
- α_{cr} Critical incident angle
- β_l Refraction angle for longitudinal wave, L
- β_s Incident angle at back surface

FIG. 6-8. Scheme of ultrasonic fields of creeping wave probe in test specimen depicting front and back surface creeping waves. Direct and indirect shear waves [6.33].

The final improvement to consider is the use of automated inspection equipment to collect and store ultrasonic data. In the past, the primary constraint for automated ultrasonic inspection was collecting and manipulating large quantities of data. However, the continued evolution of computers has allowed for storage of gigabytes of data, and the speed to collect and manipulate the data.

Modern computers have also provided a more efficient means of processing data and integrating processing with specialized search units. A good example of this is the TestPro/FATS system [6.39]. FATS, combined with the TestPro ultrasonic acquisition system, results in a complete system for acquisition, analysis, and imaging of the ultrasonic data, and interfacing with scanning devices.

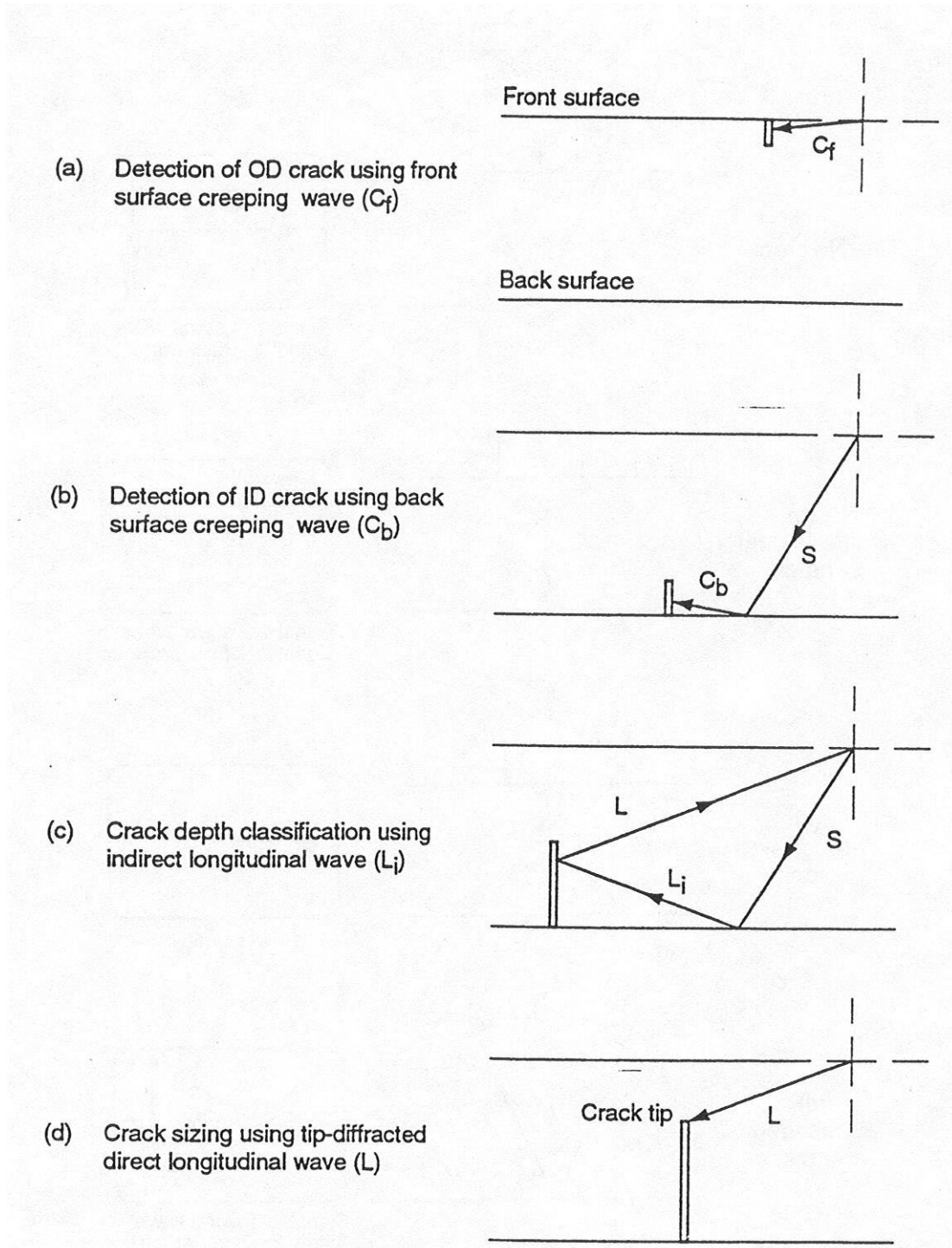


FIG. 6-9. Potential beam propagation paths for multimode approach using creeping wave probe [6.33].

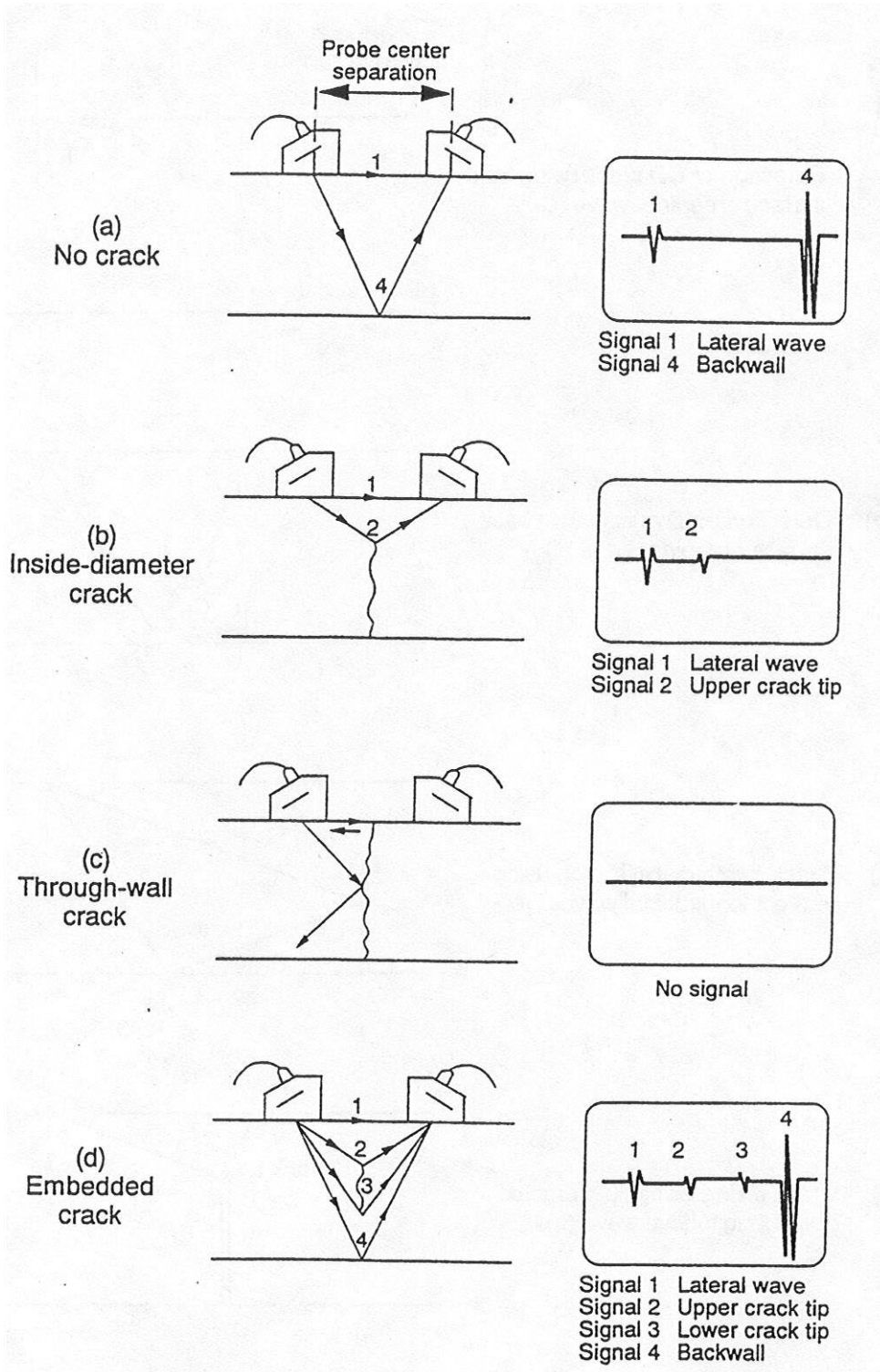


FIG. 6-10. Examples of time-of-flight (TOFD) diffraction signals [6.36].

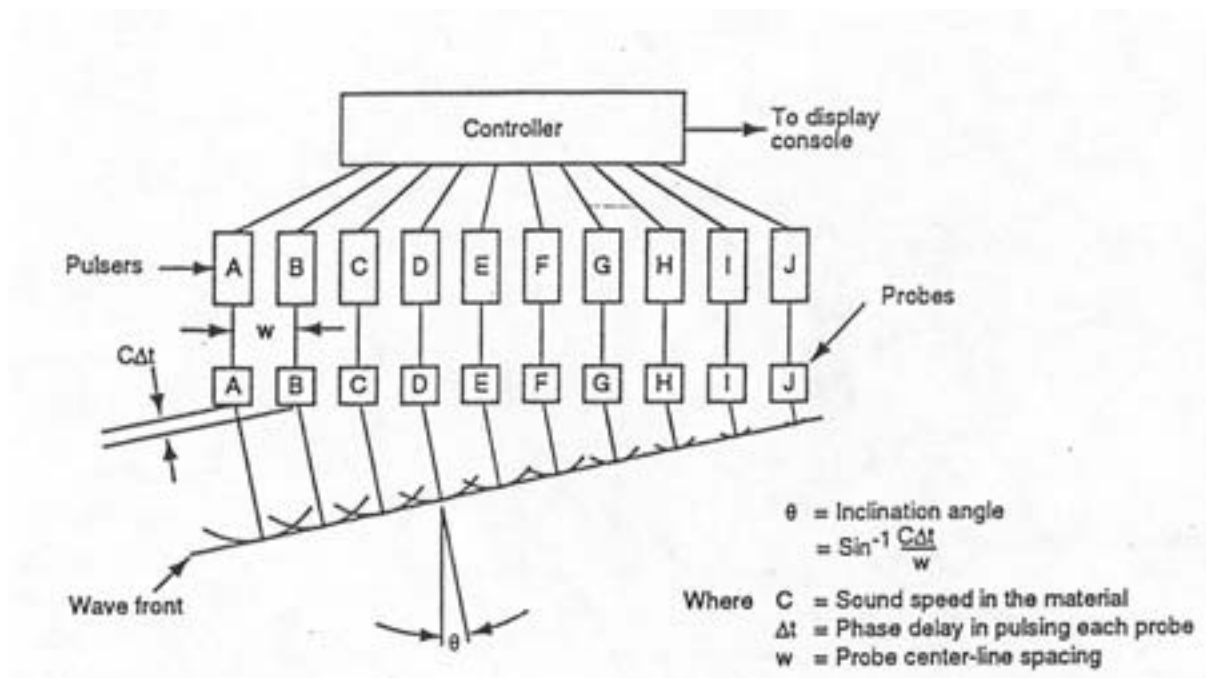


FIG. 6-11. Typical phased-array transducer.

The use of electromagnetic acoustic transducers (EMATs) can offer several advantage over conventional ultrasonic methods [6.40]. With EMATS, horizontally polarized shear waves (SH) can be generated, which have two advantages over longitudinal waves and vertically polarized shear waves (SV):

- (1) Shear waves offer better sensitivity to defects due to the corner effect¹⁰ [6.41],
- (2) SH are less influenced by weld and metallurgical features than SV waves, which tend to be easily redirected by grain structure [6.42].

In addition, EMATs techniques require no liquid couplants since the ultrasonic waves are induced in the metal electromagnetically. This approach is especially useful for dissimilar metal welds and austenitic stainless steel materials where attenuation and beam redirection are a problem and sensitivity to small flaws is critical.

Another possible crack detection method is acoustic emission. Acoustic emission methods can potentially provide global information regarding defects in the piping and may be capable of detecting the location and growth of small flaws that are not detectable by other non-destructive testing methods. Acoustic emission should be viewed as complementary to in-service inspection methods, not as their replacement.

Fatigue crack detection by acoustic emission depends on the ability of the instrumentation to detect the acoustic signals caused by crack growth under reactor operating conditions, specifically in the presence of reactor coolant flow noise. The acoustic signal produced by crack growth consists of discrete burst-type sounds with a duration ranging from a few microseconds to a few milliseconds. The source of the signal is determined from the time of signal arrival at several different sensors installed at various locations. However, some test results indicate that the acoustic signal produced during tensile crack growth in Type 304

¹⁰ Shear waves striking a right-angle corner reflector are totally reflected in the incident direction, whereas for longitudinal waves, significant energy is lost due to mode conversion to a shear wave, except where the incident wave is "flat" to one of the two surfaces.

stainless steel may not be detectable at certain stages of the crack growth [6.43]. On the other hand, the preliminary results from the in-service acoustic emission monitoring of a Peach Bottom Unit 3 recirculation-bypass line, core spray line, and feedwater nozzle indicate that pipe cracking can be detected using acoustic emission techniques [6.44]. Several significant steps have been taken to validate continuous, on-line acoustic emission monitoring in the field. Recent work on the application of the acoustic emission method at Watts Bar Unit 1 has shown that it can be effectively used for in-service monitoring of crack growth in thick wall, geometrically complicated components such as RPV nozzles [6.45]. Field application of continuous acoustic monitoring is also currently being evaluated by Pacific Northwest Laboratory at the Limerick Unit 1 reactor to monitor a flaw indication in an inlet nozzle safe end weld [6.46]. In addition, ASME Code Case N-471, which provides for continuous on-line acoustic monitoring for growth of known flaws, has been developed and approved by the NRC¹¹. The Code Case applies to components in which flaws exceeding the acceptance criteria (ASME Section XI, IWB-3410.1) have been identified, and for which the analytical evaluation of the flaws found the components acceptable for continued service according to ASME Section XI, IWB-3132.4.

Risk-Informed inspection. A proposed alternative to the selection criteria of ASME Section XI is the use of risk-informed selection rules. A draft Code Case for this alternative is currently being developed and supported by NRC research with support coming from the Westinghouse Owners Group¹². The intent of risk-informed inspection criteria is to allow ISI examinations to be focused on critical components. Components would be categorized as either risk-significant or non risk-significant, and would receive examinations commensurate with their risk-significance. The result would be an overall reduction in the quantity of examinations as illustrated in a pilot study performed at Surry, Unit 1 [6.47]. In the pilot study performed on the Surry reactor coolant system (RCS), 161 inspection locations were identified under the Section XI programmes. Under the risk-informed pilot study programme, this number would be reduced to 20 inspection locations, but with a corresponding increase in the inspection confidence¹³ from 81% to 88%.

The current concern with risk-informed inspection and the draft Code Case is how to implement it in a consistent manner across the industry. In its current state, the draft Code Case is limited to examination of Class 1, 2, and 3 piping. The implementation requirements are not specified, but are based on the risk-informed selection procedure that is developed by each utility. Currently, the owners groups (BWR, Westinghouse, CE and B&W) are performing preliminary analysis (e.g., pilot studies) separately, but in parallel in preparation for industry wide implementation of the draft Code Case¹⁴. Similar pilot studies are in progress in France, Sweden, Spain and Switzerland.

6.2. Monitoring of low-cycle fatigue

Fatigue monitoring is a process by which the temperature, pressure, and other parameters that contribute to fatigue are monitored so that the CUF at a location can be computed more accurately [6.48]. Since the plant process instruments are not located at the critical fatigue locations, and since these locations are almost always inaccessible for direct

¹¹ Approved in Regulatory Guide 1.147, In-service Inspection Code Case Acceptability, ASME Section XI, Division 1, Revision 9, April 1992.

¹² Personal communication with Steve Gosselin at the EPRI NDE Center, 8 November 1994.

¹³ For the purpose of risk-informed inspection, the confidence is defined by the percentage of locations that contribute to the core damage frequency that are addressed by the inspection programme.

¹⁴ Personal communication with K.W. Hall on 1 March 1995.

measurements, fatigue monitoring is generally accomplished through indirect measurements; which may limit its application to low-cycle thermal and mechanical fatigue from a practical standpoint. In some cases, data from laboratory tests or special in-field testing can be used to approximate the fatigue usage from high-cycle thermal fatigue. Fatigue monitoring does not include high-cycle vibration monitoring, for which the magnitude of vibration and source of the stressors are determined, but no fatigue usage is actually calculated.

Fatigue monitoring can contribute to ensure the safe operation of nuclear plants and assist in ageing management efforts. Fatigue monitoring at critical locations may be useful because:

- NPPs are getting older and important components are accumulating progressively more fatigue damage. Fatigue monitoring can provide more accurate measurements of the plant parameters than were assumed in the design analyses, and this in turn can result in more reliable prediction and mitigation of fatigue.
- Fatigue monitoring can identify and quantify the stressors that were not accounted for in the original design of LWRs, and can assist in determining if nonconservative assumptions were made in the design fatigue analysis.
- Fatigue monitoring can assist in identifying the locations that are most susceptible to significant fatigue damage by providing better quantification of the stressors.
- Since the use of fatigue monitoring data can result in more accurate quantification of fatigue usage, it (indirectly) assists in directing inspection efforts to those areas that have the highest CUFs.
- Fatigue monitoring can support efforts to identify actions to mitigate fatigue damage and to verify their success. For example, plant procedures (startup, shutdown, or operating) can be revised to reduce the severity of those loads that contribute most to the CUF, once the magnitude of those loads are identified by fatigue monitoring.
- Fatigue monitoring can be used to better quantify stressors and/or fatigue usage so that required inspections can be reduced or the required inspection interval lengthened, for example, BWR feedwater nozzles.
- Monitoring of the operating environment and the cyclic loading history could assist in evaluating the effects of environment (including temperature effects) and the loading sequence on fatigue damage.
- Fatigue monitoring along with reliable in-service inspection would provide more accurate crack growth rates.

Fatigue monitoring takes two forms:

- (1) In the Design Basis Approach, the historical operating data are reviewed, and, in some cases, the assumptions used in the design analyses are changed, and
- (2) On-line Fatigue Monitoring of plant parameters uses existing or, if needed, supplementary plant instrumentation.

To more accurately define the CUF at the critical locations, it is necessary to determine what the fatigue usage has been to date, and then to update it as new cycles occur. It would be highly desirable if there were a method to non-destructively test the material to determine the CUF. However, microcracking from fatigue cannot be measured using current conventional in-service inspection techniques. Therefore, indirect methods must be used, that is, estimating the CUF analytically. Either or both of the two methods listed above can be used to accomplish this estimation. Because the past operating logs are available and plant

operation may have changed over the years, the first consideration should be to consult and systematically catalog the categories, numbers, and severity of the transients from the records of past plant operation. The past usage can be estimated by reviewing the historical plant data, redefining the plant design analysis assumptions as necessary to conform to the actual parameters, reperforming stress analyses if necessary, and computing the CUF based on the actual number and severity of the cycles. The revised assumptions can be extrapolated to predict future usage. In the second method, the stresses induced by transients can be computed as they occur, by taking into account the plant process parameters measured during the various transients. It can be used to assess the past fatigue usage, assuming that the past transients have induced the same stresses as the present transients. However, this second method may not be nearly as acceptable as the first for estimating past usage, because plant operating procedures may have changed, and extrapolating backwards is not as likely to produce an accurate result without review of the plant records. Unfortunately, in a few cases the required information on past operation may not be available, and the past usage can only be estimated from current operation.

6.2.1. Design basis approach

This type of fatigue monitoring programme involves using the plant operating data and procedures to update the fatigue usage. The advantages of such programmes are:

- The transients can be classified according to actual number and severity, so that a more accurate CUF can be calculated. Design analysis assumptions can be modified, if necessary.
- The fatigue analysis can be revised to include changes to operating procedures and design.
- Fatigue damage caused by newly discovered transients can be estimated.
- In many cases the existing stress models can be used.

Programmes relying solely on historical operating data are still not entirely rigorous, because the plant parameters needed to determine the presence and severity of thermal stratification, turbulent mixing, and thermal striping may not be recorded. However, present knowledge of conditions (temperatures and flow rates) and plant operation that cause or accompany these transients can assist in identifying instances during which these transients might have occurred and in estimating their severity.

The success of this type of programme is dependent on the accessibility and accuracy of the plant's historical data. For example, the logs may in some cases not contain sufficient details, or the entries may not be clear enough to provide the desired accuracy to determine the temperature changes during the transient. Significant personnel time may be involved in reviewing logs and updating the CUF.

6.2.2. On-line fatigue monitoring

In an attempt to more precisely define the thermal stresses leading to fatigue usage and to provide an automated method to track the fatigue usage being accumulated at critical locations, several firms have developed online fatigue monitoring systems that directly query the plant process information system. For each critical location chosen to be monitored, the vendor has developed a model to compute the stress and fatigue usage. The fatigue usage algorithm (based on the ASME Section III method) is general, but the stress model is component-specific.

Once the fatigue monitoring system is in operation, calculation of fatigue usage is much less labor-intensive than the system of manually inputting the plant process data. However, the problem of determining the fatigue usage accumulated before the system was placed on-line is the same as for the fatigue monitoring process by log review.

In the design basis stress analyses, detailed thermal and stress models (in many cases finite element models) were often used to determine the temperature and stress distributions in the components being analyzed for fatigue. It is impractical to directly incorporate detailed thermal and stress models in an online fatigue monitoring system so that the entire analysis would have to be performed for each transient. To achieve the same results for each transient, analytical models have been developed that rely on the results of a few representative thermal and stress analyses that predict the fatigue usage for a given transient by using the results from the analysis that most closely matches the transient.

Vendors and several utilities such as EDF have developed algorithms to compute the stresses from the plant process parameters with minimal computational effort. For some effects, such as pressure or thermal expansion, the stresses can be computed directly using closed-form solutions; there are linear relations between pressure/temperature and stresses. However, for stresses caused by thermal gradients such as through the nozzle walls, the stresses are generally computed by the use of Green's (influence) functions. For high-frequency stressors such as thermal striping or turbulent mixing, a spectrum approach can be used.

There are various levels of sophistication that can be used in fatigue monitoring systems. In general, the more sophisticated the monitoring, the less conservative the assumptions can be, and thus a more accurate and generally a lower CUF can be determined. Simple fatigue monitoring by design-basis transients is effective if the conservative assumptions used result in an acceptable CUF. For online fatigue monitoring systems, the actual plant parameters can be used to more accurately determine the stress by reducing excessive conservatism. Two approaches have been taken:

- (1) to use the existing plant instrumentation that in most cases is located remotely from the critical locations to be monitored, and to use benchmarking and conservative assumptions to validate the results, or
- (2) to use additional instrumentation for local monitoring, which reduces the validation requirements.

The first approach has been used in the USA and France, while the second is used in Germany. It is important that those assumptions that do have to be made are conservative, especially for such phenomena as thermal striping and turbulent mixing. As the online systems are further developed, some of the conservative assumptions may be eliminated by more precise monitoring. What must be ensured, however, is that no nonconservative assumptions are included.

There are at least five active vendors of fatigue monitoring programmes in the USA: four are NSSS vendors and the fifth is a programme that was sponsored by the Electric Power Research Institute (EPRI). There are also several overseas vendors. The Japanese pressurized-water reactor group has developed an advanced transient and fatigue usage monitoring system which can cope with thermal stratification phenomena and inner surface heat transfer coefficient change on the critical locations during plant operations [6.49]. This system estimates the thermal transient changes making use of plant process data and calculates the stress vs. time history and fatigue usage factor on the critical locations. Summaries of these

fatigue monitoring programmes can be found in Ware [6.48]. Three of the five USA vendors as well as several overseas vendors include various amounts of online data from the plant process parameters in their fatigue monitoring systems, and they use computer algorithms to determine the fatigue usage accumulated during the transients. The fatigue usage calculated by the online monitoring system is combined with the fatigue usage accumulated before the online system was initiated, which is estimated using the design basis approach. Some reactor coolant system locations that are candidates for fatigue monitoring are shown in Figure 6-12.

EDF has developed an integrated fatigue monitoring system, SYSFAC [6.50] with 3 complementary modules:

- functional classification of the plant transient in the design list
- mechanical classification of the plant transient in the design list, through comparison of stress range
- direct and periodic evaluation of the usage factor, in some specific location (like charging line nozzle or surge line nozzles).

All the SYSFAC system use standard instrumentation and thermohydraulic transfer functions from instrumentation location to the fatigue sensitive locations.

During the validation process of this system, and from the beginning of the life of each plants, EDF operators perform manual transient bookkeeping and compare all these bookkept transient with initial design transient list (number of cycles and load amplitude). The initial transient list can be modified if some transient appears frequently on the site and are not considered at the design stage. In this case all the consequences on the design stress report has to be analysed in order to justify a maximum usage factor of 1 in all locations with the new transient list.

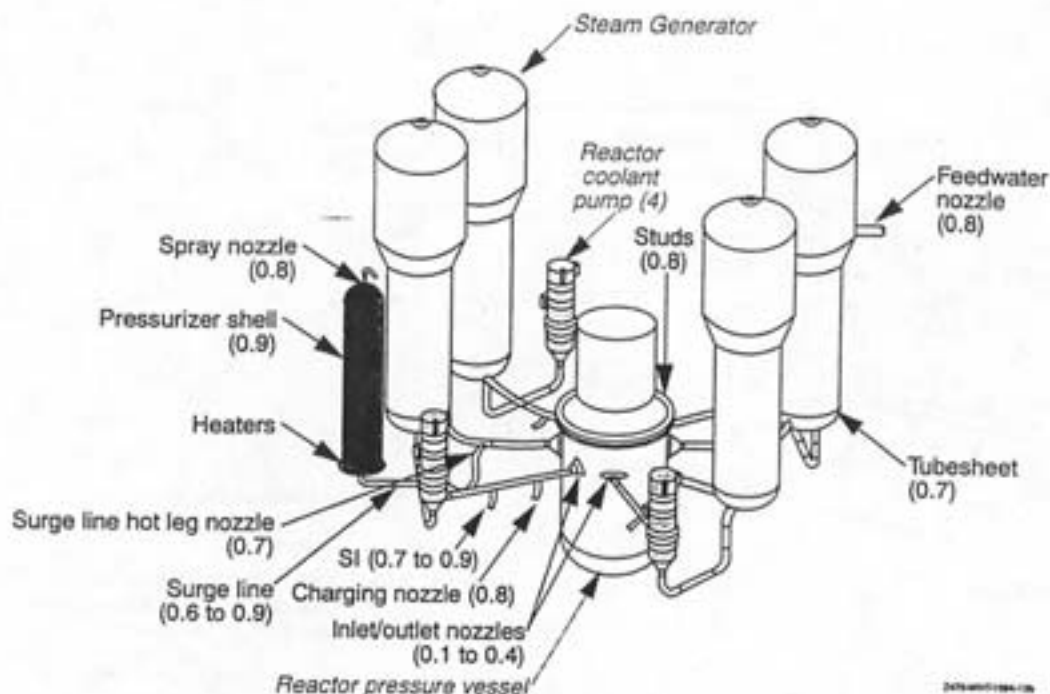


FIG. 6-12. Potential locations for fatigue monitoring in PWR plants. Cumulative usage factors are listed in parantheses.

6.3. Leak detection

The safety significance of PWR primary system leaks can vary widely, depending on the location of the leak, leakage rate, and its duration. The location of a leak may be such that the leak or leak repair action disables or degrades a safety system and contributes to an increased likelihood of core damage as a result of reduced accident mitigation capability. A leak may initiate a small-break LOCA if its rate is higher than the charging pump capacity. In the absence of a safety system response or appropriate operator actions, this leak would eventually lead to core damage. Sometimes the leak location is such that a manually isolable leak could not be isolated until the plant is placed in cold shutdown and airborne activity levels decreased sufficiently to allow containment entry. Such a leak took place at Oconee 3 and lasted for about 11 hours [6.51]. A high-rate, long-duration leak increases the likelihood that some other malfunction will occur and thus compound the recovery actions.

Leak detection systems are employed in the case of LBB behavior of primary pressure retaining components to ensure the detectability of leakage from a crack before it grows to critical crack size. Early leak detection and appropriate response will help to adhere to the design conditions for the power plant components and may play a potentially important role in accident prevention. Some welds are inaccessible for in-service inspection, and early leak detection and localization can timely identify the presence of a through-wall crack. Some base metal sites are susceptible to cracking but not inspected during in-service inspection; early leak detection and localization of a through-wall crack at these sites would allow for orderly shutdown of the reactor or other appropriate actions. Quick localization of leakage could reduce the radiation exposure to plant personnel inside containment. Thus, the use of a leak detection system would lead to detection of functional deterioration of component or system and is consistent with the defense-in-depth concept. In addition, use of leak detection systems with the capability to detect a leak of less than 38 L/min would be one of the factors that will allow application of LBB concept to smaller size piping. The other limiting factors, for example, include accuracy of stress analysis of some of these lines and uncertainty in the measurements. Sometimes, the leak detection systems have identified the presence of through-wall cracks that were not detected by the plant in-service inspection methods. Some through-wall fatigue cracks in PWR primary system branch lines, such as one in the Farley safety injection line, were found because of leakage, not in-service inspections. Similarly, many IGSCC cracks in boiling water reactor piping have been missed during ultrasonic in-service inspection and were detected only because of leakage [6.52]. The reason is that the fatigue and IGSCC cracks may close when the reactor is shut down, and their detection by in-service inspection becomes difficult. A sensitive leak detection system can detect a presence of a through-wall crack in the reactor pressure boundary when it is still small.

6.3.1. USNRC Regulatory Guide 1.45 recommendations

Regulatory Guide 1.45, Reactor Coolant Pressure Boundary Leakage Detection Systems, provides recommendations regarding acceptable leak detection methods, sensitivity of leak detectors, detector response time, and seismic qualification of instrumentation employed for leak detection. These recommendations are for detecting leakage inside the containment. The main recommendations are summarized as follows:

- Flow rates of identified leakage¹⁵ should be monitored separately from unidentified leakage¹⁶.
- Flow rates of unidentified leakage should be monitored with an accuracy of 3.8 L/min (1 gpm) or better.
- At least three separate leak detection methods should be employed to ensure effective monitoring during periods when some detection systems may be ineffective or inoperable. Two of these methods should be sump level and flow rate monitoring, and airborne particulate radioactivity monitoring. A third method may be either condensate flow rate monitoring or airborne gaseous radioactivity monitoring. (The Japanese PWRs are designed to have all four of the leak detection methods mentioned [6.53]). Use of humidity, temperature, or pressure monitoring of the containment atmosphere is also recommended as part of a leak detection system.
- Each of the three selected leakage detection systems should be able to detect an unidentified leakage with a leakage rate of 3.8 L/min (1 gpm) or smaller in less than one hour.
- The leakage detection systems should be capable of performing their function following seismic events that do not require plant shutdown.
- Indicators and alarms for each leakage detection system should be located in the main control room.

The recommendations are limited to reactor coolant leakage into the primary containment, not to the outside of the containment. The regulatory guide also recommends monitoring systems, such as monitoring of coolant radioactivity, to detect intersystem leakage, for example, steam generator tube leakage. Intersystem leakage poses an important safety issue but it is not within the scope of this project; therefore, it is not discussed hereafter.

Based on our investigation and the information presented in USNRC [6.54], it appears that most PWRs in the USA employ at least two of the leak detection systems recommended by Regulatory Guide 1.45, but these systems cannot detect a 3.8 L/min leak under all conditions. Several utilities, for example, Duke Power, are not committed to the Regulatory Guide. But some other utilities are committed to the Guide because their LBB applications for primary coolant loop, which were based on USNRC approved topical reports submitted by owners group, were approved by USNRC under the condition that their plant-specific leak detection systems satisfy Regulatory Guide 1.45 [6.55].

6.3.2. Effectiveness of current leakage detection systems

When a leak of primary system coolant occurs, a portion of the leakage evaporates and the resulting vapor is transported to the containment vessel atmosphere and mixed by the containment vessel air circulation system, and the remaining portion of the leakage (which is in the liquid phase) is routed to the containment sump. Then, the leak detection systems typically installed in both the containment atmosphere and the sump could detect the leakage. Some of the leak detection systems, such as containment sump level and flow monitor and condensate flow rate monitor, monitor both primary and secondary leakage, so the samples have to be analyzed to evaluate the respective part of each type of leakage. Therefore, more

¹⁵ Identified leakage shall be (a) leakage into collection systems, such as pump seal or valve packing leaks, that is captured and conducted to a collection tank, or (b) leakage into the containment atmosphere from sources that are both specifically located and known not to interfere with the operation of the leakage detection systems or not to be pressure boundary leakage.

¹⁶ Unidentified leakage is all leakage that is not identified leakage.

than one leak detection system is used to accurately and reliably estimate the total leakage rate. We evaluate the effectiveness of these leakage detection systems in this section.

In 1984, the USNRC PWR Pipe Crack Task Group evaluated the capabilities of different available leak detection systems and concluded that none of the systems would be acceptable for complete characterization of a leak, detecting and locating a leak, and accurately estimating its rate, as shown in Table XXV. Of 11 systems presented in the table, three are capable of quantitative leak determination: sump monitoring, condensate flow rate monitor, and primary coolant inventory. However, the third system is only accurate if used to determine the leak rate for a 6- to 24-hour period. This system would be unacceptable for measuring 1 gpm within 1 hour. The best systems for leak detection and location are tape moisture sensor and acoustic monitoring, but these systems have poor capability for measuring the leak rate [6.54].

TABLE XXV. CAPABILITIES OF LEAKAGE MONITORING METHODS USED INSIDE CONTAINMENTS ([6.54] MODIFIED)

Method	Leak Detection Sensitivity	Leak Measurement Accuracy	Leak Location
Sump Level Monitor	G ^a	G	P ^c
Containment Air Cooler condensate Flow Rate Monitor	G	F ^b	P
Airborne Gaseous Radioactivity Monitor	F	F	F
Airborne Particulate Radioactivity Monitor	F	F	F
Primary Reactor Coolant Inventory ^d	G	G	P
Humidity Dew Point Monitor	F	P	P
Tape Moisture Sensor	G	P	G
Temperature Sensor	F	P	F
Pressure Sensor	F	P	P
Visual Inspection ^e	F	P	G

^a G (Good) - can generally be applied to meet intent of this standard if properly designed and utilized.

^b F (Fair) - may be acceptable, marginal, or unable to meet intent of this standard depending upon application conditions and the number of measurement points or locations.

^c P (Poor) - not normally recommended but might be used to monitor specific confined locations.

Siemens has developed an integral leakage monitoring systems that has been implemented on several German reactors [6.56]. The leakage is based on detectable changes in the associated measured variables (for example, an increase in moisture can be determined based on the increase in the dew point temperature by 10 degrees above the normal dew point

temperature or an increase in the condensate flow rate of the recirculation air cooler). The specified detector sensitivity is below 0.1 kg/s (100 cm³/s). Siemens considers that monitoring the room moisture is one of the most sensitive leak-detection methods. Monitoring the recirculation air coolers directly evaluates the leakage rate. The dew point temperature is measured separately for each loop at three positions: the shield cooling bypass, the steam generator, and the main coolant pump.

A recent study of the reportable leak events during the period 1985 to 1996 indicates that the leak detection systems are used to detect leaks and determine their rate but not to locate them; determination of location is accomplished by visual examination [6.57]. The main finding of the study is that some of the current leakage detection systems are effective in detecting 3.8 L/min (1 gpm) leakage inside the containment within an hour, but are not fully effective in detecting leakage that is ten times smaller. These smaller leakages were detected by visual inspection. Other findings follow:

- A sump level and flow rate monitor can detect a 3.8 L/min (1 gpm) leak in less than 1 hour. The cross section of the sump determines the sensitivity of this leak detection system. At some plants, for example, this system could detect a 3.8 L/min leak in less than 10 minutes. The detection time for a smaller leak will increase inversely as the leak rate decreases. Several variables, including location of leak source from sump and time it takes for leakage to leak out from the insulation, may increase the detection time.
- An airborne particulate radioactivity monitor can detect a 3.8 L/min (1 gpm) leak within one hour under certain conditions related to percentage of fuel failure and corrosion product concentration. Under certain conditions, the monitor can detect a much smaller leak of 0.38 L/min in less than 10 minutes. The study has, however, identified several 0.38 L/min leakages that were not detected by the plant leak detection systems which most likely include airborne particulate radioactivity monitors.
- An airborne gaseous radioactivity monitor cannot detect a 3.8 L/min leak in less than 1 hour because of the improved fuel performance.
- A method based on weight balance of primary reactor coolant inventory cannot detect a 3.8 L/min leak within an hour.
- A method based on monitoring volume control tank (VCT) level may be used to detect a leak during steady state operation. The response time of this method to detect a leak of 3.8 L/min (1 gpm) depends on the volume between two adjacent graduations on the makeup tank. At one plant, this method can detect a 3.8 L/min leakage within about one-half hour.
- Leakage detection systems are currently not used to detect primary system leakage outside the containment. Visual inspection is generally relied upon for detecting this leakage.
- Current leakage detection systems are not designed for locating a leak source inside the containment. Generally, containment entry and visual inspection are required. During some leak events, it takes considerable time to determine the location of the leak source while the plant is operating; therefore, a leak source, possibly located in the pressure boundary, may remain unidentified for that period of time.

6.3.3. Capabilities of advanced leakage detection systems

The advanced leakage detection systems are focusing on two aspects of leakage detection: early detection of leakage of <3.8 L/min (<1 gpm) and locating the leak while the plant is operating. Early detection of leakage from the reactor coolant pressure boundary is vital for reliable plant operation and accident prevention. Reliable detection of a leak smaller than 3.8 L/min in less than a hour may allow application of the LBB concept to small diameter piping, i.e. <102 mm (4 in.).

Use of a detection system to locate a leak while the plant is operating would help avoid containment entry by plant personnel to determine the leak location, which is a slow process, and it would facilitate earlier identification of whether the leak is a pressure boundary leak.

The capabilities of three advanced leakage detection systems are summarized here: nitrogen-13 (N-13) monitor, local humidity monitor, and acoustic emission monitor. The sensors for these devices may be installed near welds and base metal sites that have unrepaired weld indications, and locations on the pressure boundary that are susceptible to cracking, as indicated by field experience. The N-13 monitor can detect a leak rate as low as 0.2 L/h (~0.001 gpm), and can detect a leak of 1 L/h (0.005 gpm) in 1 hour. The N-13 monitors have been installed at several French PWRs to detect leakage from reactor pressure vessel head penetration.

Local humidity monitors are installed directly along the outside surface of the piping under the insulation. They can detect leakage by measuring a local increase in the humidity and determine the leak location. A detection system was tested at a WWER-440 plant in the Slovak Republic, which shows that the system can detect leakage smaller than 4L/min, and determine the leak location within $\pm 1\%$ of the sensor tube length. The local humidity monitoring system is qualified for a German PWR to detect a small potential leak from the reactor pressure vessel closure head. The test results showed that this system can reliably detect a leak rate 2.5L/min with a response time of as little as 15 minutes.

Acoustic emission monitoring with externally fitted probes can be used to detect high-frequency structure-borne noise emitted by escaping high-energy fluid. As in acoustic emission for crack growth, the principal involves arranging several detectors at strategic locations, and based on the time of arrival of signals to the separate detectors, the leakage location is determined. Siemens has developed such a system which can localize the leak within 1 to 3 m, and detect leaks of 0.025 to 0.065 kg/s (25 to 65 cm³/s) [6.56]. The acoustic leak monitoring system is based on the principle that discharging fluid induces high-frequency structure-born noise of a continuous signal characteristic in a component. This noise is detected by externally fitted probes.

Acoustic emission monitoring systems have been installed at US NPPs to monitor valve stem leakage. The monitors can detect a leak rate as low as 0.5 gpm. Acoustic emission monitors are also installed on a 711-mm (28-in.) recirculation line elbow at a BWR in the USA.

6.4. Loose parts monitoring

The Loose Parts Monitoring (LPM) system is an in-service monitoring programme to detect and monitor loose parts in light-water reactor (LWR) power plants. One of the objectives of the LPM programme is to provide timely indication of component degradation. This in-service LPM programme is based on the recommendations from the American Society of Mechanical Engineers operation and maintenance standards and guides (ASME OM-S/G)-1997, Part 12, “Loose Part Monitoring in Light-Water Reactor Power Plants.” The loose parts monitoring system includes measures to monitor and detect metallic loose parts by using transient signal analysis on acoustic data generated due to loose parts impact. The detection and monitoring system includes a set of accelerometers installed in the vicinity of regions where loose parts impact is likely to occur. The system incorporates the capability of automatic annunciation (audible and visual), audio monitoring, automatic and manual signal recording, and acoustic signal analysis/evaluation [6.5].

6.5. Water chemistry monitoring

Monitoring of primary water chemistry is necessary because it affects different ageing mechanisms such as general corrosion, PWSCC, and possibly, environmental fatigue. Typically, in the USA, the EPRI guidelines (EPRI TR-105714) are used for PWR primary water chemistry. The programme includes periodic monitoring and control of known detrimental contaminants such as chlorides, fluorides, dissolved oxygen, and sulfate concentrations below the levels known to result in loss of material or crack initiation and growth. Water quality (pH and conductivity) is also maintained in accordance with the guidance [6.5]. In Germany, the chemistry handbook of PWRs requires:

- to control the content of lithium, hydrogen, oxygen, chlorides, and boron 3 times per week;
- to control the conductivity and pH value once a week by taking specimens from one loop;
- to measure periodically the boron content by an automatic device.

REFERENCES TO SECTION 6

- [6.1] ASME 1989, ASME Boiler and Pressure Vessel Code, Section XI, Rules for In-service Inspection, American Society of Mechanical Engineers, New York.
- [6.2] ASME 1992, Interpretation #XI-1-92-56 Issued October 4, 1993, American Society of Mechanical Engineers, New York.
- [6.3] ASME 1974 Edition/Summer 1974 Addenda, ASME Boiler and Pressure Vessel Code, Section XI, Rules for In-service Inspection, American Society of Mechanical Engineers, New York.
- [6.4] MATTHEWS, M.T., et al., Final Submittal in Response to Nuclear Regulatory Commission Bulletin 88-11, Pressurizer Surge Line Thermal Stratification, BAW-2127, Babcock & Wilcox, Lynchburg (1990).
- [6.5] United States Nuclear Regulatory Commission, Generic Ageing Lessons Learned, NUREG-1801, Office of the Nuclear Reactor Regulation, USNRC, WA (2001).
- [6.6] DOZIER, J., WICHMAN, K., KUO, P.T., Potential Enhancements for Codes and Standards to Support License Renewal, Proc. 2001 ASME Pressure Vessel and Piping Conference in Atlanta, GA, ASME, New York (2001).

- [6.7] RSE-M Code, “Surveillance and in-service inspection rules for mechanical components of PWR nuclear islands”, AFCEN Paris, 1997 edition + addenda 1998 and 2000.
- [6.8] CODRON, P., LAURIOT, B., DUBREUIL-CHAMBARDEL, A., “EDF’s «OMF-Structures» RI-ISI Process: Overview of the Methodology, Applications and Comparison with the Other Existing RI-ISI Initiatives”, ICONE-9, International Conference on Nuclear Engineering, paper 9829, Nice, France, April 2001.
- [6.9] Rules 1973, Rules for Design and Safe Operation of Components in NPPs, Test and Research Reactors and Stations, Metallurgia, Moscow, Russian Federation (1973).
- [6.10] Rules 1990, Rules for Design and Safe Operation of Components and Piping of NPP, PNAE G-7-008-89, Energoatomizdat, Moscow, Russian Federation (1990).
- [6.11] HARKER, A.H., et al., Modeling Ultrasonic Inspection of Austenitic Welds, Journal of Nondestructive Evaluation, **9** 213 (1990) 155–165.
- [6.12] JEONG, P., AMMIRATO, F., Ultrasonic Material Characterization of Cast Stainless Steel, Nondestructive Evaluation: NDE Planning and Application, R.d. Streit (ed.), 1989 ASME Pressure Vessels and Piping Conference, Honolulu, Hawaii, 23–27 July 1989, NDE-Vol. No. 5, American Society of Mechanical Engineers, New York (1989).
- [6.13] TAYLOR, T.T., An Evaluation of Manual Ultrasonic Inspection of Cast Stainless Steel Piping, NUREG/CR-3753 (1984).
- [6.14] JEONG, P., AMMIRATO, F., Ultrasonic Examination of Cast Stainless Steel, EPRI NP-6299, Electric Power Research Institute, Palo Alto, CA (1989).
- [6.15] EDELMANN, X., HORNING, R., Investigation of an Ultrasonic Techniques for Detection of Surface Flaws During In-service Inspection of Dissimilar Metal Welds, Proceedings of the Fifth International Conference of Nondestructive Evaluation in the Nuclear Industry, CA, May 1982. (1983).
- [6.16] USNRC, Safety Injection Piping Failure, USNRC Information Notice 88-01 (1988).
- [6.17] USNRC, Pressurizer Surge Line Thermal Stratification, USNRC Bulletin 88-11 (1988).
- [6.18] USNRC, Pressurizer Surge Line Thermal Stratification, USNRC Bulletin 88-11 (1988).
- [6.19] STRAUCH, P.L., et al., “Stratification Issues and Experience in Operating Power Plants”, High Pressure Technology, Fracture Mechanics, and Service Experience in Operating Power Plants, ASME Pressure Vessels and Piping Conference, Nashville, TN, PVP Vol. 192 (1990) 85–92.
- [6.20] MERLE, P., Thermal Fatigue in French Primary Circuits: the Safety Authority Point of View, presented at the NEA/CSNI Specialists’ Meeting on Experience with Thermal Fatigue in LWR Piping Caused by Mixing and Stratification, OECD Nuclear Energy Agency, 7–12 June 1998, Paris, France.
- [6.21] SHAH, V.N., WARE, A.G., In-service Inspection of Base-Metal Sites Susceptible to Thermal Fatigue Damage, Changing Priorities of Codes and Standards: Failure, Fatigue, and Creep, ASME PVP Vol. **286** 18 (1994) 9.
- [6.22] GAUTHIER, V., Thermal Fatigue Cracking of Society Injection System Pipes Non Destructive Testing Inspections Feedback, presented at the NEA/CSNI Specialists’ Meeting on Experience with Thermal Fatigue in LWR Pipig Caused by Mixing and Stratification, OECD Nuclear Energy Agency, 7–12 June 1998, Paris, France.
- [6.23] USNRC, Ultrasonic Inspection Techniques for Dissimilar Metal Welds, UNSRC Information Notice 90-30 (1990).
- [6.24] DOMBRET, P., Main Results of PISC III Action 3: Nozzles and Dissimilar Welds, Determining Material Characterization: Residual Stress and Integrity with NDE, 1994,

- Pressure Vessels and Piping Conference, PVP Vol. 276, NDE Vol. 12 (1994).
- [6.25] CZAJKOWSKI, C.J., Survey of Boric Acid Corrosion of Carbon Steel Components in NPPs, NUREG/CR-5576, USNRC (1990).
 - [6.26] TVA 1995, Letter W.C. Ludwig (TVA) to V.N. Shah (INEL), WA 16 February 1995.
 - [6.27] BUSH, S.H., Impact of PISC II on ASME XI, Rules for In-Service Inspection of NPP Components, Ultrasonic Inspection of Heavy Section Steel Components: The PISC II Final Results, R.W. Nichols and S. Crutzen (eds.), Elsevier Applied Science, London, (1988) 617.
 - [6.28] COWFER, C.D., Basis/Background for ASME Code Section XI Proposed Appendix VIII: Ultrasonic Examination Performance Demonstration, Nondestructive Evaluation NDE Planning and Application, R.D. Streit (ed.), presented at the 1989 ASME Pressure Vessels and Piping Conference, Honolulu, Hawaii, NDE – Vol. 5, American Society of Mechanical Engineers, New York, 23–27 July (1989).
 - [6.29] USNRC 1988, Generic Letter 88-01, NRC Position on IGSCC in BWR Austenitic Stainless Steel Piping, 25 January 1988.
 - [6.30] AMMIRATO, F., et al., Performance Demonstrations for In-service Inspection of NPP Components, Eleventh International Conference on NDE in the Nuclear and Pressure Vessel Industries, April 1992, Albuquerque, NM (1992).
 - [6.31] BECKER, F.L., et al., Performance Demonstration Test Blocks to Meet the Requirements of the ASME Code, Eleventh International Conference on NDE in the Nuclear and Pressure Vessel Industries, April 1992, Albuquerque, NM (1992).
 - [6.32] ASME Code, Section XI, Addenda 1994 of 1992 edition, ASME, New York.
 - [6.33] BROOK, M.V., Ultrasonic Transducers Design for Detection and Characterization of Cracks in Nuclear Primary Pressure Piping, 8th International Conference on NDE in the Nuclear Industry, Kissimmee, Florida, November 1986.
 - [6.34] DAVIS, M.J., ID Creeping Wave Techniques for Detection Characterization, and Sizing of Planar Flaws, NDE: Applications, Advanced Methods, and Codes and Standards, Pressure Vessels and Piping Conference, San Diego, CA, PVP Vol. 216, NDE Vol. 9 (1991).
 - [6.35] PERS-ANDERSON, E., An Alternative Approach to ISI Using ZIPSCAN/TOFD, BWR Reactor Pressure Vessel & Internals — Inspection & Repair Workshop, Charlotte, NC, 16–18 July 1991.
 - [6.36] PERS-ANDERSON, E., PWR Vessel Head Penetration Inspections, Assuring Structural Integrity of Steel Reactor Pressure Boundary Components, 12th SMIRT-Post Conference Seminar No. 2, Paris, France, 23–25 August 1993.
 - [6.37] GRIGSBY, J.C., et al., Phased-Array Techniques and Manipulators: An Advanced Modular Approach for Inspection of Boiling Water Reactor Pressure Vessels, Materials Evaluation, May 1992.
 - [6.38] WÜSTENBERG, H., et al., Improvement of Detection of Stress Corrosion Cracks with Ultrasonic Phased Array Probes.
 - [6.39] BISBEE, L.H., Enhanced Ultrasonic Examination of Feedwater Pipe-to-Nozzle Welds, Nuclear Plant Journal, March–April (1994) 42–53.
 - [6.40] VON BERNUS, L., et al., Current in-service inspections of austenitic stainless steel and dissimilar metal welds in light water power plants, Nuclear Engineering and Design, No. 151 (1993) 539–550.
 - [6.41] KRAUTKRÄMER, J., KRAUTKRÄMER, H., Ultrasonic Testing of Materials, Springer-Verlag, Berlin Heidelberg New York (1983).
 - [6.42] OGILVY, J.A., The influence of austenitic weld geometry and manufacture on ultrasonic inspection of welded joints, British Journal of NDT, 29 (1987).

- [6.43] USNRC 1980, Investigation and Evaluation of Cracking Incidents in Piping in Pressurized Water Reactors, NUREG/CR-0691, F-9-F-11.
- [6.44] HARTMAN, W.F., MCELROY, J.W., Acoustic Emission Surveillance of Boiling Water Reactor Piping, Nozzles, and Valves, STP 679, American Society for Testing and Materials, Philadelphia (1979) 205–218.
- [6.45] HUTTON, P.H., et al., Acoustic Emission System Calibration at Watts Bar Unit 1 Nuclear Reactor, NUREG/CR-5144, PNL-6549 (1988).
- [6.46] DOCTOR, S.R., et al., Advanced NDE Technologies and Characterization of RPV Flaw Distribution, Proceedings of the Eighteenth Water Reactor Safety Information Meeting, Rockville, MD, 22–24 October 1990, NUREG/CP-0114, Vol. 3 (1991) 137–156.
- [6.47] EPRI, 1995, Risk-Based Inspection Workshop, Charlotte, NC 20–22 February.
- [6.48] WARE, A.G., Fatigue Monitoring for Ageing Assessment of Major LWR Components, NUREG/CT-5824, EGG-2668, Draft (1994).
- [6.49] SAKAI, K., et al., On-Line Fatigue-Monitoring System for NPP, Nuclear Engineering and Design, 153, Elsevier (1994) 19–25.
- [6.50] SAVOLDELLI, D., FAIDY, C., “Transient Monitoring Experience in French PWR Units”, ASME Pressure Vessel and Piping Conference, Vol. 332, Montreal, July 1996.
- [6.51] USNRC 1992c, Failure of Primary System Compression Fitting, Information Notice 92–15, 24 February (1992).
- [6.52] KUPPERMANN, D.S., et al., Leak Detection Technology for Reactor Primary Systems, Nuclear Safety, Vol. 28, April–June (1987) 191.
- [6.53] AOKI, K., Reactor Coolant Pressure Boundary Leak Detection Systems in Japanese PWR Plants, Nuclear Engineering and Design, 128 (1991) 35–42.
- [6.54] USNRC 1984a, Investigation and Evaluation of Stress Corrosion Cracking in Piping of Boiling Water Reactor Plants, Report of the U.S. Nuclear Regulatory Commission Piping Review Committee, Volume 1, NUREG-1061.
- [6.55] WICHMAN, K., et al., LBB Application in the US Operating and Advanced Reactors, NUREG/CP-0155, Proceedings of the Seminar on Leak Before Break in Reactor Piping and Vessels, Lyon, France, 9–11 October 1997, 1–7.
- [6.56] BARTHOLOMÉ, G., KASTNER, W., KEIM, E., Design and Calibration of Leak Detection Systems by Thermal Hydraulics and Fracture Mechanics Analyses, Nuclear Engineering and Design, 142 (1993) 1–13.
- [6.57] SHAH, V.N., et al., Assessment of Pressurized Water Reactor Primary System Leaks, NUREG/CR-6582, INEEL/EXT-97-01068 (1999).

7. AGEING MITIGATION METHODS

Section 4 of this report describes the ageing mechanisms that could impair the integrity of PWR primary piping during its service life. For three of these mechanisms (thermal fatigue, vibratory fatigue, and PWSCC) mitigation methods are available to prevent or reduce the rate of ageing degradation (*managing ageing mechanisms*). Piping repair or replacement is an option to correct unacceptable degradation caused by any ageing mechanism (*managing ageing effects*).

Managing ageing mechanisms

7.1. Mitigation of thermal fatigue

There are three basic ways to mitigate/slow down the rate of fatigue of primary piping: (1) by operational changes that will reduce temperature differences causing thermal fatigue, (2) by maintenance to minimize valve leakage causing thermal stratification, and (3) by design changes to reduce fatigue usage.

7.1.1. Operational changes

To reduce thermal stratification in *surge lines* and thus the rate of thermal fatigue, changes in operating procedures can be implemented, such as limiting the differences in pressurizer and reactor coolant system temperatures to no more than 93°C (200°F) during heatups and cooldowns. An important controlling parameter in limiting this temperature difference is the method used to form the bubble in the pressurizer [7.1]. The two methods of heatup and cooldown in a PWR are the steam-bubble and water-solid modes. The steam-bubble mode creates large temperature differences between the pressurizer and reactor coolant system (approximately 167°C (300°F)), while the water-solid mode generally results in temperature differences of only about 111°C (200°F). All Japanese PWR plants have adopted the water-solid mode and this has contributed to the fact that neither leakage or fatigue crack has been found in surge lines in Japanese PWR plants. The disadvantage of the water-solid mode is that without the cushioning effect of the steam bubble, pressure control is difficult. Westinghouse also has evaluated the use of a nitrogen bubble in the pressurizer during startups and shutdowns to both minimize the temperature difference and provide a more stable pressure control than is possible with the water-solid mode; however, its implementation is expensive.

To mitigate *pressurizer spray line* fatigue damage caused by stratified flow and thermal shock, plant operating procedures can specify minimum flow through the spray line and continuous spray during plant cooldowns. A typical minimum flow in the pressurizer spray line of approx. 60 mL/s has been specified, in order to have a good thermal conditioning of the pressurizer spray nozzle and absence of steam in the spray line. This is accomplished by providing a bypass line around the main spray nozzle. The continuous spray flow keeps the spray line warm during plant operation. With no flow, the line could cool down by losing heat to the surroundings and then, when spray flow is initiated, there would be a thermal shock. In other locations where thermal stratification could occur, such as in makeup lines, increased minimum flow rates have been specified to eliminate the stratification.

Low-cycle transients due to heat-up/cooldown operation are sometimes responsible for excessive fatigue usage. Modification of operating procedures in order to reduce heat-up/cooldown and flow transients are suitable corrective actions, due to the fact that a large part of CUF is due to thermal loads during these operations.

In Westinghouse plants, a quarterly check of the charging line valves are performed, where the system is isolated. During this test, the temperature at the charging nozzle undergoes a thermal shock of 250°C (450°F). If the tests are performed so that the normal charging nozzle is used for one half of the tests, and the alternate *charging nozzle* is used for other half of the tests, then the fatigue usage is spread between the two nozzles.

7.1.2. Maintenance to reduce valve leakage

Low leak-through rates in closed valves (<60 mL/s), can cause stratified flow conditions in piping with virtually no flow and hot water layers over the cold. The valve leak-through represents a quasi-equilibrium where the hot-cold interface leads to cracking. Effective options to restrict the valve leakage are replacing of valve packing or increasing valve seat gap to eliminate cyclic opening/closing. If leakage cannot be avoided, installing of monitoring equipment and/or a redesign of the thermal sleeve should be considered to minimize contact with the pipe wall.

7.1.3. Design changes

Nuclear plant designers were aware of conditions that would result in high CUFs and took steps to reduce the fatigue usage, including analyses that identified critical locations, and operating procedures designed to limit high thermal gradients. Examples of features incorporated into designs for mitigating fatigue are thermal sleeves and the use of rounded fillets to reduce stress concentrations. However, experience has shown instances in which original design had to be modified. Introducing a definite slope and limiting stagnant horizontal lines are highly recommended for mitigation of thermal mixing concerns.

Design modifications that have been implemented to suppress thermal stratification in spray and surge lines include one made by Combustion Engineering at several plants which uses a *sloped section of the pressurizer spray line* in place of the horizontal portion: in one plant, a *10-ft piping section was inclined 45 degrees* to mitigate the thermal loads caused by stratified flows [7.2].

Incorporation of properly sized *bypass valves* which provide full flow through the spray lines during normal operations is another means for suppressing thermal stratification and decreasing fatigue usage.

The *gaps between the surge line and the pipe whip restraints* have been increased in some plants to eliminate plastic deformation from contact between pipe and restraints that may occur from large pipe displacements caused by thermal stratification.

To mitigate flow stratification caused by leaking valves, design modifications include an extra isolation valve downstream of the leaking check valve to offer another barrier against flow in a leaking emergency core cooling line, and additional instrumentation to monitor the temperature distribution between the top and bottom of the pipe (e.g. for a residual heat removal line).

Since the weld region in pipe elbows is a susceptible region for cracking, newly designed German plants have fabricated the elbow section with an integral straight run on each end so that a straight run-to-straight run butt weld can be made. Changes in pipe direction also can be accomplished by bends rather than elbows thereby *eliminating welds*.

Many nuclear plants have carried out *snubber reduction programmes* that reduce the probability of a locked snubber contributing to unanticipated fatigue usage. Snubbers are support devices that are designed to allow piping and equipment to freely expand and contract during thermal events and lock during dynamic events. In a number of cases, mechanical snubbers were in the locked mode so that the piping could not freely expand and contract; hence, higher than intended stresses and fatigue usage were induced.

7.1.4. Examples of ageing mitigation actions for thermal fatigue

- To reduce thermal fatigue in the spray line, close to the pressurizer, it is possible to increase the minimum continuous flow rate in the spray line, balanced by pressurizer heaters, in order to have a good thermal conditioning in the spray line (and a pressurizer spray nozzle).
- To reduce the surge line stratification effects, modify the heat-up and cooldown procedure to minimize the difference between pressurizer and hot leg.
- To reduce thermal fatigue in a safety injection connected line, assure a good leak tightness of the isolation valves to minimize the risk of high temperature difference in the penetrating vortex area.
- To assure free thermal expansion of a piping system, inspect periodically the piping supports.
- To minimize environmentally accelerated fatigue degradation, assure the specified water chemistry (oxygen contents, etc.) in all situations; if any chemical contamination of a system is detected, perform a complete review of potential consequences.
- In high fatigue sensitive locations, replace and change design of some pipe fittings with high thickness variation or longitudinal welds.
- To protect nozzles from thermal fatigue and to assure inspect ability of thermal sleeve attachment, repair or replace thermal sleeves, as appropriate.
- For each susceptible location with a high computed usage factor or with complex local loads (such as, dead legs, piping between two isolation valves or mixing areas) perform transient monitoring and periodic inspection.
- For mixing tees with large temperature difference and large number of hours of operation, define a specific surveillance programme.

7.2. Mitigation of vibration fatigue

Vibration (high cycle) fatigue results usually from small amplitude displacements in a fraction of millimeter range and often results in a leak short time after crack initiation. The most effective method for mitigating vibration fatigue is to eliminate the sources of vibration by changing the frequency of the exciting forces originating in rotating machines, pressure variation in valves, or cavitation.

Another effective method of mitigating vibration fatigue is adding integral stiffeners to piping at the location of shell mode response. For example: support all massive devices (e.g. valves) on small connected lines; add stiffness on tees to reinforce the connection of a small pipe to a large pipe; reinforce tees at socket-welds by increasing the fillet weld size.

7.3. Mitigation of PWSCC of Alloy 600

Typically susceptible components of PWR primary piping include primary loop and pressurizer instrument penetrations (instrument nozzles) welded to the piping using Alloy 182 filler material. Since the PWSCC initiation and crack growth rate depend on the presence of high tensile stress, time at operating temperature, coolant chemistry, and susceptible microstructure, PWSCC can be mitigated in a limited way by suitable coolant chemistry and lower temperature. Low lithium content (2 ppm) and low hydrogen concentration (25–35 cm³/kg) have been used to minimize PWSCC.

Managing ageing effects

7.4. Piping repair and replacement

If a pipe crack develops, options available include repair (such as grinding out the crack) or replacing the component (possibly with a different geometry and/or material). In some cases the most effective and economic corrective action for degraded piping may be its replacement after an adequate root cause analysis to preclude recurrence of the problem.

All analyses before any replacement have to consider both safety and economical aspects (plant availability, replacement cost, ISI and monitoring cost with or without replacement, dose to workers). The new component should include improvement in accordance with root causes analysis. And detailed expertise of the replaced component should be performed to confirm root cause analysis results. Finally, similar piping location with similar potential ageing degradations should be reviewed.

If unacceptable PWSCC is detected, a specific weld repair has to be studied with less sensitive material to PWSCC (such as Alloy 690 or Alloy 152-52 filler metal), or the Alloy 600 material has to be protected against any contact with primary water (stainless steel cladding can be used).

A more complex problem is one when the CUF exceeds the ASME Code allowable value of 1.0 but in-service inspection detects no cracking. NUMARC [7.3] has proposed that for locations where the CUF cannot be shown to be less than unity, fatigue transient monitoring to better quantify the stressors, or periodic in-service inspection in accordance with the ASME Code Section XI requirements (plus perhaps enhanced or augmented methods) could be used to justify continued operation. The NRC has not accepted increased inspection as an acceptable corrective action, but has acknowledged that a staff position is needed to specify the appropriate corrective action to be taken when the CUF limit has been exceeded; replacement with modification of operation procedure has to be considered and analysed on a case by case basis.

Jamali [7.4] reports that the repair/replacement decision percentages for nuclear plant piping failures (not limited to the reactor coolant system) have been as follows:

<i>Action</i>	<i>%</i>
Modify	20
Repair	38
Replace	30
Temporary measures	11
Unknown	1

REFERENCES TO SECTION 7

- [7.1] ARNOLD, E.C., et al., Changing Nuclear Plant Operating Limits During Startup and Shutdown, Proceedings of the American Power Conference, Vol. 52 (1990) 960-966,.
- [7.2] SHAH, V.N., MACDONALD, P.E., (Editors/Authors), Ageing and Life Extension of Major Light Water Reactor Components, Elsevier Science Publishers B.V., Amsterdam, June 1993.
- [7.3] NUMARC 1992, PWR Reactor Coolant System License Renewal Industry Report, NUMARC Report Number 90-97.
- [7.4] JAMALI, K., Pipe Failures in US Commercial NPPs, EPRI TR-100380 (1992).

8. PWR PRIMARY PIPING AGEING MANAGEMENT PROGRAMME

The information presented in this report indicates that the operating environment including primary system pressure, temperature and chemistry can cause ageing degradation of PWR primary piping. In particular, ageing mechanisms of thermal fatigue, vibratory fatigue, thermal ageing, stress corrosion cracking, boric acid and atmospheric corrosion can lead to both safety and economic concerns. Therefore, a systematic ageing management programme for PWR primary piping is needed at all plants.

The preceding sections of this report dealt with important elements of an PWR primary piping ageing management programme whose objective is to maintain the integrity of the PWR primary piping at an NPP throughout its service life. This section describes how these elements are integrated within a plant specific PWR primary piping ageing management programme utilizing a systematic ageing management process which is an adaptation of Deming's Plan-Do-Check-Act cycle to ageing management (Fig. 8.1). Such an ageing management programme should be implemented in accordance with guidance prepared by an interdisciplinary ageing management team for PWR primary piping organized at a corporate or owners group level. For guidance on the organizational aspects of a plant ageing management programme and interdisciplinary ageing management teams refer to IAEA Safety Report "Implementation and Review of NPP Ageing Management Programme" [8.1].

A comprehensive understanding of PWR primary piping, its ageing degradation, and the effects of the degradation on the ability of the PWR primary piping to perform its design functions is the fundamental basis of an ageing management programme. This understanding is derived from a knowledge of the design basis (including applicable codes, and regulatory requirements); the design and fabrication (including the materials properties and specified service conditions); the operation and maintenance history (including commissioning and surveillance); the inspection results; and generic operating experience and research results. Sections 1.1, 2, 3 and 4 contain information on important aspects of the understanding of PWR primary piping and their ageing.

In order to maintain the integrity of PWR primary piping, it is necessary to control within defined limits its age related degradation. Effective ageing degradation control is achieved through the systematic ageing management process consisting of the following ageing management tasks, based on understanding of PWR primary piping ageing (which includes, among other things, identification of all sensitive locations for each significant ageing mechanism):

- operation within operating guidelines aimed at minimizing the rate of degradation — *managing ageing mechanisms* (Sections 8.1.3 and 7)
- inspection and monitoring consistent with requirements aimed at timely detection and characterization of any degradation (Section 6);
- assessment of the observed degradation in accordance with appropriate guidelines to determine integrity (Section 5); and
- maintenance (repair or parts replacement) to correct unacceptable degradation — *managing ageing effects* (Section 7)

A PWR primary piping ageing management programme co-ordinates programmes and activities contributing to the above ageing management tasks in order to detect and mitigate

ageing degradation before the PWR primary piping safety margins are compromised. This programme reflects the level of understanding of the PWR primary piping ageing, the available technology, the regulatory/licensing requirements, and plant life management considerations/objectives. Timely feedback of experience is essential in order to provide for ongoing improvement in the understanding of the PWR primary piping ageing degradation and in the effectiveness of the ageing management programme. The main features of a PWR primary piping ageing management programme, including the role and interfaces of relevant programmes and activities in the ageing management process, are shown in Fig. 8.1, and discussed in Section 8.1. Application guidance is provided in Section 8.2.

8.1. Key elements of PWR primary piping ageing management programme

8.1.1. Understanding PWR primary piping ageing

Understanding PWR primary piping ageing is the key to effective management of PWR primary piping ageing, i.e. it is the key to: co-ordinating ageing management activities within a systematic ageing management programme, managing ageing mechanisms through prudent operating procedures and practices (in accordance with procedures and technical specifications); detecting and assessing ageing effects through effective inspection, monitoring, and assessment methods; and managing ageing effects using proven maintenance methods. This understanding consists of: a knowledge of PWR primary piping materials and material properties; stressors and operating conditions; likely degradation sites and ageing mechanisms; condition indicators and data needed for assessment and management of PWR primary piping ageing; and effects of ageing on safety margins.

The understanding of PWR primary piping ageing is derived from the PWR primary piping baseline data, the operating and maintenance histories, and external experiences. This understanding should be updated regularly to provide a sound basis for the improvement of the ageing management programme consistent with operating, inspection, monitoring, assessment and maintenance methods and practices.

The PWR primary piping baseline data consist of the performance requirements, the design basis (including codes, standards, regulatory requirements), the original design, the manufacturer's data (including materials data), and the commissioning data (including pre-service inspection data). The PWR primary piping operating history includes the pressure-temperature records, system chemistry records, and the ISI results. The PWR primary piping maintenance history includes the inspection records and assessment reports, design modifications, and type and timing of maintenance performed. Retrievable up-to-date records of this information are needed for making comparisons with applicable external experience.

External experience consists of the operating and maintenance experience of (a) PWR primary piping of similar design, materials of construction, and fabrication; (b) PWR primary piping operated with similar operating histories, even if the designs are different; and (c) relevant research results. It should be noted that effective comparisons or correlations with external experience require a detailed knowledge of the PWR primary piping design and operation.

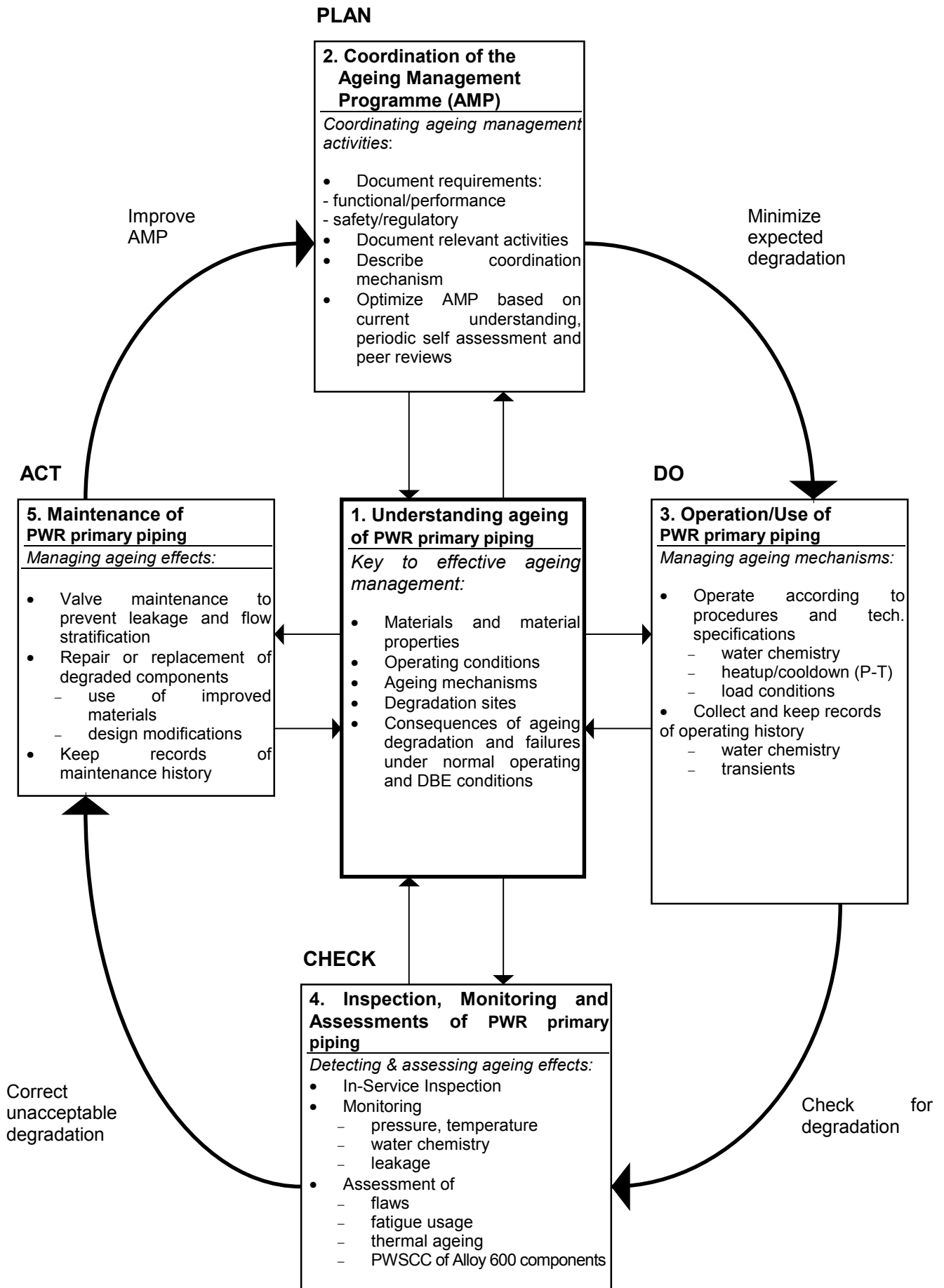


FIG. 8.1. Key elements of PWR primary piping ageing management programme utilizing the systematic ageing management process.

The present report is a source of such information. However, this information has to be kept current using feedback mechanisms provided, for example, by owners groups. External experience can also be used when considering the most appropriate inspection method, maintenance procedure and technology.

8.1.2. Co-ordination of PWR primary piping ageing management programme

Existing programmes relating to the management of PWR primary piping ageing include operations, surveillance and maintenance programmes as well as operating experience feedback, research and development and technical support programmes. Experience shows that ageing management effectiveness can be improved by co-ordinating relevant programmes and activities within an ageing management programme utilizing the systematic ageing management process. Safety authorities increasingly require licensees to implement such ageing management programmes for selected SSCs important to safety. The co-ordination of a PWR primary piping ageing management programme includes the documentation of applicable regulatory requirements and safety criteria, and of relevant programmes and activities and their respective roles in the ageing management process as well as a description of mechanisms used for programme co-ordination and continuous improvement. The continuous ageing management programme improvement or optimization is based on current understanding of PWR primary piping ageing and on results of periodic self-assessments and peer reviews.

8.1.3. Operation of PWR primary piping

NPP operation has a significant influence on the rate of degradation of plant systems, structures and components. Exposure of PWR primary piping to operating conditions (e.g. temperature, pressure, water chemistry) outside prescribed operational limits could lead to accelerated ageing and premature degradation. Since operating practices influence PWR primary piping operating conditions, NPP operations staff have an important role within the ageing management programme to minimize age related degradation of the PWR primary piping. They can do this by maintaining operating conditions within operational limits that are prescribed to avoid accelerated ageing of PWR primary piping components during operation. Examples of such operating practices are:

- operation within the prescribed pressure and temperature range during startup and shutdown to avoid critical transients and the risk of overpressure (this risk varies, depending on the material's fracture toughness)
- performing maintenance according to procedures designed to avoid contamination of PWR primary piping components with boric acid or other reagents containing halogens
- on-line monitoring and record keeping of operational data necessary for predicting ageing degradation and defining appropriate ageing management actions.

Operation and maintenance in accordance with procedures of plant systems that influence PWR primary piping operational conditions (not only the primary system but also the auxiliary systems like water purification and injection systems), including the testing of the PWR primary piping components, and record keeping of operational data (including transients) are essential for an effective ageing management of the PWR primary piping and a possible plant life extension.

8.1.4. PWR primary piping inspection, monitoring and assessment

Inspection and monitoring: The PWR primary piping inspection and monitoring activities are designed to detect and characterize significant component degradation before the PWR primary piping safety margins are compromised. Together with an understanding of the PWR primary piping ageing degradation, the results of the PWR primary piping inspections and monitoring provide a basis for decisions regarding the type and timing of maintenance actions and decisions regarding operational changes and design modifications to manage detected ageing effects.

Current inspection and monitoring requirements and techniques for PWR primary piping are described in Section 6. Inspection and monitoring of PWR primary piping degradation falls in two categories: 1) in-service inspection, and 2) monitoring of pressures and temperatures, water chemistry, transients (relative to fatigue), and piping leakage. Results of the ISI are used for flaw tolerance/crack propagation assessments. Transient monitoring provides realistic values of thermal stresses as opposed to design basis thermal stress values for fatigue assessments. Finally, leakage monitoring aims for an early detection of cracks before growing to a critical size the LBB scenario.

It is important to know the accuracy, sensitivity, reliability and adequacy of the non-destructive methods used for the particular type of suspected degradation. The performance of the inspection methods must be demonstrated in order to rely on the results, particularly in cases where the results are used in integrity assessments. Inspection methods capable of detecting and sizing expected degradation are therefore selected from those proven by relevant operating experience.

Integrity assessment: The main safety functions of PWR primary piping is to act as a barrier between the radioactive primary side and the non-radioactive outside environment and to carry water for cooling of fuel. Safety margins are part of the design and licensing requirements of an NPP to ensure the structural integrity of the PWR primary piping under both normal and accident conditions. An integrity assessment is used to assess the capability of the PWR primary piping to perform the required safety function, within the specified margins of safety, during the entire operating interval until the next scheduled inspection.

Integrity assessments have used a variety of methods in response to the particular conditions and circumstances present at the time of the assessment. Section 5 of this report describes the assessment methods used. Included in the PWR primary piping integrity assessments is utilization of the ISI results along with fatigue crack growth models and fracture mechanics technologies to assess the flaw tolerance of the PWR primary piping. These include assessment of the fatigue usage factors utilizing information/data from the on-line transient monitoring system, assessments of the stress corrosion cracking susceptibility of the Alloy 600 components, and thermal ageing assessments.

8.1.5. Maintenance of PWR primary piping

Maintenance actions that can be used to manage ageing effects detected by inspection and monitoring methods in different parts of PWR primary piping are described in Section 7. Decisions on the type and timing of the maintenance actions are based on an assessment of the observed ageing effects, available decision criteria, and understanding of the applicable ageing mechanism(s), and the effectiveness of available maintenance technologies.

Maintenance actions for managing thermal fatigue include replacing valve packing or increasing valve seat gap to minimize valve leakage and thus prevent flow stratification, and for vibratory fatigue installing pipe stiffeners. Maintenance options for managing degraded piping (cracked or with CUF >1.0) are repair or replacement. (Cracks may be removed by grinding and the cavity filled with weld metal or a pipe section may be replaced, perhaps with different geometry and/or material.)

8.2. Application guidance

The PWR primary piping ageing management programme should address both safety and reliability/economic aspects of PWR primary piping ageing to ensure both the integrity and serviceability of the PWR primary piping during its design life and any extended life. The following subsections provide guidance on dealing with the relevant age related degradation mechanisms.

8.2.1. Fatigue

Thermal fatigue: Several aspects of thermal fatigue should be understood by the user when developing a plant specific AMP for this degradation mechanism. Generally, both stainless and carbon steels should be considered susceptible to thermal fatigue. Thermal fatigue degradation may be found in either weld or base metal locations, but it is restricted to non-main coolant loop piping, except for high cycle fatigue in high temperature difference mixing nozzles. The specific design (i.e. layout) of the piping system is also a critical factor in determining its susceptibility to thermal fatigue since the layout may promote thermal stratification, thermal striping, and/or turbulent penetration. Finally, while previous experience has indicated that leakage rather than rupture is the primary mode of failure when thermal fatigue is present, LBB analyses are not acceptable for the evaluation of small diameter lines. Therefore, the plant safety analysis should consider the implication of a potential small-break loss of coolant-accident.

The user's ageing management programme should consider several specific common regulatory requirements and sources of information. Heatup and cooldown rates (normally determined by analysis of the reactor vessel materials) will influence the potential for thermal fatigue in some lines (e.g. the pressurizer surge line). Also, requirements on maintaining fatigue cumulative usage factors below 1.0 should be examined when the impact of thermal fatigue is assessed. In-service inspection requirements should be followed and augmented if necessary. The user should pay particular attention to information to data from their own facility or sister plants (which may have similar piping layouts), plants of similar design (i.e. NSSS vendor), when developing the ageing management programme, but information from all sources should be reviewed. Information from operation and startup testing activities at the user's facility should include a review of all data relevant to the pressure, temperature, and coolant flow conditions at potential degradation sites. Operational procedures should be reviewed and modified as necessary to minimize conditions which could lead to thermal fatigue, and operational data collection should be implemented to acquire the information noted above.

The in-service inspection, monitoring, and assessment element should rely on qualified inspection techniques (e.g. those qualified to the requirements of Appendix VIII of Section XI of the ASME Code or French RSE-M Code) since the detection of fatigue cracking is difficult. Effective local leakage detection techniques and thermal fatigue monitoring

systems (e.g. local thermocouple matrices arranged azimuthally on the piping OD) should be considered. The user should also be aware that enhanced inspection and monitoring techniques may be available and should be considered to supplement the qualified techniques noted above. If thermal fatigue degradation is discovered, the user should analyze the flaw to determine if operation for another cycle is justified. If not, replacement of the degraded component should be the appropriate corrective action. During replacement, consideration should be given to any design changes (e.g. modification of the slope of a piping section) which could be made to reduce the likelihood of future thermal fatigue. If the decision to replace the component is made, the component should be inspected and tested after removal from service. Operational regime modifications should be implemented to reduce the possibility of reoccurrence.

Vibratory fatigue: Vibratory fatigue is a high cycle mechanical fatigue mechanism which may effect any PWR primary piping system material, however the degradation sites have been generally limited to small diameter piping and socket weld locations in particular. In these cases, vibratory fatigue cracking is caused by pump- or cavitation-induced pressure pulsations if an excitation frequency coincides with the structural (natural) frequency of the piping, as determined by the piping dimensions and layout. Pump-induced pressure pulsations occur at distinct frequencies (multiples of the pump speed) and are associated with positive-displacement pumps such as those which may be found in charging systems. Cavitation induced pulsations consist of broadband frequencies (a band with a wide range of frequencies) and are associated with cavitating components such as an orifice in the letdown system.

Field experience has shown a variety of failure behavior depending on the location of the vibratory fatigue cracking. The typical failure mode is pipe rupture for cracking in socket welds. In a sound socket weld, the crack initiates at the toe of the weld and may be detected with visual inspection. In a poorly fabricated socket weld, the crack initiates at the root of the weld and is unlikely to be detected prior to rupture. In the absence of socket welds, the base metal near the small-diameter piping attachment becomes the most susceptible to such cracking and the typical failure mode becomes leakage.

Some operational activities can be initiated to assist in monitoring vibratory fatigue. The piping systems and sites susceptible to vibratory fatigue cracking can be identified by monitoring the vibration amplitude during operation. However, damaging frequencies may be present only during certain modes of operation and particular attention should be paid to monitoring during startup and shutdown operations. With regard to the inspection element of the AMP, visual inspection and radiographic testing should be considered to detect cracking at susceptible locations.

The appropriate maintenance activities to address vibratory fatigue degradation are based on the source of excitation. In the case of pump-induced vibrations, the natural frequency of the affected piping system may be increased by augmenting the piping system stiffness and reducing the mass of the components attached to the system. In the case of cavitation-induced vibrations, degraded socket welds locations should be replaced with butt welds, which are more resistant to high-cycle fatigue damage. In the case of cracks in the base metal, a weld repair or replacement of the piping should be carried out. In the event of a vibratory fatigue failure, it is recommended that the user inspect and test the similar locations in the piping system to identify all the susceptible locations.

8.2.2. Thermal ageing

The thermal ageing degradation mechanism is primarily of interest for cast stainless steel materials and welds made from stainless steel filler material. Cast stainless steels and stainless steel weld materials have a duplex structure consisting of austenite and (delta)-ferrite phases. Materials with high (delta)-ferrite content (>15%) have increased susceptibility to thermal ageing due to an increased potential for extensive spinodal decomposition of the (delta)-ferrite phase at primary system operating temperatures. This (delta)-ferrite decomposition results in a reduction in the material's fracture toughness and Charpy-impact strength. In addition, some data exists which may indicate that the welding process may also affect the potential degradation of stainless steel welds.

The effect of thermal ageing should be taken into account for any location where cast or weld stainless steel materials are used. This is especially true if an LBB analysis is to be justified for an affected piping component (e.g. sections of the main coolant loops). Thermal ageing of primary coolant piping can be a safety issue if a material develops a very low level of fracture toughness (which reduces the material's critical flaw size) and a significant flaw is present. Specific attention should be paid to cast elbows and cast inclined safety injection nozzles for flaw tolerance of these components and for their role in the LBB demonstration. As an example, the French LBB demonstration considers possible through-wall crack in elbows base metal to assure that all lower toughness locations of the main coolant lines are considered.

The options available for managing thermal ageing in the operational, inspection/monitoring, and maintenance elements of the ageing management programme are generally limited. Adjustment of the primary system operating temperatures may not be practical since operating temperatures are normally determined by other considerations; however temperature data should be recorded to aid in estimating the degree of thermal ageing. It is recommended that inspection and monitoring programmes consider: the replication of the surfaces of the affected area for metallographic examination (to determine (delta)-ferrite content), ageing surveillance specimens from the affected (or similar) materials to monitor the progression of the thermal ageing degradation, and, possibly volumetric examination of affected locations. Repair or replacement of a degraded component must be considered in the event that a significant flaw is discovered or an unacceptably low level of fracture toughness is reached. If a decision is made to replace a degraded component, an improved material (with lower (delta)-ferrite content) should be used in the new component and a comprehensive analysis of the removed component is recommended.

8.2.3. Corrosion

Stress corrosion cracking (SCC): in general, SCC is not a major concern in PWR piping, but it is a concern for instrument penetrations made from Alloy 600 and welded to the piping via Alloy 182 filler material. The most susceptible degradation site is the inside surface of the penetration where some Alloy 182 can be directly in contact with primary water. The ageing mechanism is PWSCC.

Degradation of PWR stainless steel piping can also occur due to SCC, but this has only been found as transgranular SCC from outside surface due to contamination by chloride residues in combination with water condensation. The stressors accelerating the degradation process are the existing residual stresses; but in the case of the stainless steel piping chloride

contamination (with the possibility for increasing concentration of residues) is the only necessary condition.

The impact on safety relating to PWSCC of Alloy 600 penetrations has been relatively small — degradation and leakage have been detected and repairs made prior to rupture. However, the impact on plant availability can be high because of the necessity to shut down the plant for difficult on-site welding repairs.

To minimize initiation and propagation of PWSCC of Alloy 600 penetrations appropriate primary system water chemistry should be maintained consistent with regulatory requirements and industry guidelines. In addition, data from installed leak monitoring systems (global containment monitoring and/or local penetration monitoring devices) should be recorded during operation and testing to provide for timely leakage detection. To prevent the possibility of contaminating stainless steel piping with chlorides, products containing chlorides (including lubricants, tape, insulation, markers, etc.) should be prohibited from use in operational and maintenance procedures and effective quality assurance. In-service inspection activities should be focused on the Alloy 600 components and, in particular on dissimilar metal welds using Alloy 182 filler material.

Development of the in-service inspection programme for the Alloy 600 penetration and Alloy 182 dissimilar metal weld should consider the use of ultrasonic and/or eddy-current technologies. Significant indications should be evaluated using appropriate flaw evaluation methodologies. Finally, since the detection of the PWSCC mechanism has not been possible until leakage was observed, external visual inspection for boron salt deposits should be conducted. In addition to those leakage detection systems necessary to meet existing regulatory requirements, the user should consider local leakage monitoring for those Alloy 600 penetrations deemed most susceptible to PWSCC. For this application, radiation (gas) detection monitoring systems should be considered.

If leakage is detected, the degradation site has to be repaired or replaced in an appropriate way. New weld materials Alloy 152 or Alloy 52 and penetrations made from Alloy 690 should be used. The technique to be applied to the replacement should keep defects and residual stresses to a minimum. Post-removal inspection of the degraded component should also be conducted.

Boric acid corrosion (wastage): leakage of primary coolant may cause boric acid corrosion of main coolant loop piping components made from carbon steel or low-alloy steel materials and lead to loss of material. The corrosion rate appears to depend upon the pH of the solution, the solution temperature, and the boric acid concentration in the solution. Some studies have shown that the corrosion rates of the steel at pH values of 8 to 9.5 are six times those at pH values of 10.5 to 11.5 [8.2]. As temperatures increase to the boiling point of water, the water evaporates, the solution concentrates, and the corrosion rate increases at much faster rates. Concentrated boric acid is highly corrosive at ~95°C (~200°F).

Field experience and test results indicate that the corrosion rates for carbon steels and low-alloy steels exposed to primary coolant leakage are greater than previously estimated and could be unacceptably high. The field experience is mainly associated with the carbon steel and low-alloy steel pressure boundary components such as closure bolting and carbon steel safety valve bonnets.

The observed boric acid corrosion rates are relatively high. Therefore, it is important to ensure that adequate monitoring procedures are in place to detect boric acid leakage before it results in significant degradation of the reactor coolant pressure boundary, such as wastage of carbon steel and low-alloy steel base metal.

The detection of boric acid corrosion of carbon steel and low alloy steel components may be performed by visual examination during surveillance walkdown inspections as required by the USNRC Generic Letter 88-05, Boric Acid Corrosion of Carbon Steel Reactor Pressure Boundary Components in PWR Plants. In response to the generic letter, utilities in the USA perform visual examination during surveillance walkdown inspection to detect any boric acid leakage. A small [0.38 L/min (<0.1 gpm)] primary system leak through pressure boundary can be detected during the walkdown; such a small leak is generally not detected by the plant leak detection systems.

REFERENCES TO SECTION 8

- [8.1] INTERNATIONAL ATOMIC ENERGY AGENCY, Implementation and Review of a Nuclear Power Plant Ageing Management Programme, Safety Report Series No. 15, IAEA, Vienna (1999).
- [8.2] BERY, W.E., Corrosion in Nuclear Applications, John Wiley and Sons, Inc., New York (1971), 173–174.

CONTRIBUTORS TO DRAFTING AND REVIEW

The original draft of this report was prepared by J. Schmidt of Siemens, Germany. M. Banic of the USNRC made extensive revisions to the draft report during 1995. The preparation of the draft versions of the report has been supported by the following participants of the IAEA Consultants Meetings and other technical experts:

Aggarwal, M.	Ontario Hydro, Canada
Banic, M.	USNRC, United States of America
Bougaenko, S.	RDIPE, Russian Federation
Campello, S.	FURNAS, Brazil
Dragunov, Y.	Gidropress, Russian Federation
Dozier, J.	USNRC, United States of America
Faidy, C.	EdF, France
Hermann, B.	USNRC, United States of America
Hudcovsky, S.	EGU Bratislava, Slovakia
Ito, N.	MHI, Japan
Kovacs, P.	Paks NPP, Hungary
Kuo, P.T.	USNRC, United States of America
MacDonals, P.	INEL, United States of America
Mitchell, M.	USNRC, United States of America
Porter, A.M.	INEL, United States of America
Saghal, S.	NOK Beznau, Switzerland
Schmidt, J.	Siemens, Germany
Shah, V.	ANL, United States of America
Sohn, G.H.	KAERI, Republic of Korea
Ware, A.G.	INEL, United States of America